

**Investigation of mechanisms for enhancing
expression of human FVIII in vitro; application
to therapeutic protein production**

BY

DOYOUNG LEE

UNIVERSITY COLLEGE LONDON

A thesis submitted for the degree of Doctor of Philosophy

2017

ABSTRACT

Haemophilia A is the most common bleeding disorder and is caused by deficiency or abnormality in coagulation Factor VIII (FVIII). Deletion of the B-domain dramatically improves secretion of this protein with no alteration of the pro-coagulant activity of the B-domainless FVIII. Previous work has shown that the codon optimisation of FVIII increases expression by 10-fold and the novel variant, FVIII-V3, is expressed at higher levels than B-domain deleted FVIII (BDD-FVIII) in the context of AAV mediated gene transfer in mice. However, the mechanisms underlying these enhancements to expression remain undefined. The purpose of this study was to investigate if (1) codon optimisation increases FVIII expression by increasing transcription of FVIII mRNA, (2) higher level of FVIII expression observed with V3 is due to *N*-linked glycosylation motifs in the B-domain linker and V3.

In this thesis, I characterised a range of novel FVIII variants to demonstrate that functional characteristics were similar to native FVIII.

Firstly, comparison of FVIII expression levels in lentivirally transduced HEK-293 stable cell lines showed codon optimised FVIII variants expressed higher than wild type FVIII not only improved mRNA transcription but also FVIII expression. The V3co variant expressed FVIII at the highest level *in-vitro* and by *in-vivo* AAV gene delivery to mice.

Secondly, the glycosylation profile of purified FVIII variant proteins was described. We show incremental formation of N-glycans within the B-domain linker sequences as detected by mass spectrometry analysis. In addition, these novel FVIII variants showed thrombin digestion patterns, identical to the commercial rFVIII protein. Furthermore, the thrombin generation and vWF/FVIII affinity assay revealed that all variants were similar to commercially available B-DD rFVIII.

Finally, the expression of *N*-linked glycosylation mutant V5 and through a deletion

analysis, short regions from the V3 linker variants using *in-vivo* AAV gene transfer confirming glycosylation of the linker sequence is not an important factor but conformation changes may be the key for the improved expression profile.

Overall, these insights will significantly increase the potential for the transition of engineered FVIII molecules to clinic.

ACKNOWLEDGEMENTS

I would like to express my sincere gratitude to my supervisor Professor Amit Nathwani, for giving me the opportunity to carry out my PhD in his group and for his expert guidance and help towards this thesis. I would like to thank my secondary supervisor, Professor Edward Tuddenham for his expert guidance and support throughout my PhD.

My sincere thanks to Dr Jenny McIntosh and Dr John McVey for their constant supports and contribution toward my research.

I have been lucky to meet a lot of good colleagues and friends at the Cancer Institute. In particular, thanks to Allison Dane, Pollyanna Goh, Cecilia Rosales, Ifrax Mohamod, Deepak Raj, Marc Davies, Nishil Patel, Marco Della Peruta, Sara Caxaria, Solange Paredes Moscosso, Azadeh Kia Kojouri, Arnold Pizzey and Gordon Cheung anyone who I have missed that made cancer institute a great place to work. I would like to express my thanks to Anne Riddell who provided advice and support for coagulation assays in Royal Free Hospital.

I would like to thank my family for their love and support throughout the most stressful times. My husband Younbok and my daughter Florence cheer me up from my distressed times.

Lastly, I dedicated this thesis to my late father (Chong Gu Lee) and my mother (Chal Ja Cho) for their love and support me to guide and making all this possible.

AUTHOR'S DECLARATION

I, Doyoung Lee, confirm that the work presented in this thesis is my own. Where information has been derived from other sources, I confirm that this has been indicated in this thesis.

Signed.....

Doyoung Lee

CONTENTS

ABSTRACT	ii
ACKNOWLEDGEMENTS	iv
AUTHOR'S DECLARATION	v
ILLUSTRATIONS.....	xii
ABBREVIATIONS.....	xvii
Chapter 1: General Introduction.....	20
1.1. Bleeding Disorders.....	21
1.1.1. Haemophilia.....	22
1.1.1.1. Pathology.....	25
1.1.2. Haemostasis.....	26
1.1.2.1. Classical coagulation pathway	26
1.1.2.2. Cell-based coagulation model.....	29
1.2. FVIII Protein Structure	32
1.3. FVIII Secretion.....	35
1.3.1. FVIII Quality control	35
1.3.2. Receptor-mediated FVIII transport.....	36
1.3.3. LMAN1 and COPI/II interaction.....	40
1.3.4. FVIII Processing in Golgi	42
1.4. FVIII activation.....	44
1.5. FVIII clearance	46
1.6. FVIII therapeutic treatments and risks.....	48
1.6.1. Haemophilia A protein replacement therapy	48
1.6.2. Inhibitor formation	49
1.7. Bioengineering of FVIII	50
1.7.1. Wild type.....	50
1.7.2. Codon optimisation	51
1.7.3. Codon optimisation for FVIII.....	52
1.7.4. B-domain deleted FVIII	54
1.7.5. Commercial recombinant FVIII.....	59
1.7.5.1. History of recombinant proteins and current developing products	59
1.7.5.2. Current strategies to improve FVIII half-life	61
1.8. Post-translational modifications (PTMs).....	63
1.8.1. Glycosylation	64
1.8.2. Human FVIII <i>N</i> -linked glycosylation	68
1.8.3. Recombinant protein production in mammalian cells	69

1.8.4. Cell type specific Post-translational modifications	71
1.8.5. Comparison of the most common epitopes between plasma-derived FVIII and rFVIIIs.....	72
1.9. Gene delivery technology	74
1.9.1. Non-viral vectors.....	74
1.9.1.1. Naked DNA delivery.....	74
1.9.1.2. Chemical Carrier.....	75
1.9.2. Viral vectors.....	76
1.9.2.1. Pseudo typed Lentiviral vectors	77
1.9.2.2. Improve Biosafety using pseudo-typed lentivirus	78
1.9.2.3. Adeno associated virus.....	80
1.9.2.4. Recombinant Adeno associated virus (rAAV).....	81
1.9.2.5. Serotypes	84
1.9.2.6. Tissue-specific promoter.....	85
1.9.2.7. AAV engineering for large transgenes	85
1.9.3. Current status of gene therapy for Haemophilia	86
1.10. Research Aim.....	90
1.10.1. Brief outline of strategy.....	90
Chapter 2:.....	92
Materials and Methods.....	92
2.1. Basic Bacterial Manipulation	93
2.1.1. Transformation of E-coli with Plasmid DNA.....	93
2.2. Molecular cloning.....	93
2.2.1. DNA Restriction Digest	93
2.2.2. Isolation of Plasmid DNA fragments by Agarose Gel Electrophoresis.....	94
2.2.3. Dephosphorylation of Backbone DNA.....	95
2.2.4. Klenow filling	95
2.2.5. DNA ligation.....	95
2.2.6. Transformation of One Shot® Stbl3™ Bacterial Cells	96
2.2.7. Screening colonies	96
2.2.8. Site -Directed Mutagenesis.....	97
2.3. Genomic copy number correction	99
2.3.1. Quantitative Real-Time PCR (qPCR) for the determination of proviral copy number for human cell lines.....	99
2.3.2. Quantitative RealTime PCR (qPCR) for the Determination of Proviral Copy Number for Mouse liver tissue	100
2.4. Total RNA extraction.....	100

2.4.1. Measurement of FVIII RNA copy number analysis	101
2.4.2. Relative quantification measurements	101
2.5. Cell Culture Methods	102
2.5.1. Propagation of adherent cell lines	102
2.5.2. Propagation of Suspension Cell Lines	102
2.5.3. Long term storage of cell lines	103
2.5.3.1. Cryopreservation for adherent cell lines	103
2.5.3.2. Cryopreservation for suspension cell lines	103
2.6. Production of Viral vectors	103
2.6.1. The 3 rd generation Pseudo-typed Lentivectors	103
2.6.1.1. Co-transfection of HEK-293T cells	103
2.6.1.2. Viral supernatant harvest and concentration	105
2.6.1.3. Titration of Lentiviral Vectors by Quantitative Real-Time PCR (q-PCR)	105
2.6.2. Production of Adeno Associate Virus	106
2.6.2.1. Co-transfection of HEK-293T cells	106
2.6.2.2. Cells and Supernatant harvest	106
2.6.2.3. Lysis of cell pellet	106
2.6.2.4. PEGylation	107
2.6.2.4.2. PEGylation of viral supernatant	107
2.6.2.5. AAV Purification	107
2.6.2.5.1. Iodixanol purification	107
2.6.2.6. AAV titring	109
2.6.2.6.1. Titration of AAV by Q-PCR	109
2.6.2.6.2. Titration of AAV by Alkaline gel	109
2.7. Viral transduction and Single clone selection	111
2.7.1. Cell preparation and transduction	111
2.7.2. Single clone selection	112
2.8. Sample preparation for Coagulation assay	112
2.8.1. Transient transfection of Huh 7 and HEK-293T cell lines	112
2.8.2. Coagulation Assays	113
2.8.2.1. Measurement of human FVIII antigen level from cell lines ...	113
2.8.2.2. FVIII Antigen ELISA	113
2.8.2.2.1. Affinity biological FVIII antigen assay (Polyclonal antibody)	113
2.8.2.2.2. Monoclonal FVIII antigen by Asserachrom Stago Kit (monoclonal antibody)	114
2.8.2.2.3. Mouse plasma FVIII antigen assay	115

2.8.2.3. FVIII Activity Assay (Chromogenic).....	115
2.8.2.3.1. Measurement of FVIII Activity level from culture medium and mouse plasma	115
2.8.2.3.2. One-stage clotting assay (Activated Partial Thromboplastin Time)	116
2.9. Thrombin activation assay	117
2.9.1. Thrombin generation assay	117
2.9.2. Thrombin digestion	118
2.10. SDS-PAGE and Western Blot.....	118
2.10.1 Preparation of samples for SDS–Poly Acrylamide Gel.....	118
2.10.2. Membrane transfer	119
2.10.3. Antibody and ECL.....	119
2.11. Protein staining.....	120
2.11.1. Silver staining	120
2.11.2. Sypro Ruby staining.....	120
2.11.3. Coomassie staining	120
2.12. PNGase F digestion	121
2.12.1. PNGase F treatment.....	121
2.12.2. FVIII polyclonal antibody.....	121
2.12.3. FVIII Monoclonal antibody	121
2.13. <i>In-Vivo</i> Procedures	122
2.13.1. Preparing Adeno Associated Virus for mouse injection	122
2.13.2. Tail vein injection.....	122
2.14. Recombinant FVIII purification	122
2.14.1. Sample preparation for Äkta Explorer	123
2.14.2. FVIII affinity column	124
2.14.3. Diethylaminoethyl (DEAE) Sepharose Fast Flow Column	125
2.15. Immunocytochemistry	127
2.15.1. Split cells on coverslips.....	127
2.15.2. Staining.....	127
2.15.3. Confocal Imaging	128
2.16. Statistical analyses	128
Chapter 3:.....	129
3.1. Introduction.....	130
3.2. Results	132
3.2.1. Construction of B-domain modified FVIII.....	132
3.2.2. Generation of pRRL hPGK mWPRE shuttle vector	135
3.2.3. Cloning of lentiviral vectors	137

3.2.4. Cell line selection for stable FVIII expression	142
3.2.5. Lentiviral vector production	144
3.2.6. Optimisation of FVIII lentiviral vectors transduction	145
3.2.7. Protein expression by the B-domain modified FVIII cell lines ..	147
3.2.8. Single cell clone selection	150
3.2.9. Secondary screen and selection	151
3.2.10. Determination of proviral copy number in stable cell lines after lentiviral transduction	154
3.2.11. Determination of mRNA expression	156
3.2.13. Assessment FVIII Activity in stable cell lines	158
3.2.14. FVIII antigen assay in stable cell lines	160
3.2.15. Membrane-bound FVIII in serum-free condition	162
3.2.16. Immunocytochemistry	164
3.3. Discussion	168
Chapter 4:	172
4.1. Introduction	173
4.2. Results	175
4.2.1. FVIII purification step	175
4.2.2. Step 1: Affinity purification with FVIIISelect column	177
4.2.3. FVIII activity assay	179
4.2.4. Identification of purified FVIII proteins from silver staining	181
4.2.5. FVIII Western blot analysis	183
4.2.6. Double harvested medium from stable cell line improve the FVIII recovery	185
4.2.7. Membrane-bound FVIII protein	189
4.2.8. Modified FVIII purification procedure	192
4.2.9. FVIII select column purification for remaining variants	193
4.2.10. Optimisation of FVIII concentration using DEAE column	194
4.2.11. DEAE purification for SQco, V5co, V1co and N6co	200
4.2.12. Dialysis	201
4.2.13. Characterisation of purified variants FVIII materials.	202
4.2.14. Thrombin digestion of BDD-FVIII and FVIII-V3	204
4.2.15. FVIII biological activity using the thrombin generation Assay and Thrombogram	207
4.2.16. Coagulation assay	210
4.2.17. FVIII activity measured by Chromogenic Assay and One stage clotting assay	211
4.2.18. FVIII and vWF affinity assay	215

4.3. Discussion	217
Chapter 5:.....	220
5.1 Introduction.....	221
5.2. Results	227
5.2.1. PNGase F digestion.....	227
5.2.2. Mass spectrometry	229
5.2.3. <i>N</i> -glycome analysis separates FVIII variants to two groups	232
5.2.4. Distribution of sugar chain and antennary structure profiles of FVIII variants	234
5.2.5. Biologically significant common epitopes	236
5.3. Discussion	238
Chapter 6:.....	241
6.1. Introduction.....	242
6.2. Results	244
6.2.1. Construction of FVIII variant expressing AAV	244
6.2.2. Comparison of AAV FVIII variants which administrated to mouse peripheral vein.....	246
6.2.3. Modification of V3 linker sequences according to the size	249
6.2.4. Other modified FVIII constructs.....	252
6.3. Discussion.....	258
Chapter 7:.....	261
Discussion and Future Directions	262
References:	272
Appendix	299

ILLUSTRATIONS

Figure 1.1. Schematic representation of common inversion of the *F8* gene

Figure 1.2. The classic cascade model of Intrinsic and Extrinsic Pathways

Figure 1.3. Cell-based coagulation model of haemostasis

Figure 1.4. Schematic diagram of human FVIII domains

Figure 1.5. Intracellular processing of FVIII synthesis and secretion in ER and Golgi

Figure 1.6. Cargo transport by the LMAN1-MCFD2 complex

Figure 1.7. Activation process of FVIII

Figure 1.8. Schematic diagram of FVIII variants

Figure 1.9. Biosynthesis of N-glycan in Eukaryotes

Figure 1.10. Most common features of glycans of plasma glycoproteins, compared with those found in human FVIII therapeutic replacement proteins

Figure 1.11. Schematic representation of the HIV provirus and the 3rd generation packaging constructs

Figure 1.12. Schematic represents of rAAV viral packaging plasmids

Figure 2.1. Schematic diagram of the third generation lentiviral vector plasmids

Figure 2.2. Separation of AAV particles from Iodixanol gradients and Amicon filtration

Figure 2.3. Encapsidation of AAV vector with extra-large genome

Figure 2.4. Recombinant human FVIII purification steps

Figure 3.1. Schematic illustration of domain structures for engineered FVIII V1co, V3co and V5co

Figure 3.2. Vector maps of lentivirus shuttle vectors used in this study and details of restriction digestion

Figure 3.3. Schematic representations of human FVIII variants, cloned into third generation lentiviral backbone

Figure 3.4. Cloning for WT SQ and WT N6

Figure 3.5. Cloning for codon optimised FVIII variants into lentivirus shuttle plasmid

Figure 3.6. Cloning for codon optimised FVIII N6 into lentivirus shuttle plasmid

Figure 3.7. Expression of FVIII V3co and SQco variants contained PGK driven FVIII transgene suitable in different cell lines

Figure 3.8. Optimisation of the multiplicity of infection (MOI) of Lenti-FVIIIs for the production of hFVIII expression levels in HEK-293T cells

Figure 3.9. FVIII protein expression from B-domain modified constructs

Figure 3.10. Initial selection of single cell lines, according to which are the best performing FVIII antigen expressing clones

Figure 3.11. Second selection of single cell line from pre-selected lines

Figure 3.12. Quantification of viral copy number from lentiviral transduction

Figure 3.13. Evaluation of relative mRNA expression of FVIII variant stable cell lines

Figure 3.14. FVIII activity comparison between the FVIII variant stable cell lines

Figure 3.15. Quantification of human FVIII expression of variant stable cell lines

Figure 3.16. Profile of membrane-bound FVIII activity from the B-domain engineered FVIII

Figure 3.17. Immunocytochemistry revealing the FVIII variant protein localisation between ER and Golgi

Figure 4.1. Purification steps of human FVIII

Figure 4.1. FVIIISelect column profiles

Figure 4.1. FVIII chromogenic assays for individually collected fractions

Figure 4.1. Silver staining for FVIII V3co, post-FVIIISelect column

Figure 4.1. FVIIISelect column V3co SDS-PAGE analysis in reducing condition

Figure 4.1. FVIIISelect chromatogram from first harvested FVIII V3co media

Figure 4.1. Assessment of FVIII activity from the first FVIII SELECT column

Figure 4.1. FVIIISelect chromatogram from second harvested FVIII V3co media

Figure 4.1. Assessment of FVIII activity from the second FVIIISelect column

Figure 4.10. FVIIISelect chromatogram from membrane-bound FVIII V3co

Figure 4.11. Assessment of FVIII activity from membrane-bound FVIII

Figure 4.12. Schematic diagram of optimised FVIIISelect Purification

Figure 4.13. FVIIISelect column chromatograms for FVIII variants

Figure 4.14. Chromatogram of DEAE Sepharose FF, Anion exchange column purification

Figure 4.15. Assessment of FVIII activity for fractions corresponding to the DEAE column chromatogram

Figure 4.16. Silver staining for fractions corresponding to the DEAE chromatogram

Figure 4.17. Western blot analysis of fractions corresponding to the DEAE chromatogram

Figure 4.18. DEAE anion exchange column chromatogram for FVIII variants

Figure 4.19. Complete procedure of FVIII purification process

Figure 4.20. Schematic representation of FL-FVIII and FVIII V3 domain cleavage by thrombin activation

Figure 4.21. Silver staining for thrombin digestion of purified FVIII-V3

Figure 4.22. Western blotting for thrombin digestion of purified FVIII-V3

Figure 4.23. Activity of FVIII measured by thrombin generation upon activation of coagulation

Figure 4.24. Quantitative parameters of the thrombograms for FVIII variants

Figure 4.25. Comparison of FVIII activity measured by chromogenic assay and one stage clotting assay

Figure 4.26. Comparison of FVIII activity measured by chromogenic assay and one stage clotting assay using plasma STD and ReFacto AF

Figure 5.1. Schematic representations of *N*-linked glycosylation sites on FVIII variant domains

Figure 5.2. PNGase F Digestion of FVIII variants

Figure 5.3. MALDI-TOF mass spectra of permethylated N-glycans in the five FVIII

Figure 5.4. Overview of FVIII variants *N*-linked glycosylation

Figure 5.5. Qualitative and semi-quantitative analysis of N-glycan structures

Figure 5.6. Common epitopes of N-glycans on FVIII variant glycoproteins

Figure 6.1. Characterisation of AAV particles harbouring FVIII variants (V1, V2, V3, and V5)

Figure 6.2. Evaluation of AAV FVIII variants *in-vivo*

Figure 6.3. Characterisation of AAV particles harbouring FVIII V3 linker deletion variants

Figure 6.4. Evaluation of AAV hFVIII V3 linker deletion variants *in-vivo*

Figure 6.5. V-S to D-S modification of N2 (N2.5) FVIII increased FVIII expression

Tables

Table 1.1. Recombinant human FVIII concentrates

Table 1.2. Viral vectors for *in-vivo* gene transfer

Table 1.3. Summary of completed and ongoing Phase I/II clinical trials for haemophilia gene therapy

Table 2.1. Primer sets for mutagenesis

Table 2.2. % CVs for Factor VIII assays: One stage APTT clotting assay on an ACL TOP 700

Table 2.3. % CVs for thrombin generation assays (CAT Fluoroskan Ascent Analyzer)

Table 2.4. Recombinant human FVIII purification steps

Table 2.5. FVIII purification buffers

Table 2.6. Antibodies for Immunofluorescence staining

Table 3.1. Quantification of vector titres for VSVG pseudotyped lentivirus

Table 6.1. Additional modified FVIII constructs cloned into single stranded AAV backbone

ABBREBIATIONS

AAV	Adeno-associated virus
ANOVA	Analysis of variance
ARS	Autonomously replicating sequence
ASGPR	Asialoglycoprotein receptor
BDD	B-domain deleted
BHK	Baby hamster kidney
BiP	Immunoglobulin-binding protein
Bp	Base pair
BSA	Bovine serum albumin
CatC	Cathepsin C
CatZ	Cathepsin Z
CCCD	Cooled charged-coupled device camera
cDNA	Complimentary DNA
CHO	Chinese hamster ovary
CIP	Calf intestinal phosphatase
CO	Codon optimised
Cppt	Central polypurine tract
CRD	Carbohydrate recognition domain
DAPI	4',6-diamidino-2-phenylindole
DEAE	Dimethyl sulfoxide, Sepharose fast flow column
DHB	2,5-dihydroxybenzoic acid
dH ₂ O	Distilled water
DMEM	Dulbecco's modified Eagle medium
dNTP	Deoxyribonucleotide triphosphate
ECL	Enhanced chemiluminescence system
EDTA	Ethylene-diamine-tetra-acetic acid
ELISA	Enzyme-linked immunosorbent assay
ER	Endoplasmic reticulum
ERGIC	ER-golgi intermediate compartment
FBS	Fetal bovine serum
FII	Coagulation Factor II, Prothrombin
FIII	Coagulation Factor III, Tissue Factor
FF	Phenylalanine-Phenylalanine
FFP	Fresh frozen plasma
FV	Coagulation Factor V
FVIII	Coagulation Factor VIII
FIX	Coagulation Factor IX
GalNAc	N-acetyl-D-galactosamine
GFP	Green fluorescence protein
GRP78	Glucose-regulated protein
HC	Heavy chain
HCC	Hepatocellular carcinoma
HCl	Hydrochloric acid

HEK	Human embryo kidney
HEPES	4-(2-hydroxyethyl)-1-piperazineethanesulfonic acid
HGTI	Harvard gene therapy Initiative
HMWK	High-molecular-weight-kininogen
HSP70	70kDa heat shock protein
HRP	Horseradish peroxidase
Huh7	Human hepatoma cell line
ITR	Inverted terminal repeat
Kb	Kilo bases
kDa	Kilo Dalton
KK	Lysine-Lysine
KMT2B	Lysine-specific methyltransferase 2B
LB	Luria-Bartani
LC	Light chain
LDL	Low-density lipoprotein
LMAN1	Mannose-binding protein lectin 1
LN	Liquid nitrogen
LRP	Low-density lipoprotein (LDL) receptor-related protein
LTR	Long terminal repeat
MALDI-TOF	Matrix assisted laser desorption /Ionisation Time of flight
MS	Mass spectrometry
MAR	Matrix-associated region
MCFD2	Multiple coagulation factor deficiency protein 2
MMWR	Morbidity and Mortality Weekly report
MOI	Multiplicity of Infection
M/Z	Mass-to-charge ratio
Nabs	Neutralizing antibodies
OD	Optical density
OPD	O-phenylenediamine
OPLS	O-phospho-L-serine
pA	Polyadenylation signal
PBS	Phosphate buffered saline
PEG	Polyethylene glycol
PEI	Polyethyleneimine
PES	Polyethersulfone
PFA	Paraformaldehyde
PGK	Phosphoglycerate kinase
PNGase F	Peptide -N-Glycosidase F
PPP	Platelet poor plasma
PRP	Platelet rich plasma
PTMs	Post translational modifications
PVDF	Polyvinylidene-difluoride
RPM	Revolutions per minute
RRE	Rev-response element
RSV	Rous sarcoma virus
RT	Reverse Transcriptase

SA	Sinapinic acid
SIN	Self inactivate
SDS-PAGE	SDS–Poly Acrylamide Gel
TBE	Tris-Borate-EDTA
TBS-T	Tris-Buffered Saline, 0.05% Tween 20
TE	Trypsin-EDTA
TERT	Telomerase reverse transcriptase
TNFSF10	Tumor necrosis factor superfamily member 10
TOF	Time-of-flight
tRNA	Transfer RNA
QC	Quality control
Q-PCR	Quantitative real-time PCR
VSVg	Vesicular stomatitis virus glycoprotein
VWF	von Willebrand factor
V/V	Volume per volume
WPRE	Woodchuck Hepatitis Virus Posttranscriptional Regulatory Element
WT	Wild type
W/V	Weight perVolume
W/W	Weight per Weight
Ψ	Packaging signal

Chapter 1

General Introduction

1.1. Bleeding Disorders

Bleeding disorders are characterised by spontaneous bleeding or excessive bleeding after traumatic injuries, often leading to life or limb threatening complications due to local pressure effects and/or exsanguination. Defects in blood clotting factors are the cause of disease due to the lack of clotting ability of blood (Nathwani *et al.*, 2005). There are two major blood clotting diseases, haemophilia, and von Willebrand disease (vWD) in order of disease severity. The World Federation of Haemophilia (WFH) estimates that more than one in 1000 men and women has a bleeding disorder equating to 6,900,000 worldwide (Skinner *et al.*, 2012).

The term haemophilia is commonly applied to two inherited bleeding disorders, which currently affect 17,131 men in the US and 6811 in the UK (WHF, Annual global survey 2014). The two conditions are a deficiency of factor VIII (FVIII) known as haemophilia A and deficiency of factor IX (FIX) known as haemophilia B, both of which show X-linked inheritance. The prevalence of haemophilia B is about a fifth that of haemophilia A. Worldwide, there are estimated to be more than half a million people with haemophilia, the prevalence varying from 105 to 160 per million of the male population (Bolton-Maggs and Pasi, 2003).

Von Willebrand disease (vWD) is the commonest inherited bleeding disorder, due to defects in the quantity and/or quality of the von Willebrand factor (vWF). vWD is present in as many as 1% of the general population. In the UK, vWD is the most commonly diagnosed bleeding disorder, with currently 10,254 patients registered (WHF, Annual global survey 2014). Most of these patients have a mild bleeding tendency, but a few have the severe type 3 variant. vWF is a large and complex plasma glycoprotein that is essential for normal haemostasis. This disorder is mild, but it is an important cause of menorrhagia in affected kindreds. vWD affects both men and women equally, though women may experience more problems linked to periods, pregnancy and childbirth. In

severe cases, internal bleeding to muscles and joints can occur in a similar way to haemophilia (Laffan *et al.*, 2014).

The mechanism by which coagulation is initiated by injury to the vascular wall is through primary haemostasis, the process in which platelets adhere to sub-endothelium (Triplett, 2000). vWF is essential for platelet adhesion. Following platelet adhesion, thrombin generation is initiated by exposure of tissue factor which binds factor VII forming a binary activated complex that in turn activates factor X and factor IX. The coagulation factors (FVIII, FIX then form a complex on platelet surfaces, which massively accelerates thrombin generation. Hence it is evident that vWF, FVIII and FIX are central to this coagulation process and consequently any deficiency of these factors leads to failure of haemostasis, which manifests as a bleeding disorder.

1.1.1. Haemophilia

Haemophilia A is the most common severe bleeding disorder and is caused by a deficiency or abnormality in coagulation FVIII. 1 in 5000 males is affected by hereditary Haemophilia A (Mannucci and Tuddenham, 2001). The *F8* gene is located on the X chromosome; therefore males are predominantly affected while females are only carriers of the genetic defect.

The genes for *F9* and *F8* were cloned in 1982 and 1984 respectively. This cloning has resulted in important advances in the molecular characterisation of the defects that cause the haemophilias and has enabled synthesis of recombinant clotting factor concentrates for therapeutic use. In detail, the *F8* gene is one of the largest human genes measuring 186 kb in length, which maps to band Xq28 at the tip of the long arm of the X chromosome (Gitschier *et al.*, 1984; Toole *et al.*, 1984; Vehar *et al.*, 1984; Wood *et al.*, 1984).

The *F8* gene has two additional genes, FVIII-associated gene A (*F8A*) and FVIII-associated gene B (*F8B*) within intron 22 and two further copies of *F8A* exist outside

(400kb telomeric) the *F8* gene (Levinson *et al.*, 1992a; Levinson *et al.*, 1992b). The functions of the *F8A* and *F8B* genes are unknown, but they are responsible for common inversion of FVIII, which is the most common genetic defect in haemophilia A, affecting about 45% of individuals with severe disease.

The large inversion and translocation of exons 1~22 (together with introns) away from exons 23~26, is due to homologous recombination between the *F8A* gene in intron 22 and one of the *F8A* copies of upstream of FVIII gene (Fig.1.1) (Lakich *et al.*, 1993). Mutations, other than the intron 22 inversions, are predominantly point mutations and cause mild haemophilia A (HAMSTeR/HADB, <http://www.factorviii-db.org/>), which are about 85% for mis-sense (a point mutation that codes for change amino acid) mutation, and 15% for non-sense (a point mutation resulting in stop codon or truncation) mutation. A similar inversion involving intron 1 of the *F8* gene has also been described in about 1~6% of patients with severe haemophilia A in which the two repeated sequences (*intron1h1/intron1h2*) of intron 1 of *F8* gene is responsible for recombination between sequence internal and external to the factor VIII gene (Graw *et al.*, 2005).

In haemophilia A, patients with mutations that severely truncate or prevent the production of FVIII (Intron 22 inversion, large deletions, non-sense mutations) have a much higher frequency (about 40%) of Inhibitors, which are antibodies that neutralise the activity of a clotting factor. Inhibitor antibodies to FVIII or FIX may arise as alloantibodies in patients with haemophilia A or B who have been transfused with exogenous FVIII or FIX, respectively. The development of functionally inhibiting alloantibodies in haemophilia represents a serious clinical problem.

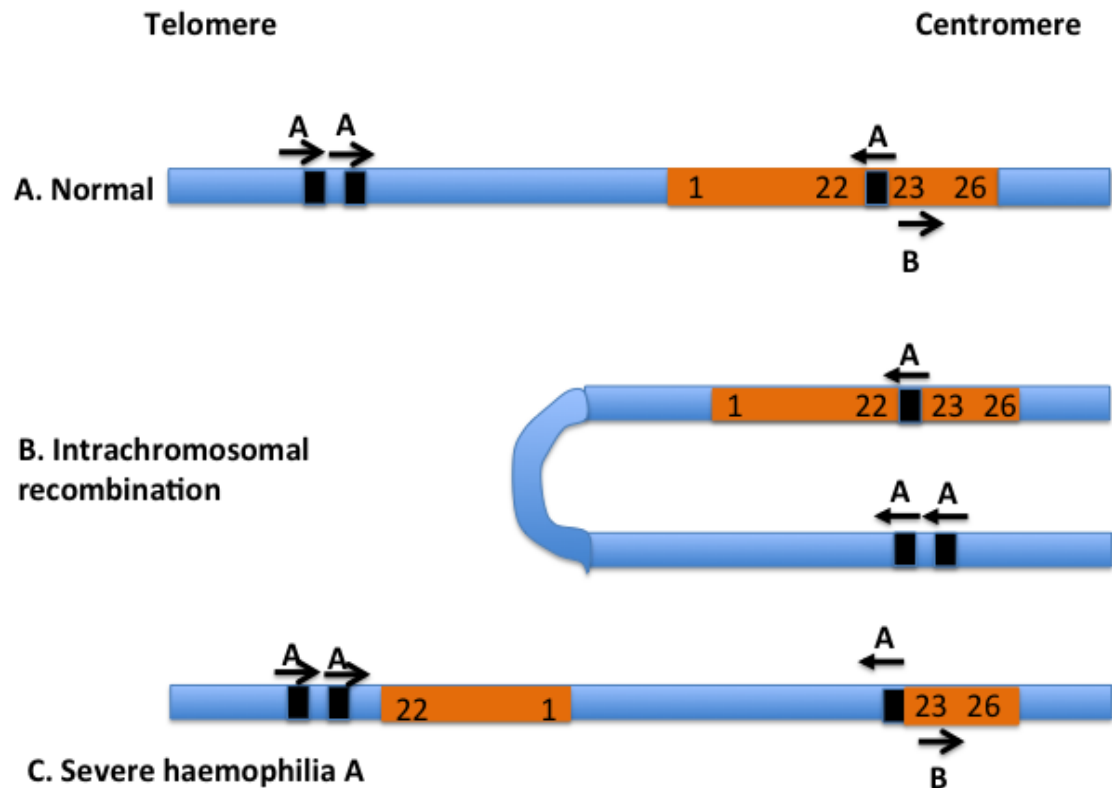


Figure 1.1. Schematic representation of common inversion of the *F8* gene

The location of *F8* gene is illustrated in the region of Xq28 that oriented with the telomere at the left to the right of centromere. A) The arrow indicates the direction of two nested genes *F8A* and *F8B* with two further telomeric copies of sequences homologous to *F8A*. Three copies of the *A* genes are indicated orientation with black arrow. B) Description of Intra-chromosomal recombination by crossing-over between the homologous *F8A* sequences. C) *F8A* recombination leading to a relocation and inversion of exons 1~22 away from exons 23~26. The diagram was adopted from Lakich et al (Lakich *et al.*, 1993).

1.1.1.1. Pathology

The disease phenotype is entirely attributed to the lack of efficiency of functional FVIII protein which normally circulates in minute amounts in the plasma (200ng/mL) (High *et al.*, 2014). FVIII has a half-life of about 12 hours in adults (shorter in children), circulating in plasma in a non-covalent complex with vWF. The vWF protects FVIII from premature proteolytic degradation and concentrates it at sites of vascular injury (Bolton-Maggs and Pasi, 2003).

Patients with mild, moderate, and severe forms of the disease have a deficiency in a FVIII activity in plasma with levels of 5~40%, 1~5%, and <1%, respectively (White *et al.*, 2001). Severe haemophilia is characterised by sporadic bleeding into the muscles, joints, or internal organs, excessive bleeding after an injury or surgery and spontaneous internal haemorrhages (Santagostino, 2014).

In the early 1960s, the only known effective treatment of haemophilia was with an infusion of fresh frozen plasma (FFP). In 1964, Dr Judith Graham Pool developed a simple method to separate a cryoprecipitate from plasma containing most of the FVIII in a more convenient concentrated form. Subsequently, lyophilised plasma-derived clotting factor concentrates were developed and widely used since the 1970s (Skinner, 2012). In the early 1990s, bioengineering technology allowed production of recombinant proteins to improve biosafety. However, current generations of treatment products have a robust safety profile (both plasma-derived and recombinant), but still more than 40% of countries report treatment product usage including FFP and cryoprecipitate, showing that they are still used for the treatment of haemophilia (Skinner, 2012). The risk of viral transmission from FFP and cryoprecipitate remains a significant concern as they are often not virus inactivated.

Recent studies estimated that mean annual cost of haemophilia A treatment per patient is \$157,180 (USA) (Duncan *et al.*, 2014). A major complication of factor replacement therapy is the development of antibody inhibitors against FVIII. Inhibitors arise in a high

proportion of patients and result in the requirement of significantly higher doses of FVIII to prevent bleeding or complete refractoriness to replacement therapy such that alternative and less satisfactory measures have to be taken to control bleeding.

1.1.2. Haemostasis

Bleeding occurs in haemophilia owing to the failure of secondary haemostasis. Haemostasis is a highly localised process in response to blood vessel injury in which cessation of bleeding is achieved by a coordinated clotting process involving both platelets and coagulation factors, while maintaining the dynamic equilibrium of an adequate blood flow but locally stemming the outflow of blood with a platelet-fibrin plug at the site of injury. The three essential roles of haemostasis for the survival of any organism that has a circulatory system are first, blockade of damaged blood vessels, second, keep the blood in a fluid state, and finally remove blood clots after restitution of vascular integrity (Versteeg *et al.*, 2013).

1.1.2.1. Classical coagulation pathway

In the 1960s, Davie and Ratnoff devised a model for blood coagulation process, which described the clotting process as a waterfall. They named this model aptly as coagulation waterfall. Independently and simultaneously Macfarlane proposed a cascade hypothesis, which was essentially identical to the Davie's waterfall, but emphasised the amplification aspect of the biochemical process invoked to explain blood clotting. The original classical waterfall or cascade of reactions involved sequential activation of various clotting factors along the intrinsic pathway. Later stimulation by extrinsic tissue factor was added and according to this model stimulation of either of these two pathways can result in the production of a large amount of thrombin and subsequent formation of a fibrin clot (Davie *et al.*, 1964; Macfarlane, 1964).

The Intrinsic pathway is triggered by auto-activated FXII cleaving pre-kallikrein into

kallikrein, which leads to a subsequent activation pathway of FXI, FIX, FX, and FII, which components are all present in the blood-along with the two cofactors FVIII and FV necessary for full FIX and FX activity respectively. The intrinsic pathway is activated when blood comes into contact with hydrophilic negatively charged surfaces *in-vitro*. In contrast, the extrinsic pathway is activated by exposure of plasma factor VII (FVII) to tissue factor (TF, FIII, Thromboplastin, CD142) on the surfaces of cells in the extravascular space, which directly induces sequential activation of factor X (FX) and prothrombin (FII) (Versteeg *et al.*, 2013).

The intrinsic and extrinsic pathway divides the initiation of coagulation into two distinct parts. The extrinsic pathway is thought to be responsible for the initial generation of activated FX (FXa), whereas the intrinsic pathway leads to amplification of FXa generation. The intrinsic and extrinsic pathways converge onto FXa, which plays a central role in the coagulation cascade (Mackman, 2009; Abdalla and Adam, 2013) (Fig.1.2).

Although this cascade concept supports laboratory evaluation of coagulation disorders and demonstrates the interactions between coagulation factors, it does not adequately explain the mechanisms leading to haemostasis *in-vivo* (Hoffman, 2003). For instance, the cascade model does not explain how the extrinsic pathway appears unable to produce sufficient amounts of FX to at least partially compensate for a deficiency of FVIII or FIX. In other words, why does activation of FX by the TF/FVIIa complex fail to substitute for the FXa that would normally be generated by FIXa/FVIIIa (Hoffman, 2003).

Those questions have recently been explained by a cell-based concept in which both FVIII and FIX are central to the process of blood coagulation and for the adequate generation of thrombin.

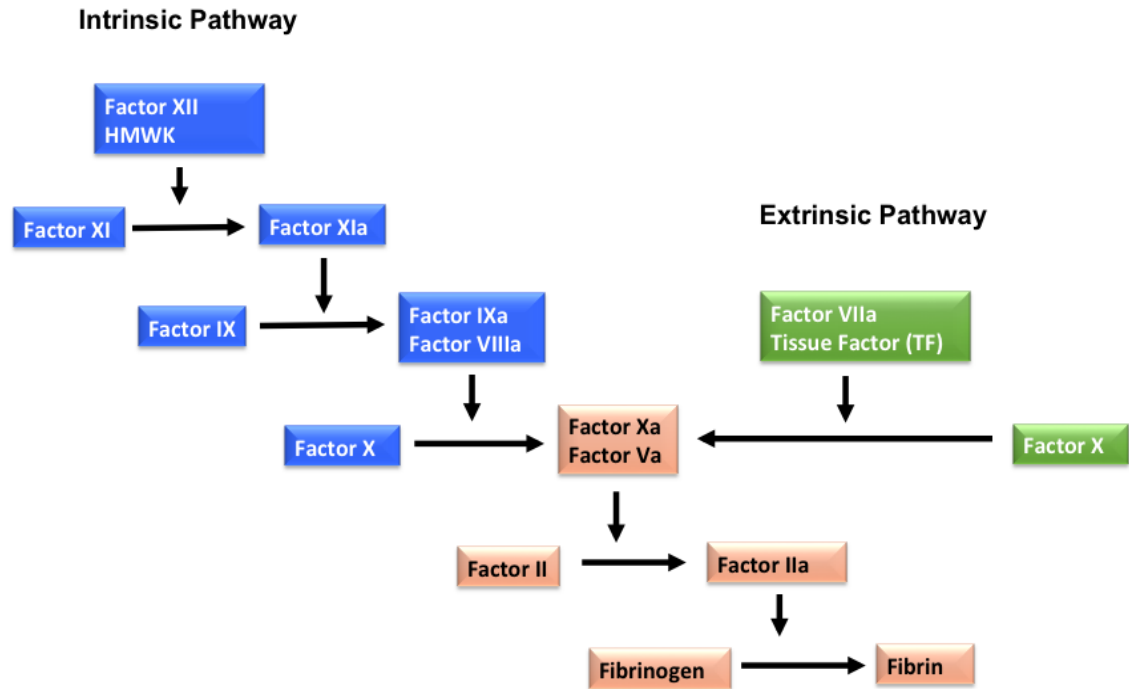


Figure 1.2. The classic cascade model of intrinsic and extrinsic pathways

The extrinsic pathway starts when an exogenous agent, tissue factor (TF) binds to and activates plasma FVII to form an active complex (TF:FVIIa), which directly induces sequential activation of FX and prothrombin (green). The TF:FVIIa complex is the key initiator of the coagulation protease cascade and activates both FIX to FIXa and FX to FXa. Components of the intrinsic pathway (FXII, FXI, FIX, and FVIII) are all present in the blood (blue). The tenase complex (FVIIIa:FIXa) plays a key role in amplifying the clotting cascade by activating FX to FXa. The final step of the cascade in which prothrombinase complex (FVa:FXa) converts prothrombin to thrombin is referred to as the common pathway. Thrombin, which is the terminal protease of the clotting cascade cleaves fibrinogen into soluble fibrin monomers that polymerise. HMWK stands for High-Molecular-Weight-Kininogen

1.1.2.2. Cell-based coagulation model

The cell-based coagulation model is based on the observation that stabilisation of fibrin, is defective if inadequate amounts of thrombin are localised to the evolving clot; the model also emphasises that coagulation occurs in a series of three overlapping steps that take place on different cell surfaces, rather than as a cascade that produces plentiful activated factors and inevitably leads to clot formation (Hoffman, 2003; Smith *et al.*, 2009).

In mammalian blood coagulation, six proteases (FVII, FIX, FX, FXII, protein C, and prothrombin) act with five cofactors (TF, thrombomodulin, Protein S, FV and FVIII) to control the generation of fibrin (Fig.1.3). The process is initiated and regulated by three stages (Initiation, Amplification and Propagation) (Hoffman and Monroe, 2001; Hoffman, 2003).

In the initiation stage, classically referred to as the extrinsic pathway of coagulation. TF binds to activated FVII (FVIIa) and forms TF/FVIIa complex, which activates small amounts of FIX and FX. FXa along with its cofactor, FVa, forms the FXa/FVa prothrombinase complex on the surface of cells that express TF. The FV can be activated by FXa or non-coagulating proteases, resulting in FVa, which is necessary for the prothrombinase complex. This complex transforms small amounts of prothrombin (FII) to thrombin (FIIa).

In the second stage, the amplification phase, the small amounts of thrombin produced by cells expressing TF interacts with platelets and the FVIII/vWF complex. This results in the activation of cofactors FV, FVIII and activation of zymogen FIX to FIXa, thus begins the haemostatic process culminating in the formation of stable fibrin (Versteeg *et al.*, 2013).

The propagation stage is characterised by the migration of large numbers of platelets to the site of injury and the production of the tenase complex and prothrombinase on the

surface of activated platelets. First, FIXa activated during the initiation phase binds FVIIIa on the platelet surface forming the FIXa/FVIIIa tenase complex. Once the intrinsic tenase complex forms on the activated platelet surface, it rapidly begins to generate FXa on the platelet. FXa is also generated during the initiation phase on the TF-bearing cell surface. Since FXa is rapidly inhibited as it moves from the TF-bearing cell surface the majority of FXa must, therefore, be generated directly on the platelet surface through cleavage by the intrinsic tenase complex. Following production, FXa generated on platelets rapidly binds to FVa, which cleaves prothrombin (FII) to thrombin (FIIa) and clot forms.

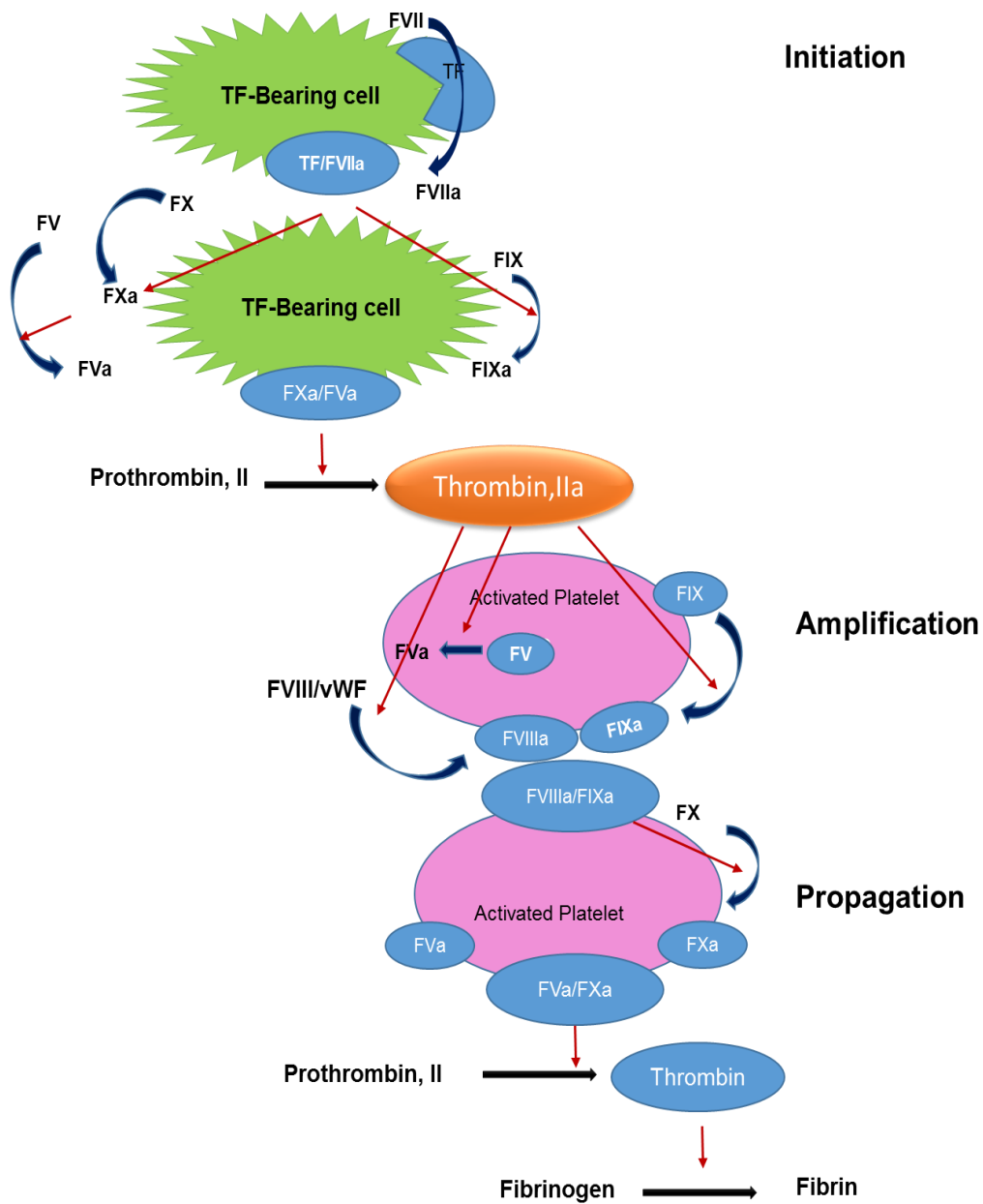


Figure 1.3. Cell-based coagulation model of haemostasis

The cell-based model describes the contribution of various cell surfaces leading to fibrin formation. In this model, thrombin generation occurs in three overlapping stages. The three phases of coagulation occur on different cell surfaces: Initiation on the tissue factor-bearing cell; Amplification on the platelet as it becomes activated; and Propagation on the activated platelet surface. TF: Tissue Factor (Factor III), The pathways were adapted from Hoffman *et al.*, 2001.

1.2. FVIII Protein Structure

Human FVIII is a large plasma glycoprotein synthesised as a single-chain polypeptide with a predicted molecular mass of 264kDa, corresponding to the mature 2332 amino acid sequence, determined from the translation of the cloned gene. After post-translational modification with *N*-linked carbohydrate chains, the molecular mass of FVIII reaches 330 kDa (Vehar *et al.*, 1984).

The FVIII protein consists of three A domains (homologous to ceruloplasmin) three a domains (acidic amino acid-rich), a B-domain (heavily glycosylated), and two C domains (homologous to discoidin), assembled into the primary domain structure: A1-a1-A2-a2-B-a3-A3-C1-C2 shown in figure 1.4 (Pemberton *et al.*, 1997; Newell and Fay, 2007).

The three A-domains are flanked by short spacers (a1, a2, and a3) that contain clusters of Aspartic acid and Glutamic acid residues as acidic regions. Those short segments of negatively charged residues occur at the C-terminal regions of the A1 and A2 domains and the N-terminal portion of the A3 domain. These 30~40 negatively charged acidic regions are segmented as a1 (337–372), a2 (711–740) and a3 (1649–1689), which are thought to function, in part, as binding sites for thrombin and other ligands (Lenting *et al.*, 1998; Fay, 2004).

The B-domain is unique and encoded by one of the largest known single exons (Exon14). It is composed of 908 amino acids that contain 19 of the potential 25 Asparagine (*N*)-linked glycosylation attachment sites on the entire FVIII molecule. The B-domain is the most heavily glycosylated region in FVIII, exhibiting no significant homology with any other known protein such as FV (Pipe, 2009).

The B-domain is proteolytically released upon activation by thrombin or FXa and is not required for pro-coagulant activity *in-vitro* or *in-vivo* (Dorner *et al.*, 1987; Eaton *et al.*, 1986a; Toole *et al.*, 1986). One function of the B-domain is to modulate the rate of thrombin activation. Factor VIII (FVIII) with a truncated B-domain is more rapidly

activated by thrombin than full-length FVIII (FL-FVIII), indicating that lower concentrations of thrombin are necessary to activate truncated B-domain FVIII, when compared to FL-FVIII. If this difference is enough to alter the functional properties of B-domain in FVIII, it suggests that B-domain deleted FVIII, may be more susceptible to proteolytic attack. Further, it is tempting to speculate that the B-domain may function to protect the functional domains of FVIII from proteolysis that may occur as the result of low amounts of circulating active protease, perhaps thrombin (Eaton *et al.*, 1986b).

More recently the B-domain has been shown to play a major role in the intracellular processing and trafficking of FVIII. Moreover, there is emerging evidence that portions of the B-domain may have functional influences throughout the life cycle of FVIII (Pipe, 2009).

The C domains are homologous to phospholipid binding proteins which suggesting a role in phospholipid interaction (Veeraraghavan *et al.*, 1998; Stoylova *et al.*, 1999). Mutations in the C1 domain are commonly identified in haemophilia A patients, yet the role of the latter domain in FVIII function or stability is not determined.

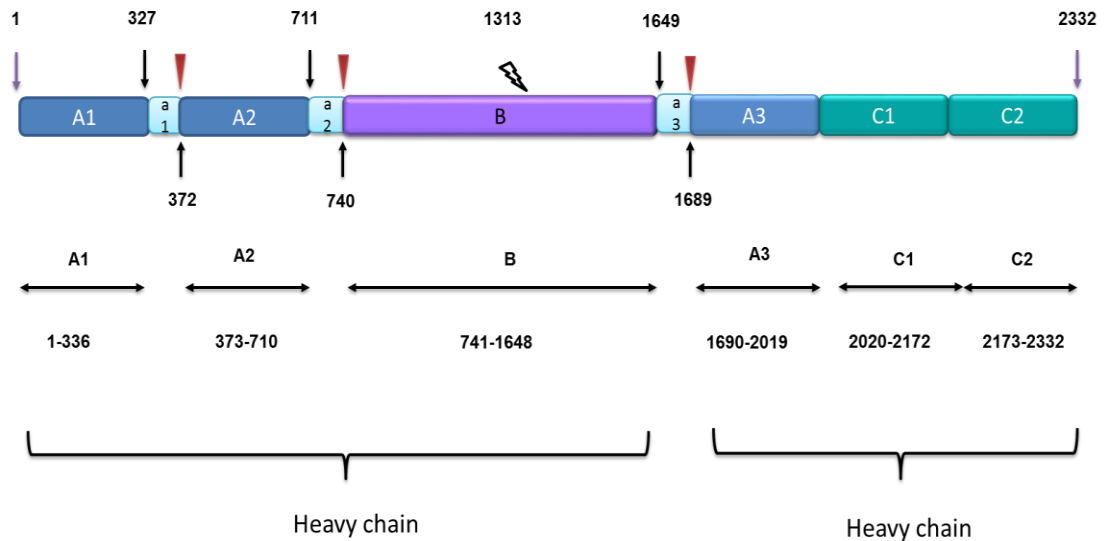


Figure 1.4. Schematic diagram of human FVIII domains

Light blue bars indicate small acidic peptides, *a1*, *a2*, and *a3*, which are located in between A and B-domain. The acidic peptides *a1*, *a2*, *a3*, and the large B-domain contains function-related cleavage sites at one or both of their N- or C-termini, and thus these sites would be predicted to be accessible to serine proteases such as thrombin and APC. Thrombin activation sites are indicated with a red arrow at 372, 740, 1689, and some of the cleavage sites within the B-domain (indicated with an open arrow, 1313), resulting in a mixture of heavy chains of variable size. Preparations of plasma-derived human FVIII contain a heterogeneous mixture of dimers because of the range of different sizes for heavy chain resulting from additional cleavage sites within the B-domain (Pemberton *et al.*, 1997; Graw *et al.*, 2005).

1.3. FVIII Secretion

1.3.1. FVIII Quality control

Human FVIII is synthesised in vascular-endothelial cells, reticulo-endothelial cells, and hepatic sinusoidal endothelial cells (Stel *et al.*, 1983; Nichols *et al.*, 1998; Nichols and Ginsburg, 1999). Moreover, FVIII mRNA was detected in a variety of extra-hepatic tissues, including kidney (glomerular microvascular endothelial cells), umbilical vein endothelial cells, spleen and lymph node so that may also produce FVIII (Wion *et al.*, 1985; Levinson *et al.*, 1992a; Levinson *et al.*, 1992b; Fahs *et al.*, 2014; Turner *et al.*, 2015). Zanolini and colleagues reported that monocytes, macrophages and megakaryocytes expressed FVIII (Zanolini *et al.*, 2015).

The initial stage of FVIII secretion begin with the translocation of mature FVIII polypeptide into the lumen of the endoplasmic reticulum (ER), the 19 amino acid signal peptide is removed by signal peptidase then *N*-linked glycosylation occurs (Lenting *et al.*, 1998).

Within the ER, the early FVIII secretory pathway appears to interact with a number of chaperone proteins, including Immunoglobulin binding protein (BiP), calreticulin, and calnexin (Dorner *et al.*, 1987; Pipe, 1998). Firstly, the BiP has been known as the glucose-regulated protein (GRP78), which is a member of the 70kDa heat shock protein (HSP70) family that exhibits a peptide-dependent ATPase activity and for which expression is induced by the presence of unfolded protein or unassembled protein subunits within the ER. The considerably less efficient secretion of FVIII, relative to that of FV, may be explained as follows: BiP binds to FVIII A1 domain hydrophobic 110 amino acid region with BiP exhibiting a peptide-dependent adenylyl pyrophosphatase (ATPase) activity. Therefore FVIII release from BiP and transport out of the ER requires high levels of intracellular adenosine triphosphate (ATP). In contrast, FV does not associate with BiP and does not require high levels of ATP for secretion (Nichols & Ginsburg 1999; Becker *et al.*, 2004). These studies show that the less efficient secretion of FVIII is due

to the interaction with these chaperone proteins, causing a significant proportion of FVIII molecules to be retained within the ER for quality control, thereby limiting the transport of FVIII to the Golgi apparatus.

Secondly, the ER-Golgi proteins (calnexin and calreticulin) are responsible for this process and preferentially interact with glycoproteins containing mono-glucosylated *N*-linked oligosaccharides. It is also suggested that while moving through the degradative and/or secretory pathways (Pipe, 1998), the quality of FVIII is controlled by a glucosyl-transferase that acts specifically on unfolded glycoproteins. The re-glucosylated protein is then once again retained on calnexin or calreticulin; but folded glycoproteins, which cannot be reglucosylated, are free to leave the ER and continue to traffic through the secretory pathway (Ashkenas and Byers, 1997). Therefore only fully folded FVIII escapes the chaperone-mediated retention mechanism and is finally transported to the Golgi apparatus and released out of the cell (Fig.1.5) (Nichols and Ginsburg, 1999). The necessity for a conformational LMAN1-binding carbohydrate-based structural motif provides an additional quality control mechanism for ER exit of properly folded proteins (Baines and Zhang, 2007).

1.3.2. Receptor-mediated FVIII transport

The FVIII transport mechanisms responsible for exit from the ER to the Golgi apparatus have been elevated as key issues for FVIII secretion and quality control. The now well established secretory pathway responsible for FVIII is Lectin Mannose-Binding Protein 1 (LMAN1, also called ERGIC) and Multiple Coagulation Factor Deficiency Protein 2 (MCFD2) complex (Nichols *et al.*, 1999; Neerman-Arbez *et al.*, 1999; Zhang *et al.*, 2005; Khoriaty *et al.*, 2012). The LMAN1-MCFD2 complex forms a specific cargo receptor for the ER-to-Golgi transport of selected proteins (Zhang *et al.*, 2003).

LMAN 1 requires Phenylalanine-Phenylalanine (FF) motifs for efficient export from ER in the context of larger export signals at the most C-terminal end of its short cytoplasmic tail. The efficient export of LMAN1 is dependent upon its oligomerisation, which is based

on amino acid residues located in its transmembrane and luminal domains. In contrast, the lack of oligomerisation leads to misfolding and protein retention by chaperones (Nufer *et al.*, 2003).

The cytoplasmic tail of LMAN1 contains an FF motif that interacts with the COPII subunit (illustrated in Fig.1.6). The majority of LMAN1 is localised to the ERGIC at steady state, it cycles the back to the ER via a Lysine-Lysine (KK) ER-retrieval signal that interacts with COPI. The luminal part of LMAN1 contains 4- α helices that are predicted to form a coiled-coil domain and a carbohydrate recognition domain (CRD) that binds mannose. The crystal structure of the CRD is similar to leguminous lectins and the calnexin (Velloso, 2002). Structural determinants in both the luminal and trans-membrane domains lead to oligomerisation of LMAN1, which exists exclusively in two homo-hexameric forms within the cell. The first form is composed of six disulfide-linked monomers and the second form is composed of three disulfide-linked dimers that might associate non-covalently through coiled-coil domains (Zhang *et al.*, 2005).

The cargo proteins of the LMAN1–MCFD2 pathway are required for efficient ER-to-Golgi transport of FV, FVIII and two lysosomal glycoproteins cathepsin C(catC), cathepsin Z(catZ) (Fig.1.6). Given the evolutionary conservation and the ubiquitous expression pattern of LMAN1 and MCFD2, additional cargo proteins also exist. For example, Nicastrin, a component of the γ -secretase complex, and a mutant immunoglobulin heavy chain have also been reported to interact with LMAN1 (Baines and Zhang, 2007). Interactions between catC or catZ and LMAN1 were also observed. Upon treatment with a chemical crosslinker, an estimated 5~20% of FVIII is detected in a tertiary complex with LMAN1 and MCFD2, which provides direct evidence for the receptor activity of the LMAN1-MCFD2 complex (Baines and Zhang, 2007). The LMAN1-MCFD2 complex and FVIII interaction are dependent on the intracellular Ca^{++} concentration. The MCFD2 possible to be dispensable for the interaction between LMAN1 and catC or catZ, which indicates that MCFD2 is specifically required for recruitment of FV and FVIII to sites of

transport vesicle budding within the lumen of the ER (Zhang *et al.*, 2005; Nyfeler *et al.*, 2006).

FV and FVIII are homologous proteins that share a common A1-A2-B-A3-C1-C2 domain structure. Although the B-domains of FV and FVIII share little sequence identity, both are heavily glycosylated. Given the lectin activity of LMAN1, an interaction between LMAN1 and the B-domains of FV and FVIII seems a likely possibility. Consistent with this, B-DD FVIII is not efficiently cross-linked to the LMAN1-MCFD2 complex. However, substantial cross-linking is still detected when glycosylation of FVIII is blocked (Zhang *et al.*, 2005). This observation, combined with the MCFD2 in the secretion of FV and FVIII, indicates that protein–protein interactions are also important for LMAN1-MCFD2 cargo-receptor function (Baines and Zhang, 2007).

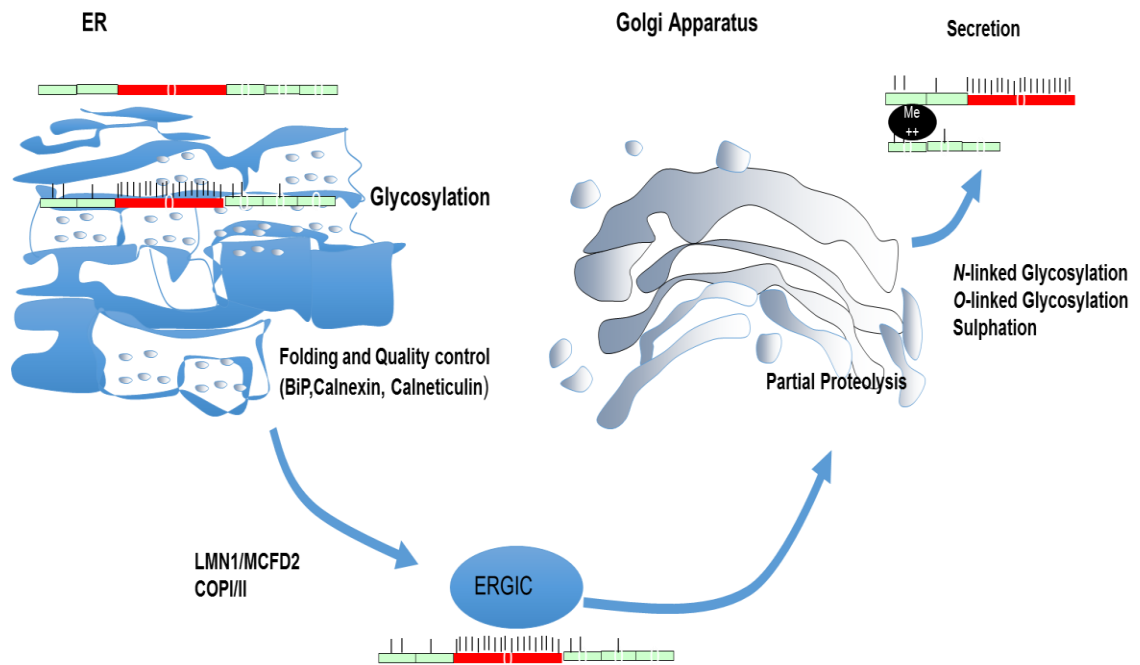


Figure 1.5. Intracellular processing of FVIII synthesis and secretion in ER and Golgi

The FVIII primary translation product is translocated into the lumen of the ER where N-linked glycosylation occurs. The majority of FVIII binds to ER chaperone proteins, which perform quality control. A proportion of the molecules attains proper conformation for transport into the Golgi where additional complex carbohydrate modification on N-linked glycosylation sites occurs. Also, O-linked glycosylation and sulphation of several tyrosine residues in the acidic regions of FVIII take place. In the Golgi, the protein is cleaved to its mature heavy and light chain (Kaufman *et al.*, 1988; Pipe, 2009).

1.3.3. LMAN1 and COPII interaction

Alternatively, MCFD2 could be required for the separation of FV and FVIII from LMAN1 in the ERGIC, which is the site of dissociation of secretory proteins for anterograde transport via packaging into COPII coated transport vesicles (Moussalli *et al.*, 1999; Zhang *et al.*, 2003). The calcium-dependent LMAN1-MCFD2 complex is an essential step in ER-to-Golgi transport for a specific subset of glycoproteins including FV and FVIII (Graw *et al.*, 2005; Zhang *et al.*, 2005). The coat proteins (COP1 and COP II) are important for FVIII transport between ER to Golgi due to the fact that COPII acts earlier in the pathway, apparently driving the initial budding of vesicles from the ER, COPII transports cargo from the ER to the Golgi complex (Becker *et al.*, 2004; Baines & Zhang 2007). Then, COPI becomes associated with new budding vesicles, the COPI complex binds to ERGIC membranes and initiates the budding of COPI-coated vesicles. COPI clearly plays a critical role in Golgi-to-ER retrograde transport and also possibly anterograde (Nichols and Ginsburg, 1999; Khoriaty *et al.*, 2012)). COPI and COPII coats bind to the ERGIC and drive the lectin-glycoprotein complex into budding vesicles (Itin *et al.*, 1996; Lavoie *et al.*, 1999).

Recruiting cargo proteins to budding vesicles can be catagorised as direct binding to components of the COPII coat and specific adaptors (receptors) to link them to COPII vesicles. The direct binding is limited to proteins that span the ER membrane due to the cytosolic COPII-coat proteins. However, specific adaptors that bind COPII serve as cargo receptors for the second class of cargo, which includes both soluble and transmembrane proteins. Several classes of ER export motifs include the interactions between COPII and transmembrane cargo, which can be recognised by the COPII coat proteins (Baines and Zhang, 2007).

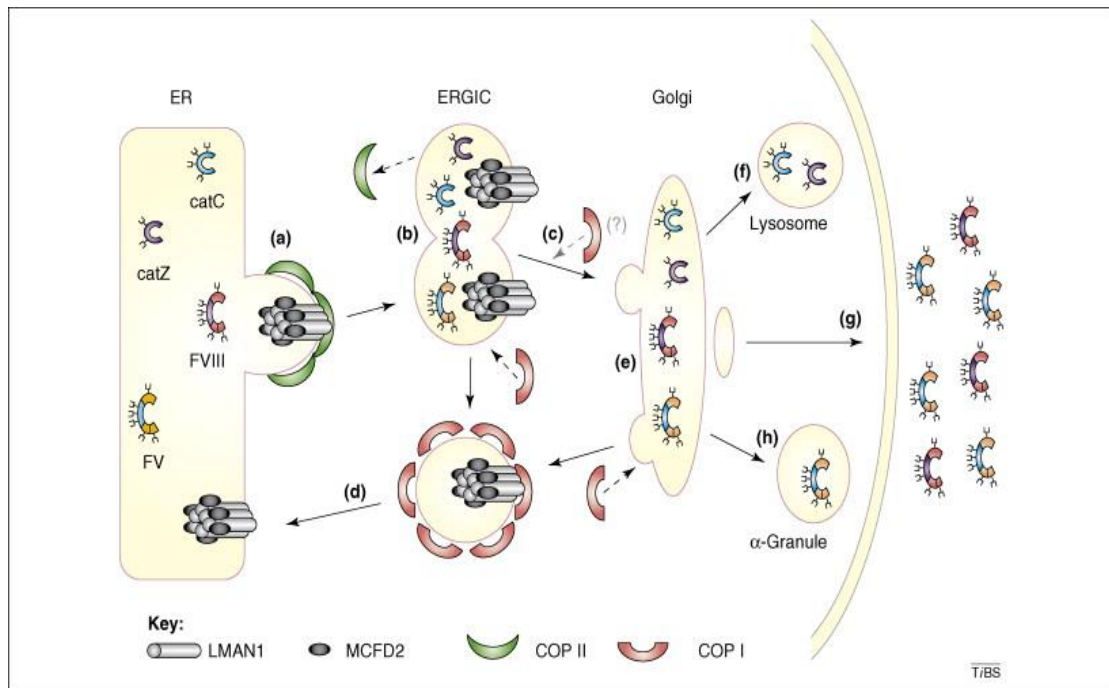


Figure 1.6. Cargo transport by the LMAN1-MCFD2 complex

A) FV, FVIII, cathepsin C (CatC), and cathepsin Z (CatZ) bind the LMAN1-MCFD2 complex and are packaged into COPII vesicles. B) COPII vesicles bud from the ER membrane and fuse together, which leads to form the ER-Golgi intermediate compartment (ERGIC). C) Anterograde transport of cargo protein to the Golgi apparatus occurs along microtubules. D) The LMAN1-MCFD2 complex is recycled back to the ER through COPI vesicles. E) Posttranslational modification of the cargo proteins occurs in the Golgi apparatus. F) CatC and CatZ are transported to the lysosomes. G) FV and FVIII are secreted outside of the cells. H) In murine megakaryocytes, FV is transported and stored in α -granules. Reproduced from Baines and Zhang 2007 (Baines and Zhang, 2007; Khoriaty *et al.*, 2012).

1.3.4. FVIII Processing in Golgi

Once in the Golgi compartment, FVIII is among the many proteins to undergo intracellular proteolysis. The tertiary structure of FVIII confers on the B-domain region a particular susceptibility to proteolysis. The heavy and light chain portions of FVIII form a globular domain structure, about 14nm in diameter, while the connecting B-domain region forms an extended rod-like structure (Kaufman *et al.*, 1988; Fowler *et al.*, 1990). Moreover, the carboxy-terminal region of the B-domain comprises a motif (R-X-X-R) similar to that recognised by intracellular proteases of the subtilisin-like family (Barr, 1991; Lenting *et al.*, 1998). Consequently, the FVIII polypeptide is cleaved in the B-domain after residues 1648 to generate the heavy chain of 200kD (A1-a1-A2-a2-B) in a metal ion complex with the light chain of 80kD (a3-A3-C1-C2). Within the Golgi apparatus, FVIII undergoes modification of the *N*-linked oligosaccharides to complex-type structures, *O*-linked glycosylation, and sulphation of specific tyrosine residues Y346, Y718, R719, Y723, Y1664, and Y1680.

FVIII protein is also subjected to further partial proteolysis of the B-domain between residues 741 and 1648 producing a range of heterodimeric molecules that circulate in plasma with varying lengths of B-domain (Fay *et al.*, 1986; Kaufman, 1998). The FVIII heavy and light chains remain non-covalently associated through the A1 and A3 domains in a metal ion-dependent manner. Considering the structural homology of FVIII to the copper-binding protein ceruloplasmin, it is not surprising that copper ions have been found in FVIII as well. Moreover, the copper/FVIII ratio, calculated for both proteins, one single copper atom present per molecule of FVIII (Bihoreau *et al.*, 1994). Most likely, the copper ion binding site is composed of residues His265, Cys310, His315, and Met320 within the A1 domain and His1954, Cys2000, His2005 and Met2010 for the A3 domain. In addition, L649, C692, F697 and M702 in the A2 domain, The copper has three protein ligands, 2 Histidine and 1 Cysteine, at this site, because the leucine, isosteric to

methionine, cannot be considered as a copper ligand (Messerschmidt and Huber, 1990).

Binding of divalent metal ions to this site may allow the A1 domain to adopt an A3 domain binding conformation. Alternatively, divalent metal ions may directly bridge the A1 and A3 domain by interacting with both domains. In the absence of divalent metal ion, the resulting heterodimers were inactive (Wakabayashi *et al.*, 2001).

Other metal ions are ineffective in promoting reassembly of dissociated heavy and light chain, but calcium or manganese ions are efficient in this respect (Nordfang and Ezban, 1988). However, the specific activity of FVIII dimers that were re-associated in the presence of calcium ions is markedly enhanced by the addition of copper ions. Apparently, divalent metal ions serve an auxiliary role to enhance cofactor function of FVIII. These observations imply that multiple sites may be involved in the association between heavy and light chain. Thus, evidence to date indicates that Cu⁺⁺ promotes the inter-chain association and contributes to the specific activity of FVIII, whereas Ca⁺⁺ or Mn⁺⁺ is required to promote the active cofactor conformation (Fay, 2004). Therefore, the metal ions are important for maintaining the heterodimeric structure of secreted FVIII.

1.4. FVIII activation

Immediately after their release into the blood stream, the inactive FVIII molecules interact with large multimeric vWF monomers, to form a tight non-covalent complex. Several groups have reported a vWF-binding domain of FVIII. Direct evidence for the binding of FVIII light chain to vWF was experimentally demonstrated by Foster and colleagues who identified the involvement of amino acid residues 1670-1684 (Lollar *et al.*, 1988; Foster *et al.*, 1989). Light chain C2 residues 2303-2332 were implicated in this binding (Saenko *et al.*, 1994; Lenting *et al.*, 1999). In addition, Saenko and colleagues demonstrated that a3 acidic region and the C2 domain are both directly involved in forming a high-affinity binding site for vWF (Saenko *et al.*, 1994; Graw *et al.*, 2005). The FVIII to vWF binding ratio in plasma is 1:50 and this heterodimeric structure of FVIII stabilised by vWF interferes with the binding of FVIII to negatively charged phospholipid surfaces and inhibited binding of FVIII to FIXa. Thereby the half-life of FVIII circulating in plasma is increased (Weiss *et al.*, 1977; Fay, 2004; Fay *et al.*, 2009). The association with the vWF protein is the most significant identified determinant of FVIII survival, as it provides protection from premature clearance or activation (Lenting *et al.*, 2007). To perform its cofactor binding functions, FVIII pro-cofactor is proteolytically cleaved by α -thrombin at three arginine residues (R372, R740, and R1689) yielding 50kDa, 43kDa, and 73kDa fragments (Fig.1.7). In this process, the variable B-domain fragments and the short a3 peptides are lost. Finally, FVIII forms an active heterotrimer (FVIIIa) (Pemberton *et al.*, 1997). Overall, FVIIIa is a heterotrimer comprised of three non-covalently linked polypeptide chains: the A3-C1-C2 subunit associated with the A1 subunit which is stabilised by divalent metal ion-dependent linkage, whereas the A2 subunit is weakly associated with the dimer through electrostatic interactions (Fay *et al.*, 1991). These weak interactions contribute to the FVIIIa heterotrimer instability, as the dissociation of the A2 domain leads to spontaneous inactivation.

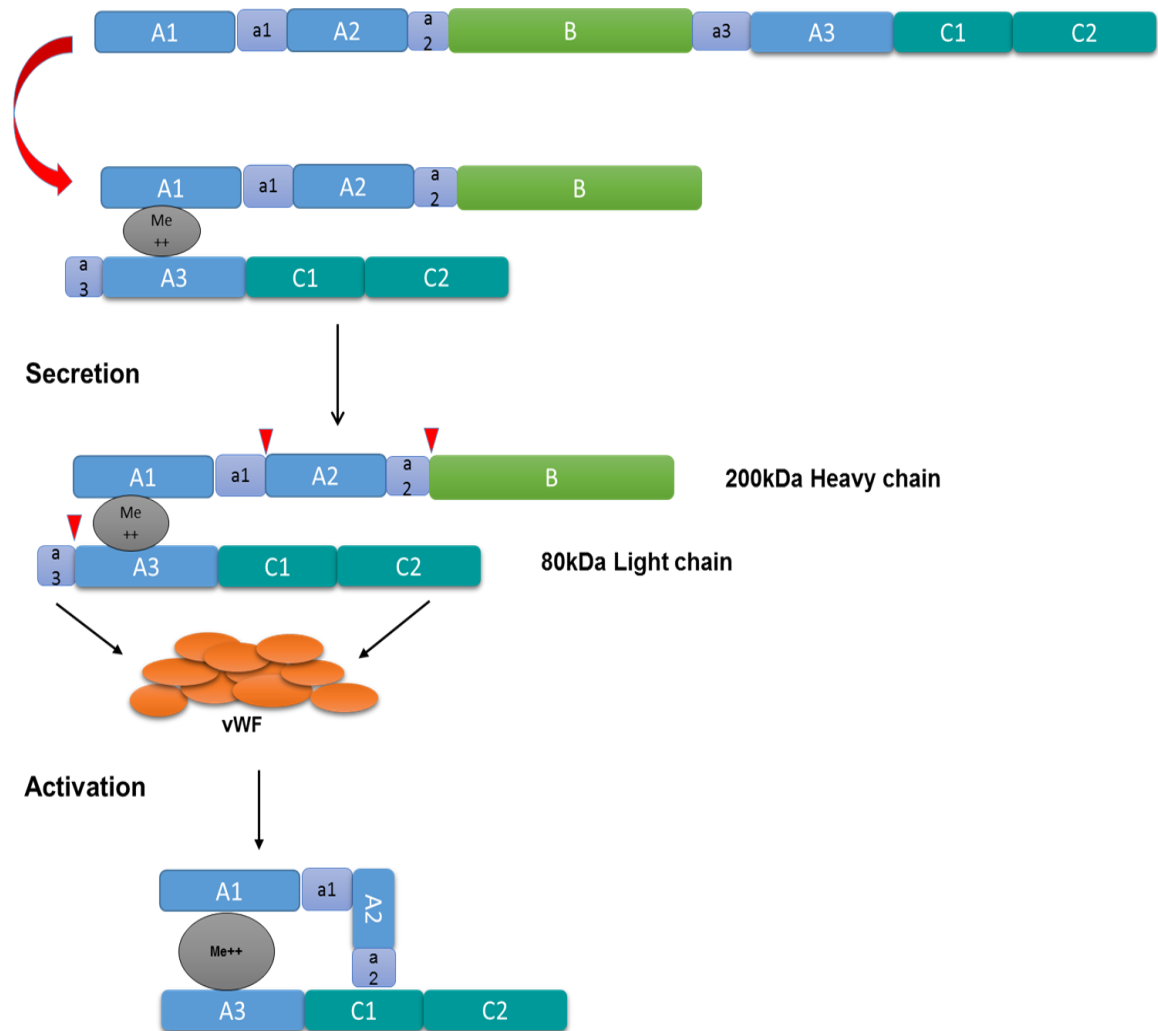


Figure 1.7. Activation process of FVIII

FVIII gene is translated to 2332 amino acid polypeptide, which consists of domain structure A1-a1-A2-a2-B-a3-A3-C1-C2. Upon secretion, the FVIII is a heterodimer of heavy and light chains bound to each other by a divalent metal ion (grey ball) and in complex with the carrier protein von Willebrand Factor (vWF). Thrombin, FXa and FIXa mediate activation by proteolytic cleavage at specific residues to form a hetero-trimer. Red arrows indicate thrombin cleavage sites at Arginine (R)372, (R)740, and (R)1689. Cleavage at (R)1689 releases the a3 acidic-rich region, which dissociates FVIIIa from vWF (Mannucci and Tuddenham, 2001; Pipe, 2009; Saenko *et al.*, 1994). Binding of metal ions to this site allows the A1 domain to adopt an A3 domain binding conformation. Alternatively, metal ions directly bridge the A1 and A3 domain by interacting with both domains simultaneously (Kaufman *et al.*, 1988).

1.5. FVIII clearance

The asialoglycoprotein receptor (ASGPR) is abundantly expressed in the liver. The ASGPR is a member of the C-type family of lectins that play a role in calcium-dependent binding as an endocytic receptor (Stockert, 1995). It is clear that the ASGPR receptor binds oligosaccharides with terminal β -linked *N*-acetylgalactosamine (GalNAc) or Gal, and hence that it can mediate the rapid clearance of glycoproteins bearing these terminal sugars from the circulation (Park *et al.*, 2003). Bovenschen *et al.*, concluded by *in-vitro* binding studies that ASGPR is involved in the catabolism of FVIII (Bovenschen *et al.*, 2005a).

Free FVIII molecules in plasma are rapidly cleared via low-density lipoprotein (LDL) receptor-related protein (LRP1, also known as a α 2-macroglobulin receptor or CD91) (Saenko *et al.*, 1999; Lenting *et al.*, 2007). LRP is a major endocytic receptor in the liver (Moestrup *et al.*, 1992), but it is also expressed in many other cell types and tissues.

LRP has been established to interact with coagulation FVIII and to mediate its cellular uptake into the lysosomal degradation pathway (Lenting *et al.*, 1999; Bovenschen *et al.*, 2005b). The region of FVIII involved in its binding to LRP was localised within the A2 domain residues 484~509, based on the ability of the isolated A2 domain and the synthetic A2 domain peptide 484~509 to prevent FVIII interaction with LRP (Saenko *et al.*, 1999; Bovenschen *et al.*, 2005a). However, Lenting and colleagues reported that LRP1 interacts with the light chain of FVIII C2 domain. Interactive sites for FIXa, phospholipids and LRP1 binding of FVIII light chain overlap so that vWF interferes with the interaction between FVIII light chain and LRP1 (Lenting *et al.*, 1999).

Removal of free FVIII forces a constant shift from vWF-bound to free FVIII. LRP1 mediated clearance of unbound FVIII is facilitated by both LDL-receptor (LDLR) and cell surface heparan-sulfate proteoglycans (HSPG) (Sarafanov *et al.*, 2001). These receptors also have the potential to internalise FVIII by themselves. The vWF prevents

binding of FVIII to LRP1 not only in a system using purified proteins but also in cellular degradation (Lenting *et al.*, 1999). Degradation of FVIII was completely inhibited by vWF because vWF binding to FVIII involves its light chain C2 domain. Moreover, LRP-directed antibodies inhibited degradation to a similar extent, suggests that LRP indeed give rise to the binding and transport of FVIII to the intracellular degradation pathway (Lenting *et al.*, 2007).

Sarafanov and colleagues reported *in-vivo* and *in-vitro* experiments revealing that HSPGs are also involved in FVIII catabolism with another LRP-independent pathway. In these pathways, HSPGs act as receptors providing the initial binding of FVIII-vWF complex to cells (Sarafanov *et al.*, 2001).

In summary, there are multiple mechanisms for FVIII and vWF complex formation, which vWF stabilises hetero-dimeric FVIII structure, and protects FVIII from proteolytic degradation by phospholipid binding proteases (activated protein C and activated FX). Moreover, vWF interferes with binding of FVIII to phospholipid surface and inhibits binding of FVIII to FIXa, thereby prevents the cellular uptake of FVIII (Lenting *et al.*, 2007).

1.6. FVIII therapeutic treatments and risks

1.6.1. Haemophilia A protein replacement therapy

The treatment option of FVIII replacement therapy became feasible in the late 1960s to early 1970s when it became known that specific FVIII concentrates could be produced from pools of donor plasma (Mannucci & Tuddenham 2001). Protein replacement therapy has been effective and has resulted in both a dramatic increase in life expectancy and a vast improvement in the quality of life. However, while this therapy proved effective, one major drawback was the frequent contamination of plasma-derived FVIII with several human viruses, such as human immunodeficiency virus and hepatitis viruses.

Approximately 70% of tested persons with haemophilia A (FVIII deficiency) and 35% with haemophilia B (FIX deficiency) became seropositive for HIV during the 1980s from infectious plasma-derived clotting factor concentrates. (The MMWR [Morbidity and Mortality Weekly Report] supplement was prepared as a report to the President and the Domestic Policy Council, which was presented to the Council on November 30, 1987). Although the coagulation factors have been produced from plasma concentrates for 15 years, genetically engineered recombinant factors are now available. In spite of developing new technology to produce recombinant proteins and improved bio-safety, the most fundamental issue in haemophilia treatment is the lack of availability of factor concentrates for two-thirds of the world's patient population. Production of bio-similar products and prioritisation of their registration will reduce the cost and make recombinant proteins more accessible for those patients coming from developing countries (Peyvandi *et al.*, 2013).

1.6.2. Inhibitor formation

Patients with haemophilia A treated with FVIII concentrates are at risk of developing FVIII neutralising antibodies (NAbs, Inhibitors). Inhibitor development is one of the most complicated matters in the treatment of haemophilia A as it increases the bleeding propensity while it provided treatment with therapeutic FVIII concentrates ineffective (Eckhardt *et al.*, 2013). The FVIII mutations that are associated with a high inhibitor prevalence are large deletions, nonsense or null mutations, and intron 22 inversions (Kempton and White, 2009).

Oldenburg and colleague are found that 68.8% of patients with large deletions had high-titer inhibitors compared with only 21.2% with missense mutations; the most common intron22 inversion with 38.5% and 30% to 40% with all other mutation types. FVIII inhibitor antibodies most frequently bind to the A2 and C2 domains of FVIII, where the risk of inhibitor formation is 4-fold greater than in patients with mutations outside this region. This finding indicates that the prevalence of inhibitor distribution shows dependence on the localisation of mutation (Oldenburg and Pavlova, 2006; Fang *et al.*, 2007).

The development of neutralising antibody to FVIII is the most significant complication of haemophilia A treatment, occurring in up to 33% of patients with severe haemophilia A, but only in 13% of moderate and mild in haemophilia A (Eckhardt *et al.*, 2013). In the presence of an inhibitor, the risks of increased mortality, major bleeding complications and the cost of care increase substantially. For this reason, developing methods which decrease FVIII inhibitor formation is an important goal (Earnshaw *et al.*, 2015).

The measurement of FVIII inhibitor potency is standardised to the Bethesda method (Kasper *et al.*, 1975), where 50% of FVIII activity, relative to control, after 2 hours of incubation is defined as one Unit of inhibitor per mL(Bethesda unit). A patient classified as a high responder shows above five units at any point after treatment while a low

responder presents a titer below five units despite repeated treatments with FVIII concentrate (Schwaab *et al.*, 1995; White *et al.*, 2001). Risk factors for developing inhibitors are i) mutation in the *F8* gene (large deletions, nonsense mutations or inversions), and ii) exposure to FVIII during the first 50 days of FVIII concentrate treatment. While the development of inhibitor antibodies after rFVIII replacement therapy is a major concern, this therapy is currently the most effective treatment option for haemophilia A. New factor replacement therapy methods, which are cost-effective and safe, are required.

1.7. Bioengineering of Factor VIII

1.7.1. Wild type

Wild-type FVIII has been consistently reported to be very weakly expressed compared with the similar coagulation protein FV (Kaufman *et al.*, 1989; Nichols and Ginsburg, 1999). The cause of the low expression of FVIII has not been fully explained. Particular inhibitory elements were discovered in the coding region of FVIII (nucleotides 1681 to 2277 and 5002 to 5582nt). The 1.2kb fragment of the FVIII cDNA coding sequences decreased mRNA accumulation and FVIII protein production because of the consensus destabilising sequences “ATTTA and TATT” nuclear matrix attachment region (MARs) (Lynch *et al.*, 1993). A similar discovery by Hoebe and colleague show that 305bp of coding sequences is the cause of the low expression of FVIII. Both suggest that the repressor sequences act as a transcriptional silencer of expression (Hoebe *et al.*, 1995; Fallaux *et al.*, 1996). More detail study has been performed that demonstrates the 305bp fragment match with “WTTTAYRTTTW” consensus sequence observed in the autonomously replicating sequences (ARS) element is responsible for the effect. Overall, the MAR or ARS in the FVIII could explain the repressing effects of the FVIII mRNA transcription.

1.7.2. Codon optimisation

The codon is a three-nucleotide RNA sequence that corresponds with a specific antisense tRNA, which transports a specific amino acid to the ribosome for protein chain elongation during synthesis. The genetic code is redundant in that multiple codons specify one amino acid, a finding that has been observed in all species. Codon usage plays a major role in determining translational efficiency and rare codons result in ribosomal stalling during translation. Recently, algorithms have been developed to optimise the translation process for efficient protein production. These codon optimisation procedures include the elimination of mRNA secondary structures, which leads to an efficient translational performance from mRNA (Johnston *et al.*, 2012).

Cannarozzi and colleagues showed that subsequent occurrences of the same amino acid do not use codons randomly in coding sequences, but favour codons are used for the same tRNA. The effect is discovered in rapidly induced genes, which involves both frequent and rare codons and diminishes only slowly as a function of the distance between subsequent synonymous codons. Therefore the translation speed can be controlled by tRNA consumption at the ribosome complex (Cannarozzi *et al.*, 2010). Thus appropriate usage of tRNA pools in host cells for mRNA translation might be developed through evolution to improve the protein yield to survive in extreme environments, which require high success rate for the selection process (Tuller *et al.*, 2010).

Boël *et al.* suggested that codon content influences protein expression more strongly than mRNA-folding parameters. The less efficiently translated protein sequences exhibited greatly reduced mRNA levels *in-vivo*. Moreover, the codon content modulates a kinetic competition between protein elongation and mRNA degradation that is a central feature of the physiology of translation in *E. coli* (Boël *et al.*, 2016).

In addition, by quantifying translational efficiency in healthy and cancerous tissues in human and mouse, they showed that many different sets of mRNAs could be equally well translated irrespective of their cell-type specificity. This stability of translational

efficiency is best explained by differences in GC (Guanine-Cytosine) content between genes. The GC variation across the mammalian genome is most likely a result of the interplay between genome repair and gene duplication mechanisms, rather than selective pressures caused by codon-driven translational rates. Consequently, codon usage differences in mammalian transcriptomes are most easily explained by well-understood mutational biases acting on the underlying genome. Therefore, the hypothesis of codon usage biases postulated to exist within mammalian transcriptomes might be explained by differences in GC content across the genome. More evidence discovered from mammalian genomes suggests that mutational bias is a sufficient explanation for variations in codon usage between sets of genes. For example, when compared to prokaryotes, the mammalian genome is better optimised for complex transcriptional and post-transcriptional regulation than for codon adaptation.

Overall, protein translation efficiency and stability can be modified according to the mammalian codon usage which can be applied for biosynthesis of stable proteins (Rudolph *et al.*, 2016).

1.7.3. Codon optimisation for FVIII

Human FVIII expression levels are significantly lower than similarly sized proteins. The main reason for this is the inefficient transport of the primary translation product from the ER to the Golgi and low mRNA expression (Dorner *et al.*, 1987; Kaufman *et al.*, 1988). There are many hurdles to overcome to improve the weak FVIII expression because transcribed mRNA levels are very low due to the wild-type FVIII genomic sequence containing multiple transcriptional silencers such as ARS/MARs (Lynch *et al.*, 1993; Hoeben *et al.*, 1995; Koeberl *et al.*, 1995; Fallaux *et al.*, 1996).

To improve FVIII expression level, deletion of the entire B-domain leads to a 17-fold increase in mRNA and primary translation product, but the amount of secreted protein improved only 30%. Which suggests that the rate of ER-Golgi transport is important in

reducing protein secretion (Pittman *et al.*, 1994; Miao *et al.*, 2004). Over the last decade FVIII bioengineering has been intensively carried out to improve secretion efficiency, plasma half-life, functional activity and reduce antigenicity/immunogenicity. As this activity has largely occurred in the commercial sector some details of production are obscure. However, in at least one academic study, FVIII expression *in-vitro* and *in-vivo* has been improved by codon optimisation (Ward *et al.*, 2011). In particular direct comparison between non-codon-optimised and codon-optimised FVIII showed that codon optimised FVIII cDNA sequence improved protein expression by 7- to 30- fold as opposed to the wild-type FVIII (Ward *et al.*, 2011). A similar result reported from Radcliffe and colleagues that lentiviral vectors which contained codon engineered FL-FVIII led to a significant increase in titre of approximately 10-fold but also achieved high secretion levels of FVIII. Non-codon optimised FVIII expression was below the limits of detection of the assay. In contrast, the codon-optimised FVIII was calculated to contain in excess of 100-fold more FVIII than the lowest standard. Therefore, codon optimisation had improved full length FVIII expression dramatically. In contrast, for B-domain deleted FVIII comparison of a non-codon optimised with a codon-engineered sequence yielded only modest improvements in titer and expression (Radcliffe *et al.*, 2007).

Moreover, Johnston and colleagues reported the controversial result that they used a codon optimised hybrid FVIII transgenes, which did not enhance Human/Porcine (HP) FVIII expression (Johnston *et al.*, 2012). They concluded that the ineffectiveness of the expression of HP-FVIII may be due to the innate high expressing characteristics of HP-FVIII. Therefore, the possible mechanism for the enhanced levels of FVIII from a codon optimised FVIII transgene could be due to either enhanced codon usage for translation or the removal of cryptic sequence, which contains transcriptional silencers and inhibitory sequences found within the human FVIII cDNA (Johnston *et al.*, 2012).

1.7.4. B-domain deleted FVIII

Current research shows that the B-domain is not required for FVIII activity and that deletion of this domain dramatically improves secretion and stability of this protein. It is reported that the removal of B-domain has no effect on the pro-coagulant activity of FVIII. Moreover, reduction in the size of the glycoprotein improves its mRNA expression and secretion (Toole *et al.*, 1986; Pittman *et al.*, 1993; Pipe, 2009). B-domain deleted recombinant FVIII (rFVIII-BDD) products are the newest subset of FVIII protein, and the B-domain is replaced with short amino acid sequences that link the 90kDa and 80kDa domains of active FVIII (heavy and light chains).

A, B-domain-deleted (BDD)-rFVIII, rFVIII SQ, was originally characterised by Pharmacia & Upjohn (Stockholm, Sweden) and clinical studies began in 1993 and rFVIII SQ was eventually developed commercially through an agreement with Genetics Institute (USA), then a subsidiary of American Home Products (and eventually Wyeth), in 1997 and was finally approved as ReFacto® in March 2000 (Pipe, 2008).

Commercial recombinant BDD-FVIII (ReFacto®) was first introduced for clinical use more than a decade ago. ReFacto® contains a neo-antigenic site (the “SQ” link) which generated by joining of Ser743 in the N-terminus with Gln1638 in the C-terminus of the B-domain. However extensive clinical use of ReFacto® has shown no increase in the frequency of neutralising hFVIII antibodies in patients treated with this product (Lind *et al.*, 1995; Sandberg *et al.*, 2001; Lusher *et al.*, 2003; Gringeri *et al.*, 2004; Pollmann *et al.*, 2007).

While ReFacto® was the first modified rhFVIII, on the market new products, have recently emerged. By 2014, Novo Nordisk introduced a 21 amino acids linker containing truncated B-domain rFVIII Turoctocog alfa (NovoEight®), which is a new rFVIII molecule with a truncated B-domain. The molecule consists of a heavy chain containing the A1-A2 domains, a truncated B-domain coding for 21 amino acids of the naturally occurring B-domain (amino acid 741-750 fused with 1638–1648) and the light chain (A3-C1-C2

domains). The modified B-domain was selected to achieve a well-defined product, which produced in CHO cells in serum-free conditions and formulated without animal- or human- derived materials thereby providing a solid basis for establishing a robust purification process (Ezban *et al.*, 2014).

Recently, the firm Octapharma introduced “Nuwiq®” for the production of which producer cell lines of human origin (human-cl) have been used for the first time to produce rhFVIII. The human-cl rhFVIII consists of a 170kDa protein comprising the functional A and C domains of human FVIII with a linker sequence of 16 amino acids inserted between the A2 and A3 domains. The first eight amino acids in the N-terminal part of the linker derive from the native protein B-domain while the remainder sequence was chosen to provide a recognition site for furin or furin-like proteases. This short sequence “QAYRYRRG” showed similarity with the sequence “QAYR-RRG” present in a protein of 800 amino acids expressed by the *KIAA1462* gene in human neural cells in the mainly cerebral cortex (Sandberg *et al.*, 2012). The reason for using a human cell line is due to generate an authentic human pattern of PTMs which leads to precisely folded and fully active FVIII. This is of particular importance as PTMs have been demonstrated to impact on rhFVIII activity. The new human cell line-derived recombinant human FVIII (Human-cl rhFVIII) protein is the first native and unmodified human rFVIII product produced in a human cell line (Sandberg *et al.*, 2012; Kannicht *et al.*, 2013). Human-cl rhFVIII is manufactured without additive animal, or human derived materials during production and purification (Valentino *et al.*, 2014).

Biogen Idec /SOBI introduced a 15 amino acids linker BDD-FVIII Fc which has a longer half-life. rFVIII-Fc is a B-domain deleted FVIII molecule, which consists of the dimeric constant region (Fc) of IgG1 and the terminal half-life of rFVIII-Fc (19 hours) was extended 1.5-fold compared rFVIII (Dumont *et al.*, 2012).

Bayer (Bayer Healthcare) has created a PEGylated rFVIII (BAY 94-9027) using site-

directed mutagenesis. They modified a B-domain deleted rFVIII through the introduction of a single cysteine at amino acid 1804 specifically conjugated to a 60kDa PEG molecule. In clinical studies, BAY 94-9027 demonstrated equivalent recovery and an improved PK profile compared with rFVIII-FS (Kogenate®, FL-FVIII), with a ~19 hours half-life (~13 hours for rFVIII-FS) (Mei *et al.*, 2010; Coyle *et al.* 2014).

CSL Behring developed a B-domain deleted rFVIII with a covalent bond between the heavy and the light chain of FVIII (Lonoctocog alfa), circulating as a single-chain FVIII molecule (Schulte, 2013). rVIII-Single chain has a single-chain design in which a truncated B-domain covalently links the heavy and light chains improved intrinsic stability. In addition, it has been shown that the affinity of rVIII-Single chain for vWF is markedly higher, and its pharmacokinetic properties are improved, compared with full-length rFVIII (Schmidbauer *et al.*, 2015).

In 2004, Pipe and colleagues created and tested FVIII expression plasmids containing human B-domain fragment with varying numbers of glycosylation sites ranging from N1-N8. They found that including a 226 amino acids linker containing six N-linked oligosaccharides, in the domain increased mRNA stability and production (Miao *et al.*, 2004). 226aa/N6 has six N-linked oligosaccharides within a truncated B-domain spacer inserted into otherwise wild-type BDD-FVIII (Fig.1.5). This variant had the most increased mRNA and primary translation product levels and improved secretion efficiency. In contrast, Kolind and colleagues have reported novel B-domain deleted mutants with varying linker lengths and numbers of N-linked glycosylation sites. Their results showed that short linker B-domain FVIII constructs were better expressed than longer B-domain linker and that presence of N-linked glycosylation sites showed no improvement to FVIII yield in serum-free condition. From this work, no unifying explanation or conclusions were derived (Kolind *et al.*, 2010).

In 2013, McIntosh and colleagues developed a novel B-domain deleted FVIII named V3, the V3 peptide was flanked by 14 amino acids SQ residues from the N- and C-terminal

ends of the B domain. This variant was developed for AAV gene therapy for haemophilia A. It was found that rAAV-HLP-codop-hFVIII-V3 mediated higher hFVIII antigen expression in two different murine models compared with codon optimised FVIII SQ containing 14 amino acids linker identical to SQ and a FVIII with a 226aa truncated B-domain each in the same AAV cassette. Significantly, the manner in which the *N*-glycosylation triplets from the B-domains are brought together appeared to be important, because minor changes to the 17 amino acids peptide (V3) markedly affected expression levels *in-vivo* and *in-vitro* (McIntosh *et al.*, 2013).

Notwithstanding theoretical objections, the practical advantages render BDD-FVIII more attractive, because, as has been suggested it is safe, efficacious, and immunologically similar to wild-type FVIII. The particular advantages of B-domain deleted FVIII for therapeutic use includes its greater level of expression and significantly reduced heterogeneity. Thus, the cost of production should be significantly less than wild-type FVIII for producing recombinant FVIII. In addition, the limited size of the cDNA construct allows its insertion in most viral vectors (including Adeno associated virus) with the aim of therapeutic gene transfer (Pittman *et al.*, 1993; Chao *et al.*, 2000; Chao and Walsh, 2001).

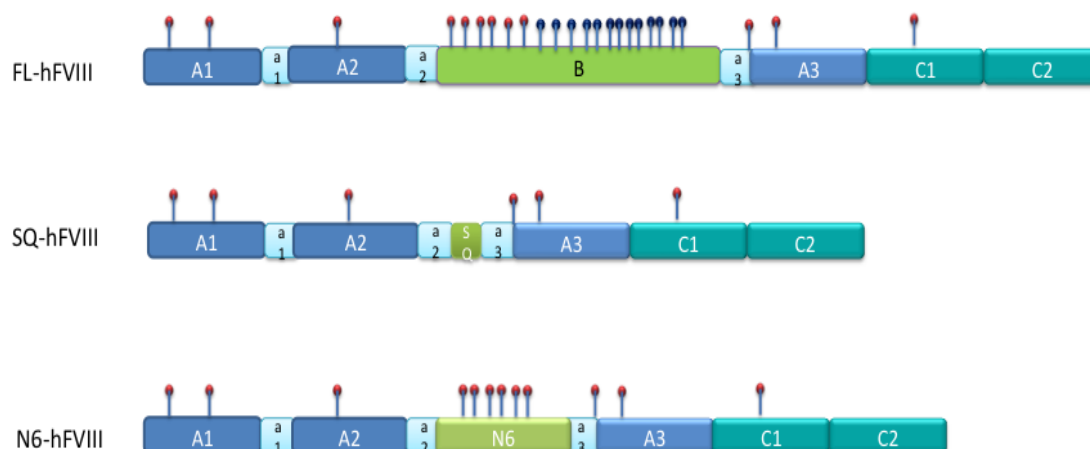


Figure 1.8. Schematic diagram of FVIII variants

FVIII variant domain structures were illustrated as full length FVIII (FL-hFVIII), B-domain deleted FVIII (BDD-hFVIII), and 226 amino acid lengths truncated B-domain of N6-hFVIII.

Full-length hFVIII (FL-hFVIII) represent 25 *N*-linked glycosylation sites and full-length B-domain with 908 amino acids. BDD-hFVIII, Ser743 was fused to Gln1638, creating a 14 amino acid "SQ" linker between the C-terminus of the 90kDa chain and N-terminus of the 80kDa chain. N6 hFVIII, 226 amino acid reserved from N-terminus of B-domain and fused to Gln1650 in a3 region, creating a 226 amino acid /N6 linker. Potential *N*-linked glycosylation sites are indicated by lollipops. Blue lollipops (*N*7-*N*19) inside of full-length B-domain were excluded in this study.

1.7.5. Commercial recombinant FVIII

1.7.5.1. History of recombinant proteins and current developing products

The *F8* gene was cloned in 1984, which allowed recombinant human FVIII (rFVIII) to be produced and purified from mammalian cell culture. Thereafter, the first generation of recombinant full-length FVIII (rFL-FVIII) was introduced in the early 1990s, which is CHO cell-derived full-length FVIII (Recombinate®, Baxter), and the following year the BHK cell derived rFL-FVIII (Kogenate®, Bayer). Ten years later, in 2000 Wyeth developed the second generation of B-domain deleted rFVIII (ReFacto®). Another so-called second-generation modification was the removal of human albumin from formulation stabilising the final product of rFL-FVIII (Kogenate®, Bayer). The third generation production method of Kogenate (also marketed as Helixate), Advate, and ReFacto® does not contain any animal or human proteins in the culture medium. However, these products were generated in non-human cell lines, which produce recombinant glycoproteins with a rodent glycosylation pattern. By this consideration, recently Biogen Idec/SOBI and Octapharma companies developed products which are produced in HEK-293 cells (Casademunt *et al.*, 2012). Their products have been tested in clinical trials and are approved by health authorities. Currently, several companies supply rFVIII, in which FL-FVIII or B-domain deleted product are present (Table 1.1). The Baxter (now Baxalta/Shire) production system includes co-expression of vWF, but this is removed from the final product.

An approach to improve coagulation factors is to extend their half-life. Obtaining half-life extension has been challenging for therapeutic proteins but is now being applied to FVIII.

Company	Product	Generation	Gene	Cell line
Baxter	Recombinate®	1	FVIII/VWF	CHO
	Advate	3	FVIII/VWF	CHO
Bayer	Kogenate®	1	FVIII	CHO
	Kogenate FS	2	FVIII	BHK
CSL Behring	Helixate	2	FVIII	BHK
Pfizer	ReFacto®	2	BDD-FVIII	CHO
	ReFacto AF	3	BDD-FVIII	CHO
Green Cross	GreenGene	2	BDD-FVIII	CHO
	GreenGene F	3	BDD-FVIII	CHO
Biogen Idec/SOBI	Eloctate®	3	BDD-FVIII Fc	HEK
Novo Nordisk	NovoEight®	3	tBDD-FVIII	CHO
Octapharma	Nuwiq®	3	tBDD-FVIII	HEK

Table 1.1. Recombinant human FVIII concentrates

Recombinant human FVIII is produced from three different cell lines by genes carrying FVIII/vWF, FVIII, BDD-FVIII and truncated BDD-FVIII. Biogen Idec and Octapharma produced rFVIII from human cell lines. The B-domain engineered rFVIII protein products enlarged in the 3rd generation of recombinant FVIII. Abbreviation: CHO, Chinese hamster ovary; BHK, Baby hamster kidney; HEK, Human embryonic kidney.

1.7.5.2. Current strategies to improve FVIII half-life

Human FVIII is large, complex protein, and its half-life is relatively short, which necessitates frequent dosing to maintain therapeutic levels. Modifications that extend the product's half-life could theoretically allow for extended dosing intervals (Schulte, 2013). Recombinant factors with longer residual time in circulation would cumulate the benefits of reducing the frequency of infusions thus improving the compliance with improved prophylaxis regimens for haemophilia A patients by reducing the frequent injection of rFVIII required by its short half-life (Pan *et al.*, 2009).

In this context, several strategies are being exploited to optimise the pharmacokinetics of therapeutic FVIII, which include coupling of the effector protein to polyethylene glycol (PEG), dimeric Fc fragments of human immunoglobulin G, or human serum albumin (Ing *et al.*, 2016).

PEGylation used for many therapeutic proteins, which have been approved for variety of chronic diseases. However, PEGylation of FVIII is difficult due to large molecular weight which lead to different characteristics and activity levels. Therefore the chemically modified PEGylation of FVIII has been developed that the selective PEGylation was achieved by a mutation in the light chain of FVIII. Other approaches to increase the functional half-life of drugs include the production of recombinant fusion proteins where the FVIII activities are modified through the fusion to a Fc-domain or albumin of an antibody (Stennicke *et al.*, 2013).

Modification with PEGylation is a method to improve the pharmacokinetic profile and extend half-life about 2.5-fold. The circulation of therapeutic proteins by increasing size leads to reduction of renal clearance. The clearance of FVIII take place primarily in the liver where interaction occur with low-density lipoprotein receptor-related protein (LRP). The FVIII modification by PEG polymers might achieve a longer-acting FVIII due to reducing binding of the PEG-conjugated FVIII to LRP (Pan *et al.*, 2009; Turecek *et al.*,

2012). PEGylation of FVIII was shown to confer prolonged efficacy in haemophilic mice, as compared to unmodified FVIII (Mei *et al.*, 2010).

rFVIII-Fc is a fusion protein, which composed of a single B-domain-deleted FVIII molecule to the dimeric Fc fragments of human immunoglobulin G. rFVIII-Fc exhibits approximately 2-fold extension in half-life in haemophilia A mice and dogs (Dumont *et al.*, 2012).

The CSL Berhring rVIII-Single chain was designed with a covalent bond between the heavy and light chains of FVIII. The heavy and light chains of native FVIII, are held together by a metal-ion bridge, which makes the FVIII molecule relatively unstable. The recombinant single-chain FVIII (rVIII-Single chain) further strengthens the interaction between these two FVIII chains and results in a significantly increased binding to vWF. The half-life of vWF bound FVIII is about 12 hours in contrast free FVIII shows only an hour. Consequently, the increased proportion of vWF bound FVIII leads to an extension of the FVIII half-life (Oldenburg and Albert, 2014; Schmidbauer *et al.*, 2015).

Reduced interaction with clearance receptor (Baxter, Bayer and Novo Nordisk), interaction with the neonatal Fc receptor and immunoglobulin molecules protecting the protein from intracellular degradation finally increased FVIII half-life by 2-fold (Biogen Idec/SOBI) (Powell *et al.*, 2012).

1.8. Post-translational modifications (PTMs)

Post-translational modifications (PTMs) are important in regulating the folding of protein, activity, and stability by covalent linkage to new functional groups, such as acetate, phosphate, and methyl groups. For many PTMs, including acetylation, glycosylation, methylation, phosphorylation, SUMOylation, succinylation and ubiquitination tens of thousands of sites can now be confidently identified and localised in the sequence of the protein (Olsen *et al.*, 2013; Liu *et al.*, 2016).

PTMs dynamically alter the compartmentalisation, trafficking, and physical interaction of key molecules that regulate immunological processes (Liu *et al.*, 2016). Some PTMs, including glycosylation, lipidation and disulfide bridge formation are stable and are important for maturation and proper folding of newly synthesised proteins. Others, such as phosphorylation, are more transient and have essential roles in intracellular signalling. A protein can be modified by more than one type of PTMs or multiply modified by the same PTMs at different residues (Deribe *et al.*, 2010). Importantly, >95% of these data are derived from mass spectrometry (MS) based proteomic which has considerably extended our knowledge about the occurrence and dynamics of protein post-translational modifications. So far, quantitative proteomics has been mainly used to study PTM regulation in cell culture models and focus on quantifying, sometimes slight relative changes of modified peptides between different sample states. Cell culture conditions may be manipulated to influence productivity and PTMs for example, temperature, growth rate and media composition (Butler, 2005).

It is suggested that analysis of aberrant PTM patterns in human disease would provide new insights that might have a direct impact in the clinic (Olsen *et al.*, 2013; Pagel *et al.*, 2015).

1.8.1. Glycosylation

Glycosylation is a post-translational protein modification that expands the diversity of the proteome. Eukaryotic glycoproteins have been implicated in cellular processes including the intracellular targeting, immune response, intercellular recognition, protein folding and stability (Varki, 1993). A variety of glycan-protein linkages have been identified in glycoproteins from bacterial organisms to a eukaryote (Weerapana and Imperiali, 2006). The intensive research of glycosylation systems in eukaryotic organisms has been carried out since the 1930s; it raised assumptions that bacteria and archaea were deprived of this important protein modification (Messner, 2004).

Glycosylation can introduce heterogeneity through the generation of different oligosaccharides, and variable addition of outer arm sugars as the glycoprotein transits in the Golgi. The presence and nature of the oligosaccharide (glycoform) may impact glycoprotein folding, stability, trafficking and immunogenicity as well as its primary functional activity (Walsh and Jefferis, 2006).

In an individual glycoprotein, more than one carbohydrate unit is often present, attached at different positions by either an *N*-linkage, *O*-linkage or both. Moreover, each attachment site frequently accommodates different glycans; a phenomenon referred to as site heterogeneity. This results in micro-heterogeneity of the whole molecule and creates discrete subsets, or glycoforms, of a glycoprotein that have different physical and biochemical properties. This may lead to functionally diversified glycosylation of any protein, which is dependent on the cell or tissue in which it is produced. Thus the polypeptide encodes information that directs its own pattern of glycosylation (Lis and Sharon, 1993).

The structural changes of glycan play critical roles on many glycoproteins in modulating functional activity and immunogenicity. Moreover, the diversification in carbohydrate structures has been associated in the pathogenesis of many human diseases, such as cancers which are related with alterations in protein glycosylation (Preston *et al.*, 2013; Holst *et al.*, 2016).

Genetic engineering makes it possible to produce glycoproteins in heterologous systems on a large scale, both for research purposes and for therapeutic use. For instance, oligonucleotide-directed mutagenesis allows for specific changes in the primary structure of glycoproteins and facilitates the examination of factors governing site-specific glycosylation and oligosaccharide processing. In glycoproteins with more than one glycan, mutagenesis provides insights into the contribution of each glycan to the overall properties of the molecule (Lis and Sharon, 1993). Several factors may influence glycan biosynthesis, namely, the under or overexpression of glycosyltransferases, the impairment of glycosyltransferase chaperone function, altered glycosidase activity, changes in the tertiary conformation of a given peptide or growing glycan, and the availability of sugar nucleotide donors, cofactors and acceptor substrates (Ferreira *et al.*, 2016).

N-linked glycans on glycoproteins are attached to the side chain of asparagine (Asn), and the *N*-linked glycosylation begins in the endoplasmic reticulum (ER). The attachment of *N*-linked carbohydrates to proteins is thought to occur during or shortly after translocation of the nascent chain into the lumen of the endoplasmic reticulum. The oligosaccharide chain is transferred by the enzyme oligosaccharyl transferase to the asparagine in the consensus tripeptide Asn-X-Thr/Ser, where X is any amino acid except proline (Mononen and Karjalainen, 1984). The initial 14 sugar core of *N*-linked glycan is mannose-rich (Glc3Man9GlcNAc2) structure, which attached during protein synthesis in the ER. Subsequently, the core glycan is modified by a series of glycosyl-transferases and glycosidases through the ER and the Golgi apparatus. The ER chaperone proteins

calnexin and calreticulin engaged with newly synthesised glycopeptides. Calnexin is a lectin that binds to *N*-linked oligosaccharides and assists glycoproteins during initial folding or oligomeric assembly to prevent aggregation, leaving the ER prematurely and to ensure quality control (Hammond *et al.*, 1994; Hebert *et al.*, 1995).

N-linked glycans are further modified in Golgi where the properly folded glycoproteins are transported from the ER. Due to the fact that more than a hundred glycosyltransferases are found in the human genome, the complexity and heterogeneity of the final *N*-linked carbohydrate structure exist in nature. Overall, *N*-linked glycans can be classified into 1 of 3 subgroups: high-mannose, hybrid, or bi- tri- tetra complex (Fig. 1.6).

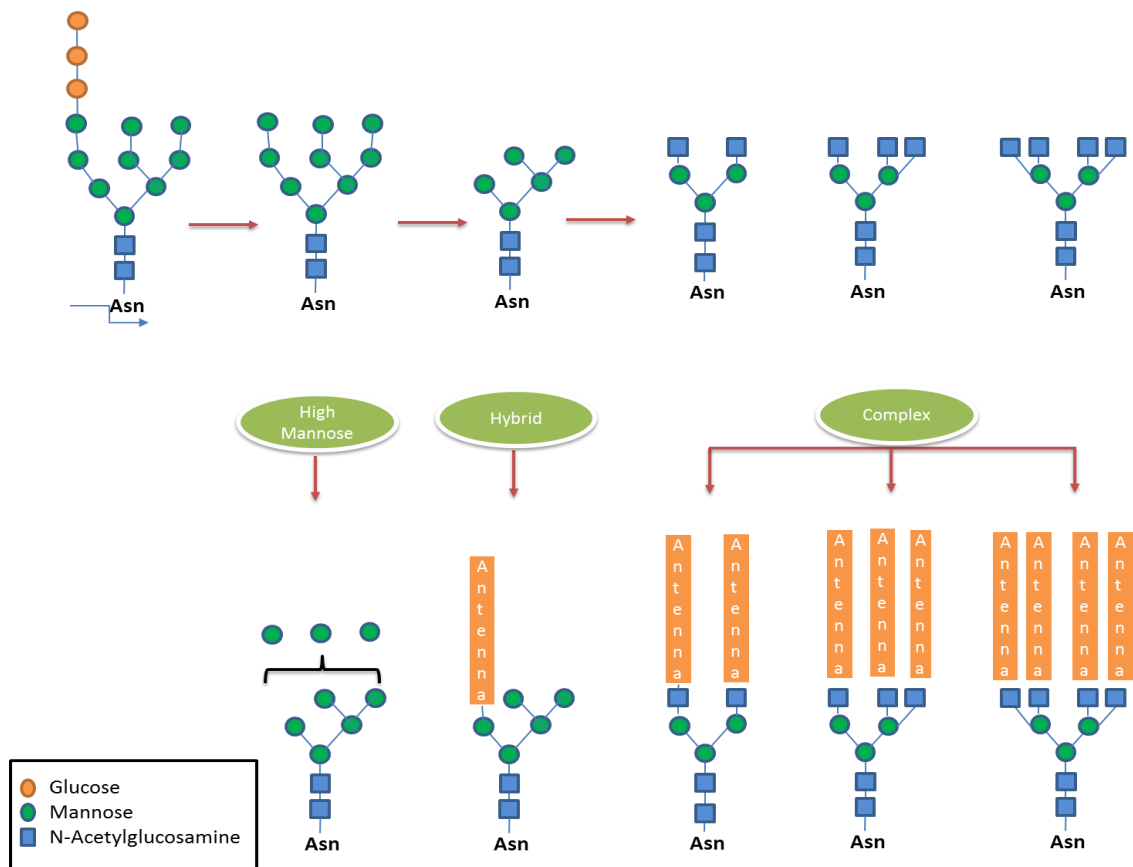


Figure 1.9. Biosynthesis of *N*-glycan in Eukaryotes

N-linked glycosylation starts in the ER and antennary structures are further processed in the Golgi apparatus. *N*-linked glycans can be classified into 1 of 3 subgroups: high-mannose, hybrid, or bi-tri- tetra complex depending on antennary structures (Preston *et al.*, 2013).

1.8.2. Human FVIII *N*-linked glycosylation

Recent studies have focused on the post-translational modifications, and specifically glycosylation of the FVIII protein, suggesting their pivotal role in FVIII biosyntheses, stability, quality control, secretion, activation and clearance. Glycoproteins that are incorrectly glycosylated fail to fold properly and/or fail to exit the ER, and are consequently degraded (Varki, 1993).

FVIII has a heavily glycosylated B-domain region containing 19 *N*-linked glycosylation sites. A large proportion of FVIII is not secreted, which was detected in a stable complex with BiP. However, the deletion of the heavily glycosylated region showed efficient FVIII secretion due to reduced binding with BiP (Dorner *et al.*, 1987). The deletion of most of the highly glycosylated internal domain of FVIII produces a protein which retains pro-coagulant activity and displays higher levels of secretion compared with FL-FVIII (Toole *et al.*, 1986).

The utilisation of *N*-linked glycosylation sites on a protein may influence the extent and stability of an association with BiP, and this can be correlated with the efficiency of secretion. In the absence of normal *N*-linked glycosylation efficient secretion is impaired. The un-glycosylated protein displays increased association with BiP and this complex is stable and not secreted. *N*-linked glycosylation sites on FVIII play a role in its efficient secretion and the extent and stability of its association with BiP. In the case of FVIII, deletion of the heavily glycosylated region by removal of protein sequence resulted in a reduced association with BiP (Dorner *et al.*, 1987).

Consequently, the 19 *N*-linked sites clustered in the FL-FVIII (B-domain: 19, Total: 25) may be presented in an appropriate conformation for too short a period of time (4~6 hours) for efficient glycosylation. Some molecules may, therefore, exhibit incomplete *N*-linked glycosylation. Further, it was observed that inhibition of *N*-linked glycosylation enhances association with BiP; incomplete glycosylation of FVIII may result in stable association with BiP and retention in the cell (Dorner *et al.*, 1987).

Interestingly, de-glycosylation of a human recombinant FVIII variant resulted in a substantial impairment of its clotting activity, suggesting the significant role of glycans in FVIII functions. Moreover, heavily glycosylated B-domain deleted FVIII, which has reduced polysaccharide moieties induces inhibitors, suggesting that glycosylation changes directly or indirectly through alteration of structure conformation, modifies the immunogenicity of the protein (Lee *et al.*, 1998). The small conformational changes in A and C domains led to the *N*-linked glycosylation to this epitope, which may play a critical role in the loss of FVIII activity (Kosloski *et al.*, 2009).

1.8.3. Recombinant protein production in mammalian cells

For large-scale production, recombinant proteins are expressed in immortalised mammalian cells. Chinese hamster ovary (CHO) cells, Baby hamster kidney (BHK), Human embryo kidney (HEK-293), Mouse myeloma (NS0), SP2-0 (hybridoma), HKB11 and human retinal cells (PER-C6) have each gained regulatory approval for recombinant protein production (Wurm, 2004; Swiech *et al.*, 2012). Mammalian cell systems are attractive to produce recombinant proteins, because of capacity for proper protein folding, assembly and post-translational modifications. Significant progress in developing and engineering new cell lines, introducing novel genetic mechanisms in expression, gene silencing, and gene targeting has been achieved. Understanding glycosylation has become one of the foci of research and development. Transient gene expression technology platforms play more important role in biopharmaceutical manufacturing (Zhu, 2012). The development of a manufacturing process for a recombinant protein in mammalian cells is well established and constantly being improved with current technology.

HEK-293 cells were first established by Dr Frank Graham in 1977. These HEK-293 cells have been widely employed as an expression host in scientific research over the last half-century. Adherent HEK-293 cell lines were adapted to suspension cell culture in 2003 by Invitrogen. Since then human cell lines have been evolved that are easily grown

in animal origin free raw materials under serum-free conditions while eliminating concerns associated with the use of animal-derived serum. A suspension cell does not require enzymatic or mechanical dissociation and typically achieves cell densities of 3×10^6 cells/mL in shaker or spinner culture and 4×10^6 cells/mL in bioreactor culture. Consequently, it is now easy to scale up a cost effective culture method (Gibco, 2003). Nowadays, human origin cells are used for bulk protein production, batch harvesting and many research applications. The human cell line contains the translational machinery and all the subcellular compartments, which is required to generate correctly folded and fully active FVIII, with a genuine human pattern of PTMs and human protein-like molecular structure assembly (Zhu, 2012). Despite the safety and efficacy of recombinant protein expression in hamster or mouse cells, the glycosylation pattern is of profound importance when considering their potential as expression systems for biosynthesis of human recombinant glycoproteins. Non-human cells simply do not glycosylate according to the human-type. These differences in glycosylation pattern may be highly immunogenic in humans, and/or may cause rapid clearance of the recombinant protein from circulation (Brooks *et al.*, 2004).

The anticipated benefit of using human cells in the production of rFVIII is avoidance of development of inhibitors due to non-human glycosylation pattern (Goudemand *et al.*, 2006). Immunogenicity not only remains a serious cause of morbidity in patients but also 4-fold increases the annual cost for treatment (Gringeri, 2003). Due to the PTMs expected to be produced in recombinant proteins, human cell line PTMs are more similar to their natural proteins and reduce the potential immunogenic reactions against nonhuman epitopes, therefore human cell lines are an attractive alternative for protein production for human therapeutic proteins (Swiech *et al.*, 2012; Zhu, 2012).

1.8.4. Cell type specific Post-translational modifications

Various host cell lines are available to express recombinant proteins. However PTMs differ between species and are organ specific, hence producing recombinant glycoprotein by a human cell line is important for prevention of potential novel immunogenicity by non-human PTMs (Böhm *et al.*, 2015; Kannicht *et al.*, 2013).

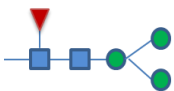







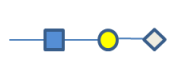

According to literature, production of FVIII in human cells produces similar post-translational modifications to those observed in the human plasma FVIII product (Sandberg *et al.*, 2012). Additionally, rFVIII expression in a human cell line avoids the expression of the antigenic carbohydrate epitopes Gala1-3Ga β 1-GlcNAc-R (α -Gal) and *N*-glycolylneuraminic acid (Neu5Gc), which are present on hamster glycoproteins, and so in CHO and BHK cell line produced proteins (Valentino *et al.*, 2014). The anti- α -Gal is the most abundant natural antibody in all humans (~1% of circulating immunoglobulins in humans), and it mediates the rejection of pig xenograft organs in humans. The α -Gal epitope has clinical potential in the production of vaccines expressing α -Gal epitopes that can be targeted to antigen-presenting cells, thereby increasing the immunogenicity. There are different types of PTMs in FVIII glycoprotein; this glycoprotein has 25 *N*-linked glycosylation sites, seven *O*-linked glycosylation sites and six sulphation in full-length FVIII (Kannicht *et al.*, 2013; Preston *et al.*, 2013). Glycosylation alters the functional and structural properties of a protein and is responsible for physiological properties, immunological properties, receptor binding and intracellular sorting. FVIII contains six tyrosine residues that are modified by posttranslational sulphation for full FVIII pro-coagulation activity and stability. These sulphation sites have a critical role in FVIII/vWF binding affinity because thrombin cleavage sites are located in the tyrosine sulphation border. Moreover, sulphation of FVIII Tyrosine1680 is vital for the interaction with vWF and influences the half-life of FVIII in the circulation. In addition, the current study uses human cell lines for the production of the FVIII protein to ensure that it is efficiently glycosylated in the hope of reducing the immunological response to the FVIII protein that

is observed in 30% of the patients treated with the current protein concentrates which are manufactured in CHO or BHK cell lines.

1.8.5. Comparison of the most common epitopes between plasma-derived FVIII and rFVIIIs

Although non-human originated cell line produced most abundant Gal- α 1,3-Gal and Neu5Gc, however, there are many epitopes represented depend on basic sources of purification or production. The most common epitopes are represented in Figure 1.10.

Although HEK-293 cell lines human origin cell line but introduced by the kidney, so fucosylated LacdiNac epitope represented with human plasma-derived protein. In blood group antigens, Lewis x/a existed plasma-derived FVIII, rodent cell line and Human cell lines derived rFVIII. Other blood A.B.O group's epitopes present human plasma protein glycans and plasma-derived FVIII.

Core structure	Terminal structure		Human plasma protein glycans	pdFVIII	rhFVIII-CHO/BHK	rhFVIII-HEK293F Nuwiq
		High Mannose N1->6	+	+	+	+
		LacNac	+	+	+	+
		Sialyl-LacNac	+	+	+	+
		Sialyl-Lewis x/a	+	+	+	+
		LacdiNac(F)	+	-	-	+
		Blood Group A,B,O	+	+	-	-
						
		Neu5GC	-	-	+	-
		Gal-α 1,3 -Gal	-	-	+	-

▲ Fucos (Fuc)
 ● Galactose (Gal)
 ● Mannose (Man)
 ■ N-acetylglucosamine (GlcNAc)
 ■ N-acetylgalactosamine (GalNAc)
 ◇ N-acetylneuraminic acid (NeuGc)
 ◆ N-acetylneuraminic acid (NeuAc)

Figure 1.10. Most common features of glycans of plasma glycoproteins, compared with those found in human FVIII therapeutic replacement proteins

Abbreviation: pdFVIII, Plasma-derived FVIII; rhFVIII, Recombinant human FVIII derived; CHO, Chines Hamster Ovary cell derived rFVIII; BHK, Baby hamster kidney cell derived rFVIII; HEK-293F, Human embryo kidney cell line 293F derived rFVIII. The structures were modified from Kannicht et al. (Kannicht *et al.*, 2013).

1.9. Gene delivery technology

In order to study the functional role of genes, it is necessary to manipulate the expression of specific genes in target cell populations. Gene manipulation has been achieved using transgenic animals or non-viral gene transfections including naked DNA (Kofler, 1998), electroporation (Li *et al.*, 1997) and liposomes (Nicolau *et al.*, 1987). However, non-viral transfer systems are relatively inefficient in post-mitotic neuronal cells. In addition, transgenic methods are expensive and time-consuming. In contrast, recombinant viral vectors are able to achieve efficient long-term transduction in a variety of cell types. A number of viral vector systems are now further developed with the aim of producing an optimised vector that can transduce with high efficiency, provide a robust and long-term expression, and elicit no host immune response.

1.9.1. Non-viral vectors

Non-viral vectors have the advantage of avoiding some of the problems associated with viral vectors such as oncogenic effects and unexpected immune response. Further, non-viral vectors have advantages regarding simplicity of use and ease of large-scale production. These techniques are categorised into two general groups: first, naked DNA delivery by physical methods, such as electroporation, second, delivery mediated by a chemical carrier such as cationic polymer and lipid.

1.9.1.1. Naked DNA delivery

Transfection of naked DNA into cells is highly inefficient because cellular uptake of DNA relies on non-specific endocytosis and these naked DNAs are degraded by the lysozyme. Therefore, naked DNA import into the nucleus is more difficult (Wiethoff and Middaugh, 2003). However, these cellular DNA uptakes can be improved by the use of electroporation which increases cell permeabilization through controlled electric fields (Coster and Chilcott, 2002). The injection of naked DNA followed by the application of

pulsed electric fields has been used for gene transfer to the liver (Liu and Huang, 2002), skin (Zhang *et al.*, 2002), and subcutaneous tumours (Lucas *et al.*, 2002).

1.9.1.2. Chemical Carrier

A common physical method of introducing DNA into cells relies on the use of cationic carrier (Pedroso de Lima *et al.*, 2001; Taranejoo *et al.*, 2015). The addition of cationic lipids (in the form of liposome) to plasmid DNA decrease the negative charge of the nucleic acid and facilitates its interaction with the cell membrane (Wiethoff and Middaugh, 2003). Liposomes are lipid bilayers entangle a fraction of aqueous fluid. DNA will spontaneously associate to the external surface of cationic liposomes, and these liposomes will interact with the cell membrane. Using this method *in-vitro* 90% transfection efficiency can be achieved. To enhance the transfection efficiency obtained with liposomes in hard to transfect cells, molecular conjugates consisting of a protein such as an asialoglycoprotein and transferrin or synthetic ligand have been used. Despite these improvements in non-viral gene delivery, transfection of certain cell types remains inefficient in comparison to viral vectors (Washbourne and McAllister, 2002). Non-viral gene transfer systems are also comparatively toxic to certain cell types. The toxicity is mainly due to its cationic nature and a non-cleavable molecular structure that restricts its biomedical applications (Taranejoo *et al.*, 2015).

1.9.2. Viral vectors

Viruses are obligate intracellular parasites that have evolved to efficiently replicate their genetic material while avoiding detection by the host immune system. Hence, by replacing non-essential viral genes with foreign genes of interest a harmless highly efficient recombinant viral vector gene delivery system can be made. Viral gene delivery allows the expression of a gene in almost any mammalian cell type. However, selecting the best viral gene delivery system for a particular experimental aim can be challenging. Viral based vector systems that are under development include Adenovirus, Adeno-associated virus and lentivirus. Table 1.2 shows most common viral vectors used in gene transfer.

Viral vector	Characteristics	Advantages	Limitation
Adenovirus	36kb double stranded DNA virus, Non-enveloped, Non-integrating	Large genome capacity, easy producing high titer	High immunogenicity
Adeno-associated virus	4.7kb single stranded DNA virus, Non-enveloped, Non-integrating	Low immunogenicity	Small genome capacity
Lentivirus	8kb, single stranded RNA virus Enveloped and Integrating	Long term gene expression, Highly efficient gene transfer	Insertional mutagenesis

Table 1.2. Viral vectors for *in-vivo* gene transfer

Viruses have advantages and limitations for gene delivery. Although adenovirus is able to package up to 35kb large genome, adenovirus is highly immunogenic. In contrast, AAV is less immunogenic and has only 4.7kb packaging capacity. The lentivirus is capable of long-term gene expression due to the viral genome integration into a host cell. However it might thereby cause insertional mutagenesis.

1.9.2.1. Pseudo typed Lentiviral vectors

The lentiviruses are a subgroup of the retroviruses, the family *Lentiviridae*, which are able to infect both proliferating and non-proliferating cells (Kim *et al.*, 1998). They are more complicated than simple retroviruses and containing six proteins *tat*, *rev*, *vif*, *vpr*, *nef* and *vpu*. *Vpr*, *Vif* and *Nef* found in the viral particle, are involved with integration, maturation and budding during the viral life cycle. *Vpu* indirectly assists in the assembly of the virion by promoting the release of newly synthesised *env* glycoproteins from CD4 molecules. This enables *env* to be transported to the cell surface, providing proteins for the outer membrane coat.

Tat and *rev* provide essential gene regulatory functions and are therefore present in all lenti viruses. They enhance the rate of transcription and mediate nuclear export of un-spliced viral RNA, respectively (Blesch, 2004). The lentivirus-encoded gag matrix protein, integrase enzyme and *vpr* protein interact with the nuclear import machinery and facilitate the import of the viral genome.

The most commonly used lentiviral vectors have been developed from the Human Immunodeficiency Virus-1 (HIV-1). An Early version of recombinant HIV vectors was of limited use due to their strict host cell tropism and the conserved potential risk of generating wild-type virus (Poznansky *et al.*, 1991). In order to overcome the host cell tropism, lentiviral vectors were pseudo typed with the vesicular stomatitis virus G (VSVG) envelope protein. This increased the host cell tropism of lentiviral vectors and substantially reduced the potential to form wild-type HIV (Naldini *et al.*, 1996). The use of a separate plasmid containing a heterologous envelope makes it extremely unlikely to generate replication-competent virus, as two independent homologous recombinant events would have to occur. VSVG pseudo-typed vectors transfect both dividing and non-dividing cells in vitro (Reiser *et al.*, 1996).

1.9.2.2. Improve Biosafety using pseudo-typed lentivirus

The possibility of insertional activation of an oncogene following transfection of lentiviral vectors has been addressed by the development of self-inactivation (Sin) lentiviral vectors. The HIV-1 provirus is separated into the *cis*-acting sequence, and *trans*-acting sequence, this split-genome, the conditional packaging system is based on existing viral sequences and acts as a built-in device safeguarding against the generation of productive recombinants to improve biosafety (Dull *et al.*, 1998). HIV contains two regulatory genes, *tat* and *rev*, essential for viral replication and four accessory genes, *vif*, *vpr*, *vpu*, and *nef* that are not crucial for viral growth *in-vitro* but are critical for *in-vivo* replication and pathogenesis. Consequently, the *cis*-acting sequences (LTR, RRE, splice donor, acceptor, Ψ , PBS, PPT and cPPT) are instead linked to the transfer vector constructor. The transacting genes (*gag*, *pol*, *env*) are located on two separate plasmids. The transfer vector consists of modified LTRs, a transgene driven by a suitable promoter and packaging signal (Figure.1.8). The 3' sequence of the U3 element has been modified remaining only 18bp, thus eliminating promoter activity and ensuring that proviruses resulting from this vector can not transcribe their full genome and therefore self-inactivating (Sin)(Zufferey *et al.*, 1998).

Further features of these vectors include an extended packaging signal the cPPT/CTS (central termination sequences) element, which enhances transduction in non-dividing cells. The 3rd generation packaging system matches the performance of its predecessors regarding both yield and transducing efficiency. However, it increases significantly the predicted biosafety of the vector (Dull *et al.*, 1998; Zuffery *et al.*, 1998).

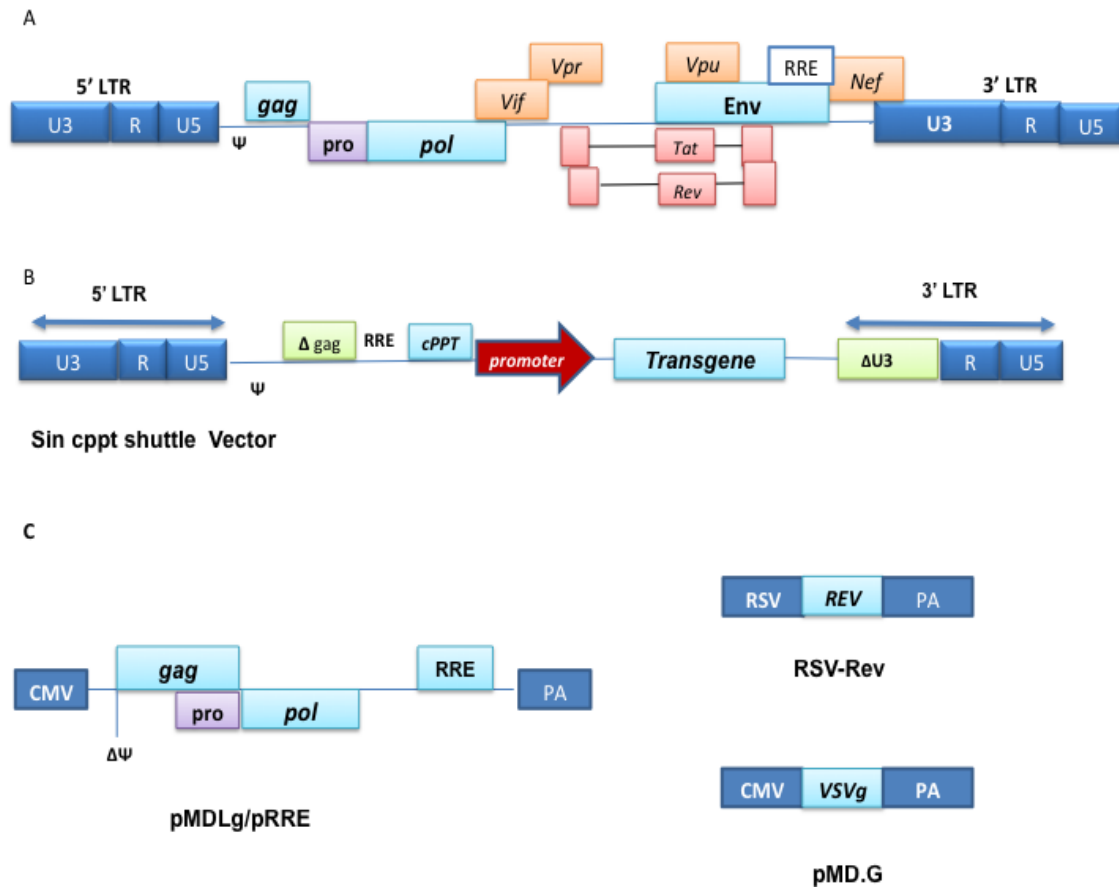


Figure 1.11. Schematic representation of the HIV provirus and the 3rd generation packaging constructs

A) The original HIV-1 provirus, B) 3rd generation self-inactivate shuttle plasmid, C) Packaging plasmids. Separate trans- and cis-acting element improve biosafety from self-inactivation pseudo-typed HIV. The self-inactivating (Sin) lentiviral shuttle vector; strong trans-activator *tat* and *rev* exons have been deleted, and the viral sequences upstream of the *gag* gene have been replaced, the 3' LTR has an almost complete deletion of the U3 region, which is replaced by the TAT-independent Rous Sarcoma Virus (RSV) promoter. The vector contains a central polypurine tract (cPPT) to enhance vector potency and transgene expression. The 3rd generation packaging constructs: pMD.G, encodes an envelope to pseudotype the vector, here shown coding for vesicular stomatitis virus glycoprotein (VSVG) gene derived from the CMV promoter. pMDLg/pRRE expresses the *gag* and *pol* genes under the CMV promoter. RSV-Rev expresses the *rev* cDNA. Ψ -packaging signal, CMV is the hCMV promoter, PA-polyadenylation signal. The plasmid structures were modified Dull et al. (Dull et al., 1998).

1.9.2.3 Adeno associated virus

AAV vectors are developed from a parvovirus, which is naturally occurring adeno-associated virus. It was first isolated in 1966 in studies of pathogens in the respiratory tract. AAV is not autonomously replicating in animal hosts or cell cultures but it is rather dependent on a helper virus, adenovirus or herpes simplex for replication (Buller *et al.*, 1981; Mingozzi and High, 2013).

AAV belongs to the Parvoviridae family of viruses. Viruses in this family are small (20 to 26 nm) non-enveloped viruses containing a single-stranded DNA viral genome approximately 4.7kb size with palindromic 145 bases Inverted terminal repeat (ITRs) at each terminal. The genome of AAV encodes two open reading frames (ORFs), one encoding the genes responsible for replication (*Rep* gene) and the other encoding the viral structural capsid genes (Srivastava *et al.*, 1989; Berns, 1990).

Four regulatory proteins (*Rep*78, 68, 52 and 40) with overlapping amino acid sequences are translated from both spliced and un-spliced forms of the two mRNAs transcribed from the left side open reading frame. The right side opens reading frame contains the *Cap* gene, which produces three viral capsid proteins (*VP1*, *VP2*, and *VP3*). The unspliced transcript produces *VP1* (87kDa), the biggest of the capsid proteins. The spliced transcript produces *VP2* (72kDa) and *VP3* (62kDa). The *VP3* represents 80% of the total virion protein mass.

The AAV life cycle has a lytic and lysogenic stage for successful infection. In the presence of helper virus (adenovirus or herpes virus), the lytic stage occurs. During this stage, AAV undergoes productive infection characterised by genome replication, viral gene expression, and virion production (Daya and Berns, 2008).

AAV genome is the only example of an exogenous DNA that integrates at a specific site (*q13.3-qter*) in the human genome chromosome 19 and integrated AAVS1 site (Linden and Winocour, 1996). This site was first identified in cell culture (Kotin *et al.*, 1992), and

has also been identified in human tissues infected with wild-type AAV. However, in human tissues AAV was predominately found non-integrating in episomal forms, mirroring what is observed with recombinant vectors (Schnepp *et al.*, 2005). In addition, *In-vitro* experiments suggest that the AAVS1 locus is a safe integration site. It remains to be evaluated that AAV integration into this site is suitable for human gene therapy applications (Daya and Berns, 2008).

Current understanding of this process implicates cis-active signals, both in the viral genome and at the site of integration, as well as *Rep* 68/78 (AAV vector virions from which the *rep* gene has been deleted do not integrate in a site-specific manner) (Kyöstiö *et al.*, 1994; Linden and Winocour, 1996).

1.9.2.4. Recombinant Adeno associated virus (rAAV)

The viral genome comprises with genes and cis-acting regulatory sequences, and it is used for the design of recombinant viral vectors (Kay *et al.*, 2001). Recombinant AAV vectors have 96% of the viral genome removed from the vector, only the two 145-base pair (bp) ITRs which is sufficient for packaging and integration (Samulski *et al.*, 1983). The original recombinant AAV (rAAV) was produced by the transfection of a plasmid encoding the transgene cassette flanked by ITRs with a plasmid encoding *rep* and *cap* genes flanked by ITRs, which involved in intermolecular recombination (Yan *et al.*, 2005). The transfected cells were then infected with a helper virus, such as Herpes or Adenovirus (Buller *et al.*, 1981; Samulski *et al.*, 1983).

Figure 1.12 shows that rAAV packaging plasmids, the *Rep/Cap* genes contained plasmid decisive viral serotype and transgene expression cassette, which included tissue specific promoter and transgene followed by a polyadenylation signal (pA), Adenoviral helper plasmid which contains the minimal relevant function of Viral RNA (VA) and *E2A* and *E4A* genes.

Due to the difficulty to achieve high titre of viral production, and possible contamination of adenovirus or wild type wtAAV, the rAAV vector production systems have been optimised in a number of ways (Peel and Klein, 2000). Safety and vector yield have been improved in a number of ways. The first, packaging plasmid optimised and second, only the relevant helper functions in adenoviral helper plasmid design (Li *et al.*, 1997b; Xiao *et al.*, 1998).

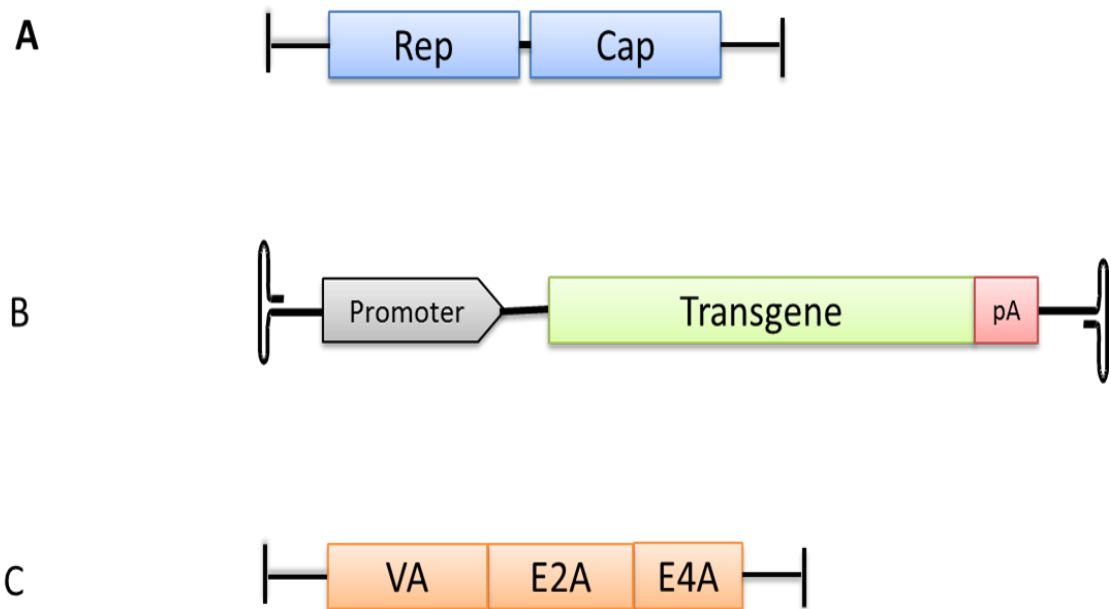


Figure 1.12. Schematic represents of rAAV viral packaging plasmids

A) Rep (*Rep* 78/68/52/40) and Capsid (*VP* 1/2/3) genes contained plasmid, B) Transgene expression cassette, which included promoter, transgene and followed by polyadenylation signal (pA), C) Adenoviral helper plasmid (Type-2 or 5 adenovirus), which is minimized to contain only relevant functions of Viral RNA (*VA*) and *E2A* and *E4A* genes minimized. *E*; denotes the early mRNAs that expressed before the initiation of viral DNA replication. The *E2* for encodes DNA polymerase that binds to the ITRs, so transcription and replicates the viral genome. The *E4* viral gene is involved in early transcription and disruption of the cytoskeleton. pA; Polyadenylation signal.

1.9.2.5. Serotypes

Recombinant AAV production requires shuttle AAV2 vector that has inverted terminal repeats (ITR), helper, and capsid plasmids (Hastie and Samulski, 2015). The capsid can be chosen for a specific tissue or cell type.

Numerous AAV serotypes have been identified with variable tropism; however, all of them share the same properties including genome size and organisation and, with small differences, the inverted terminal repeats share structure and function. At least 13 human and more than 100 nonhuman primate AAV serotypes have been identified so far, and rational design and evolution-based strategies have further engineered AAV capsides (Daya and Berns, 2008; Hastie and Samulski, 2015). The virus particles are purified by either column chromatography or gradient centrifugation. Caesium chloride (CsCl₂) or iodixanol is the most used for the gradient centrifugation, which can provide flexibility because a single method can be used to purify different AAV serotypes (Ayuso *et al.*, 2009).

One of the obstacles to AAV gene therapy is the presence of neutralising antibodies (NAbs) in human populations consequent on naturally occurring infection by wild type AAV. Current AAV-based vectors of common serotypes have significant rates of seropositivity ranging from 30% of the population with Nabs to AAV8 and about 60% of the population with pre-existing anti AAV2 immunity. It has been shown that pre-existing NAbs to the viral vector limits effective gene transfer in a way that is influenced by the route of administration and organ targeted. Whether AAV capsid modifications or the use of novel AAV serotypes will circumvent this obstacle remains to be seen (Calcedo *et al.*, 2011).

1.9.2.6. Tissue-specific promoter

The expression cassette consists of promoter, transgene and polyadenylation signal in addition to the viral ITRs. Vector properties that could reduce some of the risks including infectivity of special cell or tissue (Kay *et al.*, 2001). Therefore, choosing the correct promoter, especially a tissue-specific promoter, is a major step toward achieving successful transgene expression (Shevtsovva *et al.*, 2005; Zheng *et al.*, 2008).

1.9.2.7. AAV engineering for large transgenes

The main limitation of using AAV is the limited genome capacity for self-complementary (sc) and single-stranded (ss) DNA - maximum 2.3kb and 4.7kb respectively; however, the transgenes required for diseases such as Cystic fibrosis, Haemophilia A, and Leber's Congenital Amaurosis (LCA, RPE65) are larger than 5kb. In order to deliver such large therapeutic genes, investigators have attempted different strategies.

AAV vectors for delivery of larger genomes have been produced; however, these vectors are inefficient, and multiple investigators have characterised their limitations (Allocca *et al.*, 2008; Lu *et al.*, 2008; Wu *et al.*, 2010). The large transgenes using AAV vectors include splitting large genomes for co-delivery using two AAV vectors, or exploiting head-to-tail concatemer formation. Despite solving the current packaging limitations of AAV with this approach, cells have to be infected with numerous virus particles to increase the efficiency of transduction, and the system is dependent on the homologous recombination (Halbert *et al.*, 2002). Using deleted transgenes that retain therapeutic potential and optimising expression cassettes with minimal transcriptional regulatory elements, when possible, have emerged as alternative solutions.

Partially packaged vectors could be able to re-enter the virus replication after infection. It would require either two packaged ITRs or ITR correction of the truncated end of the genome. The large-gene reassembly mechanism of the partial packed vectors are different since the partially packaged genomes are missing an ITR and because the ITRs

are thought to stimulate intermolecular recombination and non-homologous end joining (Inagaki *et al.*, 2007; Lai *et al.*, 2010).

There are many ways to approach fitting a bigger gene into a smaller virus, for example, truncating the gene and use the short transcriptional regulatory elements (Ghosh *et al.*, 2008; Ostedgaard *et al.*, 2005). Moreover, there are dual AAV trans-splicing or hybrid vectors for large transgenes. The trans-splicing system transgene cassette is split between two rAAV vectors containing appropriately placed splice donor and acceptor sites. Transcription from rAAV molecules is followed by correct splicing of the mRNA transcript, resulting in a functional gene product. This application enables AAV to deliver therapeutic genes up to 9kb in size; however, it is less efficient than rAAV.

The major problem in the current dual-vector approaches is that they all depend on the molecular property of the target gene itself. Essentially, an optimal gene-splitting site must be present in order to efficiently express a gene with the trans-splicing and overlapping AAV vectors (Ghosh *et al.*, 2008). The hybrid vectors significantly improved transduction of the trans-splicing vectors. Trapani and colleagues generated efficiently transduced dual hybrid AAV vectors, which reconstitute a large gene by either trans-splicing, homologous recombination, or a combination of the two (hybrid) (Trapani *et al.*, 2014). These strategies for large transgene expressing via AAV vectors have potential to be effective depending on the transgene and provide evidence of the efficacy of over-sized transgene delivery.

1.9.3. Current status of gene therapy for Haemophilia

Haemophilia has been an attractive target for investigation of gene therapy approaches because biologically active clotting factors can be delivered by various viral delivery methods, which could lead to a modest increase in clotting factor levels that can rescue haemophilia (High and Anguela, 2015). Particularly, here are several reasons why haemophilia A is suitable candidate for gene therapy: i) FVIII production is not regulated in response to bleeding; ii) The broad therapeutic index of FVIII minimises the risk of

overdoses; iii) Delivery of FVIII into the bloodstream does not require expression of the gene by a specific organ and iv) even low levels of the protein can be beneficial (Kaufman *et al.*, 1999; Roth *et al.*, 2001). In the last two decades, gene therapy approaches have been applied to haemophilia via non-viral or viral gene deliveries summarised in table 1.3 (Roth *et al.*, 2001; Powell *et al.*, 2003; Manno *et al.*, 2003; Manno *et al.*, 2006). AAV-based gene transfer for haemophilia B has been one of the highlights of successful clinical viral gene therapy advances in the past five years (Nathwani *et al.*, 2011; Nathwani *et al.*, 2014). In contrast, clinical trials for haemophilia-A using viral vectors (Adenovirus, Retrovirus and AAV) showed unsuccessful results that failed to achieve persistent phenotypic correction, which utilised *ex-vivo* fibroblast transduction, a retrovirus vector, or AAV for FVIII gene delivery (Monahan *et al.*, 2010) (Table 1.3).

The big obstacle for AAV gene transfer for haemophilia A is that at 7kb the cDNA of full length FVIII far exceeds the 4.7kb limit of AAV packaging capacity. Because the large B-domain is not necessary for pro-coagulant activity, a B-domain deletion version of FVIII could be created and named FVIII-SQ, which has only a 14 amino acid linker between a2 and a3. Therefore, current gene therapy applications for haemophilia A have focused on B-domain deleted FVIII due to its advantages of reduced overall cDNA size for packaging into viral vectors and increased mRNA levels (Pipe, 2009).

The B-domain deleted hFVIII trial has been carried out recently, in which the AAV vector contains single stranded rAAV2/5 FVIII SQ, sponsored by BioMarin therapeutics, (clinical trials identifier #: NCT02576795) (High and Anguela, 2015). The preliminary data has been released from an ongoing Phase I/II clinical trial in which nine severe haemophilia A patients have received a single dose of the therapy and seven of those have been treated at the high dose, 6×10^{13} vg/kg. For the seven patients treated with the high dose, as of each patient's most recent reading (12~28 weeks, post- administration), six of seven patients had FVIII levels above 50%, and the seventh was above 10%. Moreover, there are no serious clinical complications observed

(<https://www.hemophilia.org/Newsroom/Industry-News/> Preliminary-Clinical-Trial-Data-Shows-Progress-for-BioMarin-s-Factor-VIII-Gene-Therapy-National haemophilia foundation).

Another novel 31 amino acid linker peptide between the $\alpha 2$ and $\alpha 3$ was generated by the Nathwani group and is currently in the process of being developed as a clinical grade single stranded HLP (liver specific) promoter-driven FVIII V3co packaged in AAV8 and produced in HEK-293T cells for human trial (Prof Amit Nathwani, personal communication).

Overall, viral gene therapy promises to deliver a significant advance over current treatment for haemophilia.

Vehicle	Transfer method	Gene	Patients treated	Best outcome	Complications	Reference
Gamma-retrovirus transduction of autologous fibroblast	Ex-vivo	F9	2	Transient expression (2%)	No adverse effects reported	Xinfang et al 1996
Electroporation of autologous fibroblasts (BDD-FVIII)	Ex-vivo	F8	12	Transient expression (2%)	No adverse effects reported	Roth et al 2001
Gamma-retrovirus (BDD-FVIII). Intra vascular	In-vitro	F8	12	Transient expression (2%)	No adverse effects reported	Powell et al 2003
Adenovirus	In-vitro	F8	1	Transient expression (2%)	Transaminitis, Thrombocytopenia	No published reports 2002
ssAAV2/2. Intramuscular	In-vitro	F9	8	Transient expression (2%)	No adverse effects reported	Manno et al 2003
ssAAV2/2. Hepatic artery infusion	In-vitro	F9	7	Transient expression (2%)	Transient transaminitis	Manno et al 2006
scAAV2/8, codon optimized FIX, Intra vascular	In-vitro	F9	10	Persistent expression (1%-6%)< 3years	Transient transaminitis	Nathwani et al 2011, 2015
scAAV2/8, FIX Padua Intra vascular	In-vitro	F9	6	Variable expression (0.5%-25%)< 6months	No adverse effects reported	Monahan et al 2015
ssAAV2/5, codon optimized BDD-FVIII, Intra vascular	In-vitro	F8	9	Variable expression (>1%-150%) < 12weeks	Transient transaminitis	Biomarin 2016

Table 1.3. Summary of completed and ongoing Phase I/II clinical trials for haemophilia gene therapy

Gene therapy clinical trials for haemophilia have used three types of viral vector, adenovirus, retrovirus and AAV. One patient received an adenoviral-mediated treatment for haemophilia A, and there has been one trial of retroviral gene transfer of FVIII, and the remaining treatment has been used AAV. The table adopted and modified from Swystun et al. (Swystun and Lillicrap, 2016).

1.10. Research Aim

The aim of this project was to investigate functional roles of modified B-domain linkers of FVIII. We aimed to determine if the length of B-domain and *N*-linked glycosylation of FVIII influences FVIII expression.

1.10.1. Brief outline of strategy:

B-domain deleted (BDD) FVIII retains full procoagulant function, while partial BDD FVIII, where 226 amino acids of the N-terminal remain (referred to as N6), increases *in-vitro* secretion of FVIII 10-fold compared with BDD-FVIII (Miao *et al.*, 2004). Since N6-FVIII retains the six *N*-linked glycosylation consensus sequences (N-X-T/S) dispersed across the proximal 226 amino acids, it was hypothesised that the *N*-linked glycosylation motifs of N6-FVIII are key for improvement of FVIII expression. This led to the development of a 31 amino acid B-domain linker, FVIII-V3, consisting of six *N*-linked glycosylation triplets juxtaposed (McIntosh *et al.*, 2013). To further improve FVIII expressions, the natural FVIII coding sequences were modified to optimal mammalian coding sequences (codon optimisation), resulting in a 20-fold increment of FVIII mRNA expression as opposed to native FVIII mRNA (Ward *et al.*, 2010).

Currently, the most effective version of engineered FVIII is FVIII-V3, which has shown efficient and sustained transgene expression *in-vivo* using AAV. However, the mechanisms behind the improved expression of FVIII-V3 has not been established.

To address this, I investigated the length effects of the *N*-linked glycosylation motifs and FVIII expression. In this study, I undertook a head to head comparison of *in-vitro* FVIII expression levels of codon optimised FVIII constructs and performed biochemical analysis for novel FVIII variants. Furthermore, I developed additional mutants to understand minimum linker length and optimal composition, which were validated *in-vivo*.

Strategy:

1. Wild type SQ, N6 FVIII variants and Codon optimised FVIII variants (V1, V3, V5, N6, and SQ) were cloned into the pRRL-PGK-WPRE-SV40 pA vector for lentivirus production.
2. Stable cell lines expressing FVIII variants were derived and evaluate mRNA transcription levels and FVIII expression.
3. Optimised purification method for FVIII proteins was developed to enable analysis of the biochemical features of FVIII variants.
4. The *N*-linked glycosylation pattern of FVIII variants was investigated using mass spectrometric analysis.
5. FVIII variants were cloned into the pAV-HLP-pA vector for AAV production, then the efficacy of AAVs was assessed *in-vivo* using the C57Bl/6 mouse model.

Chapter 2

Materials and Methods

2.1. Basic Bacterial Manipulation

2.1.1. Transformation of E-coli with Plasmid DNA

Plasmid DNA (0.1-0.01 ng/5 μ L) was incubated with 50 μ L of competent cells (DH5 α , New England Biolabs[NEB], Hitchin, UK) in a 2mL tube (supplied with competent cells) for 30 minutes on ice. The cells were then heat shocked for 40 seconds in a 42°C water bath and immediately returned on ice for a further 2 minutes. Subsequently, 450 μ L of sterile SOC medium (supplied with competent cells) were added, and the cell suspension was incubated at 37°C and shaken at 200 rpm for an hour. Following incubation, 50 μ L of cell suspension was spread using a sterile plastic rod onto a 90mm Petri-dish (VWR , Lutterworth, UK) containing solid Luria-Bartani (LB, MP Biomedicals, Cambridge, UK) agar medium (10g bacto-trypton, 5g yeast extract, 10g NaCl and 15g Agar) containing the appropriate antibiotics. The Petri dishes were then incubated overnight at 37°C in an inverted position to allow for bacterial colony growth.

2.2. Molecular cloning

2. 2.1. DNA Restriction Digest

DNA was cut with restriction enzymes to excise the required DNA fragments from plasmids. Restriction digests were carried out using the following conditions. 5 μ g DNA was added to 5 μ L of the appropriate reaction buffer (10X, NEB), 0.5 μ L 100X BSA (Bovine serum albumin), 1unit of the required enzyme (NEB) and molecular biology water added up to 50 μ L. Reactions were carried out at 37°C for 1.5 hours. All digested vector backbone and FVIII insert DNA samples were analysed on a 1% agarose gel at 120V.

2.2.2. Isolation of Plasmid DNA fragments by Agarose Gel Electrophoresis

Electrophoresis grade agarose (Bioline, London, UK) was dissolved at the desired final concentration (usually 1% [w/v] depending on DNA size) in 1x TBE (Tris-Borate-EDTA) buffer. To dissolve the agarose, the solution was boiled in a microwave oven. The gel mix was then allowed to cool to 60°C, following which SYBR® Safe (Fisher Scientific, Loughborough, UK) was added to the mix at the final concentration 0.5µg/mL. The gel mix was immediately poured into a gel former containing a suitably sized comb and allowed to set. Subsequently, it was submerged in a horizontal gel electrophoresis tank containing a 1XTBE buffer. Sample loading dye was added to each DNA sample, a ladder was added to one well of the gel for size determination (Hyperladder 1Kb, Bioline). Required bands were excised and purified using the Gel Purification kit (Qiagen, Crawley, UK) according to the manufacturer's instructions. The agarose gel was viewed under blue light illuminator, and a gel fragment (containing the DNA fragment of interest) was excised from the rest of gel with a clean scalpel and placed in a 1.5mL microcentrifuge tube (Eppendorf, Stevenage, UK). Three volumes of binding buffer QG (supplied by the manufacturer) was added to one volume of gel, followed by incubation at 55°C for 10 minutes to assist dissolution of the gel slice into the buffer. When agarose gel had dissolved, one gel volume of Propanol-2 (VWR) was added, and then the sample was transferred to QIAquick® spin column (supplied by the manufacturer) and centrifuged down at one minute, 12,000xg. The flow-through was discarded and 750µL wash buffer PE was applied to the column, which was spun down and the eluent discarded. Finally, 30µL of ddH₂O (double distilled water) was added to the column, and allowed to stand for one-minute incubation. Then finally centrifugation of the column for one minute at 12,000xg enabled collection of the eluate containing isolated DNA.

2.2.3. Dephosphorylation of Backbone DNA

To remove 5' phosphate groups from vector backbone DNA (to prevent self-ligation) remaining DNA was incubated at 37°C for an hour with 1X NEB buffer 3 (NEB) and 0.5units/ μ g DNA Calf Intestinal Phosphatase (CIP, NEB). DNA was purified by using the gel extraction kit (Qiagen) as per the manufacturer's instructions.

2.2.4. Klenow filing

Sticky ended DNA was blunt ended by 3' overhang removal and 3' recessed end fill-in. For this DNA was dissolved in 1X NEB buffer 4 (NEB) at a final concentration of 33 μ M deoxyribonucleotide triphosphates (dNTP, Life technology). Then 1 unit DNA Polymerase I, Large Fragment (Klenow, NEB) per microgram DNA was added and the mixture incubated for 15 minutes at 25°C. 0.5M ethylene-diamine-tetra-acetic acid (EDTA) was added to a final concentration of 10mM and heated at 75°C for 20 minutes to stop the reaction. DNA was cleaned by PCR purification (Qiagen) to remove enzyme.

2.2.5. DNA ligation

All ligations for the cloning of FVIII elements into the pRRL PGK WPRE backbone and FVIII elements into the pAV2 HLP pA backbones were carried out using Quick DNA ligase (NEB) according to manufacture's recommendations. Briefly, an insert to vector molar ratio of 1:1 to 5:1 was used. To the DNA 10 μ L of 2X Quick DNA ligase buffer (supplied by the manufacturer), 1 μ L of Quick DNA ligase (400U/ μ L, supplied by the manufacturer) and up to 10 μ L molecular biology water was added. As negative control vector backbone DNA alone or insert DNA were used under the same reaction conditions. Control reactions were later used to determine relative background levels of self-ligated backbone DNA. All reactions were incubated for 10 minutes at room temperature; the ligated product was then transformed into One shot® Stable3 competent E.coli (Invitrogen Life Technologies, Paisley, UK).

2.2.6. Transformation of One Shot® Stbl3™ Bacterial Cells

For transformation of plasmid DNA, 50µL of individual One shot® Stable3 competent cells were thawed briefly on ice. 5µL of each ligation mixture including negative control was then added to one individual aliquot of competent cells and left for 10 minutes on ice. For positive control 1µL of 50pg/µL, PUC19 plasmid DNA (Life Technology) was also added to 50µL of One shot® Stable3 cells and incubated on ice for 30 minutes. Next, to allow for the uptake of DNA, all samples and controls were heat shocked at 42°C for 40 seconds and immediately placed on ice for a further two minutes. 250µL of SOC medium (Life Technology, supplied by the manufacturer) was then added to each sample followed by one hour incubation at 37°C 220rpm with shaking. As all constructs contained an ampicillin resistance gene, total reactions were spread onto agar plates containing 100µg/mL carbenicillin (Melford, Suffolk, UK) under aseptic technique. Plates were incubated at 37°C overnight for the colony formation then selection of colonies was performed the following day.

2.2.7. Screening colonies

To determine whether ligations had been successful plates were first checked to ensure that higher numbers of colonies were present for each construct in comparison to negative control. The positive control plate was used to verify that transformation had occurred. Following these checks colonies were picked using pipette tips and placed in 5mL of LB medium (MP Biomedicals) containing carbenicillin 100µg/mL. Samples were left in a 37°C shaking incubator overnight.

The following day, DNA was extracted from 1mL of the cultures using the NucleoSpin® Plasmid Kit (Fisher Scientific) as per the manufacturer's instructions. 4mL of each culture was reserved and stored at 4°C. To ascertain whether the correct clones had been generated the extracted DNA was used in a diagnostic restriction digest whereby the enzymes selected would generate fragments of sizes that enabled correct constructs to

be differentiated from the incorrect only. All diagnostic digests were carried out at 37°C for 2 hours with the following components per sample: 5µL DNA, 1µL 10X Buffer (supplied by the manufacturer), 0.1µL 100X (BSA), 0.25µL enzyme and 3.65µL molecular biology water. Samples were run on a 1% agarose gel at 120V for an hour. Where positive digests were identified the corresponding 4mL of reserved bacterial culture was used to inoculate a further a 500mL of LB medium containing ampicillin. These cultures were incubated at 37°C overnight with 225rpm shaking. The next day DNA was extracted from the cultures using the endonuclease free MAXI Prep kit (Qiagen) as per the manufacturer's instructions.

2.2.8. Site-Directed Mutagenesis

The linker peptide variants were generated using the Q5® Site-Directed Mutagenesis kit and primer designated NEB program (NEB). The pair of primers for FVIII variants were designed using NEBase Changer. pAV HLP FVIII-V3 pA was used as the PCR template. Table 2.1 shows each primer pair for PCR.

To prepare PCR mixture: Q5 Hot Start High-Fidelity 2X Master Mix 12.5µL, 10µM each forward and reverse primer, 10ng of template DNA and top up Nuclease-free water until 25µL. Mix reagents completely and then transfer to a thermocycler. Perform the following cycling conditions: Initial denaturation, 98°C 30 seconds, then followed by 25cycles 98°C 10 seconds, 50~72°C 10~30 seconds, 72°C 20~30 seconds/kb. The final extension is 72°C 2 minutes. After PCR, there is one more step: Kinase, Ligase & DpnI (KLD) treatment assemble the following reagents: 1µL of PCR product, 5µL of 2X KLD Reaction Buffer, 1µL of 10X KLD Enzyme Mix and 3µL of Nuclease-free Water, mix well and incubate at room temperature for 5 minutes. After PCR and DNA transformed as recommended *E.coli* strain (DH5α).

Colonies pick up then performed mini-prep for DNA extraction. All mutations were confirmed by DNA sequencing (Beckman, UK).

N0	Forward	5' CCCCAGTGCTGAAGAGG
	Reverse	5' CTGGCTGAAGCTCCTGGG
N1	Forward	5' CCCCAGTGCTGAAGAGG
	Reverse	5' AGTGGCATTCTGGCTGAAG
N2	Forward	5' CCCCAGTGCTGAAGAGG
	Reverse	5' AGACACATTAGTGGCATTCTGG
N3	Forward	5' CCCCAGTGCTGAAGAGG
	Reverse	5' GCTGTTGTTAGACACATTAGTGG
N4	Forward	5' CCCCAGTGCTGAAGAGG
	Reverse	5' GCTGGTGTGCTGTTGTTAG
N5	Forward	5' CCCCAGTGCTGAAGAGG
	Reverse	5' GCTGTCATTGCTGGTGTG

Table 2.1. Primer sets for mutagenesis

FVIII variants N0 to N5 generated based on pAV2 HLP V3 plasmid. Primer pairs were designed for NEB Q5 site direct mutagenesis using NEBase Changer.

2.3. Genomic copy number correction

2.3.1. Quantitative Real-Time PCR (qPCR) for the determination of proviral copy number for human cell lines

To determine FVIII genome copy number per cell, genomic DNA was extracted from stable cell lines using the DNeasy® Blood and Tissue kit (Qiagen) as per the manufacturer's instructions. For each sample DNA was diluted to an approximate concentration of 7.5ng/μL and loaded in 5μL per well in duplicate to a 96 well Q-PCR plate. 20μL of Q-PCR master mix (12.5μL 2X SYBR Green master mix, 1μL forward PGK primer- 5' TCTCGCACATTCTTCAC GTC-3', 1μL reverse PGK primer- 5' GTCCGTCTGCGAGGGTACTA-3' each 2.5μM, 5.5μL molecular biology water per well) was then added to each well and cycling conditions were carried out. Thermal cycling was started with denaturation at 95°C for 10 minutes, followed by 35 cycles of 95°C for 5 minutes, 95°C 10 seconds and 60°C for 30 seconds. The amplification was followed by melting curve analysis. Copy number was determined by a pRRL PGK WPRE plasmid DNA standard (PGK primers above), and DNA concentration for each sample was determined from levels of housekeeping gene expression (derived from a human genomic DNA standard using GAPDH primers in a separate reaction). To calculate copies per cell of PGK copy number results were divided by the amount of DNA in each sample (ng); these Figures were then multiplied by 37.5 (the theoretical amount of DNA loaded in each well) and divided by 5,681 (the approximate number of cells from which 37.5ng of DNA is derived from human diploid copy per cell). To normalise FVIII levels for viral genome copy number (FVIII/copy/cell) values of % normal FVIII was divided by copy number from the corresponding cell line's DNA sample.

2.3.2. Quantitative RealTime PCR (qPCR) for the Determination of Proviral Copy Number for Mouse liver tissue

To determine viral genome copy number per cell, genomic DNA was extracted from mouse liver sample using the DNeasy® Blood and Tissue kit (Qiagen) as per the manufacturer's instructions. For each sample DNA was diluted to an approximate concentration of 7.5ng/μL and loaded in 5μL aliquots in duplicate to a 96 well Q-PCR plates. 20μL of Q-PCR master mix (12.5μL 2X SYBR Green master mix, 1μL forward FVIII HC primer 5' -AAGGACTTCCCCATCCTGCCT-3', 1μL reverse FVIII HC primer 5'-GGGTTGGCAGGAACCTCTGG-3' each 2.5μM, 5.5μL molecular biology water per well) was then added to each well and cycling conditions were carried out as described previously. Copy number was determined by a FVIII V3 plasmid DNA standard (using FVIII HC primers), and DNA concentration for each sample was determined from levels of housekeeping gene expression (derived from a mouse genomic DNA standard using mouse GAPDH primers in a separate reaction). To calculate copies per cell FVIII HC copy number results were divided by the amount of DNA in each sample (ng); these Figures were then multiplied by 37.5 (the theoretical amount of DNA loaded in each well) and divided by 6528.5 (the approximate number of mouse diploid cells from which 37.5ng of DNA is derived). To normalise FVIII levels for viral genome copy number (FVIII/copy/cell) values of % normal FVIII was divided by copy number from the corresponding liver DNA sample.

2.4. Total RNA extraction

To determine RNA levels per viral genome copy per cell, stable cell lines were homogenised using 1mL syringe and RNA was then extracted using the RNeasy Plus® kit (Qiagen) as per the manufacturer's instructions.

2.4.1. Measurement of FVIII RNA copy number analysis

500ng of RNA was converted to cDNA by using the Superscript III RT cDNA synthesis kit (Life technology). 2µL of cDNA samples, cDNA standards and negative controls (-RT and water) were then loaded onto 96-well Q-PCR plates in duplicate. 18µL of master mix (10µL 2X SYBR Green master mix, 1µL forward WPRE primer-5' TTCTGGGACTTTCGCTTTCC-3', 1µL reverse WPRE primer- 5' CCGACAACA CCAC GGAATTA-3', each 2.5µM and 6µL molecular biology water per well) was then added to each well, and Q-PCR cycling conditions were carried out as previously described. To normalise the data for the amount of cDNA loaded for each sample, a separate Q-PCR to quantify levels of housekeeping gene cDNA was performed using human GAPDH primers (5'-GGAGTCAACGGATTTGGTCGT-3', 5'-GGCAACAATATCCACTTT ACC-3') suitable for cDNA samples (Qiagen). To calculate RNA/copy/cell values of WPRE copies were divided by results for cDNA concentration (ng). Results were then divided by viral genome copy number per cell to give an approximation of transcription levels per copy.

2.4.2. Relative quantification measurements

The mRNA copy numbers of each cell types were calculated as follows: mRNA copy numbers = 2^{-CT} , where CT is the average threshold cycle number of the gene of interest. The normalised gene mRNA copy number is the copy number of the gene of interest divided by the copy number for GAPDH. The change in threshold cycle for each gene = ΔCT : The change in threshold cycle number relative to FVIII variants= $\Delta\Delta CT$: The fold-changes of FVIII variants are calculated by raising 2 to the negative power of the $\Delta\Delta CT$ value for each gene. For each FVIII gene $\Delta\Delta CT = 0$, and $2^0 = 1$.

2.5. Cell Culture Methods

2.5.1. Propagation of adherent cell lines

Dulbecco's Modified Eagle Medium (DMEM, Gibco, Paisley, UK) was purchased from Life technology. HEK-293T adherent cells (St Jude Children's Hospital, Memphis, USA) were grown in DMEM containing 4.5g glucose, 1mM L-glutamine and 10% (v/v) heat inactivated Foetal Bovine Serum (FBS, Gibco). Cells were grown at 37°C in a humidified 5% CO₂ incubator (Eppendorf) until cell populations were 80% confluent. Prior to subculturing to new flasks cells were washed in PBS (Phosphate Buffered Saline). Cells were detached by incubating in Trypsin-EDTA (TE, Invitrogen) for 5 minutes at 37°C. Trypsin was inactivated by dilution in 10 times complete cell culture medium, cells were then centrifuged at 400xg (Beckman Coulter, High Wycombe, UK) for 5 minutes. The supernatant was then discarded and the pellet re-suspended in DMEM containing 10%.

2.5.2. Propagation of suspension cell lines

Suspension HEK-293F cells (Invitrogen Life Technologies, Paisley, UK) were grown at 37°C in a humidified incubator with 8% CO₂ on 130rpm shaking incubator until cell populations reached 2.5x10⁶cells/mL. Prior to subculturing to new flasks, cells were centrifuged at 100xg (Beckman) for 5 minutes. The supernatant was then discarded and the pellet re-suspended in Glutamax containing Freestyle293 SFM (Life Technology) media. Cells were inspected daily for viability and were maintained in 125mL Erlenmeyer flasks (Corning, Appleton Wood, Birmingham, UK).

2.5.3. Long Term Storage of Cell Lines

2.5.3.1. Cryopreservation for adherent cell lines

Adherent HEK-293T Cells were centrifuged at 400xg for 5 minutes and re-suspended at a final density of 1×10^7 cells /mL of cryopreservation medium (9 volumes of FBS, 1 volume of Dimethyl sulfoxide [DMSO, Sigma]). The suspension was quickly transferred into 1mL labelled cryovials (Nunc, VWR) and the vials were then frozen at -80°C in a Mr Frosty containing isopropanol for 24 hours to ensure a -1°C /minute freeze rate. Finally, the vials were transferred to liquid nitrogen for long-term storage.

2.5.3.2. Cryopreservation for suspension cell lines

Suspension HEK-293F cells were centrifuged at 100xg for 5 minutes (Beckman bench top) and then re-suspended in a minimal volume of medium, vortexed for 45 seconds, and viability examined with trypan blue (Sigma) and counted. Cells were diluted 1×10^7 cells per ml in a 1:1 (v/v) mixture of conditioned medium and fresh Freestyle 293 SFM with 7.5% DMSO. The vials were frozen in the same manner as the adherent HEK-293T cells.

2.6. Production of Viral vectors

2.6.1. The 3rd generation Pseudo-typed Lentivectors

2.6.1.1. Co-transfection of HEK-293T cells

Early passage ($\leq P30$) of HEK-293T cells were cultured in 150cm^2 round tissue culture plates (Greiner, Stonehouse, UK) until they reached 80% confluence. Cells were cultured at 37°C , 5% CO_2 in DMEM (Gibco, Paisley, UK) with 10% FBS (Gibco) and enzymatically passaged every 2~3 days. For each virus construct $2 \times 150\text{cm}^2$ plates of HEK-293T cells were used at 2×10^7 cells on the day of transfection. For the transfection mixture 60 μL of 1mg/mL Polyethyleneimine (PEI Max, Polysciences Inc, Northampton, UK) was added to 3mL serum free DMEM. In a separate tube 5 μg of VSVG plasmid

(containing enveloping genes), 4.6µg of KGP3R plasmid (containing gag/pol genes), 2.4µg of RTR2 plasmid (containing RRE gene), 48µg of a transgene containing plasmid, were added to serum-free DMEM to a final volume of 3mL. The mixture containing DNA was then filtered into the PEI-containing mixture through a 0.45µm syringe filter. The solution was mixed and incubated at room temperature for 15 minutes in the hood (light off). The 3mL of transfection solution was then added dropwise to each 150cm² dish.

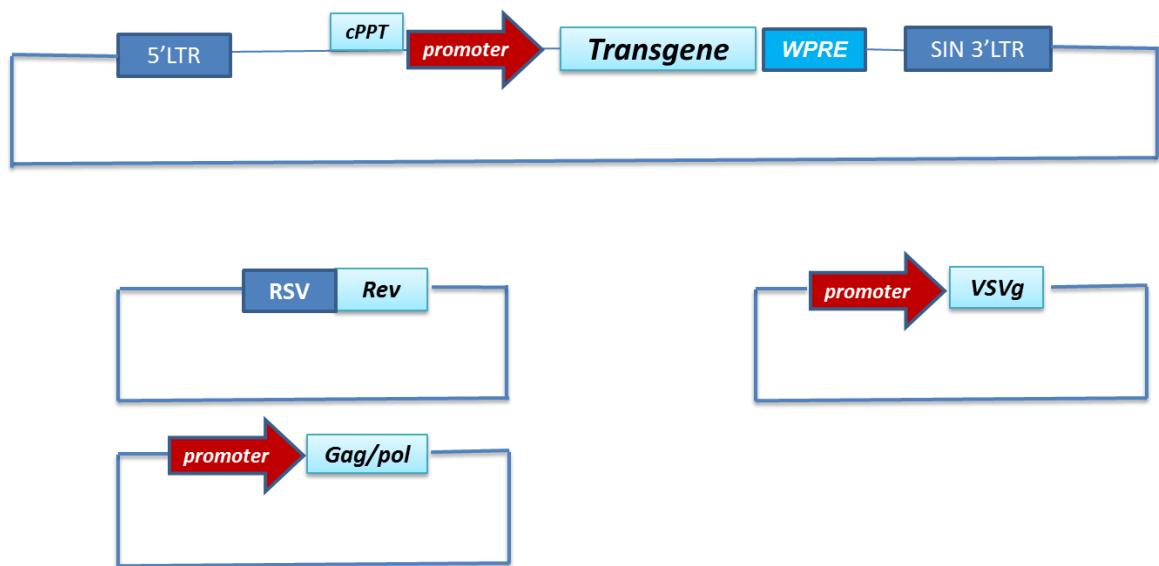


Figure 2.1. Schematic diagram of third generation lentiviral vector plasmids

The 3rd generation lentiviral vectors were improved bio-safety, because the original HIV-I provirus was separated to four plasmids. Shuttle vector comprised the transgene, the gag/pol packaging construct, Rev protein construct, and Envelop construct (Commonly use VSVg). 3rd generation lentivirus particles were produced by transient transfection to HEK-293T cells.

2.6.1.2. Viral supernatant harvest and concentration

After 24 hours of incubation, mediums were changed with 15mL of fresh 10% FBS-containing DMEM medium. The first harvest was taken after 24 hours, and another 15mL of fresh medium was added; after a further 24 hours, the second harvest was carried out. The combined first and second harvest of virus-containing cell culture mediums were centrifuged at 400xg for 5 minutes. Virus-containing mediums were then spun at 400xg for 5 minutes at 4°C, passed through a 0.45µm filter and spun at 46,600xg for 120 minutes at 4°C Beckman SW32 rotor. The supernatant was discarded, and the viral pellet was dissolved in 200uL of DMEM or 150-fold concentrated. Finally, each virus was aliquoted in a 10µL vial and stored at -80°C.

2.6.1.3. Titration of Lentiviral Vectors by Quantitative Real-Time PCR (q-PCR)

The viral titer was determined using the Q-PCR Lentivirus Titration Kit (Applied Biological Materials, ABM, London, UK), per the manufacturer's instructions. In brief, 2µL of the diluted purified viral preparation was added to 18µL of Virus Lysis Buffer and incubated at room temperature for 3 minutes. This solution is now referred to as the viral lysate. 2.5µL of viral lysate, 10µL reagent mixer, and 12.5µL of master mix were then loaded onto 96-well Q-PCR plates in duplicate. Two positive controls (STD1 and STD2) and negative controls were then added to each well. The Q-PCR primers supplied in this kit which is designed for all HIV-1 based vectors were added. Detection and cycling conditions were carried out as described in the manufacturer's instructions. The Ct value of the viral lysate is used to determine the titer of the unknown viral sample. The titer of viral samples can be calculated from Ct values by using company supplied on-line lentiviral titre calculator at [https://www. Abm good. com/ viralexpress/ LentiTitre. php](https://www.Abm good. com/ viralexpress/ LentiTitre. php).

2.6.2. Production of Adeno Associate Virus

2.6.2.1. Co-transfection of HEK-293T cells

For each virus 10x150cm² plates of low passage (\leq P30), HEK-293T cells were used at approximately 80% confluence on the day of transfection. Cells were cultured at 37°C, 5% CO₂ in Dulbecco's Modified Eagle Medium (DMEM, Gibco) with 10% heat-inactivated FBS and enzymatically passaged every three days. For the transfection mixture 750µL of 1mg/mL PEI was added to 15mL serum free DMEM. In a separate tube 225µg of Adeno helper plasmid (containing essential genes from the adenoviral genome that support rescue and replication of AAV genomes), 75µg of Rep2/Cap8 plasmid and 75µg of single stranded transgene containing plasmid was added to serum free DMEM to a final volume of 30mL. The mixture containing DNA was then filtered into the PEI-containing mixture through a 0.45µm of polyethersulfone (PES, Sartorius, Epsom, UK) syringe filter. The solution was mixed and incubated at room temperature for 15minutes. 3mL of transfection solution was then drop wise to each 150cm² dish.

2.6.2.2. Cells and supernatant harvest

After 24 hours of incubation, the medium was replaced with serum-free DMEM, and further 48 hours later cells were harvested using cell scrapers. Cells and supernatants were centrifuged at 800xg for 10 minutes. Supernatants were kept at 4°C for further PEGylation step, and cell pellets were re-suspended in TD buffer, pH7.5 (140mM NaCl, 25mM Tris, 3.5mM MgCl₂, 5mM KCl, and 0.7mM K₂HPO₄ in one litre of distilled water)

2.6.2.3. Lysis of cell pellet

Cell pellets were re-suspended in TD buffer. To lyse the cells and release viral particles freeze-thaw cycles of 5 minutes at liquid nitrogen (LN) followed by 5~10 minutes at 37°C were repeated at least five times.

2.6.2.4. PEGylation

2.6.2.4.1 Preparation for 40% PEG (2.5M NaCl)

Prior to preparing solution of 40% polyethylene glycol (PEG, Sigma), the 2.5M NaCl has prepared. First, add 146.1 g of NaCl (Sigma) to 800mLs distilled water, and dissolved properly then add 200g of polyethylene glycol (PEG). Allow PEG to dissolve by stirring and heating at 37°C. Then add a further 200g of PEG. Once fully dissolved adjust the volume to 1L and store at 4°C.

2.6.2.4.2. PEGylation of viral supernatant

Prior to purification, the supernatant was PEGylated by the addition of 40% PEG solution to a final concentration of 8% PEG. The supernatant and PEG solution was incubated on ice for 2 hours followed by centrifugation at 4000xg 30 minutes at 4°C. After centrifugation viral particles are sedimented with the PEG, the supernatant was discarded, and the pellet was dissolved in 1% Sarkosyl final concentration (Sigma). Finally, viral supernatant pellet and cell pellet were mixed (maximum volume: 12mL) and incubated at 37°C for 30 minutes with 50units/mL Benzonase (Sigma). Lysates were then spun at 4000xg for 20 minutes at 18°C, passed through a 0.45µm PES filter to remove cellular debris.

2.6.2.5. AAV Purification

2.6.2.5.1. Iodixanol purification

First, place 12mL of crude AAV prep in 89mm sorvall tubes using a long metal needle. This was then underlay with 9mL of 15% iodixanol using a syringe and long needle or kwill tube. Additional layers of 7mL 25% iodixanol, 5mL 40% iodixanol, and finally 5mL 60% iodixanol were also underlayered. Tubes were heat sealed and placed in a 70Ti rotor (Beckman Dickson), and centrifuged at 270,217xg, 75 minutes, 18°C and deceleration brake 1. After the centrifugation, the virus is contained in the 40% iodixanol layer.

To remove the virus, the tube was pierced with a 19-gauge needle, then swapped to a 19-gauge needle with a syringe attached. To allow the virus to be drawn out the top of the tube was pierced with a needle. The 40% layer was removed, taking the interphase between 40% and 60%, but avoiding the interphase between 40% and 25% as empty AAV particles collect in this interphase. The iodixanol-containing virus was placed into Amicon 100K filter device (Amicon, Millipore), which is pre-washed with PBS, the iodixanol is centrifuged for 20 minutes at 3000xg. After centrifugation, the virus is retained in the top of the device, and the iodixanol is in the flow through. The virus/iodixanol was topped up with PBS and mixed, then centrifuged 400xg again for 5 to 10 minutes. This was repeated until the iodixanol had been removed and final volume was 1mL. Purified AAV was filter sterilised through 0.22µm PES syringe filter (Sartorius) and stored at 4°C for further use.

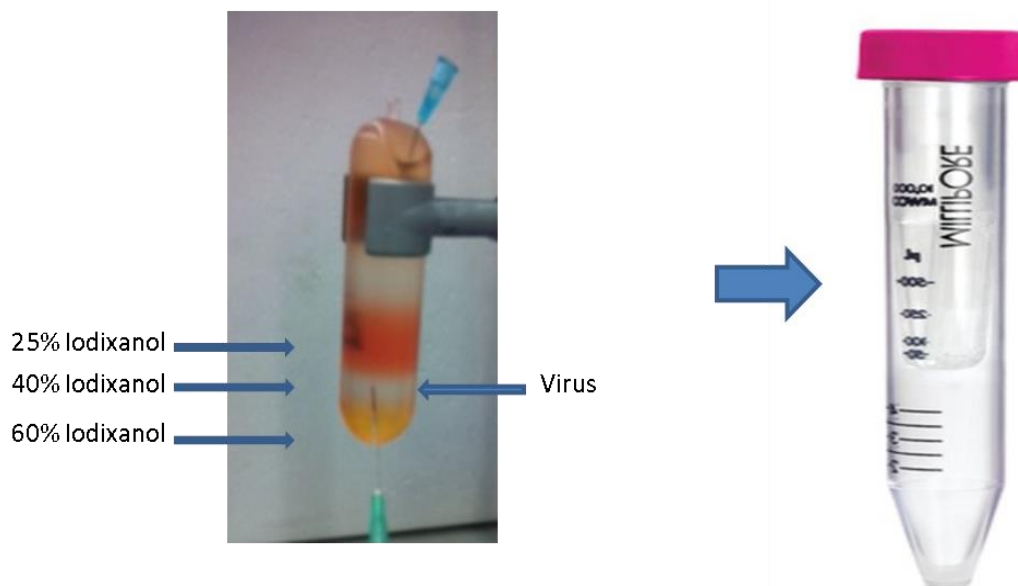


Figure 2.2. Separation of AAV particles from Iodixanol gradients and Amicon filtration

Three layers of iodixanol gradients separate AAV in the ultracentrifuge step. AAV can be collected from 40% iodixanol layer by using syringe needle. Virus contained 40% iodixanol layer was dilute with PBS, then iodixanol was removed by amicon 100k filter system.

2.6.2.6. AAV titrating

2.6.2.6.1. Titration of AAV by Q-PCR

To determine viral titre for single-stranded AAV HLP FVIII pA viruses, primers against the FVIII HC (Heavy chain) were used, and the titer of all AAV2/8 viruses was determined from a standard generated from a linearized FVIII HC containing plasmid DNA. Each virus was quantified in three different dilutions (1:100, 1:1000 and 1:10000). 10µL of virus samples, negative control samples (Water) and standards were added to 96-well plates in triplicate. To each well the following master mix was added: 12.5µL 2X QuantiFast SYBR Green PCR master mix (Qiagen), 1µL forward primer, 1µL reverse primer (each 2.5µM), 0.5µL molecular biology water (15µL master mix/well). Plates were then sealed, briefly spun by centrifugation and placed in a thermal cycler (Realplex, Eppendorf). After an initial heating period of 5 minutes at 95°C, the following steps were carried out for 40 cycles: 95°C 10 seconds and 60°C 30 seconds. The copy number of viral genomes was calculated from the standard curve using Realplex software (Eppendorf). To calculate viral genome copies per mL, copy number recorded per 10µL reaction was multiplied by the dilution factor and 100.

2.6.2.6.2. Titration of AAV by Alkaline gel

AAV was titred under denaturing conditions. The alkaline agarose gel was prepared by melting 0.8g agarose in 98mL water; once the gel had cooled to 50°C, 2mL alkaline electrophoresis buffer (50X; 2.5M NaOH, 50mM EDTA), was added, the gel was poured and allowed to set.

To 25µL of AAV, 8.5µL of alkaline sample loading buffer (4X; 20% Glycerol, 4X alkaline running buffer, 1.2% SDS, the tip of Xylene cyanol) was added and mixed; samples were cooled on ice before loading on the gel. When setting the gel was transferred to the electrophoresis chamber in the cold room after ensuring that the apparatus and the alkaline electrophoresis buffer were at 4°C. Samples and 5µL Hyperladder I (Bioline) to

wells on either side of the samples were loaded onto the gel. The gel was run overnight, 16~18hrs at 20V in the cold room.

To stain the gel, the gel was gently rocked in three gel volumes of 0.1M Tris, pH 8.0 for an hour to neutralise the gel. The gel was then transferred to a one gel volume solution of 4XGelred (GelRed Nucleic Acid Gel Stain, 10,000X, Biotium, Cambridge Bioscience, Cambridge, UK) in 0.1M NaCl and rocked gently for 2 hours. The gel was rinsed twice in water. Gel image was captured using a UV transilluminator (Genesys), bands were quantitated using Gene Tools, and virus concentration were calculated by DNA concentration of the band and the genome size of the virus.

In the sense of limited packaging capacity of single stranded AAV (approximately 4.7kb), linker modified FVIII viral particles were tested for DNA packaging condition using alkaline gel analysis, which exhibits total genome of AAV. Fully packaged self-complementary AAV viral DNA, which is containing a 2.3kb transgene of human FIX (hFIX) exhibit clear one band on the alkaline gel (Fig.2.3.A), while the FVIII carrying AAV genomic DNA bands showed multiple bands across the gel suggesting fragmented FVIII DNAs were packaged into the virus. These results suggested that not all the vector sequences were completely packaged into AAV capsids. The wide range of smears confirmed that a heterogeneous mixture of genomes with different lengths was packaged into AAV capsids (Lu *et al.*, 2008). The size of top the band was approximately between 4.87kb to 5.13kb, which was followed by fragmented DNAs (Fig. 2.3.B).

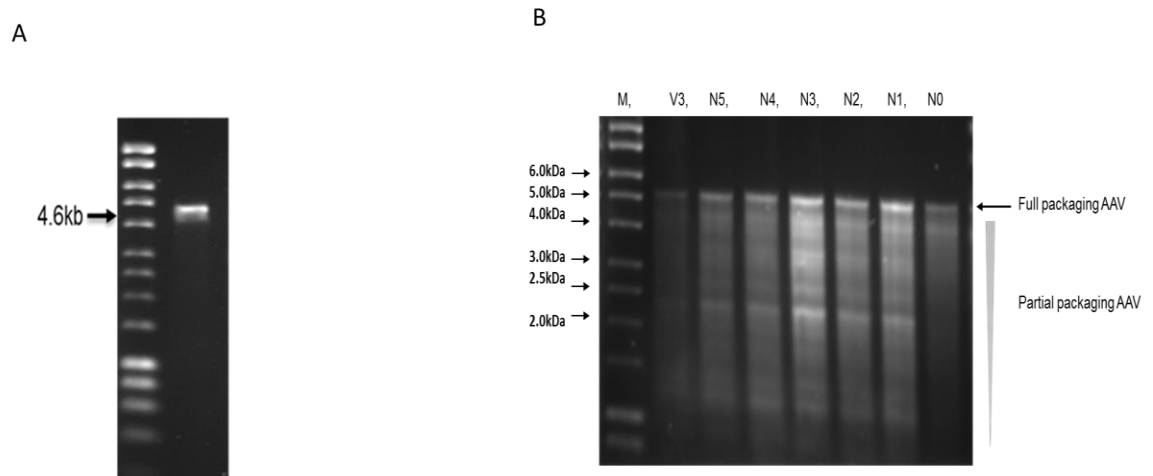


Figure 2.3. Encapsidation of AAV vector with extra-large genome

Alkaline gel analysis of packaged AAV genomes. Viral DNA visualized by Gel-red staining in 0.8% alkaline gel electrophoresis.

A) A typical alkaline gel with a DNA standard and full packaged 2.3kb human FIX small transgene, which packaged by self-complementary shuttle vector, presented double size of 4.6kDa single DNA band B) Alkaline gel analysis of viral genomes extracted from single stranded rAAV8 HLP hFVIII variants, 5.13kDa 31aa V3, 5.12kDa of N5, 4.9kDa of N4, 4.9kDa N3, 4.9kDa of N2, 4.9kDa of N1 and 13aa 4.87kDa of N0, viral particles. Each viral DNA shows the size and those over-sized AAV heterologous bands spreading from 5.2kb down to 1kDa. Full packaging size we expect to be 4.87kb to 5.13kb.

2.7. Viral transduction and Single clone selection

2.7.1. Cell preparation and transduction

Early passage ($\leq p30$) adherent HEK-293T cells were seeded at a density of 1×10^5 cells/well into 12-well plates. The following day media was removed and replaced with 300 μ L of media containing lentivirus at a multiplicity of infection (MOI) of 10. After 4 hours the media volume was restored by the addition of 700 μ L of 10% FBS containing DMEM.

2.7.2. Single clone selection

After lentiviral transduction, a heterogeneous population of cells with viral inserts will be achieved, in order to achieve a homogenous selection a single cell was isolated and expanded. We diluted a cell suspension and plated into 96-well plates so that on average, each third well will contain a single cell. We harvested polyclonal cells and counted cells using a chamber slide. After carefully visually inspecting cells in the counting chamber slide by microscopy, two separate chambers were counted four times and cells were then re-suspended in 1×10^6 cells/mL. Cells were then diluted to 5 cells/mL, 200 μ L of the solution was transferred into each well of a 96-well plates using a multichannel pipette.

2.8. Sample preparation for Coagulation assay

Cells were seeded at 1×10^6 cells/well in 6-well plates. 24 hours later the media was discarded and cells washed with PBS, 1mL of serum-free DMEM was added to each well, and 24 hours later media was used in an Enzyme-Linked Immunosorbent Assay (ELISA) to screen clones for FVIII expression.

2.8.1. Transient transfection of Huh 7 and HEK-293T cell lines

To test hFVIII expression from plasmid DNA, transient transfection was carried out on Huh 7 and HEK-293T cells for subsequent FVIII ELISA on supernatants. The day before transfection 5×10^5 cells was plated per well in 6-well plates. On the day of transfection 2 μ g of the plasmids were added to 100 μ L of serum-free X-VIVO (Lonza, Nottingham, UK). In a separate tube 1 μ L of PEI (1mg/mL) was added to 100 μ L X-VIVO. The two solutions were then mixed, incubated at room temperature for 20 minutes and added to the cells. After 4–6 hours, the medium was replaced with 10% FBS containing DMEM. After 48 hours transient transfection, the medium was changed with 1mL of serum-free

X-VIVO, then further incubated at 37°C and finally, supernatants were harvested and stored at -80°C.

2.8.2. Coagulation Assays

2.8.2.1. Measurement of human FVIII antigen level from cell lines

To determine FVIII antigen levels, two different ELISA methods have been used. The Affinity Biologicals FVIII antigen kit (Affinity Biologicals, Quadratech, Epsom, UK) is polyclonal, and the other one is monoclonal anti-(FVIII light chain)-IgG detection antigen kit (Diagnostica Stago, Reading, UK). We used Affinity Biologicals FVIII antigen kit for our earlier screening test, which we used for single clone selection for each variant. However, it later transpired that this kit was not detecting accurately the FVIII levels in the B-domain deleted and truncated B-domain linker constructors. However, it is valid for internal comparison for each variant. Six well plates were coated with 1X Geltrex (Life Technology) at room temperature for 60 minutes then 1×10^6 cells per well added. 24 hours later FBS containing medium was discarded, and the cells were washed with 2mL of PBS. Finally 2mL of the fresh serum-free medium was added. The media was harvested after a further 24 hours, by centrifugation at 400xg for 5 minutes, the FVIII levels in the supernatant were then determined by ELISA.

2.8.2.2. Factor VIII Antigen ELISA

2.8.2.2.1. Affinity biological FVIII antigen assay (Polyclonal antibody)

An immunocapture assay was used to determine hFVIII: Ag levels in cell culture samples from HEK-293T cells. In brief, 96-well plates were coated overnight at 4°C (Maxisorp, Nunc, Fisher Scientific) with an Affinity-purified antibody to FVIII (Affinity Biologicals, Polyclonal Antibody). After blocking at room temperature for one hour (PBS/6% BSA/0.05% Tween 20), an hFVIII ELISA kit was used for subsequent steps (*F8C-EIA*, Quadratech Diagnostic). Standards and samples were diluted 1:10 ELISA kit diluent in

the diluent buffer and were loaded in duplicates (50µL/well). Standards were made by serial dilutions of murine plasma spiked with recombinant human FVIII, starting concentration 4 IU/mL (11th FVIII British Standard: 95/608, 6.9 IU/mL, National Institute for Biological Standards and Control, South Mimms, UK). We set up a FVIII antigen assay using recombinant human FVIII standard (IU/mL) as described above and assumed parity between 1 IU/mL and 100% FVIII antigen value. It should be noted, however, that this is not correct, and that the units used are not appropriate for a standard used to measure % FVIII antigen.

After washing the plate to remove unbound material, a total of 100µL/well of the polyclonal horseradish peroxidase–labelled detecting antibody was used as a secondary antibody. A peroxidase conjugated the second antibody to FVIII was added to the plate to bind to the captured FVIII. After washing the plate to remove unbound conjugated antibody, the peroxidase activity was detected by incubation with O-phenylenediamine (OPD, Sigma). After 15 minutes incubation time the reaction was quenched with the addition of 50µL of 3M Hydrochloric acid (HCl, Sigma) and the colour produced was quantified using microplate reader at a wavelength of 490nm.

2.8.2.2.2. Monoclonal FVIII antigen by Asserachrom Stago Kit (Monoclonal antibody)

To determine FVIII antigen levels per stable cell lines the ASSERACHROM FVIII: Ag kit (Diagnostica Stago) was used. This kit is an antigenic assay for the quantitative determination of FVIII by ELISA. FVIII to be measured is captured by monoclonal anti-FVIII light chain IgG antibody coated on the internal walls of plastic microplate wells. Calibrator (lyophilised human plasma calibrator, assay value provided in the kit) for analysis were prepared as kit instruction. Samples were diluted with supplied kit buffer and assayed as per the manufacturer's instructions. Results were then divided by viral genome copy number per cell to calculate FVIII Ag /copy/cell

2.8.2.2.3. Mouse plasma FVIII antigen assay

Mouse blood was collected in 0.136 Molar, trisodium citrate anticoagulant (1:9 v/v to blood, Sigma) with the gentle mix. Blood was centrifuged 2500×g for 15 minutes at 4°C. Plasma samples were quickly snap frozen in dry ice then stored at -80°C. Plasma concentration of mouse FVIII antigen was determined by the ASSERACHROM FVIII: Ag kit (Diagnostica Stago) as per the manufacturer's instructions.

2.8.2.3. Factor VIII Activity Assay

2.8.2.3.1. Measurement of FVIII Activity level from culture medium and mouse plasma

FactorVIII: C is a chromogenic assay for testing the cofactor activity of FVIII:C (BIOPHEN FVIII:C, Quadrtech). In the presence of FIXa, phospholipids and calcium, thrombin-activated FVIII:C forms an enzymatic complex, which activates FX to FXa. This activity is directly related to the amount of FVIII: C, which is the limiting factor in the presence of a constant and excess amount of FIXa. Generated FXa is then exactly measured by its activity on specific FXa chromogenic substrate. FXa cleaves the substrate and releases p-nitroaniline (pNA). The amounts of pNA generated are directly proportional to the FXa activity. Finally, there is a direct relationship between the amount of FVIII:C in the assayed sample and FXa activity generated, measured by the amount of pNA released. Samples were diluted 1:10 and 1:20 in sample diluent provided (R4) and run in duplicate on plates. A standard curve plotting FVIII cofactor activity against pNA released was constructed by diluting Biophen normal control plasma (Quadrtech Diagnostics). The Kit contained two controls, which were also used as a further quality control for the assay. The assay was performed as per the manufacturer's instructions. Results were then divided by viral genome copy number per cell to calculate FVIII:C / copy /cell values.

2.8.2.3.2. One-stage clotting assay (Activated Partial Thromboplastin Time)

FVIII levels were measured using a one-stage clotting assay (Activated Partial Thromboplastin Time; APTT) on an ACL TOP 700 (Instrumentation Laboratory, MA, USA). Hemos/L SynthASil APTT reagent and FVIII deficient plasma (contains vWF levels at ~90 IU/dL) were used against frozen plasma calibrator (CRYOcheck reference plasma, Precision BioLogic Inc, Dartmouth, Canada).

Purified FVIII variants were diluted into FVIII deficient plasma (Hemos/L). An eight point calibration curve was constructed by the ACL TOP (range 0~150%) from the plasma calibrator in triplicates. The diluted FVIII variant samples were then analysed by parallism dilutions (1:10, 1:20 and 1:40). Values for variants were calculated in IU/dL by the ACL TOP coagulometer. The Coefficient variation (CV) value of the Intra and inter assay are represented in table 2.2.

	One stage FVIII Assay
Intra assay	
Normal Level	3.8%
Abnormal Level	4.0%
Inter Assay CV	
Normal Level	4.0%
Abnormal Level	5.5%

Table 2.2. Percentage of CVs for Factor VIII assays: One-stage clotting assay on an ACL TOP 700

Intra and inter level of normal and abnormal exhibited similar CV value.

CV: Coefficient variation, kindly provided by Anne Riddell at Haemophilia and Thrombosis Centre in the Royal free hospital.

2.9. Thrombin activation assay

2.9.1. Thrombin generation assay

Thrombin generation was measured with the Calibrated Automated Thrombogram System (CAT, Diagnostica Stago) based on Fluoroskan Ascent Analyzer (390nm excitation 460nm emission wavelength: Thrombinoscope, Diagnostica Stago). Before starting the assay, all reagents [PPPlow (1pM tissue factor and 4μM phospholipid reagent, thrombinoscope, Diagnostica, Stago), Thrombin Calibrator (Thrombinoscope, Diagnostica Stago) to which had been added 1mL double distilled H₂O and vortexed] were put on ice; meanwhile warming up the FluCa buffer in the 37°C water bath for 15 minutes. The CAT machine has a calibrator step. In the 96-well round bottom plates set up for the experiment, all samples were assayed in triplets and the calibrator used two wells, and quality control (QC) samples were assayed for internal control. Protein sample and the calibrator were vortexed and 20μL from each added to the round-bottom 96-well plates. Then 80μL samples were added into 20μL of the trigger (PPPlow). Next, the plate was put in the machine for 5 minutes at 37°C. The pre-warmed buffer with Fluca substrate was diluted 1:40 and vortexed immediately the mixture and adds 20μL FluCa/well with a repeater. After adding the FluCa to each well and then start the programme. For the negative control, FVIII deficient plasma was used (Hemos/L, Werfen). This assay has been performed at Katharine Dormandy Haemophilia and Thrombosis Centre in the Royal free hospital (London, UK). Table 2.3 represents the precision values of CV for CAT Fluoroskan Ascent Analyzer.

	LT	Time to PH	ETP	Peak Height
Intra assay				
Normal Level	5.1%	16.25	6.2%	12.7%
Abnormal Level	6.1%	7.5%	6.4%	16.3%
Inter Assay CV				
Normal Level	23.6%	14.9%	19%	18%
Abnormal Level	21.0%	9.6%	17.3%	22.3%

Table 2.3. Percentage of CV values for thrombin generation assays (CAT Fluoroskan Ascent Analyzer)

The CV values of inter assay were higher than intra assay. LT: Lag time, PH: Peak height, ETP: Endogenous Thrombin Potential. The values of CVs were provided by Anne Riddell in the Royal free hospital London.

2.9.2. Thrombin digestion

Cleavage reactions containing 50nM rFVIII and 1nM thrombin (Sigma-Aldrich) was performed by incubating at 37°C for an hour followed by SDS-poly acrylamide gel was performed.

2.10. SDS-PAGE and Western Blot

2.10.1. Preparation of samples for SDS–Poly Acrylamide Gel

Total volumes of 13µL sample and 2.5µL of 4x loading dye with 1µL of reducing agent were added.

Samples mixed then heat-treated at 98°C for 5 minutes. After briefly cooling down they were spun down without delay. Samples were loaded onto the gel and add anti-oxidant added into the running buffer. The samples were then run on a 4~12% NuPage Bis-Tris gradient protein gel with MOPS buffer at 200V, 120mA, 90 minutes with reducing agent.

2.10.2. Membrane transfer

Proteins separated by SDS-PAGE gels were electrophoretically transferred onto polyvinylidene-difluoride (PVDF, GE Healthcare) membranes by using mini-gel transfer kit (Invitrogen).

One hour before starting membrane transfer, 200mL of transfer Buffers were prepared and cooled down at 4°C. Six pieces of Whatman 3MM paper (5mm) to be a little larger than the gel. Cut one piece of PVDF membrane to be the same size as the gel. Take a small container and pour in a small amount of transfer buffer. Soak three pieces of 3MM papers in the buffer then place in the apparatus. Then soak the PVDF membrane and place on top of the 3MM papers. Separate the gel from the metal plate and carefully place on top, then add three more pieces of 3MM papers soaked in transfer buffer. Roll over a pipette to remove any air bubbles. Set apparatus to run at 0.8mA/cm² for an hour.

2.10.3. Antibody and ECL

At the end of the transfer remove the gel from the membrane, cut or mark one corner to indicate the correct orientation. Place in blocking buffer (Roche Diagnostics, Burgess Hill, UK) for an hour at room temperature on shaker or overnight in the 4°C. Dilute the primary antibody 1:1000 with 50% blocking buffer and 50% TBS-T (0.05% Tween 20). Place on a shaker for two hours at room temperature or overnight in the fridge. Washing with TBS-T three times at 10 minutes each. Dilute secondary antibody anti-mouse HRP 1:10000, place on a shaker for one hour at room temperature. Washing with TBS-T three times again. The bound HRP was subsequently detected using an Enhanced Chemiluminescence system (ECL[™], Fisher Scientific). The membrane was then exposed to X-ray film (GE Healthcare) to detect the resulting light emissions. Exposure times were then increased or decreased according to the strength of the signal.

2.11. Protein staining

2.11.1. Silver staining

Silver staining is a sensitive procedure to detect trace amounts of proteins in gels. Purified recombinant FVIII protein quantities are present at a very low concentration; we used silver staining for detection of individual protein bands under reducing conditions. The samples were treated PNGase F (Invitrogen) endoglycosidase for an hour before analysis to demonstrate proteolytic activation and the presence of *N*-linked glycan modifications.

A purified protein or PNGase F treated glycoproteins were mixed with protein loading dye and NuPAGE sample reducing reagent (Invitrogen), the mixture was heated at 95°C for 5 minutes. The denatured samples were then separated on 4~12% Bis-Tris gel (Invitrogen) with MOPS running buffer. After electrophoresis, the SDS-poly acrylamide gel was stained by SilverXpress silver staining kit (Invitrogen) according to the manufacturer's instruction.

2.11.2. Sypro Ruby staining

Sypro Ruby staining is a very simple staining with sensitivity comparable to silver staining. Pre-staining preparation steps are the same as silver staining, after SDS-PAGE, the BIS-TRIS gel was fixed with methanol and staining solution (Thermo Scientific) for overnight staining at room temperature. The stained gels were washed with ultra-pure water for 30 minutes. The staining was visualised by placing on a UV transilluminator document system.

2.11.3. Coomassie staining

Coomassie blue is commonly used to stain proteins in SDS-PAGE gels. The gels are soaked in dye, and the excess stain is then eluted with a solvent destaining step. This treatment allows the visualisation of proteins as blue bands on a clear background. Pre-

staining preparation steps same as Silver and Sypro Ruby staining, after SDS-PAGE, staining solution (50% Methanol, 40% Water, 10% Acetic acid and 0.25% Coomassie R-250 [Sigma]) was added cover the gel. Staining was carried out for 2~3hours with gentle rocking, followed by destaining solution (25% Methanol, 68% Water, 7% Acetic acid) overnight.

2.12. PNGase F digestion

2.12.1. PNGase F treatment

Peptide -*N*-Glycosidase F, also known as PNGase F (NEB), is an amidase that cleaves between the innermost GlcNAc and asparagine residues of high mannose, hybrid, and complex oligosaccharides from *N*-linked glycoproteins. For the analysis, 200~500ng of purified recombinant FVIII glycoprotein was combined with 2μL of 10X Glycoprotein Denaturing Buffer and H₂O (if necessary) to make a 20μL reaction volume. The glycoprotein was denatured by heating at 95°C for 5 minutes followed by chilling on ice. Make a total reaction volume of 40μL by adding 4μL 10X G7 Reaction Buffer, 4μL 10% NP40 and 6μL H₂O. The reaction was divided into two and a half treated with 1μL PNGase F, mix gently and incubate reaction at 37°C for one hour, a sample without PNGase F was kept on ice.

2.12.2. FVIII polyclonal antibody

The blots were probed either with a 1:5000 dilution of polyclonal sheep anti-hFVIII horseradish peroxidase antibody (SAF8C-HRP, Affinity Biologicals, Quadrantech Diagnostic).

2.12.3. FVIII Monoclonal antibody

The heavy chain was identified by monoclonal ab78876 (Abcam, Cambridge, UK) which has an A2 domain for epitope recognition site. Light chain was identified by Ab41188

(Abcam), which has an a3 binding epitope; both primary antibodies were used at 1:1000 dilution. Monoclonal heavy and light chain antibodies were then detected with anti-mouse HRP (Horseradish Peroxidase) conjugated IgG secondary antibody.

2.13. *In-Vivo* Procedures

2.13.1. Preparing Adeno Associated Virus for mouse injection

All mice used in the study were male C57BL/6 aged between four and eight weeks (Charles River, Margate, UK). Single-stranded AAV2/8 FVIII viruses were prepared in up to 200µL in X-VIVO 10 media, and 5×10^{10} vg/mouse was administered via tail vein injection with 3~4 mice per group. Intravenous tail vein injections of FVIII expressing AAV into C57BL/6 mice were performed by Dr Cecilia Rosals (University College London), according to approved UK Home Office and Institute guidelines at University College London via the tail vein using no anaesthetics.

2.13.2. Tail Vein Injection

Blood samples in mice were collected in 0.136 Molar trisodium citrate anticoagulant (1:9 v/v to blood) tubes 4 weeks after the injection date by terminal blood collection after sacrifice. Liver tissues were also collected and snap frozen on dry ice for genomic DNA extraction.

2.14. Recombinant FVIII purification

The purification process for rhFVIII produced in the adherent HEK-293T cells is illustrated below. A total of two purification steps is employed to remove host cells, medium components, and a chemical reagent during culture and purification.

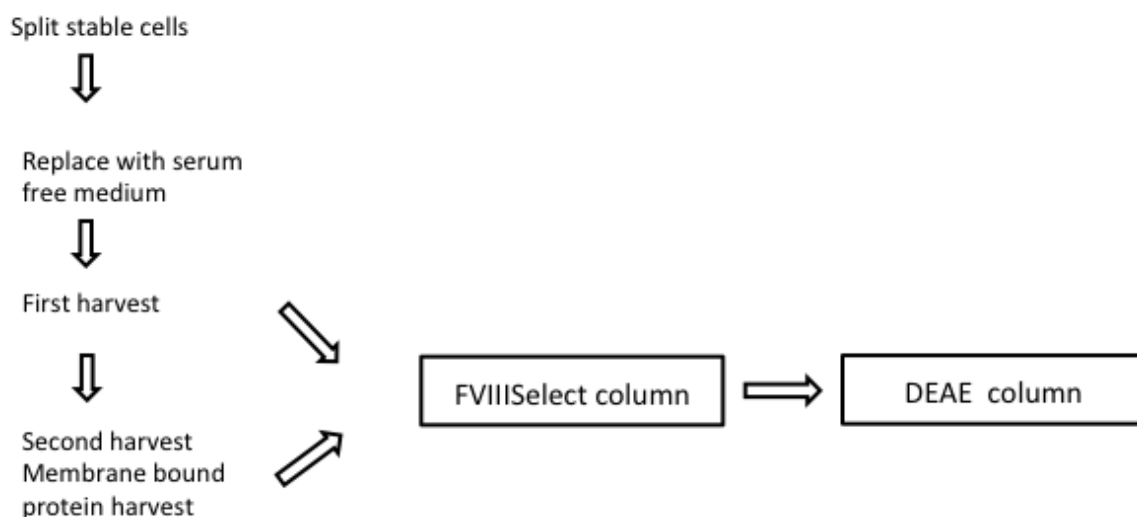


Figure 2.4. Recombinant human FVIII purification steps

FVIII containing media were collected twice from stable cells, and membrane-bound FVIII was harvested by using 0.5M NaCl. Purification was performed by affinity column (FVIIISelect, Healthcare, Stevenage, UK) then total eluants were applied to a weak anion exchange column (DEAE FF, Healthcare, Stevenage, UK).

2.14.1. Sample preparation for Äkta Explorer

Purification of recombinant FVIII proteins was carried out using a two-step purification method. The first step is an affinity column chromatography procedure and the second column is weak anion exchange column for the polishing step. Stable expressing adherent cells were grown up in a large T-1000, five-layer flask (Fisher Scientific). Day1, 3×10^8 cells were split into T-1000 flask with 200mL of DMEM containing 10% FBS. 24 hours later FBS contained medium was discarded, and cells washed twice with PBS, then 200mL of DMEM serum free media was added. A further 24 hours later media was harvested and replaced with fresh 200mL of serum free DMEM. To the harvested media 1mM benzamidine (Sigma) was added to prevent trypsin, trypsin-like enzymes, and serine protease from inactivating rFVIII. Media was centrifuged at 400xg for 5 minutes and filtered through a 0.22µm vacuum filter (Corning) and keep at 4°C for purification. 24 hours later a 2nd harvest was done, cells were washed, and 100mL of additional 0.5M

NaCl containing serum free DMEM was then incubated at 37°C for 5 minutes to harvest membrane bound recombinant FVIII. The second harvest and membrane-bound FVIII were diluted with 100mL of serum free DMEM. In total 200mL of membrane-bound FVIII supernatants were treated in the same way as the first harvest. The chromatographic operations were performed at 4°C on Äkta Explorer (GE Healthcare) Fast protein liquid chromatography (FPLC) systems controlled by Unicorn Version 5.2 Software. All purification steps followed according to Tang et al (Tang *et al.*, 2013).

2.14.2. FVIII affinity column

FVIII purification is based on highly cross-linked agarose base matrix, which enables rapid processing of large sample volumes. The ligand is a 13kDa recombinant protein, the structure of which is based upon a *Saccharomyces cerevisiae* derived single domain antibody fragment. The ligand is attached to the porous base matrix via a hydrophilic spacer arm making it easily available for binding to recombinant B-domain deleted FVIII (McCue *et al.*, 2009). Briefly, following line washing with the appropriate buffers, the affinity medium was equilibrated in 20mM Imidazole/ 10mM CaCl₂/ 400mM NaCl/ 100ppm Tween 80, pH 7.0 at a flow rate of 1mL/minutes. The cultivated media obtained from T-1000 flask preparations was then loaded onto the 1mL FVIIIselect (GE Healthcare) packed column at 1mL/minutes (traceable as an increase in absorbance at 260nm and 280nm as unbound protein and DNA exits the column). Residual unbound protein and cellular debris were washed off. After washing with buffer A and then with a mixture of 30% Buffer A (Table 2.2) and 70% of Buffer B. The protein was eluted with 50% ethylene glycol containing Buffer B (pH 6.5), which was collected in 1mL fractions into tubes. The FVIII containing fractions were identified by a peak in absorbance at 260nm and 280nm. All fractions were pooled, and normally a pool volume of around 10mL was obtained. The fractions were stored at -80°C until sufficient material was ready for the polishing DEAE FF column.

2.14.3. Diethylaminoethyl (DEAE) Sepharose Fast Flow Column

FVIII containing fractions were diluted (9-fold) in Buffer C (20mM MOPS/ 10mM CaCl_2 /100ppm Tween80, pH 7.0). The sample proteins were loaded onto the column at 1mL/minute (traceable as an increase in absorbance at 260nm and 280nm as unbound protein exits the column). After washing the column with a mixture of 80% Buffer C and 20% of Buffer D, the bound FVIII was eluted with a mixture 60% Buffer C and 40% of Buffer D, Residual unbound protein and cellular debris was washed off. The pure recombinant FVIII protein was eluted in 1mL fractions into tubes. The FVIII containing fractions were identified by absorbance at 280nm. All fractions were pooled and 1% sucrose (Sigma) w/v was added as a stabiliser, and aliquots stored at -80°C.

Equilibration buffer	20mM Immidazole 10mM CaCl ₂ 400mM NaCl 200ppm Tween 80 pH 7.0
Buffer A	20mM Immidazole 20mM CaCl ₂ 1mM NaCl 200ppm Tween 80 pH 6.5
Buffer B	20mM Immidazole 20mM CaCl ₂ 1.5M NaCl 200ppm Tween 80 50% W/W Ethylene glycol pH 6.5
Buffer C	20mM MOPS 10mM CaCl ₂ 100ppm Tween 80 pH 7.0
Buffer D	20mM MOPS 10mM CaCl ₂ 1M NaCl 100ppm Tween 80 pH 7.0

Table 2.5. FVIII purification buffers

All buffers filtered with 0.45um filter system and kept at 4°C.

Abbreviation: ppm; parts per million.

2.15. Immunocytochemistry

2.15.1. Split cells on coverslips

13mm cover glass (VWR) was sterilised in 100% ethanol for two hours, and replaced into the wells of 24-well plates. The lid was left open to allow the ethanol to evaporate in a class II cabinet. The coverslips were then coated with 200µL of 1x Geltrex (Life Technology) diluted with DMEM and incubated at room temperature for an hour. After incubation, the coating media was discarded, and 5×10^4 cells were added per well in a volume of 500µL.

2.15.2. Staining

Stable cells grown on coverslips were washed in 1X PBS and fixed in 4% PFA (Para formaldehyde) for 10 minutes at room temperature. Following fixation, cells were blocked and rehydrated for 10 minutes in 1XPBS supplemented with 1% BSA and 0.1% Triton X-100 (Sigma). Cells were transferred into primary antibodies (appropriately diluted in 1X PBS, 1% BSA, 0.1% Triton X-100, Table 2.3) and incubated with constant shaking for either 1 hour at room temperature or overnight at 4°C. Following incubation with primary antibodies, cells were washed in 1XPBS, 0.1% Triton X-100 and then incubated for 30 minutes with secondary antibodies. Cells were then washed three times with PBS before counter-staining with 0.5mg/mL DAPI (4',6-diamidino-2-phenylindole, Sigma). Coverslips were mounted onto gelatin-coated slides with Vectashield non-quenching mounting medium (Vector Laboratories). Immunocytochemical staining was then assessed microscopically using an upright Leica Imaging system and Inverted Leica Confocal Imaging system (Leica).

	Primary antibody	Secondary antibody
FVIII	FVIII-Abcam (Cambridge, UK)	DyLight Donkey anti mouse Ig-g, 450 (Thermo, USA)
ER	Calnexin-Cell Signaling (Danvers, USA)	DyLight Donkey anti rabbit Ig-g, 550 (Thermo, USA)
Golgi	Golgin97-Abcam (Cambridge, UK)	DyLight Donkey anti goat Ig-g, 650 (Thermo, USA)
Nucleus	Dapi staining (Sigma, USA)	

Table 2.6. Antibodies for Immunofluorescence staining

Monoclonal FVIII primary antibody used for human FVIII detection (Ab41188, the light chain of FVIII). Calnexin is an ER chaperone protein, which binds early stages of protein processing and rabbit calnexin purchased from cell signalling. Golgin 97 is a broad Golgi marker, which was purchased from Abcam (Cambridge, UK). DAPI (4',6'-diamidino-2-phenylindole) and used for nucleus counterstaining.

2.15.3. Confocal Imaging

Double stained Stable cell lines were viewed using an inverted microscope equipped with a 60x oil objective and a confocal system. Fluorophores were excited at 406nm, 488nm, 543nm He/Ne green, and 647nm. Each image was volume rendered from 10 Z-stacks of 0.85µm thickness using LCS Lite software (Leica). The timed series was acquired at a rate of one minute per frame, and each frame represents a volume-rendered image.

2.16. Statistical analyses

Statistical analyses were performed using Analysis of Variance (ANOVA) and t-test. Groupwise comparisons were performed by using one way ANOVA (Bonferroni simultaneous test) and two way ANOVA. The Mann–Whitney *U* test and two-tailed paired tests were used for the independent two groupwise test (GraphPad Prism 5 and 6; Graph-Pad Software Inc).

Chapter 3

**Engineering B-domain of human FVIII to
generate stably expressing cell lines
producing FVIII proteins using Lentiviral
vectors**

3.1. Introduction

Haemophilia A is bleeding disorder that is caused by very low or absent FVIII expression. Even normal FVIII expression is lower than any other coagulation factor due to poor mRNA expression, inefficient protein folding with subsequent misguided extracellular transport by ER and Golgi systems, resulting in approximately two to three-fold decrease of FVIII expression level compared with similar sized secretory proteins (Kaufman *et al.*, 1989; Lynch *et al.*, 1993). Studies of FVIII structure and function have led to opportunities to bioengineer forms of improved recombinant FVIII that share an identical domain structure (A1-A2-B-A3-C1-C2) (Vehar *et al.*, 1984; Sandberg *et al.*, 2001; Zheng *et al.*, 2013).

It has been shown that entire B-domain of FVIII is dispensable for the blood pro-coagulation process (Toole *et al.*, 1986) and that deletion of the B-domain improved mRNA levels as well as FVIII activity. Therefore the B-domain has been a favoured strategic target for human FVIII bioengineering to improve FVIII properties of biosynthesis, secretion efficiency, functional activity and long half-life in plasma (Pittman *et al.*, 1993; Miao *et al.*, 2004).

However, the production of recombinant FVIII has proved to be costly due to the expense of production, purification, and formulation. The manufacturing technology used has required specialised production and distribution, limiting access to developed first world countries but leaving less developed countries without such treatment. For this reason, recombinant FVIII production from stable cell lines is becoming important for the clinical field (Wurm, 2004). However there are hurdles to overcome for the stable cell line techniques: i) Labour-intensive process due to heterologous DNA integration into the genome by current transfection methods, ii) Time-consuming for the selection step to pick up efficiently expressing FVIII from the large scale of cell lines, which should be monitored for gene silencing overtime of passaging of the lines,

iii) The post translational modification of FVIII from the host cells line should be identical to human FVIII. Therefore, alternative gene delivery with highly effective lentivirus will facilitate the stable cell line establishment and selection steps (Trono, 2000) because lentivirus delivers the target gene efficiently into the host genome by viral integrase with a high-frequency manner to active chromatin (Bushman *et al.*, 2005). Lentivirus-based gene transfer used to establish stable cell line has been reported for Chinese hamster ovary (CHO) cells, and the result shows that efficient, stable cell lines are established compared to non-viral DNA delivery methods (Oberbek *et al.*, 2011). Non-human material contamination in the FVIII protein is an important issue for the production methods because antigenicity may cause an immune response in patients to the contaminated FVIII products. In this respect, optimisation of the serum-free culture condition for established stable cell lines is required as an important step for FVIII production.

The aim of this chapter is to address the overall hypotheses that the length of B- domain and *N*-linked glycosylation of FVIII may have important roles in FVIII production. In testing these hypotheses, human FVIII variants (wild type SQ, N6 versus V1co, V3co, V5co and N6co) and their B-domain modification will be described. Finally, characterisation of FVIII producing stable cell lines will be performed for efficient production of FVIII.

3.2. Results

3.2.1. Construction of B-domain modified FVIII

To enhance translation efficiency of FVIII, DNA sequences derived from the B-domain were engineered according to preferred codon usage based on human albumin, to create codon optimised version of FVIII SQco and FVIII N6co (McIntosh *et al.*, 2013) (Fig. 3.1).

The “SQ” linker consists of 14 amino acids: SFSQNPPVLKRHQR, which contains the proteolytic furin cleavage recognition motif RXXR (RHQR) at the C-terminal end of B-domain and before the a3 region. The B-domain deleted SQ-linker FVIII molecule is a heterodimer of a unique 90kDa heavy chain and an 80kDa of the light chain, which has a great advantage regarding expression efficiency compared to full-length FVIII products which have variable heavy chain fragments ranging in size from 90~200kDa (Pittman *et al.*, 1993).

The N6 linker 226 amino acid (aa) sequence was developed by Miao *et al.* It is a truncated partial 226aa B-domain consisting of the N-terminal portion of the B-domain. Miao *et al.*, concluded that glycosylation was important for high expression of N6/226aa due to the presence of six of Asn-X-Thr/Ser (N-X-T/S) motifs, sites of high mannose attachment, which support ER to Golgi transport of FVIII. However removal of five of the six *N*-linked glycosylation sites still leads to increased expression compared with B-domain deleted FVIII (Miao *et al.*, 2004).

The V3 linker fragment is composed of 31 amino acids that consist of the six *N*-linked glycosylation motifs from N6 placed adjacent to each other and juxtaposed in front of the native PPVLKRHQR sequence of FVIII. Thereby the linker sequence becomes SFSQ-NATNVSNNNSNDSNTSNVS-PPVLKRHQR.

Preston *et al.*, demonstrated that glycosylation plays a role in both stability and activity of FVIII (Preston *et al.*, 2013). To further understand the role of glycosylation in the B-domain, we developed several further constructs by varying length, sequence and

glycosylation potential. The first of these contains six *N*-linked glycosylation sites with an increased spacer between glycosylation motifs, leading to a 44 amino acid linker (designated V1co). Subsequently, to test whether glycosylation has a critical role for V3co, we modified the six Asparagine (*N*) to Alanine (*A*) in the V3co linker (designated V5co) (Fig. 3.1).

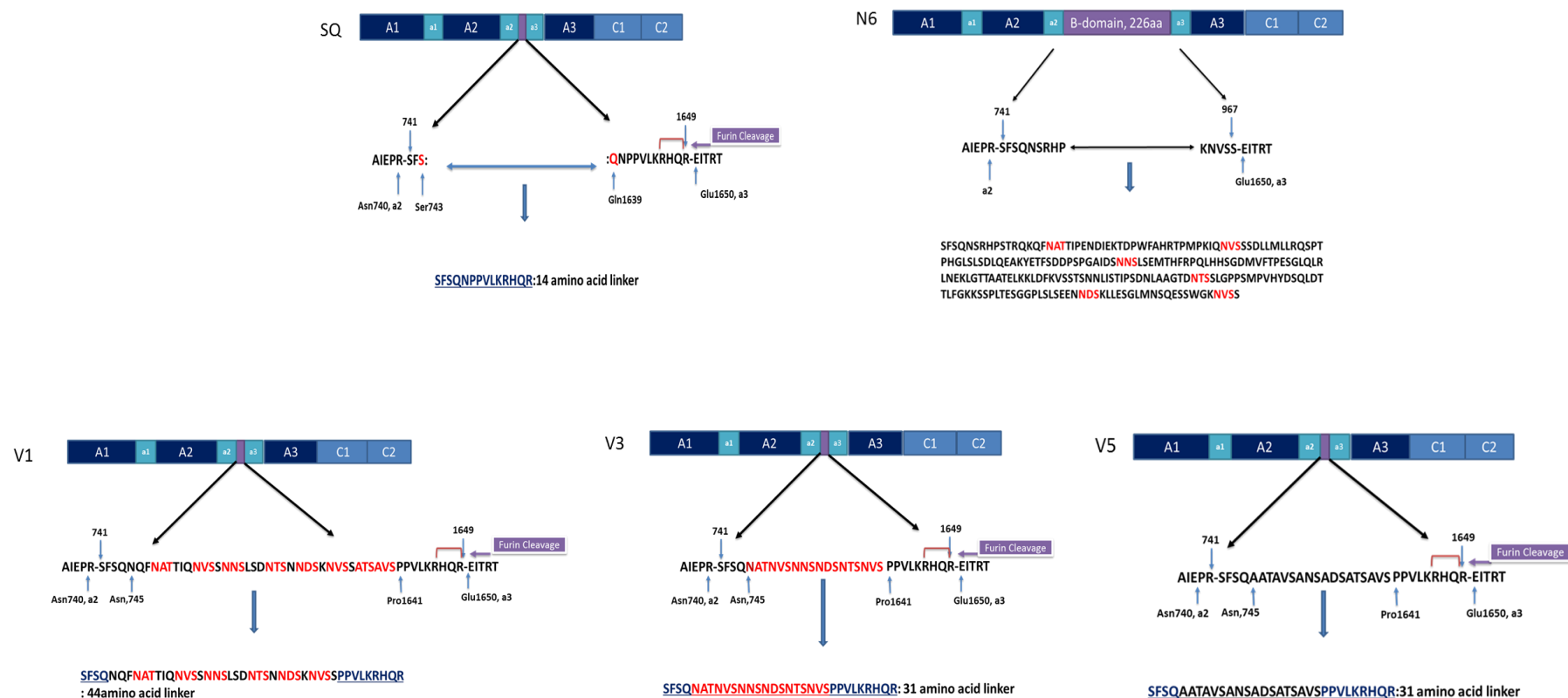


Figure 3.1. Schematic illustration of domain structures for engineered FVIII V1co, V3co and V5co

The newly generated five FVIII variants linker peptide sequences are illustrated. Truncated B-domain constructs of SQco and N6co are shown on top. Newly synthesised peptide linker sequences substituted into SQco, leading to V1co, V3co, and V5co. N-linked glycosylation sites are indicated as N (red) except SQco and V5co. The number of substituted B-domain linker amino acid (aa) are SQco, 14aa; V5co, 31aa; V3co, 31aa; V1co, 44aa and N6co, 226aa. Furin cleavage site RHQR naturally exists in SQco, V1co, V3co and V5co. However, the furin cleavage site of N6 was removed, due to the absence of B-domain proximal to the a3 region. Abbreviation: co; codon-optimised.

3.2.2. Generation of pRRL hPGK mWPRE shuttle vector

Although AAV expressing the FVIII variants can efficiently transduce cell lines, the transgenes are episomally maintained, and integration into the host genome is a rare event; therefore AAV is not a suitable viral choice for creating stable cell lines as the transgene will be gradually lost with the host cell division. Therefore, lentiviral vectors, which efficiently integrate into the target cell genome were used to establish stable cell lines. Lentivirus shuttle vector plasmid pRRL PGK perforin mWPRE (originally provided by Professor Adrian Thrasher [UCL.UK]) was prepared by removing the transgene using *Pst* and *Age*I restriction enzymes and then re-ligating the rest of the backbone DNA to create minimum shuttle plasmids. Thereby a 6668bp empty shuttle plasmid (pRRL.PGK.mWPRE) was generated for further cloning of FVIII transgenes (Fig.3.2.A.B).

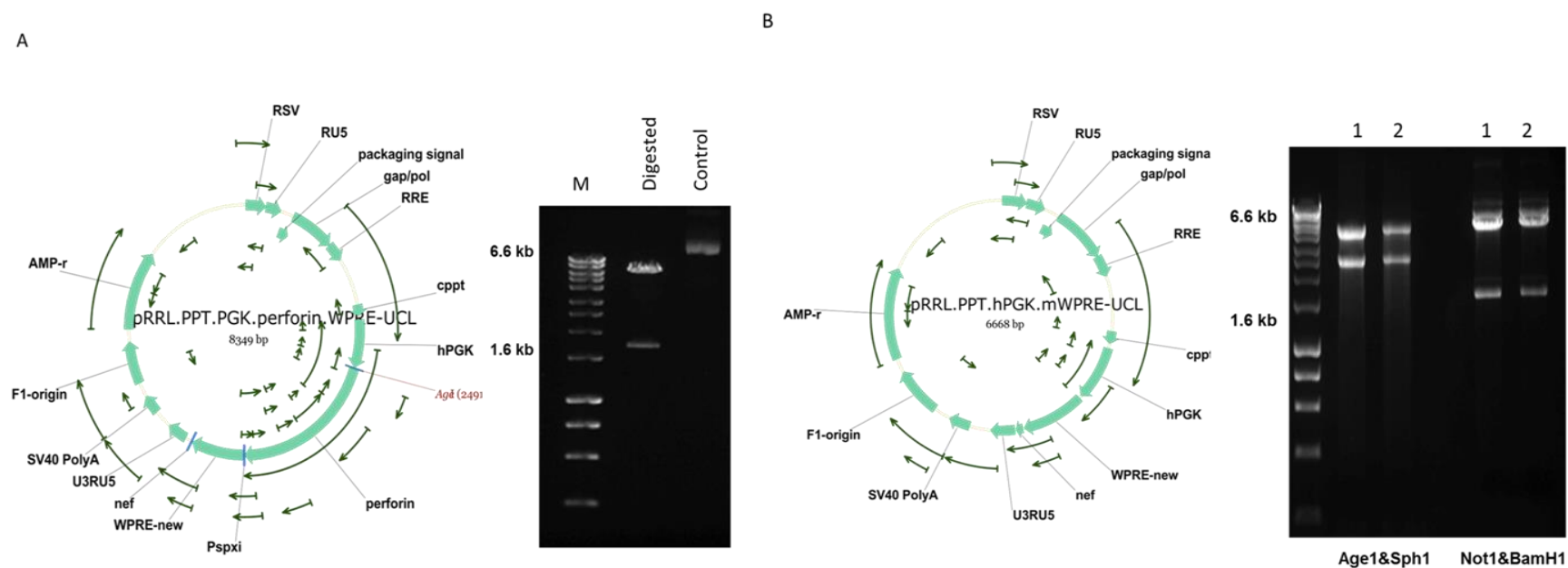


Figure 3.2. Vector maps of lentivirus shuttle vectors used in this study and details of restriction digestion

A) The original lentivirus shuttle plasmid (kindly provided by Professor Adrian Thrasher, UCL) harbour human PGK promoter, perforin gene and woodchuck post-transcriptional response element (WPRES). Restriction digestion with *PspXI* and *AgeI* generate 6668bp and 1681bp band showed on 1% agarose gel.

B) The DNA (6668bp) fragment re-ligated and two positive colonies were selected either by *AgeI/SphI* or *NotI/BamHI*, finally chose the clone number one for main backbone plasmid.

3.2.3. Cloning of lentiviral vectors

The FVIII variants are in two groups; Group one consisting of wildtype SQ and N6; Group two including the other groups are codon optimised (co) SQco, N6co, V1co, V3co and V5co. All transgenes were cloned into third generation self-inactivated pRRL vector driven by PGK promoter (Fig.3.3).

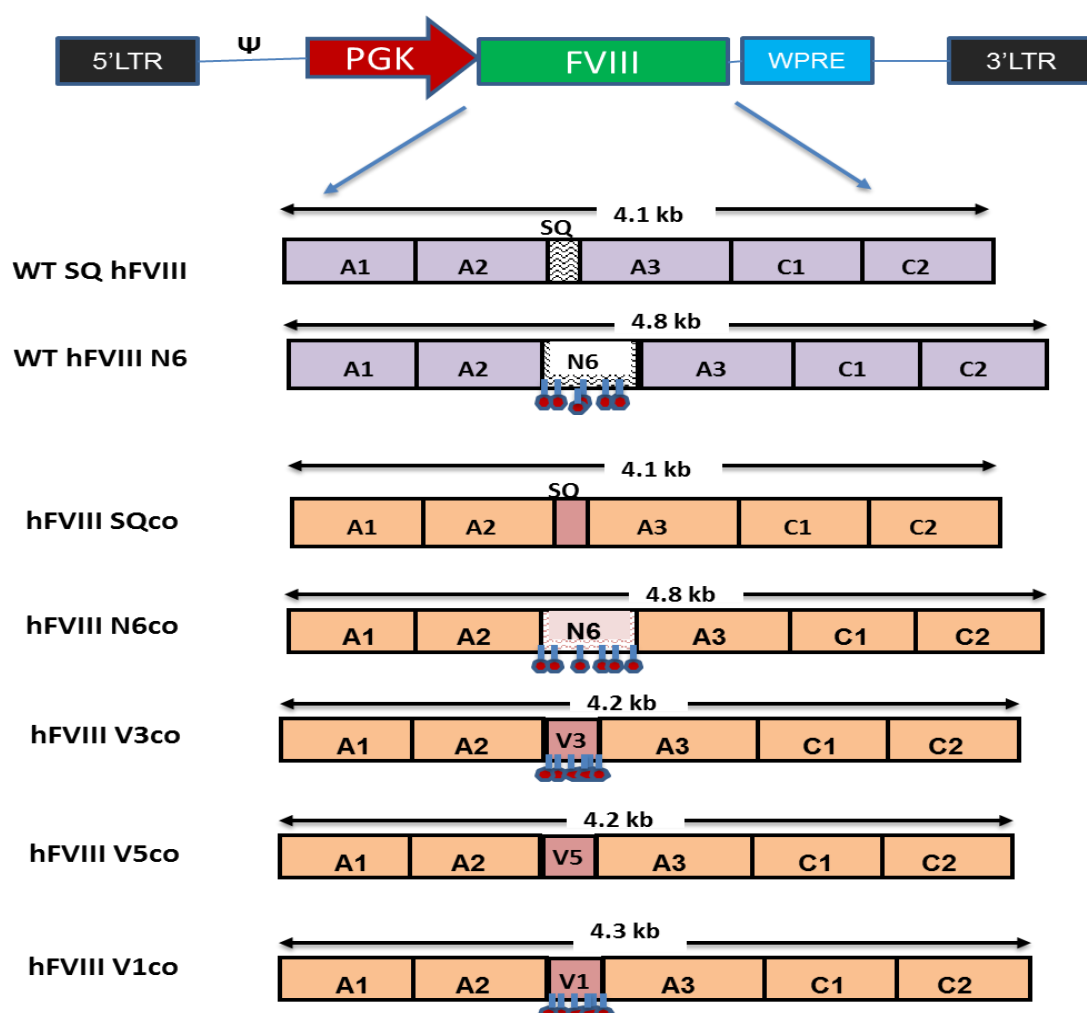


Figure 3.3. Schematic representations of human FVIII variants, cloned into third generation lentiviral backbone

The SIN (Self-inactivate) HIV-pseudo typed lentiviral vector includes, Ψ : packaging signal, phosphoglycerate kinase (PGK) promoter to drive transgene expression, and woodchuck hepatitis virus posttranscriptional regulatory element (WPRE), which enhances expression of transgenes. Lollipop indicates potential N-linked glycosylation inner linker of FVIII transgenes.

Initially, the WT SQ and WT N6 (kindly provided by Professor Steven Pipe), human FVIII variants, containing the wild-type DNA sequences were cloned into the 3rd generation pRRL transfer vector driven by PGK promoter. pRRL PGK WPRE backbone was digested with *Bam*HI, and then the sticky end was filled with Klenow reaction to create a blunt end. pAV2.HLP.WTN6 (4.3kb) and pAV2.HLP.WTSQ (4.2kb) was digested with *Not*I and *Sca*I to excise the insert. The blunt ends were filled with the Klenow reaction (Fig.3.4.A). The digested inserts and backbone DNAs were ligated, and positive colonies were selected by *Bgl*II or *Spe*I digestion (Fig.3.4.B).

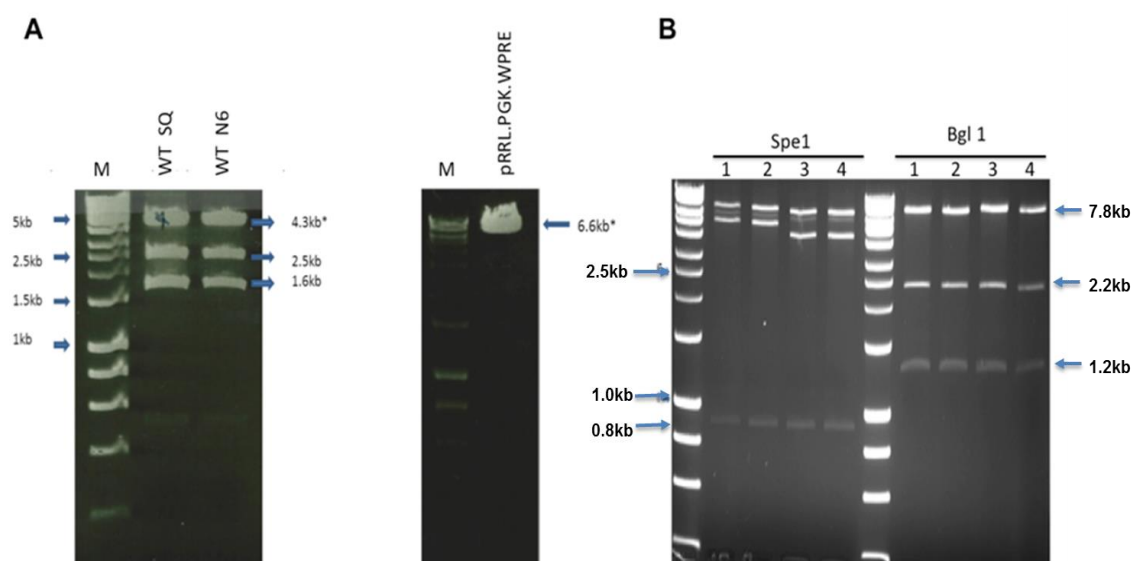


Figure 3.4. Cloning for WT SQ and WT N6

A) Agarose gel electrophoresis of restriction enzyme (*Not*I and *Sca*I) digested WT SQ and WT N6. Among the three digested bands, 4.3kb DNA was extracted for the insert. pRRL.PGK.mWPRE was linearized by *Bam*HI digestion, and then each end was blunt ended by Klenow. The backbone DNA was ligated with 4.3kb inserts. B) Positive clones were selected using *Spe*I or *Bgl*II digestion. Predicted *Spe*I digestion of WT N6 plasmid is 6.2kb, 4.4kb and 0.8 kb. The colony 1 and 2 showed correct band size upon *Spe*I digestion. Whereas the WT SQ predicted digested band illustrated as 6.2kb, 3.9kb and 0.8kb. Agarose gel separation shows correct bands for both clones 3 and 4. *Bgl*II digestion is used for full plasmid check, which corresponds to 7.8kb, 2.2kb, and 1.2kb bands respectively.

One of the goals of this project is to enhance the efficacy of expression of currently used FVIII-SQ and FVIII-N6. Therefore, codon optimised N6, SQ, and V3 DNAs, which were initially cloned into AAV shuttle plasmids (pAV2. HLP FVIII pA), were digested with *NruI* (blunt end) and *BamHI* (sticky end) to excise inserts. To create lentiviral backbone compatible ends, pRRL.PGK.mWPRE was digested with *AgeI* and *BamHI*. The digestion was performed in two steps. The first step was *AgeI* digestion, followed by Klenow fill-in, which created a blunt 5' end to create a compatible end to *NruI*. Then a second digestion was performed with *BamHI*, which creates compatible sticky 3' end to *BamHI* (Fig.3.5.A). Insert, and backbone DNAs were ligated using T4 ligase overnight then transformed into Stbl3 E.coli competent cells. Following overnight culture, colonies were selected, grown for 16 hours and then DNA was extracted. In total 12 colonies were tested and these were digested with *SbfI* and *BamHI*. Positively cloned plasmid DNA digestion bands are approximately 4.4kb and 7.3kb. Figure 3.5.B showed that colonies 1, 3, 8, 10 and 12 were positive for the *SbfI/BamHI* digestion. Clone number one was selected for final V3co lentivirus plasmid for maxi-prep. The same cloning strategy was applied to generate SQco and N6co lentiviral constructs (Fig.3.5.C, D). Although SQco and V3co cloning were successful, N6co cloning with this method was unable to achieve the correct positive colony. Figure 3.5 D showed that the *SbfI/BamHI* digestion exhibits an unwanted DNA band at 1.8kb instead of 4.4kb DNA band. To resolve this issue, we used the newly generated pRRL PGK V3co WPRE vector (Fig.3.5.B) as backbone plasmid. N6co and lentiviral backbone plasmid were digested with *KpnI* (Fig.3.6.A), and positive colonies were selected by *KpnI* digestion (Fig.3.6.B). The correct direction of the insert was checked by *SbfI* digestion, which shows 2.2kb and 9kb DNA bands (Fig. 3.6.C).

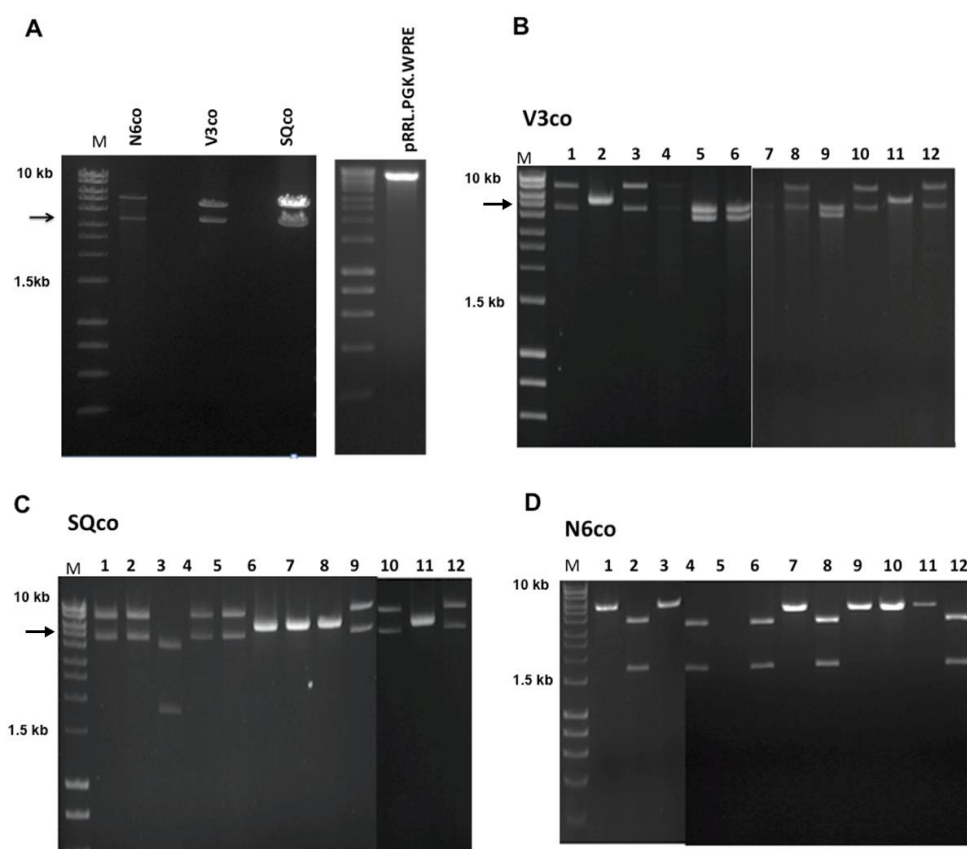


Figure 3.5. Cloning for codon optimised FVIII variants into lentivirus shuttle plasmid

A) Agarose gel electrophoresis of *NruI/Bam*HI digestion for N6co (4.9kb/ 3.3kb), V3co (4.5kb/ 3.3kb), and SQco (4.5kb/ 3.3kb). Each inserts indicated by arrow (4.9kb for N6co, 4.5kb for V3co and SQco). pRRLL.PGK.WPRE digested with *AgeI/Bam*HI as used for backbone plasmid. B), C), D) Positive colonies were selected according to correct digestion pattern with *SbfI/Bam*HI.

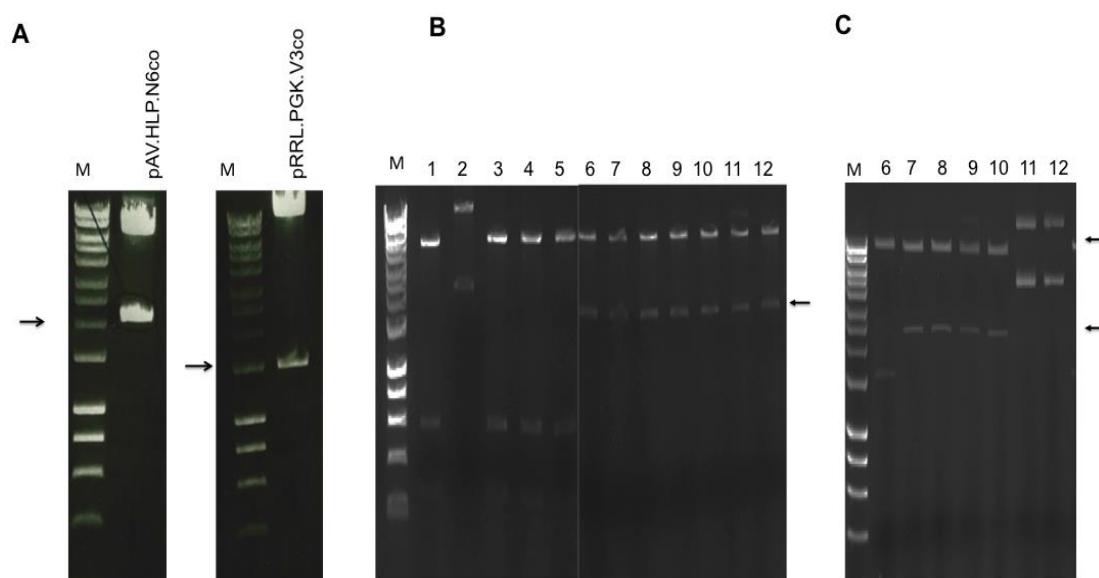


Figure 3.6. Cloning for codon optimised FVIII N6 into lentivirus shuttle plasmid

A) The Agarose gel image shows 6.3kb and 2.1kb bands for pAV2 HLP N6co synPA and 9.7kb and 1.3kb bands for pRRL PGK V3co WPRE respectively. B) Positive colony selection with *KpnI* digestion. The arrow shows 2.1kb positive DNA band. Colonies 6~12 was selected as a positive colony. C) Direction checked by *SbfI*, which digest positive plasmid DNA to 2.2kb and 9.6kb respectively (Arrow).

3.2.4. Cell line selection for stable FVIII expression

To select the most efficient cell line, which is suitable for this study, the lentiviral vector plasmid DNAs were transfected into either HEK-293T or Huh 7 cell lines. Two different cell lines were evaluated for FVIII production. The HEK-293T cell lines originated from the human embryonic kidney. It is widely used in industry for recombinant protein production because of its well-characterised genome and relatively ease of handling for scale up. In contrast, Huh 7 cell is a human hepatocyte-derived cellular carcinoma line, which allows systematic studies *in-vitro* of FVIII expression in cells that are similar to those of the target organ liver cells (Nakabayashi *et al.*, 1982). For plasmid transfection into these two cell lines, two variants were selected: FVIII B-domain modified plasmids SQco and V3co. FVIII antigen (%) ELISA assay showed that V3co ($28\% \pm 6.2$) and SQco ($18\% \pm 4.8$) were highly expressed in HEK-293T cells. In contrast, Huh 7 cells showed poor expression of V3co ($7\% \pm 1.4$) and SQco ($2\% \pm 1.2$). Statistics show between the two cell lines produced FVIII expressions yielded significant difference between HEK-293T cells and Huh 7 cells (** $P < 0.005$, Two-tailed paired t-test). The results suggest that HEK-293T cells are a more appropriate choice for stable expression of FVIII (Fig. 3.7).

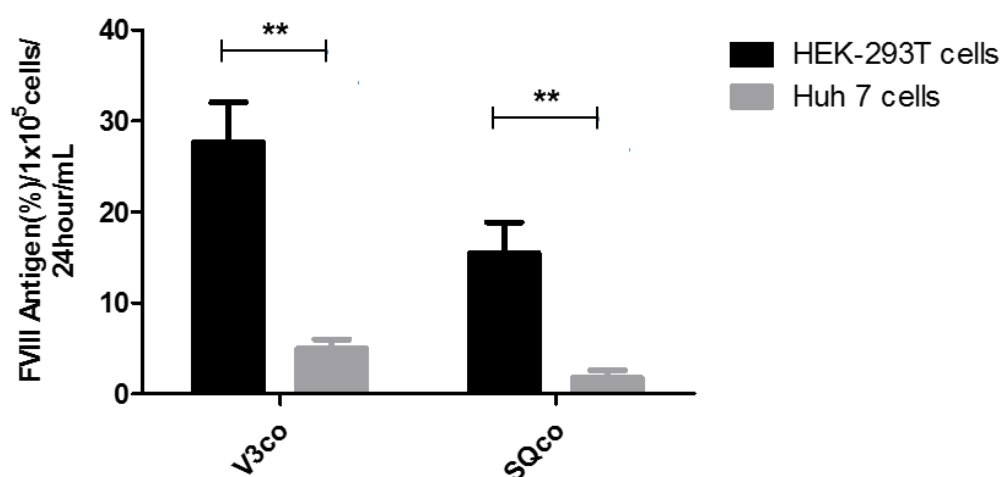


Figure 3.7. Expression of FVIII V3co and SQco variants from PGK driven FVIII transgene in different cell lines

Cells were transiently transfected with two variant expressing plasmids, and fresh medium was changed after 48 hours. FVIII containing medium was harvested after a further 24 hours of incubation and analysed for FVIII expression by ELISA. The graph shows secreted FVIII protein expression from HEK-293T and Huh 7 cells under a serum-free condition. Results are reported as mean \pm SEM, (n=2). Two-tailed paired t-test (**P<0.005). Prism 6.0 (Graph Pad).

3.2.5. Lentiviral vector production

Lentiviral vectors were produced using 3rd generation pRRL packaging system with PEI transfection, and viral titers were determined by Q-PCR (details in materials and methods). Here we achieved high viral titres using small scaled viral preps and include Green fluorescence protein (GFP) viral controls; all variants produced more than 1×10^8 viral genomes. In the context of viral titre, there was no difference between wild-type and codon optimised B-domain deleted FVIII, as illustrated in Table 3.1.

sin pRRL PGK WPRE, FVIII viruses	Titer by Q-PCR
pRRL PGK GFP WPRE	5.78×10^8 Viral genome/mL
pRRL PGK WTSQ WPRE	1.0×10^8 Viral genome/mL
pRRL PGK WTN6 WPRE	1.0×10^8 Viral genome/mL
pRRL PGK SQco WPRE	1.01×10^8 Viral genome/mL
pRRL PGK V1co WPRE	1.0×10^8 Viral genome/mL
pRRL PGK V3co WPRE	1.24×10^8 Viral genome/mL
pRRL PGK V5co WPRE	1×10^8 Viral genome/mL
pRRL PGK N6co WPRE	1×10^8 Viral genome/mL

Table 3.1. Quantification of vector titres for VSVG pseudo-typed lentivirus

The RNA based lentiviruses are unstable at room temperature, due to that fact all processing was performed at 4°C, except cell culture and production in incubators. Twice harvested viral supernatant was merged then concentrated 150 times using ultra-centrifugation. Viral pellet was re-suspended with cold DMEM and aliquots kept at -80°C. Viral titres were determined by qPCR-based assay. pRRL PGK GFP WPRE virus produced for viral control. Each Q-PCR titre is a mean of the values.

3.2.6. Optimisation of FVIII lentiviral vectors transduction

To identify, optimal FVIII expression condition, Human embryonic kidney derived HEK-293T cells were transduced serially with lentiviral vectors encoding FVIII variants. A previous report showed codon optimised FVIII cDNA produced 7~30 fold higher levels of FVIII expression level compared to the wild-type sequence (Ward *et al.*, 2011; Shestopal *et al.*, 2017). Therefore, the codon optimised lentiviral constructs harbouring SQco, V3co and N6co were used to transduce HEK-293T cells at various multiplicities of infection (MOI). The FVIII levels were assessed by FVIII antigen ELISA (Affinity Biologicals). At day four post-transduction, the maximum expression levels were detected at MOI of 10 (FVIII-N6co: 80%, FVIII-V3co: 28% and FVIII-SQco: 18%). N6co variant, which contains 226 amino acid out of 908 amino acid partial B-domain linker, expressed 3 to 4-fold higher expressions at the MOI of 10. Although results are not corrected for proviral copy number a positive correlation between FVIII antigen (Polyclonal FVIII antigen, Affinity Biologicals) and MOIs is clearly demonstrated (Fig. 3.8).

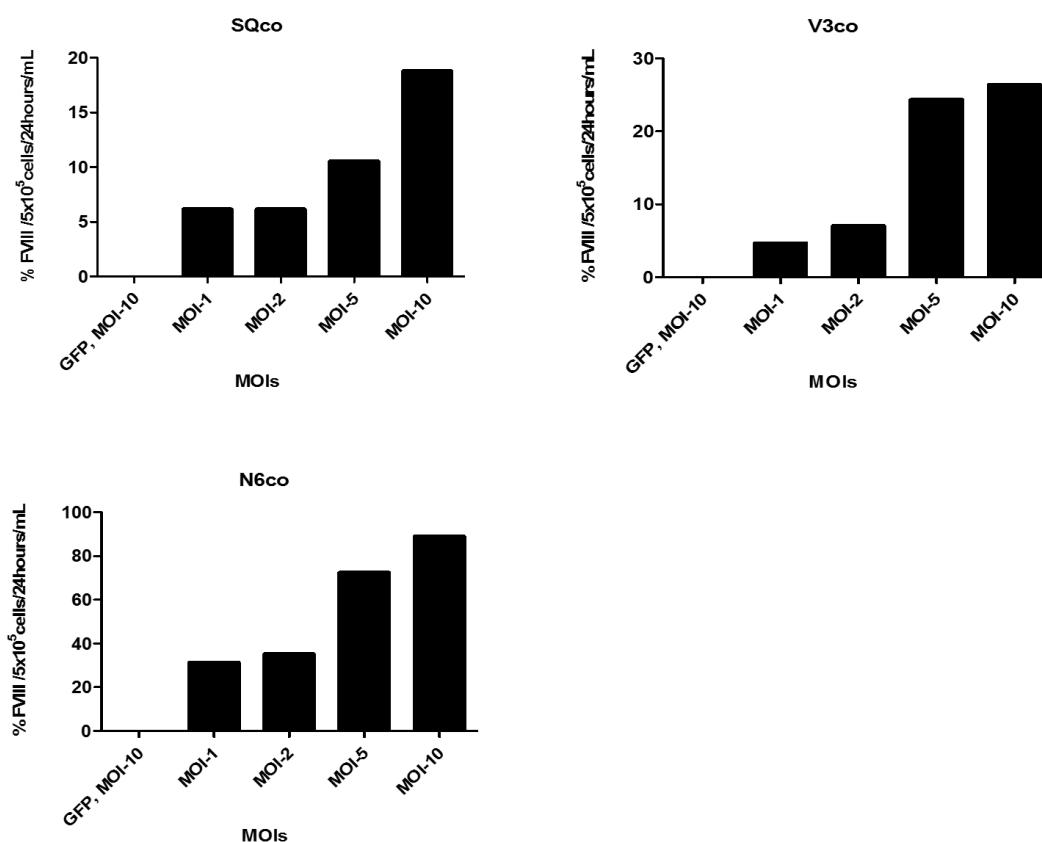


Figure 3.8. Optimisation of the multiplicity of infection (MOI) of Lenti-FVllls for the production of hFVlll expression levels in HEK-293T cells

Serial transduction of HEK-293T cells using lentiviral vectors were performed at a multiplicity of infection (MOI) of 1, 2, 5, and 10 for single transduction. Secreted FVlll was assessed using a polyclonal FVlll antigen assay after 72 hours following each transduction. Columns represent FVlll antigen expression levels for different MOIs. Cell viability and growth rates were also determined and found to be similar among all conditions. GFP lentiviral vector used as positive control for viral transduction. GFP-transduced at MOI 10 produced more than 95% GFP positive cells (Data not shown).

3.2.7. Protein expression by the B-domain modified FVIII cell lines

All FVIII lentiviral vectors (SQco, V3co, and N6co) produced FVIII Antigen. Our next interest was to test how the FVIII protein cleavage pattern is affected by the modified B-domain.

To characterise protein expression pattern, the total cell lysate of the B-domain modified FVIII (SQco, V3co, and N6co) were separated on the SDS-PAGE gel followed by western blot and detected with a polyclonal antibody directed against the full-length FVIII to determine the cleavage pattern of the modified FVIII.

The B-domain of FVIII-SQ is composed of 14 amino acids that are truncated from the original FVIII B-domain sequence. ReFacto® (Pfizer) is the commercial product of FVIII SQ, which we used as a control for the cleavage pattern. Figure 3.9 showed that ReFacto® appeared as a 170kDa (SC: Single chain), 90kDa (HC: Heavy chain) and 80kDa (LC: Light chain). It should be noted that the ReFacto® is purified and concentrated, therefore; the intensity of the cleaved product is too strong to compare with our cell lysate. Next, the codon optimised version of SQ, SQco (lane five) showed 170kDa, 90kDa and 80kDa of FVIII chains identical in mobility to those present in commercial ReFacto®.

In contrast, N6co with its 266 amino acid of B-domain is predicted to generate bands at 240kDa (single chain), 90kDa (heavy chain) and 150kDa, 80kDa (light chain). The 150kDa (226aa+80kDa light chain) is generated by cleavage of the heavy chain (A1, A2) from a single chain with B- domain (226 Amino Acid) still attached to 80kDa light chain. The actual result showed that 240kDa single chain is not detected while 150kDa was the strongest band among the cleaved N6co bands. The result suggests that 240kDa single chain might be efficiently processed to a small fragment of the cleavage products such as 150kDa chain and 90kDa heavy chain. However, the 80kDa light chain is weaker than 90kDa implying intermediate 150kDa is not efficiently processed to 80kDa of light chain.

Although a weak band representing the light chain appeared from analysis of N6co, it does not necessarily mean a reduced activity. In fact, thrombin generation assay showed no difference with ReFacto®, as will be discussed in chapter 4.

The B-domain of V3co contains an additional 17 amino acid with six *N*-linked glycosylation motifs (31aa linker) between the B-domain of SQ. Therefore the predicted size of cleavage products are 190kDa (single chain), 110kDa (heavy chain + 31aa linker), 90kDa (Heavy chain) and 80kDa (light chain). Similar to N6co, the single chain of V3co is not detected and as we predicted the 110kDa is generated from cleavage of the light chain from single chain due to the furin cleavage site and as a result B-domain linker (31aa) is still attached to 90kDa heavy chain (Fig.3.9, lane 4). It is interesting to note that the light chain is the most efficiently cleaved amongst these constructs.

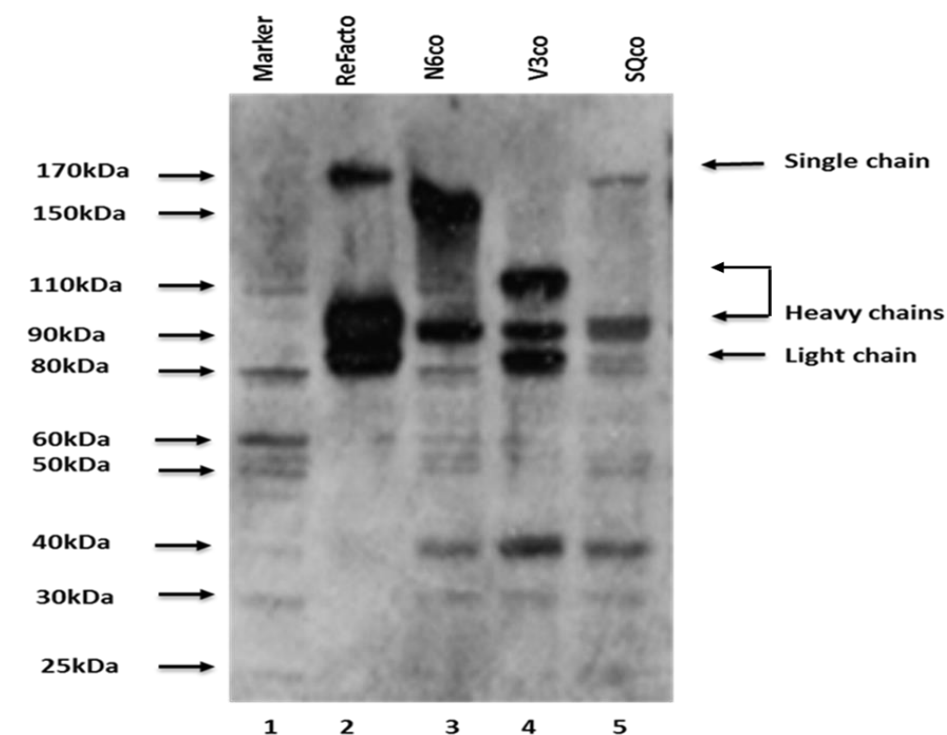


Figure 3.9. FVIII protein expression from B-domain modified constructs

HEK-293T cells were transfected with V3co, N6co, and SQco then the cell lysates were used for western blot analysis. Polyclonal antibody (Sheep, Affinity Biologicals, UK) used for the FVIII detection. Lane 1: Marker, Lane2: ReFacto® 14aa B-DD, Lane3: 226aa/N6 B-domain, Lane4: 31aa linker contained V3co, Lane5: 14aa SQco.

3.2.8. Single cell clone selection

To establish a FVIII expressing stable cell line, lentivirus with different FVIII variants were used to transduce HEK-293T cells at MOI of 10. From the population of cells that underwent ten rounds of transduction, clonal isolates were obtained by limiting dilution in 96-well plates. After two weeks, ten clones were selected for each variant and assessed for FVIII antigen levels using ELISA (%FVIII/1x10⁶cells/ 24hours expression). This ELISA assay using a polyclonal antibody against FVIII antigen shows variable expression levels in individual groups of variants (Fig. 3.10). Therefore, the four highest FVIII expressing clones were expanded for further analysis.

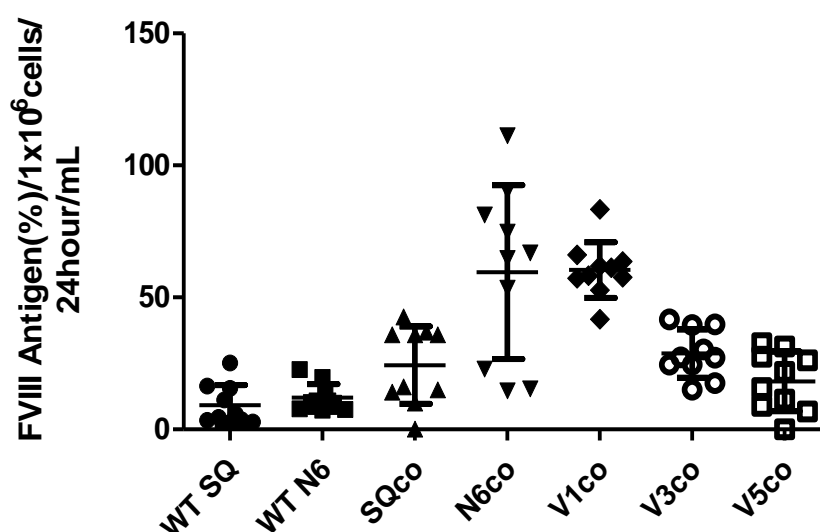


Figure 3.10. Initial selection of single cell lines, according to which are the best performing FVIII antigen expressing clones

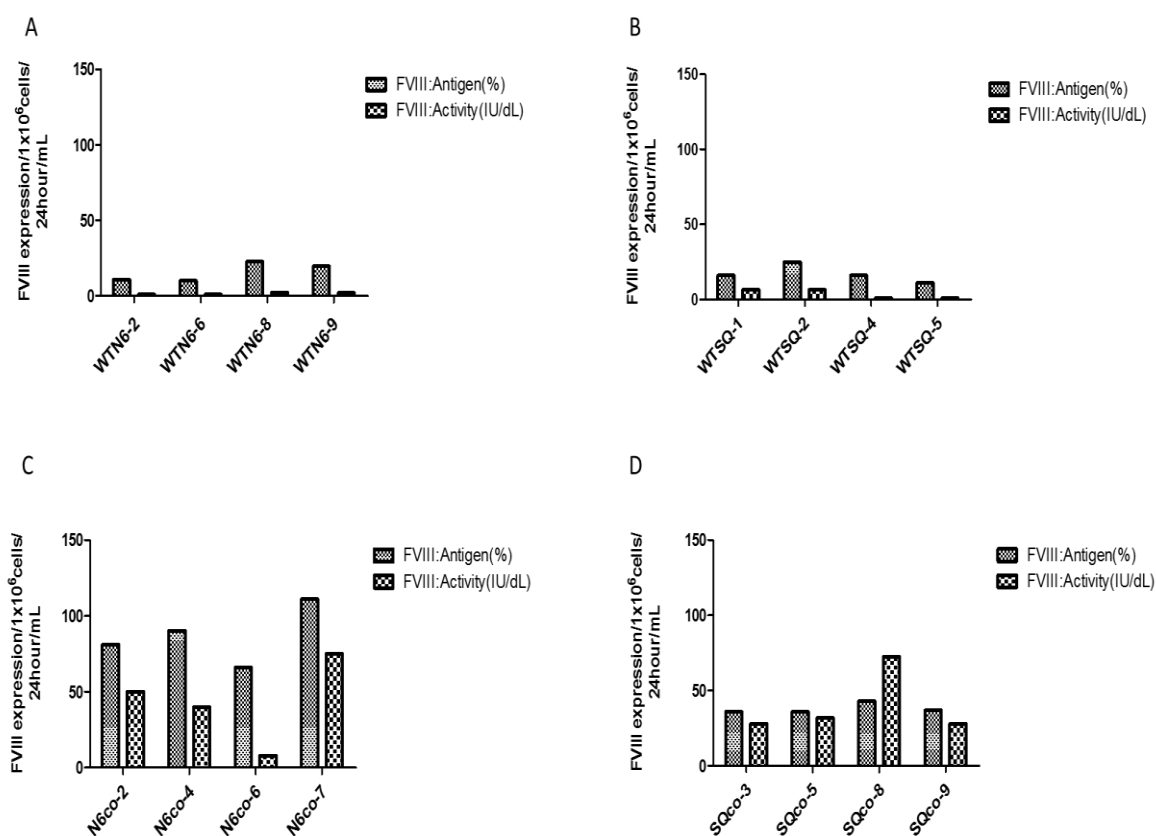
Individual clones were assayed for FVIII antigens by Affinity biologicals kit (ELISA), a total of 10 clones per variants were analysed. Horizontal bars represent the mean of each set of clones and \pm SEM, (n=10). Prism 6.0 (Graph Pad).

3.2.9. Secondary screen and selection

To select the best performing single cell clone, I chose four out of the ten initially selected clones according to FVIII antigen level and activities from the medium. The four clones of WTN6 selected are illustrated in Figure 3.11.A. Clone WTN6-8 showed the best antigen expression (23%), and activity (2.3 IU/dL). Although the protein levels are highest from the colony, we chose the clones according to the level of activity because the highly secreted FVIII protein may not be properly processed in the cells. The same selection method was applied to all constructs. The WTSQ clone 1 and clone 2 had same activity level. Clone 2 was selected for future work due to high antigen level (Fig. 3.11.B). In this study, it is important to note that we can separate into two groups according to codon optimisation. The WTN6 and WTSQ have non-codon optimised FVIII, and the rest (SQco, N6co, V3co, V1co and V5co) are all codon optimised FVIII. The FVIII antigen level of the non-codon optimised group was between 10~25 (%) for antigen level and 1~8 IU/dL for activity level (Fig.3.10. A and B). However, the codon-optimised variants showed higher FVIII antigen (40~80 %) and activity (20~80 IU/dL) (Fig.3.11. C-F). These results suggest that the codon-optimisation increases not only the antigen level up to 4-fold but also FVIII activity by 10-fold respectively. However, the fold differences between FVIII antigen level and activity may be due to discrepancy of the assay. As we mentioned in chapter 2, we applied 1 IU/mL to 100% FVIII antigen value for FVIII antigen standards that the units are not appropriate for percentage of FVIII antigen.

The N6co-7 clone was selected according to the highest activity level amongst the N6co group at 75 IU/dL of FVIII. Unlike N6co, the levels of FVIII activity of SQ derivatives (V3co, V1co and V5co) are either similar to antigen level or much higher as illustrated by the selected colony SQco-8. The results suggest that codon optimised SQ transcripts may provide optimal conditions for cellular processing of FVIII (Fig.3.11.D-G). V3co group showed a consistent FVIII antigen level, the clone (V3co-2), selected expressed

FVIII at activity levels of 170 IU/dL (Fig. 3.11.E). V1co clones (44 amino acid B-domain linker) showed high FVIII activity consistently in all four-selected colonies. Therefore I chose a clone V1co-4, according to its highest activity (139 IU/dL). In FVIII-V5co, the *N* (Asn) amino acids are substituted to *A* (Ala). Amongst V5co clones, V5co-10 showed the highest FVIII activity (222 IU/dL). All subsequent experiments were conducted with the clones selected.



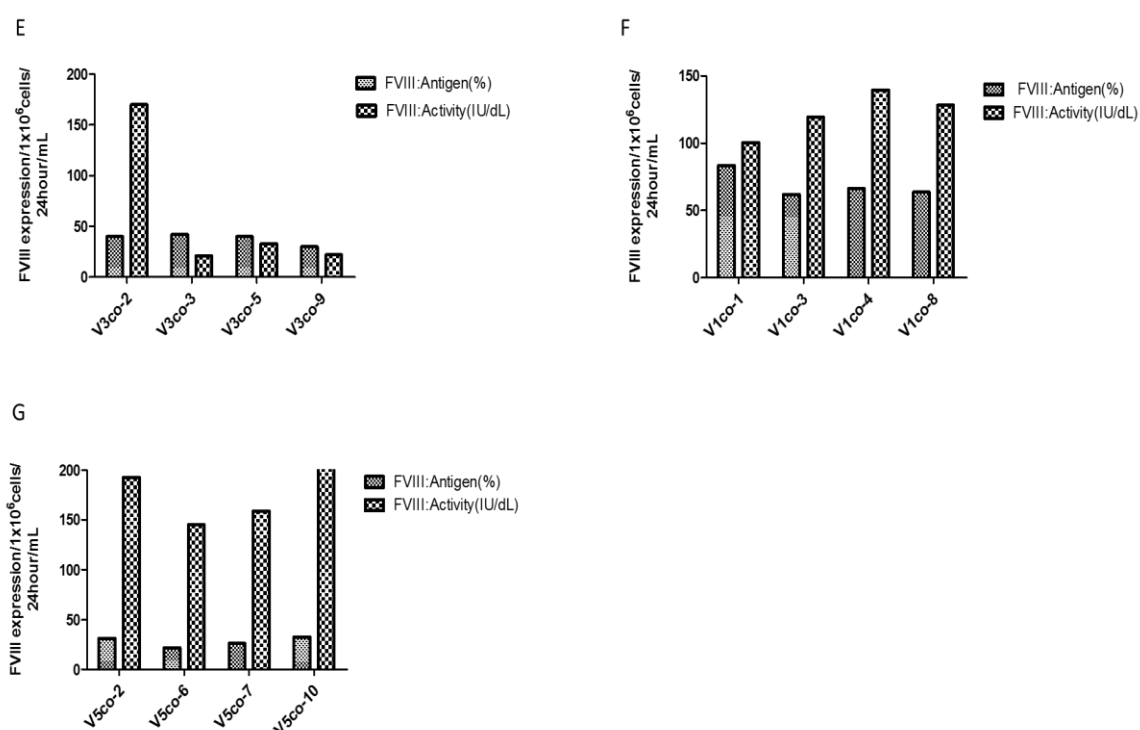


Figure 3.11. Second selection of single cell line from pre-selected lines

Further clone selections were performed. Four clones were selected from previous ten selected clones. The FVIII antigen (%) and activity (IU/dL) were tested from second stage-selected clones from the group of wild-type (WT) and codon-optimised groups. A) WTN6, B) WTSQ, C) N6co, D) SQco, E) V3co, F) V1co, G) V5co. Abbreviation: co; codon-optimised.

3.2.10. Determination of proviral copy number in stable cell lines after lentiviral transduction

To investigate if variation in transgene expression was caused by variation in the number of vector genomes integrated into the host gene, viral copy number was determined for all our transduction HEK-293T clones, since it is possible that variation in relative gene transfer efficiency for each of the lentiviral preparation may result in disparate levels of FVIII expression. Therefore the copy number was characterised from genomic DNA, which was extracted from stable cell lines so that transgene copy number could be determined using Q-PCR for each stable cell line (Fig.3.12). The average integration rate of the selected stable line for each variant was 0.5 to 1.2 copies per cell, with the exception of the WTSQ line, which had 3-fold greater copy number than the other cell lines. This raises a possibility that the WTSQ line may have been highly transduced with lentiviral vectors by chance. Therefore, three more WTSQ cell lines, which expressed lower FVIII antigen levels were tested for genome copy number. According to the Q-PCR (3.5, 3.7 and 4.1 copies per cell), we observed that there was consistently higher integration rate found among another three WTSQ lines implying that the respective lentivirus preparation had higher potency when compared to other vector preparation for the other FVIII variants. Therefore to allow for variation in gene transfer efficiency at the genomic levels we used genome copy values to normalise FVIII antigen and activity levels and expressed the results as FVIII antigen or activity levels per copy of the FVIII transgene in the target cells.

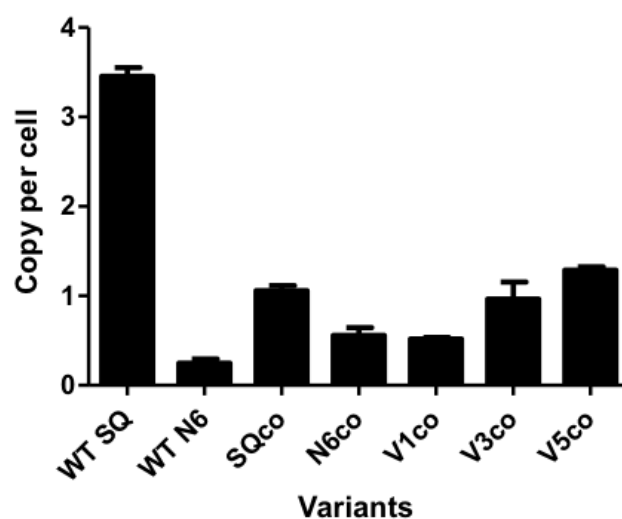


Figure 3.12. Quantification of viral copy number from lentiviral transduction

To quantify viral genome copy numbers from stable cell lines, genomic DNA was extracted from stable cell lines and q-PCR carried out for each sample for both human house-keeping GAPDH gene and viral WPRE sequence to determine integrated proviral copy number per cell.

Mean (\pm SEM), proviral copy number in FVIII stable cell lines, (n=3). Prism 6.0 (Graph Pad).

3.2.11. Determination of mRNA expression

Total RNA was extracted from the stable cells, and the relative level of FVIII mRNA was assessed using Q-PCR. Glyceraldehyde 3-phosphate dehydrogenase (GAPDH) was used for normalisation of the loading mRNA. Figure 3.13 shows that FVIII mRNA level of two wild-type variants; SQ (WTSQ) and N6 (WTN6) were very similar. Codon optimised variants had 5 to 20-fold higher FVIII mRNA levels when compared with wild-type variants. Statistical analysis between both wild-type variants and codon-optimised variants (N6co, V3co and V5co) were significant ($***p < 0.0001$, One-way ANOVA, Bonferroni simultaneous test). The V3co variant showed a 20-fold increase in mRNA expression compared with the WTSQ and 4-fold higher than codon-optimised SQ. The difference in mRNA levels between WTN6 and codon-optimised N6co was 16-fold. However, we did see a difference in FVIII mRNA levels between the V3co and N6co clones ($*p < 0.05$). The FVIII mRNA levels for the SQco and V1co clones were similar (ns). In contrast, we observed a 2-fold higher level of FVIII mRNA level in the V3co clones compared to the V5co ($**p < 0.005$).

It has been shown that deletion of the entire B-domain leads to a 17- fold increase in mRNA and primary translation product compared with full-length FVIII; however, only a 30% increase in the levels of secreted protein (Pittman *et al.*, 1994; Kaufman *et al.*, 1997; Miao *et al.*, 2004). Our results are consistent with other published reports that indicate that codon optimisation results in improvement gene expression through enhancement of translation and mRNA stability (Foster *et al.*, 2008; Presnyak *et al.*, 2015).

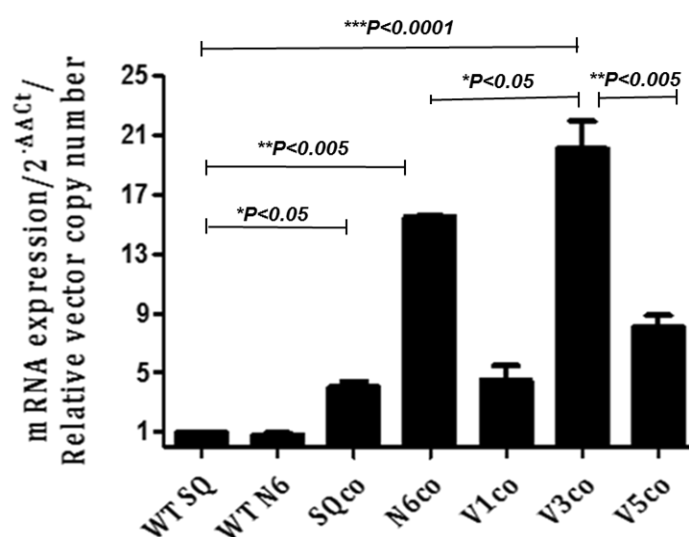


Figure 3.13. Evaluation of relative mRNA expression of FVIII variant stable cell lines

The relative expression of FVIII variants mRNA expression determined as $\Delta\Delta C_t$ value by real-time RT-PCR. WTSQ value used as a control, Total cellular RNA was prepared and FVIII transgene expression quantified by RT real-time quantitative PCR analysis of the WPRE element which lentiviral shuttle present in all transcripts. Data presented as mean \pm SEM, (n=3). One-way ANOVA (Bonferroni simultaneous test), Prism 6.0 (Graph Pad).

3.2.13. Assessment FVIII Activity in stable cell lines

The cofactor activity of stable cell lines culture media samples was assessed using the FVIII: Activity (Biophen, Quadragech Diagnostics) according to the manufacturer's instructions.

Using the chromogenic assay, the WTSQ showed activity (0.08 ± 0.01 IU/mL), which is similar with WTN6 activity (0.1 ± 0.07 IU/mL), whereas the codon optimised variants SQco (0.83 ± 0.23 IU/mL), N6co (2.19 ± 0.24 IU/mL), V1co (0.87 ± 0.12 IU/mL), V3co (2.05 ± 0.12 IU/mL) and V5co (1.64 ± 0.03 IU/mL) were significantly increased compared to wild-type variants (Fig.3.14). Statistical analysis between wild type variant and the codon-optimised variant was significant ($***p < 0.0001$, One-way ANOVA, Bonferroni simultaneous test). These results suggest that codon optimisation significantly enhanced expression of FVIII activity in these cell lines.

It is important to mention that in terms of FVIII activity, the B-domain is dispensable and that smaller B-domain deleted variants have significantly increased stability and activity (Pittman *et al.*, 1994). Moreover, *N*-linked glycosylation has been suggested to be an important modification for FVIII activity. Therefore, it is interesting to compare from our FVIII activity assay which codon optimised B-domain truncated (N6co, V3co, V5co) FVIII variants are significantly more expressed compared with SQco. As a result of statistical analysis (One-way ANOVA, Bonferroni simultaneous test), the SQco vs V3co, V5co, and N6co was significant ($**p < 0.005$) whereas SQco vs V1co were not significantly different from each other (ns). These results suggest that the six *N*-linked glycosylation sites are not affecting FVIII activity due to the fact that FVIII activity from mutated *N*-linked glycosylation construct V5co was not significantly changed. Moreover, the six *N*-linked glycosylation site containing V1co was significantly less active compared with V3co and N6co ($**p < 0.005$).

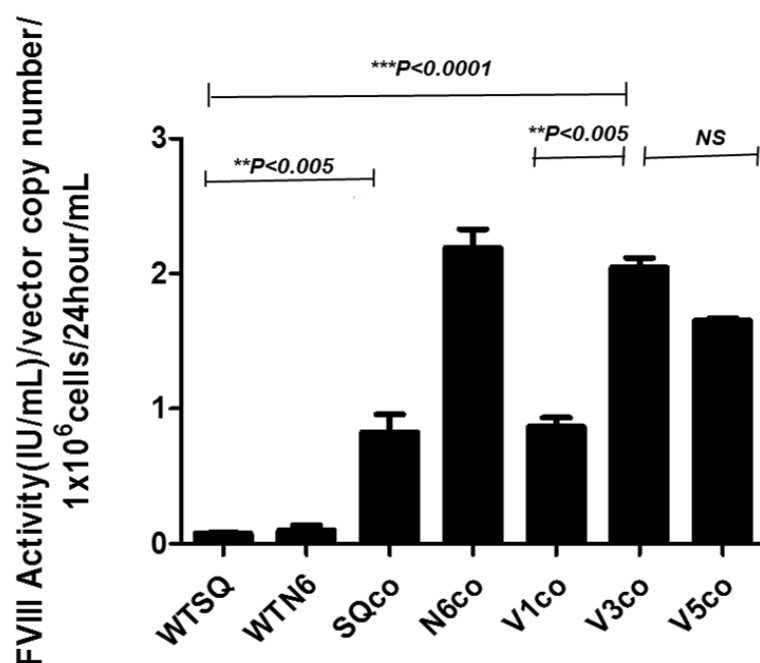


Figure 3.14. FVIII activity comparison between the FVIII variant stable cell lines

FVIII activity was determined by chromogenic assay, the data was obtained from the conditioned medium, and FVIII expressions were normalised by vector copy number. Data presented as mean \pm SEM, (n=3). One-way ANOVA (Bonferroni simultaneous test), Prism 6.0 (Graph Pad).

3.2.14. FVIII antigen assay in stable cell lines

Following the activity assay, we sought to determine the protein expression level of FVIII using FVIII antigen assay (ELISA) in the same batch of samples. The FVIII antigen expression was evaluated using the Stago kit (Asserachrom). The kits contain prepared plates coated with a monoclonal, which has a FVIII A2 domain epitope antibody. It is more sensitive than polyclonal antibody for detecting low levels of protein in culture media because monoclonal antibodies are much more specific and with less background noise than polyclonal antibodies, however very sensitive to small changes in the antigen. Figure 3.15 shows a similar pattern of FVIII protein expression as FVIII activity assay. The FVIII expression levels were WTSQ ($10.6\% \pm 1.66$), WTN6 ($4\% \pm 0.01$) whereas the codon optimised variants expression levels were SQco ($123\% \pm 3.45$), N6co ($163\% \pm 32$), V1co ($100\% \pm 4.0$), V3co ($296\% \pm 18.5$) and V5co ($182\% \pm 5.8$). Statistical analysis (One-way ANOVA, Bonferroni simultaneous test), between wild type variant and codon-optimised variants, were significant ($***p < 0.0001$). These results suggest that codon optimisation significantly enhanced FVIII protein expression corresponding to elevated mRNA levels.

We hypothesised that *N*-linked glycosylation may affect FVIII protein trafficking. V3co which encodes the shortest linker peptide with six *N*-linked glycosylation sites among the variants had the most significantly increased FVIII expression level. The V5co with its *N*-linked glycosylation sites mutated to Alanine shows significant difference ($*p < 0.05$) levels of FVIII expression compared with V3co, however six *N*-linked glycosylation sites encode N6co, and V1co shows significantly decreased FVIII expression level compared with V3co ($*p < 0.05$). These observations suggest that *N*-linked glycosylation is not the only factor influencing FVIII expression. Therefore we used immunocytochemistry to investigate the FVIII cellular trafficking from ER to Golgi in established single FVIII variant cell lines.

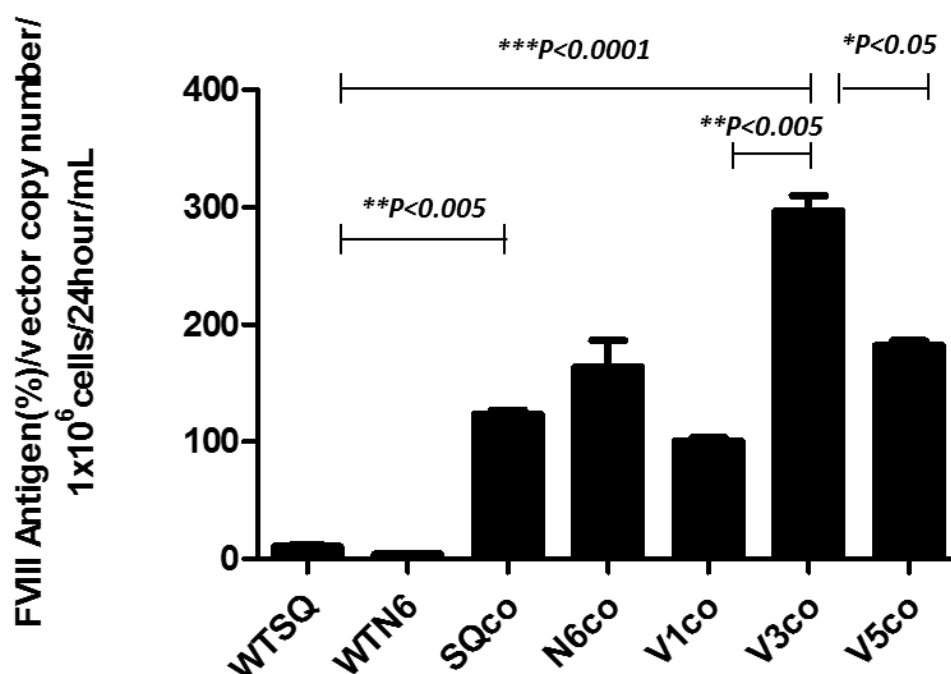


Figure 3.15. Quantification of human FVIII expression of variant stable cell lines

Quantification of human FVIII antigen expression levels were determined by a commercial ELISA (Stago kit). The data was obtained from the conditioned medium and FVIII expressions were normalised by vector copy number. Data presented as mean \pm SEM, (n=3). One-way ANOVA (Bonferroni simultaneous test), Prism 6.0 (Graph Pad).

3.2.15. Membrane-bound FVIII in serum-free condition

Previous studies showed that 90% of recombinant FVIII is attached to the cell membrane of the producing cell when the B-domain has been reduced to around 21 amino-acids. Increasing the length of the B-domain reduces the membrane attached fraction by 50% of the total FVIII expressed (Kolind *et al.*, 2010). Further studies showed that the *N*-linked glycosylations within the B-domain did not influence either total FVIII expressed or the membrane-bound fraction. The addition of *O*-phospho-*L*-serine (OPLS) and Annexin V was shown to reduce binding of FVIII to the producer cell membrane (Kolind *et al.*, 2011). These observations encouraged us to investigate if we could increase the yield of our novel B-domain modified FVIII molecules by washing the producer cells with 0.5M NaCl. The FVIII activity profile of both supernatant and membrane bound fraction are shown in Figure 3.16. As described before, low FVIII activity was detected from SQco (0.55 IU/mL) and V1co (0.6 IU/mL) HEK-293T producer cells, while the N6co (2.3 IU/mL), V3co (2.02 IU/mL) and V5co (1.53 IU/mL) producer cells showed two to 3-fold higher FVIII expression than SQco and V1co (Fig. 3.16.A).

Membrane-bound FVIII activity from the stably transduced HEK-293T producer cells showed a different pattern with amount bound being similar for SQco (0.23 IU/mL), N6co (0.18 IU/mL), V1co (0.16 IU/mL), and V3co (0.17 IU/mL) producer cells (average = 0.2 IU/mL) but surprisingly 2.4-fold higher (0.48 IU/mL) for V5co, which suggests that this variant binds more to the producer cells (Fig. 3.16.B).

Overall, these data suggest that N6co and V3co will be ideal candidates for large-scale production of recombinant protein.

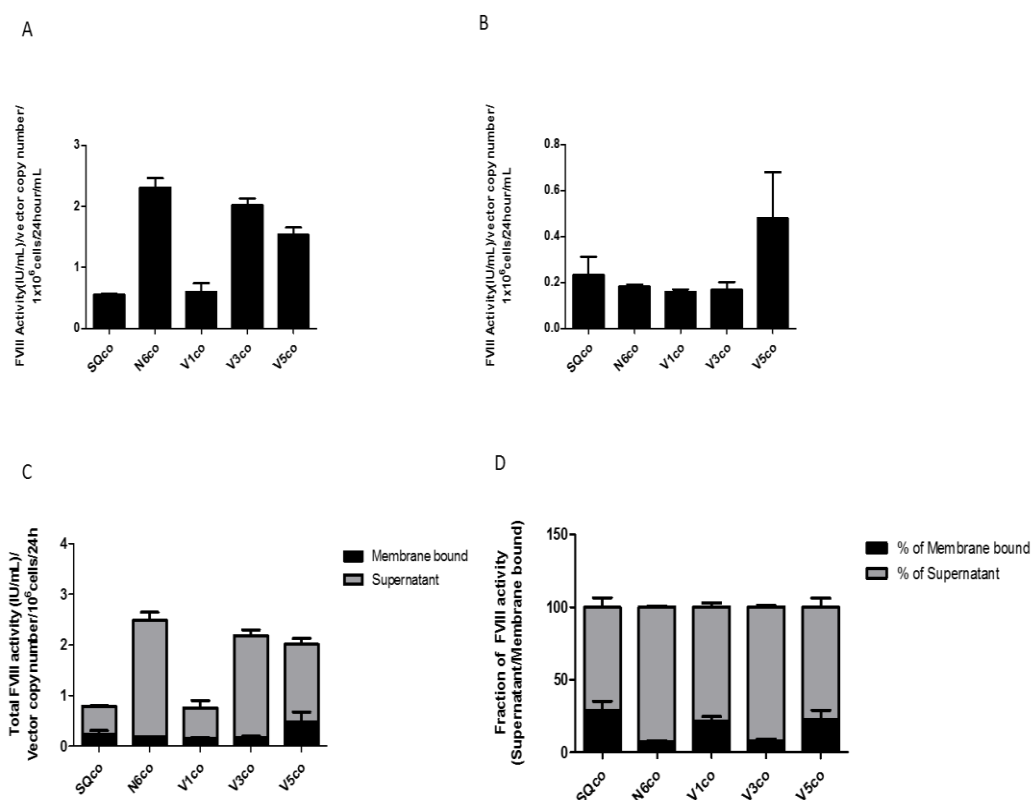


Figure 3.16. Profile of membrane-bound FVIII activity from the B-domain engineered FVIII

Established stable cell lines were plated as 1×10^6 cells per well in 6-well plates. 24 hours later mediums replaced with serum free DMEM. Further 24 hours later, cultivated medium harvested (supernatant) and cells were wash with PBS then add 1mL of 0.5M NaCl contained DMED for incubated in 37°C incubator (membrane bound fraction) both samples performed the chromogenic assay. A) FVIII activity in the supernatant. B) Cell membrane bound FVIII activity. C) Total FVIII activity, which combined with cell culture medium and cell membrane bound fraction. D) Semi-quantative (%) graph for supernatant and membrane-bound FVIII activity. Data presented as mean \pm SEM, (n=3). Prism 6.0 (Graph Pad).

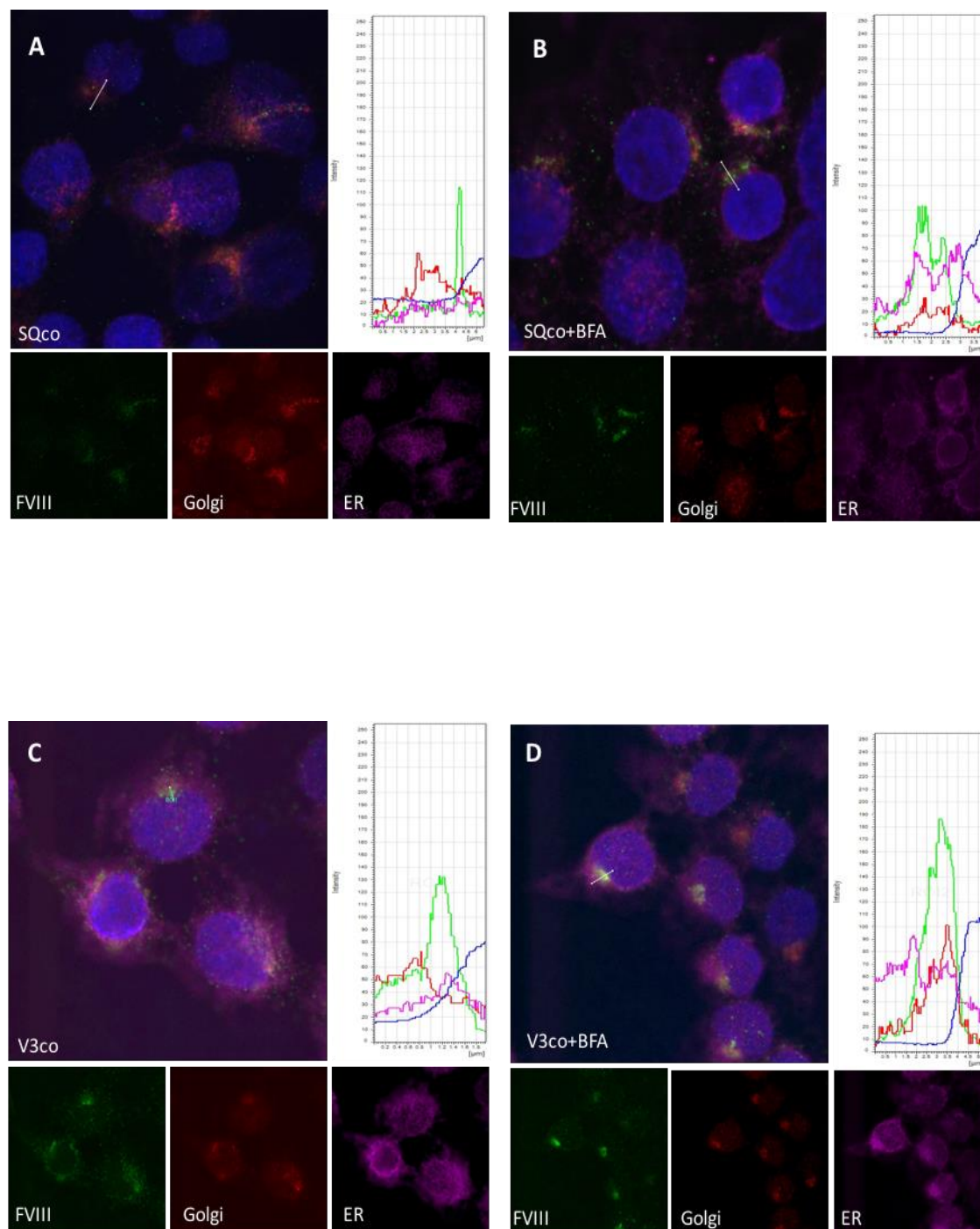
3.2.16. Immunocytochemistry

The use of bioengineering of the FVIII molecule has resulted in an improvement of FVIII mRNA expression and FVIII secretion. There are two important issues for the FVIII so produced, one is protein secretion, and the other is the biological activity of the released protein in the cultivated medium. B-domain modified constructs have *N*-linked glycosylation, which is important for protein secretion. This raised a question whether the *N*-linked glycosylation is important for the FVIII secretion to the cell culture medium. FVIII-V5co, in which all asparagine (*N*) of B-domain (FVIII-V3co) have been converted to alanine (*A*) to disable the *N*-linked glycosylation, may have decreased protein secretion to the medium. Therefore, we decided to investigate the cellular trafficking of FVIII variant proteins using immunocytochemistry. FVIII (SQco) is stained as small speckle in the cytoplasm, which is distributed to ER and Golgi apparatus (Fig.3.17.A). The majority of immunochemically detectable FVIII proteins were found in the place where Golgi and ER are over-laid (see in figure 3.17 of intensity histogram). To assess the protein localisation, image analysis was performed using software (LSF-AF, Leica), which allows drawing a specific region of interest (ROI) in the vicinity of FVIII accumulated region. It confirms that the FVIII granules were located in the overlapped region of ER and Golgi (Fig.3.17.A).

We hypothesised that blocking there trafficking system may lead to specific FVIII accumulation either in ER or Golgi. To test this hypothesis, FVIII stable cell lines (SQco) were incubated with BFA (Brefeldin A, Abcam), which prevents constitutive vesicular transport from the trans-Golgi network. Treatment with BFA increased FVIII accumulation in ER and Golgi compartment. Image analysis confirms that the intensity histogram of FVIII overlapped with the ER and Golgi (Fig.3.17.B). These findings suggest that the majority of FVIII (SQco) protein is released through ER and Golgi network.

Next, the most highly expressing FVIII cell line (V3co) was tested for the cellular localisation using immunocytochemistry. Figure 3.17.C shows a similar pattern of FVIII distribution as SQco cell line. FVIII is stained as large granules in the cytoplasm where ER and Golgi are located. The image analysis reveals that the histogram plot of FVIII is overlapped with ER and Golgi. In addition, we found an intensity difference between SQco and V3co, which may due to the different protein expression level illustrated in figure 3.9.C. The BFA inhibition increased the intensity of FVIII (V3co) in Golgi and ER compartment (Fig.3.17.D). This suggests that there was no functional difference in terms of trafficking between SQco and V3co. We next tested the FVIII V5co cell line, which contains disabled *N*-linked glycosylation sites. Figure 3.17.E shows that again the majority of FVIII is localised in ER and Golgi. The BFA inhibition increased the accumulation in ER and Golgi (Fig.3.17.F), which behaved in a similar manner to other FVIII lines (SQco and V3co). Brown and colleagues reported that human FVIII was notably absent in the Golgi apparatus and most FVIII was located in the ER. The study suggested that human FVIII is not efficiently trafficked from the ER to the Golgi (Brown *et al.*, 2011). In contrast, we observed codon-optimised human FVIII was co-localised to both ER and Golgi. Overall, my immunocytochemistry study demonstrates that FVIII proteins are predominately accumulating in the site where ER and Golgi compartments are overlapped. It suggests that ER and Golgi are both equally essential places for FVIII trafficking. It is important to note that ER and Golgi compartment are the places where the FVIII post-translational modification is occurring. The movement of proteins from the ER to Golgi apparatus has been identified as the rate-limiting step in intracellular transport (Lodish *et al.*, 1983), although immunochemistry has failed to detect any difference between FVIII variants tested, notably, V3co, which contains six additional *N*-linked glycosylation sites compared with SQco and V5co. It should be emphasised that the six *N*-linked glycosylation sites are putative and characterisation of post-translational modifications needs to be performed before a firm conclusion can be drawn. Therefore,

it is necessary to establish methods for production of purified FVIII protein to enable Mass Spectrometry analysis.



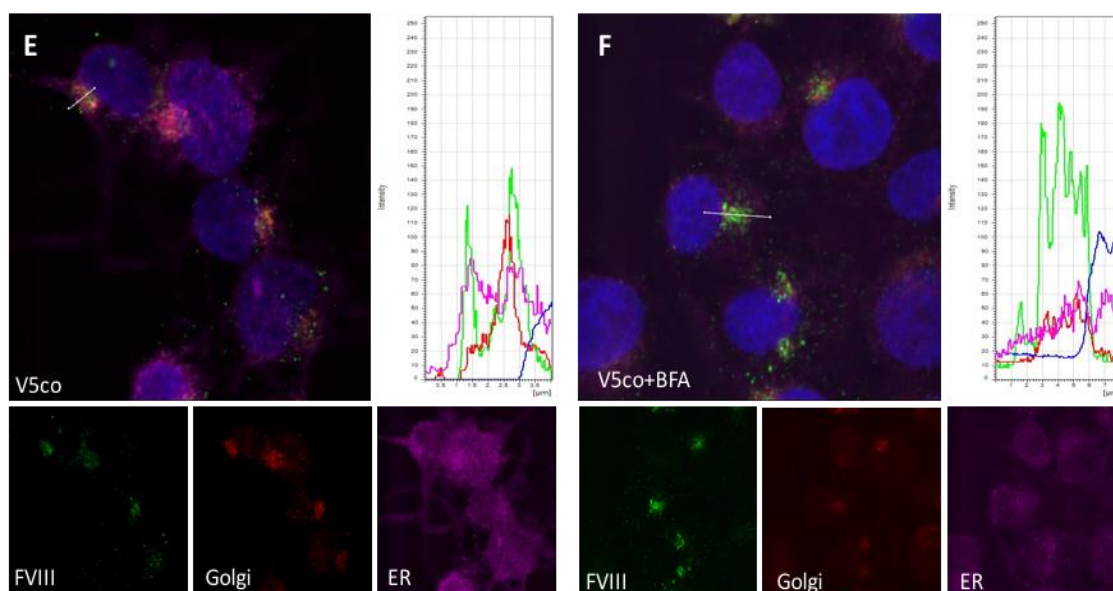


Figure 3.17. Immunocytochemistry revealing the FVIII variant protein localisation between ER and Golgi

Three FVIII variants cell lines, SQco, V3co and V5co were cultured on glass coverslip then fixed with 4% PFA for 15 minutes then immune-stained with antibodies (Green; FVIII, Red; Golgi, Purple; ER and Blue; Nucleus). Brefeldin A (BFA) was added to stable cells for an hour then cells were fixed with 4% PFA. A) SQco, B) BFA+ SQco, C) V3co, D) BFA+V3co, E) V5co and F) BFA + V5co.

Co-localisation of FVIII and ER or Golgi is represented by the colour (Green; FVIII, Red; Golgi, Purple; ER, and Blue; Nucleus). The merged images were analysed for intensity histogram using LSA-AF Leica imaging software (on the right panel). 100nM BFA- treated in 37°C for an hour then cells fixed for staining. Scale bar: 10 μ m.

3.3. Discussion

Currently, various forms of B-domain modified recombinant human FVIII (rhFVIII) are in clinical use for haemophilia A as replacement therapy (High and Anguela, 2015). ReFacto® was the first B-domain deleted FVIII commercial product, which is purified from the media of the Chinese Hamster Ovary cell line (CHO) that exogenously release engineered FVIII (Sandberg *et al.*, 2001; Booth *et al.*, 2007; Pipe, 2009). However, the current production procedure of the rhFVIII protein is very expensive, and consequently, the cost of FVIII regular infusion therapy (prophylaxis treatment) is too high for patients not living in economically developed countries. Alternatively, unlike protein replacement, gene therapy would allow endogenous expression of FVIII, which could eliminate the ongoing cost of haemophilia A treatment by replacement therapy.

Most gene therapy is based on delivering therapeutic genes to the patient using viral vectors. However, the engineered FVIII so produced must be characterised and optimised before human trial. Therefore, the first goal of this study was to characterise B-domain engineered FVIII isoforms. One of the most important hurdles was the short half-life of FVIII, which means that achieving a high concentration of the FVIII is challenging (High *et al.*, 2014).

To address these issues, three strategies were applied for enhancing FVIII expression in the cell. Firstly, to engineer the FVIII genomic sequence by codon optimisation, which increases transcription efficiency, either by stabilising the RNA transcripts with reduced cryptic splice sites and /or by enhancing protein translation. Secondly, modifying protein sequence of B-domain of FVIII to improve protein secretion. Finally, we isolated producer cells with maximal FVIII expression following lentivirus-mediated gene transfer of the FVIII variants.

In the context of establishing such a stable cell line, delivering high copy number of the gene may be essential, where copies can then be integrated into the genome. Although

transient transfection of DNA is able to establish a stable cell line by antibiotics selection process, it was not efficient enough to increase the FVIII expression due to low copy number insertion into the genome. In contrast, lentiviral vectors are ideal for long-term transgene expression either in dividing or non-dividing cells, which is suitable for establishing high copy number containing stable cell lines. Prior to transducing cell lines with lentiviral vectors, we identified that HEK-293T was better than Huh 7 cells. According to the comparison, HEK-293T cells showed approximately 4.5-fold higher FVIII expression than Huh 7 cells. The result indicates that the HEK-293T cells are more suitable for stable cell line production. Our observation recapitulates the Kalkhoran's findings that HEK-293T is more efficiently produced recombinant protein than Huh 7 cells (Kalkhoran *et al.*, 2013). In addition, Meex *et al.* reported that HepG2 cells produced more transgene protein than Huh 7 cells (Meex *et al.*, 2011). Finally, the transfection efficiency between two cell lines might vary. Considering that the observed difference in transfection efficiencies of Huh 7 and HEK-293T cells is likely due to inherent differences between the two cell lines. Because the DNA uptake and dividing times of HEK-293T cells (~24 hours) are two times quicker than Huh 7 cells (≥ 48 hours), implying HEK-293T cells are more active in the metabolic process (Nakabayashi *et al.*, 1982).

In the context of lentiviral vectors production, all the FVIII variants were efficiently produced with a titration range that was relatively high giving titres between 1×10^8 and 5×10^8 /mL. After the transduction of the FVIII variants carrying lentivirus to HEK-293T cells, the best performing single cell clone were selected according to the result of FVIII antigen level and activities from the medium. In this study, we can confirm that two group can be separated according to the codon optimisation of FVIII gene. Our results showed that FVIII activity of codon optimised group (SQco, N6co, V3co, and V1co) was 4-fold higher than that observed with FVIII variants that contained wild-type FVIII sequence (Fig. 3.11). The codon optimisation increases FVIII mRNA expression level. Therefore it

is necessary to confirm the level of FVIII transcripts from stable cell lines. The figure 3.13 shows that FVIII mRNA level of two wild typed SQ (WTSQ) and N6 (WTN6) are very similar, whereas the codon optimised variants were sharply increased from 5 to 20-fold when compared with wild-type variants suggesting indeed the FVIII mRNA increased level. We can argue that the high copy number of WTSQ is not corresponding to the mRNA transcription level, which suggests that the integrated FVIII of WTSQ is silenced or poorly transcribed. Zieiske *et al.*, showed that position effects, i.e. the regulatory environment of genomic integration sites could influence levels of expression. Others have shown that the presence of multiple copies of a transgene in a target cell can result in an epigenetic silencing and a variegated pattern of expression that the increased copy number of the lentiviral vectors into the host genome may disable the transgene transcription due to the integrated location such that becomes transcriptionally inactive heterochromatin (Garrick *et al.*, 1998; Zieiske *et al.*, 2004). Regarding protein expression, we measured FVIII by using FVIII antigen assay (ELISA) demonstrating by statistical analysis a significant difference between wild type variant and codon-optimised variant ($***p<0.0001$) demonstrating that codon optimisation enhanced FVIII protein expression and that it corresponds to increased mRNA expression. Finally, FVIII activity confirms that codon optimised FVIII constructs are all significantly increased as opposed to non-codon optimised, suggesting the stability and activity of FVIII have been improved by codon optimisation

FVIII potency confirmed that a certain level of size or sequences of the B-domain linker peptide is important rather than *N*-linked glycosylation sites for activity and also it suggests that outside of the B-domain the other six *N*-linked glycosylation of FVIII are important, most likely for protein-protein interaction with LMAN1 (Miao *et al.*, 2004; Zhang, 2005).

With regard to FVIII secretion, Kolind et al. reported that majority of recombinant FVIII binds to cell membrane when the natural B-domain is replaced with short linker sequence (21 amino acid), while *N*-linked glycosylation of the B-domain did not affect FVIII secretion (Kolind et al., 2010). Here, we showed that de-glycosylated B-domain carrying FVIII-V5co (31 amino acid) exhibited 2.4-fold increased membrane bound FVIII as opposed to V3co (31 amino acid), suggesting that lack of *N*-linked glycosylation on B-domain linker leads to accumulation of FVIII on the membrane surface of the HEK-293T cells (Fig.3.16). Our observation implies that *N*-linked glycosylation on B-domain linker might have an important role for FVIII secretion through an effect on membrane binding which is reduced in some glycosylated variants.

Taken together the results of this study using stable cell lines established by lentiviral integration of B-domain engineered FVIII variants, demonstrated that the codon optimised variants were significantly improved mRNA transcription and FVIII protein expression.

In conclusion, six *N*-linked glycosylation motifs juxtaposed the short linker version; FVIII-V3co has the best expression of FVIII protein. The superiority of this variant is due to the higher mRNA transcription and lower membrane binding together with enhanced protein translation.

The role of glycosylation in membrane binding and protein secretion requires further elucidation and dissection.

Chapter 4

Recombinant FVIII protein purification and characterisation

4.1. Introduction

The main aim of the studies outlined in this chapter was to define an optimised chromatography step that is highly selective for FVIII to enable isolation of a large quantity of FVIII protein without losing activity for the further biochemical characterisation of the FVIII variants including functional studies and *N*-linked glycosylation pattern by mass spectrometry. Achieving high purity FVIII is challenging by current purification methods because FVIII in the inactive state is a heterodimer in which the heavy and light chain are linked by a relatively unstable non-covalent metal ion bridge that makes FVIII compounds highly prone to degradation under acidic conditions. Consequently, the chromatographic purification of FVIII compounds must be performed under mild conditions to prevent product degradation.

Commercial large-scale recombinant protein products are purified by several steps including chromatography. Novo Nordisk's new rFVIII (Novo Eight) is purified in a five steps process, including the Capto MMC affinity column, which captured rFVIII from culture media and highest yields of proteins were achieved by combining high concentrations of both NaCl and ethylene glycol in the elution buffer. An anti-rFVIII immune-affinity chromatography using monoclonal antibody (F25), anion exchange step and size exclusion chromatography steps were added to attain a high degree of purity (Ahmadian *et al.*, 2016). The first human cell line derived rFVIII Nuwiq® (Octapharma) production process included nine steps from harvest cultivated medium to final formulation and polishing steps of size exclusion chromatography (Winge *et al.*, 2015). Recombinant FVIII Fc fusion protein (rFVIII Fc, Biogen Idec) production process also uses chromatography purification with steps including FVIIISelect affinity column (GE Healthcare), Anion exchange chromatography and Hydrophobic interaction chromatography methods (McCue *et al.*, 2015).

We therefore collected a large number of media from FVIII stable lines described in the previous section as illustrated in Figure 4.1. We then

1. Performed small-scale studies with a two-step chromatographic purifications processes to enable purification of FVIII at high yields without compromising function.
2. Used the optimised purification method to generate sufficient quantities of purified FVIII to enable biochemical characterisation including mass spectrometry.

While we need a relatively high concentration of pure FVIII, we don't need to the FVIII to be purified at levels required for infusion into patients.

4.2. Results

4.2.1. FVIII purification step

Recombinant human FVIII protein isolated from our stable producer cell lines (V3co, N6co, V1co, SQco and V5co) was initially purified by two-step chromatography as described by Tang et al. (Tang *et al.*, 2013). Step 1 entailed the capture step for which we used FVIIISelect a specifically designed affinity adsorbent molecule designed for purification of B-domain deleted FVIII. The second polishing step entailed concentration of eluant from step 1 by positively charged resin DEAE anion exchange column (GE Healthcare) as described in Figure 4.1. The buffer used for both column purifications methods are described in Table 2.2. FVIIISelect matrix consists of a 13kDa recombinant Camelid single domain antibody fragment that is attached to the porous base matrix via a hydrophilic spacer arm made available commercially by GE Healthcare (McCue *et al.*, 2009). We modified the standard protocol to include an additional harvest of the cell surface membrane bound FVIII using a buffer containing 0.5M NaCl.

All except cell culture step were processed at 4°C due to the instability of FVIII. Minimum exposure of FVIII to room temperature was necessary to prevent protein degradation. The final products were stored at - 80°C pending further analysis.

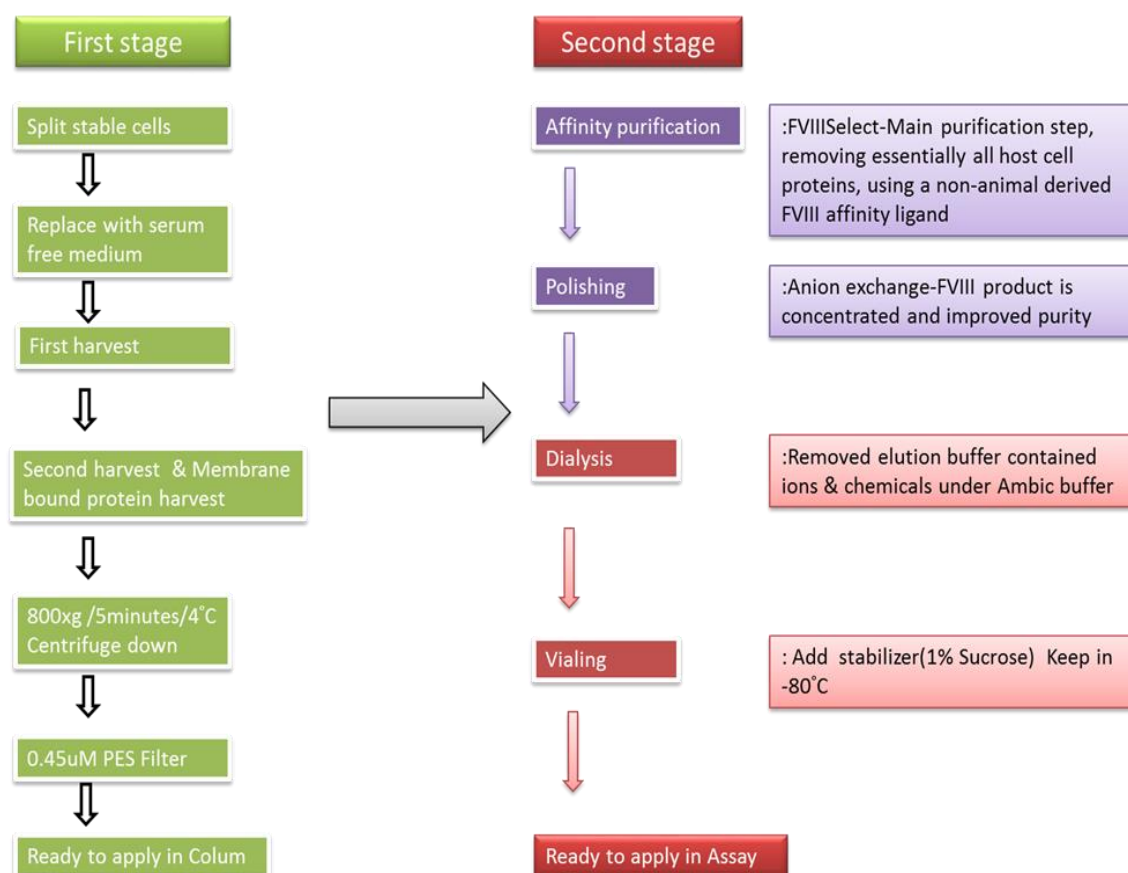


Figure 4.1. Harvesting and purification steps of human FVIII from cell lines.

In the first stage, cellular membrane bound FVIII was collected by using 0.5M NaCl followed by the first harvest of the medium. Cultivated mediums and membrane-bound fractions were spin down and filtered prior to applying on the second stage. In the second stage, the actual purification starts with two purification steps of FVIII, collected from the stable cell lines (V3co, N6co, V1co, SQco and V5co). In this simple two-step purification, the medium was applied to FVIIIselect affinity column then to the DEAE anion exchange for polishing and concentration.

4.2.2. Step 1: Affinity purification with FVIIISelect column

To test whether this FVIIISelect column enables us to achieve efficient yield of high purity FVIII, initially, a small-scale column was packed for a pilot purification run (1mL column resin used). The FVIIISelect column was equilibrated with the equilibration buffer (20mM Imidazol/ 10mM CaCl₂/ 400mM NaCl/ 100ppm Tween 80, pH 7.0) at a flow rate of 60mL/minute using an ÄKTA explore FPLC instrument. Then, the media obtained from V3 stable cell lines grown on 5-layer cell culture flask (T-1000, Millipore, total surface area: 1000cm²) was loaded onto the column at the rate of 1mL/minute. Full ÄKTA explore profiles in shown in Appendix 1.

Figure 4.2 shows absorbance A280 of FVIIISelect eluants (blue) and gradient salt concentration for elution step (green). To collect eluents, automated square fraction collector (FRAC-950, 15x15) was used (red: tube number). Automated gradient mixture of buffer A (30%) and buffer B (70%) resulted in Elution of two peaks, one at low salt concentration and the other at a higher salt (fractions E3 to F11) concentration, the latter we speculated FVIII contained peak (Fig. 4.2).

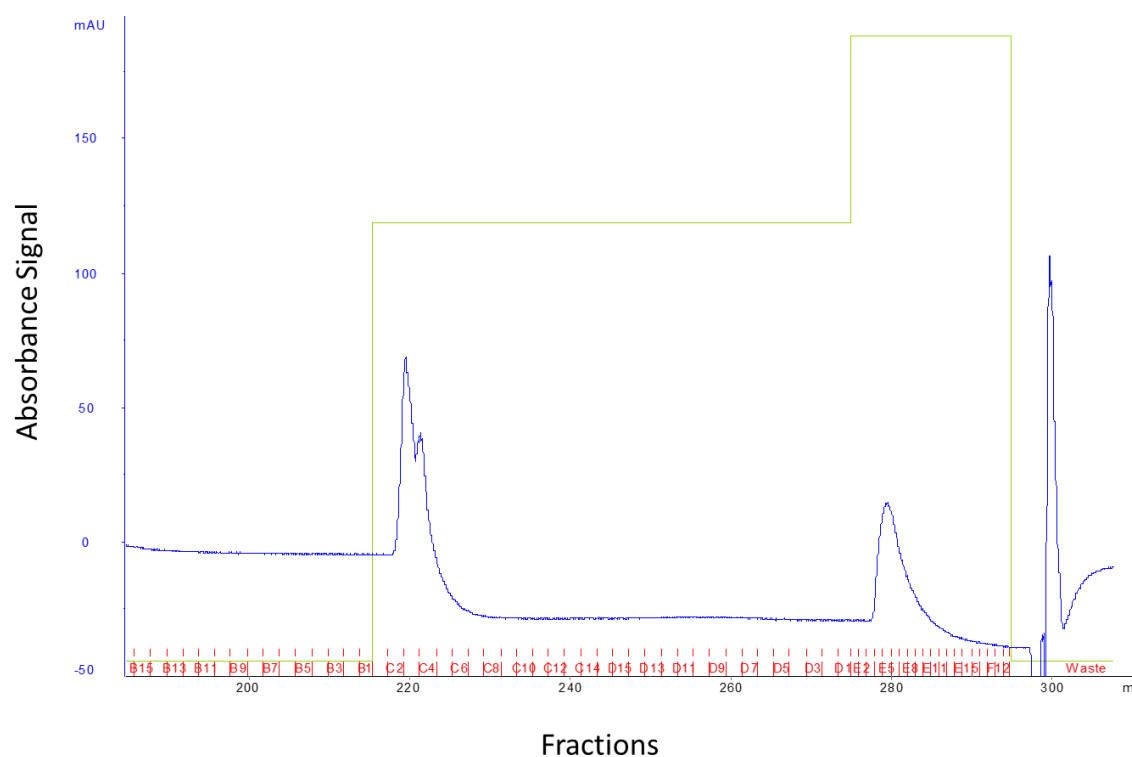


Figure 4.2. FVIIISelect column profiles

Chromatogram (UV absorbance and fractions) of the FVIIISelect purification process performed at small scale. The blue line indicates at A280 in protein absorbance units (mAU). A pilot running for FVIII V3 stable cell lines cultivated media, two step gradient (depend on salt concentration) shows elution pattern in the green box. The bottom lane shows individual collection tube number in fraction collector (red). The first peak collection C2 to C7 tubes and second peak collect E3 to F11.

4.2.3. FVIII activity assay

To identify the eluted fractions that contained rFVIII, a chromogenic FVIII activity assay was used. The elution buffer was included as a negative control. The FVIII activity of pooled first peak (fractions C2~C7) showed the the FVIII activity of ~0.43 IU/mL (5.15 Unit in 12mL), while the FVIII activity in the second peak was 5.65 IU/mL. The FVIII activity in the individual fractions (E7~E12) varied between 4~6 IU/mL. These results suggest:

1. The elution buffer does not inhibit or interfere with FVIII chromogenic activity assay.
2. The first A280 absorbance peak probably represents elution of cellular proteins bound non-specifically to the affinity matrix as illustrated by the fact that these proteins came off at relatively low salt concentrations.
3. The second peak is contained biologically active FVIII as illustrated by the FVIII Chromogenic assay.

In order to calculate the total recovery of FVIII from FVIIISelect, the FVIII activity of starting cell culture media was measured (2.73 IU/mL), which revealed total FVIII in the starting material was approximately 409 Units (Fig.4.3). The calculated total FVIII activity for the second peaks was 101.7 Units, which is a recovery of only 25%. This implies that the 75% of FVIII is unaccounted. The amount of FVIII in the flow-through (FT) was measured. However, the activity of this material was only 0.07 IU/mL, so only 2.5% of FVIII was detected in total FT. Therefore, it appears that about 70% of FVIII is degraded during the purification process. Alternatively, the chromogenic assay may have underestimated the activity of FVIII in the second peak, perhaps because of the high concentration of FVIII, which may have saturated the assay.

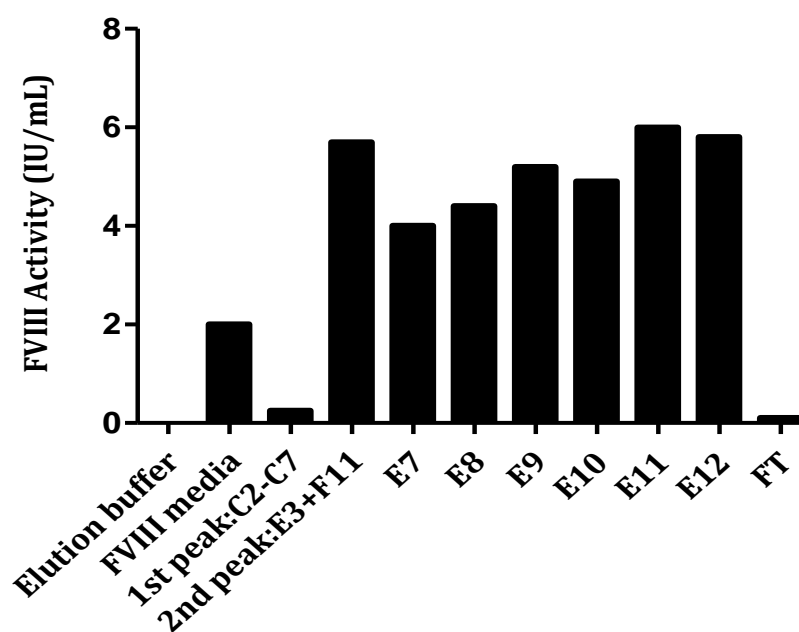


Figure 4.3. FVIII chromogenic assays for individually collected factions

To validate FVIII expression in individual samples; the elution buffer FVIII activity was negative control, Full media: Benzamidine treated harvest media, FT (collect flow through line): validation of unbound protein, First peak: C2~C7, Second peak: E3~F11, highest fractions in the second peak, E7 to E12 individual fractions. FVIII activity determined by chromogenic assay.

4.2.4. Identification of purified FVIII proteins from silver staining

To test FVIII protein levels in the key elution fraction, 10 μ L of eluents were separated on SDS-PAGE followed by silver staining (Fig.4.4). Silver staining was chosen because of higher sensitivity with the ability to detect protein in the nanogram (ng) range.

Figure 4.4 shows that full-length-FVIII (Kogenate®, Bayer) exhibits the typical FVIII components consisting of a single full-length peptide, heavy, and light chain variants as indicated by the arrows. Silver staining of the un-purified, un-concentrated medium (Total, lane 2) and FT (lane 3) demonstrated multiple bands of varying sizes. The 1st peak in lane 4 shows predominantly light chain of FVIII which has been described before (McCue *et al.*, 2009). The 2nd peak fractions (lane 5~11) exhibit that non-specific protein bands are reduced and heavy and light chains are more prominent in lane 8 and 9, which correspond to the peak amongst the fractions collected. These results suggest that FVIIISelect column is efficiently able to isolated FVIII from culture media and helps to remove non-FVIII proteins.

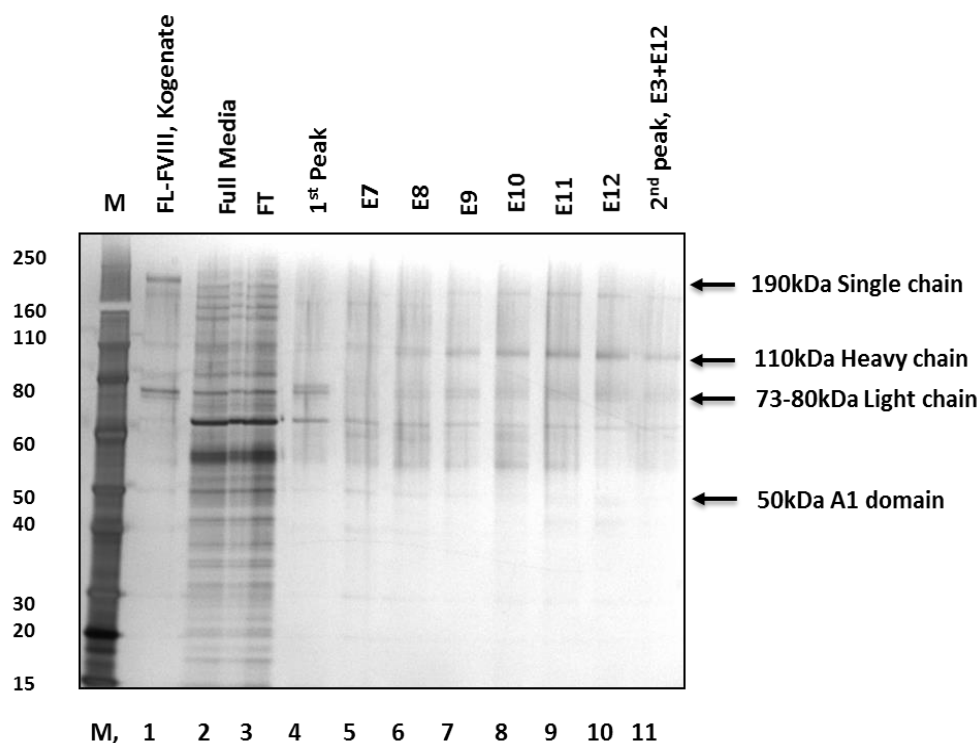


Figure 4.4. Silver staining for FVIII V3co, post-FVIIISelect column

FVIIISelect column purified rFVIII fractions performed SDS-PAGE and silver staining. Lane1: Full length FVIII, Kogenate® (Bayer), Lane2: Cultivated medium, Lane3: Flow through (FT), Lane4: 1st peak, Lane5: E7, Lane6: E8, Lane7: E9, Lane8: E10, Lane9: E11, Lane10: E12, Lane11: E3+E12 (pooled 2nd peak).

4.2.5. FVIII Western blot analysis

Specificity of FVIIISelect to isolate the FVIII protein was tested by Western blot analysis using FVIII specific antibody. Figure 4.5 shows that the fragments of Kogenate® (Bayer) that were detected comprised of a single chain, heterologous heavy chains and light chain. The starting cell culture medium shows only a small portion of V3 in the single chain format probably because of the presence of the furin cleavage site. The remainder of FVIII V3 consisted of heavy chain plus the 31 amino acid V3 B-domain linker, cleaved heavy chain and light chain (as discussed in chapter 3). However, the Flow through (FT) shows that FVIII V3 protein is predominately the heavy chain with 31 amino acid linker attached form (lane 3). This result suggests that the heavy chain with linker form of FVIII may not bind to the FVIIISelect resin efficiently. Based on FVIII activity, which was uniform across the fractions we choose to pool the fractions of the second peak.

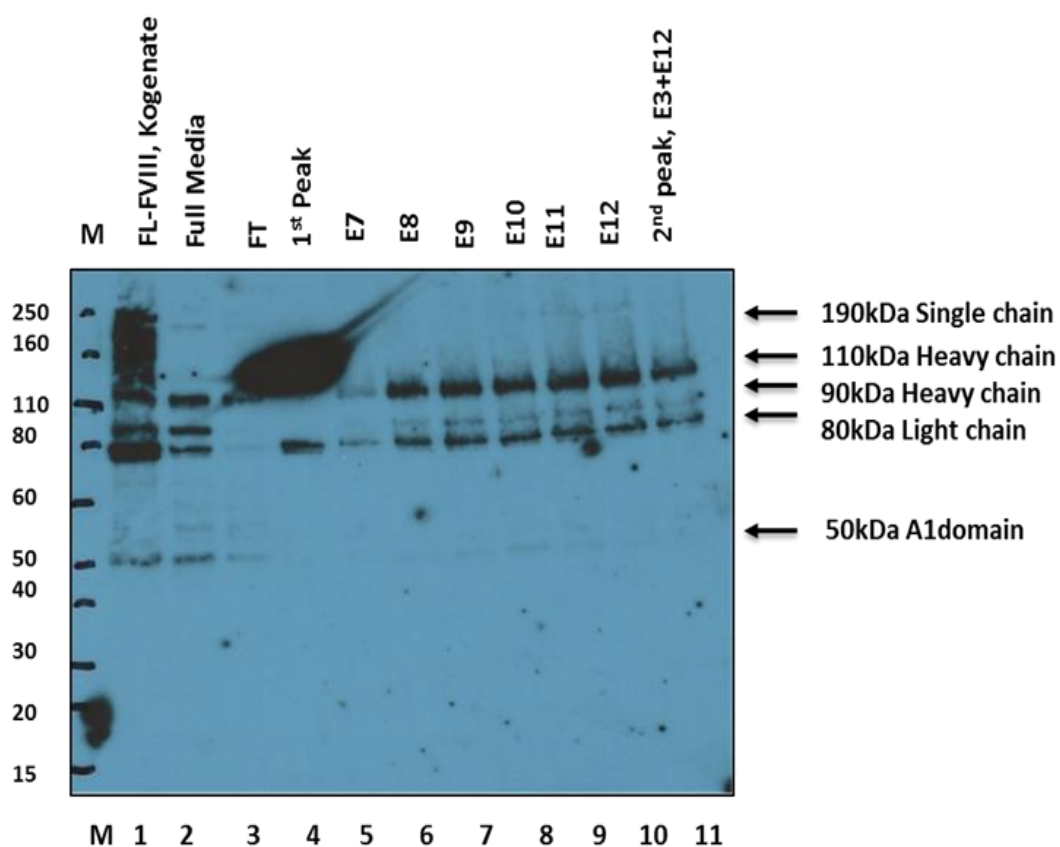


Figure 4.5. FVIIISelect column V3co SDS-PAGE analysis in reducing condition

FVIIISelect Purified FVIII V3 protein performed Western blot, polyclonal antibody (sheep polyclonal antibody: affinity biologicals) detects in full media (Harvest stable cell culture media): 190kDa single chain, 110kDa linker contained heavy chain, 90kDa of A1 and A2 heavy chain, 80kDa of Light chain. The commercial FL-FVIII (Kogenate®, Bayer) lane1, shows 200~90kDa heterologous heavy chains and 80kDa light chain. Flow through (FT) shows dominant heavy chain band, but the 1st peak shows dominant light chain band. All of the individual second peak fractions show two heavy chains (110kDa, 90kDa) and light chain (80kDa).

4.2.6. Double harvested medium from stable cell line improve the FVIII recovery

In order to improve the yield of FVIII, we tested whether it was possible to collect a second harvest from the stable cell line and increase the amount of FVIII protein purified. First, stable cell lines were seeded at 3×10^8 cells in 200mL of 10% FBS containing DMEM in T-1000 flask. Following overnight incubation, cells were washed twice with Dulbecco's phosphate-buffered saline (D-PBS) then the 150mL of serum free DMEM added for further 24 hours. The 1st harvest of media was performed 24 hours later and 150mL fresh serum-free DMEM added for a second harvest. The first harvest was processed as described above with the FVIIISelect method and the chromatogram was similar to that previously observed (Fig. 4.5 and 4.6).

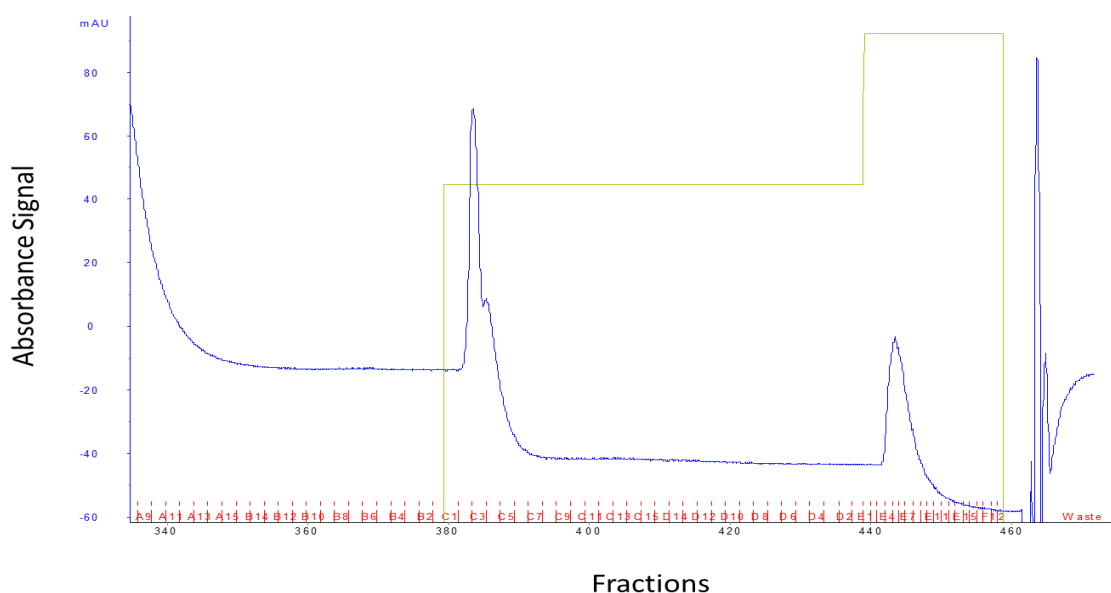


Figure 4.6. FVIIISelect chromatogram from first harvested FVIII V3co media

The FVIIISelect chromatogram shows that two dominant peaks. Absorbance A280 of FVIIISelect eluents represents protein concentration (blue), and the green colour line represents salt gradient for elution step. Second peak fractions were collected and kept at freeze for next purification step.

Since the first peak did not have any biologically active FVIII activity, we only collected and pooled the fractions from the second (E4 to E15, ~12mLs in total). The FVIII activity of starting unprocessed medium was 600 IU in total and the yield of FVIII in the entire second peak was 236 IU/mL, representing a recovery of 39%, and improvement of >50% on the initial experiment (Fig. 4.7).

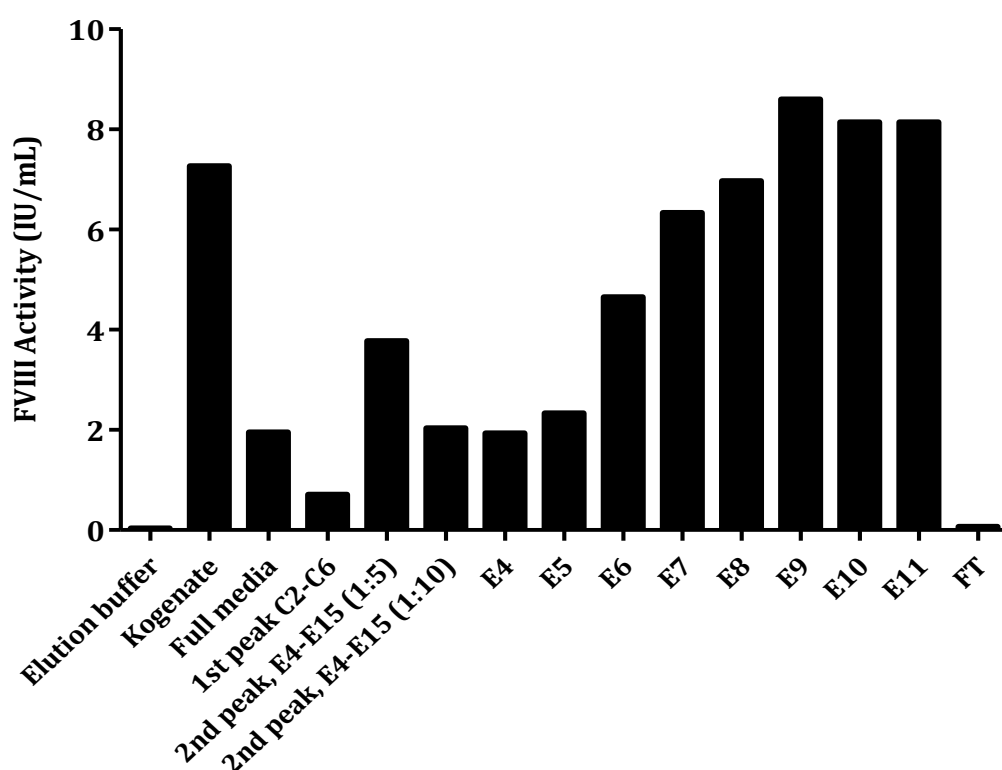


Figure 4.7. Assessment of FVIII activity from the first FVIII SELECT column

Elution buffer alone used for negative control and Kogenate (FL-FVIII, Bayer) used as positive control. FVIII activity determined by using chromogenic assay from starting material (Full media), Flow through (FT), 1st peak fraction (C2~C6), 2nd peak (E4~E15), which diluted to 1: 5 and 1:10 for the sensitivity of the assay.

Following the first harvest, the medium was collected the next day (second harvest, Fig.4.8) and purified using the FVIIISelect column even though the condition of the cells had deteriorated as many cells were observed floating in the medium; likely due to the prolonged culture in serum-free conditions.

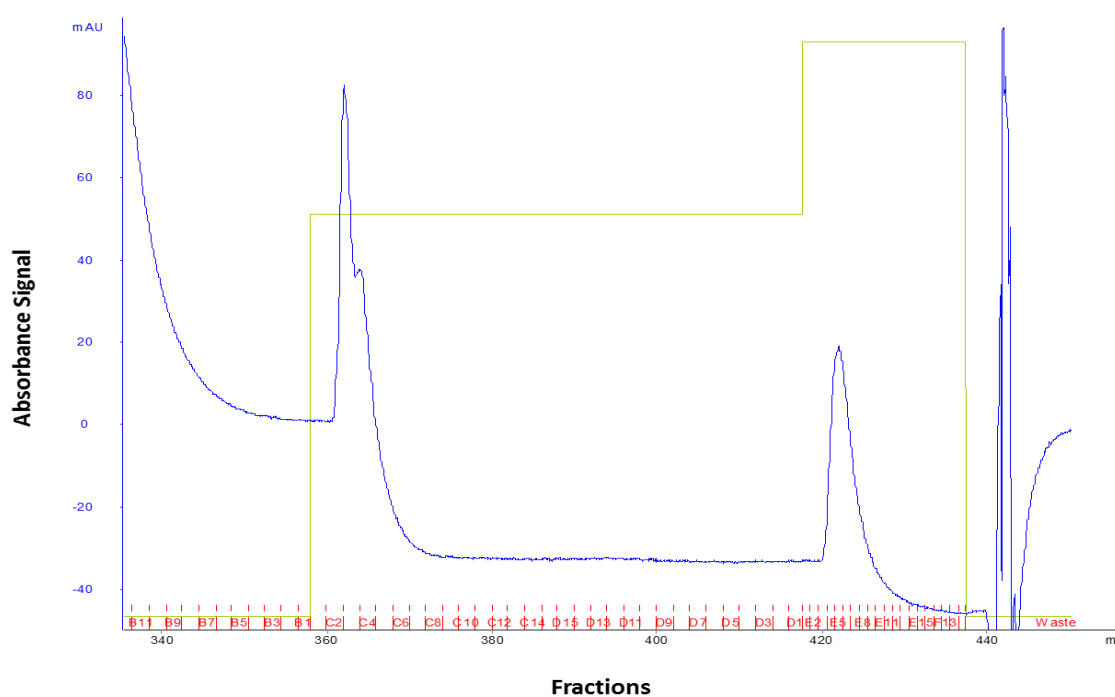


Figure 4.8. FVIIISelect chromatogram from second harvested FVIII V3co media

The purification pattern shows similar as the first harvest, Absorbance signal shows A280, Fraction number means individual tube in an automated fraction collector. The second peak, E4 to E15 tubes collect and merged for further purification.

The purification pattern was similar to that of the first harvest. We collected eluates from first peak (C2~C6) and the second peak (E4~E15) (Fig.4.8) as before. According to the FVIII activity assay, total activity of FVIII in the starting unpurified material was 600 IU in total, the activity in the first peak was 1.2 IU/mL and that in the second peak was 25 IU/mL, giving a total FVIII yield of 300 IU in Total. This result shows about 42% recovery was achieved from the second harvest for purification using FVIIISelect column (Fig. 4.9).

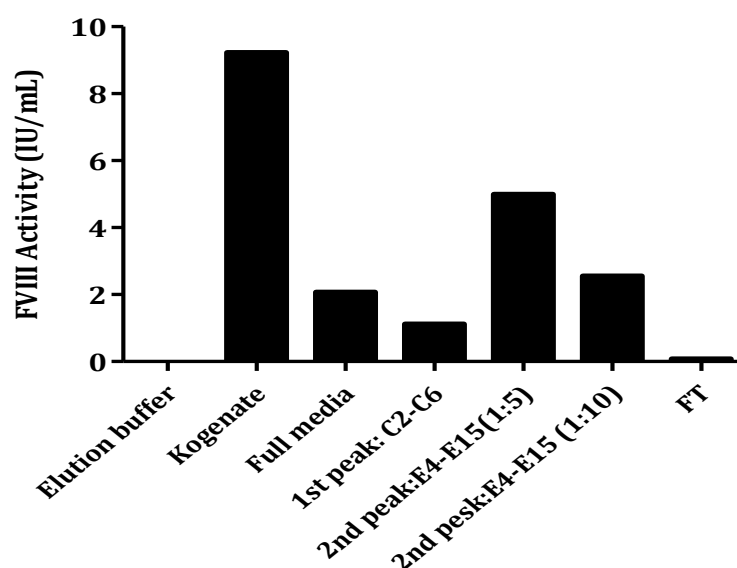


Figure 4.9. Assessment of FVIII activity from the second FVIII SELECT column

Elution buffer alone used for negative control and Kogenate (FL-FVIII, Bayer) used as positive control. FVIII activity determined by using chromogenic assay from starting material (Full media), Flow through (FT), 1st peak fraction (C2~C6), 2nd peak (E4~E15), which diluted to 1: 5 and 1:10 for the sensitivity of the assay.

4.2.7. Membrane-bound FVIII protein

Our previous study in chapter three shows that 10 to 40% of total FVIII was found on the cell surface membrane, which suggests that we can increase FVIII recovery if we include one more collection steps for membrane bound FVIII proteins. To determine the proportion of FVIII bound to cell membrane our established FVIII expressing cell lines, were incubated with 50mL of 0.5M NaCl for five minutes to dissociate membrane bound FVIII proteins followed by the second harvest of the medium. Then 100mL of fresh cold DMEM was added to dilute the high salt (NaCl) then and subsequently loaded onto the FVIIISelect column. The chromatogram for the membrane-bound FVIII was similar to that of the 1st and 2nd harvest (Fig. 4.10).

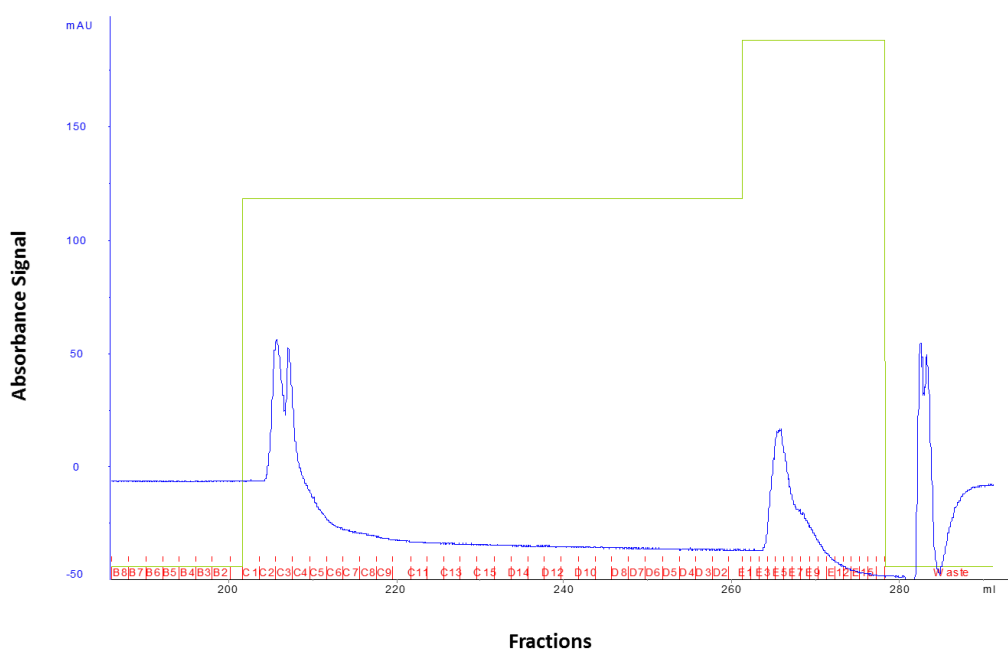


Figure 4.10. FVIIISelect chromatogram from membrane-bound FVIII V3co

Two T-1000 flask cells harvest, add 0.5M NaCl to dissociate recombinant protein from cell surface membrane. Membrane-bound media was five times diluted with DMEM (110.3mM NaCl) to reduce salt concentration before loading on the FVIIISelect column; Chromatogram shows membrane bound V3co profile, Absorbance signal shows A280, Fraction number means individual tube in an automated fraction collector.

The FVIII activity of starting materials was 300 Units (2 IU/mL, 150mL) and 154 Units was recovered (11.8 IU/mL, 13mL) in the second peak, which shows about 51% recovery (Fig. 4.11).

The overall membrane bound fraction was 25% which was higher than that observed in our previous small-scale experiment using 6-well plates, in which membrane-bound fraction was 10%. The differences between the two experiments are the 6-well plates seeded 1×10^6 cells per well (4.67 cm^2) after only 24 hours both cultivated and membrane-bound rFVIII was harvested, On the other hand T-1000 flask were seeded with 3×10^8 cells, which is maximised seeding on plates and also membrane-bound fractions were harvested after a 48 hours time gap. The possible reasons are three times more densely seeded cells and increased harvesting time. A confounding factor may be that serum-free condition, may increase the amount of FVIII bound to the cell membrane as reported before (Swiech *et al.*, 2011).

These results taken together suggest that the total yield of FVIII can be improved by combining two harvests of the cell culture media and collection of the FVIII membrane bound protein. This strategy was adopted for large-scale production of the FVIII variants.

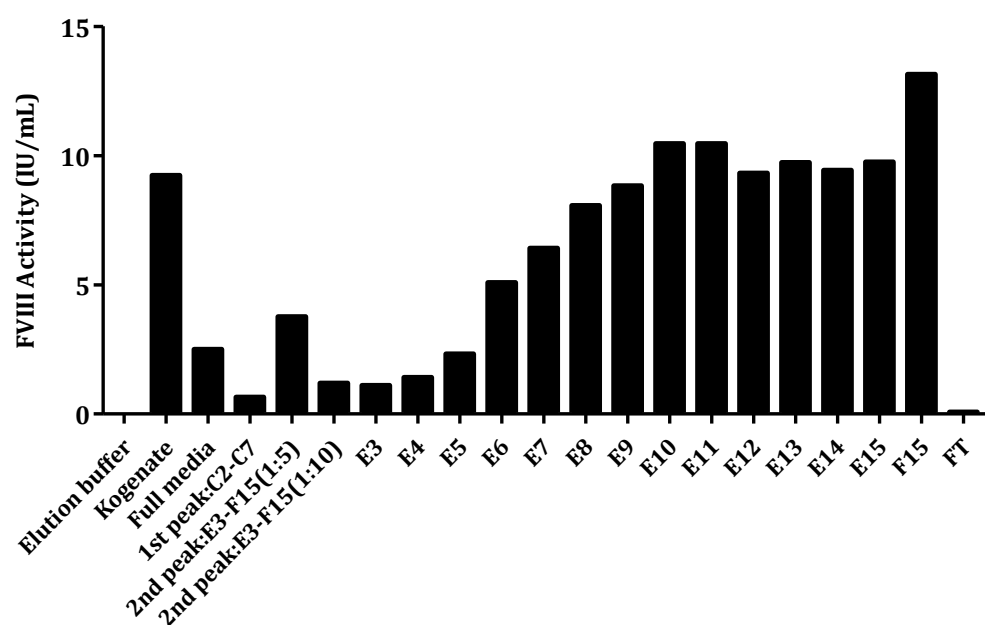


Figure 4.11. Assessment of FVIII activity from membrane-bound FVIII

Elution buffer alone used for negative control and Kogenate (FL-FVIII, Bayer) used as positive control. FVIII activity determined by using chromogenic assay from starting material (Full media), Flow through (FT), 1st peak fraction (C2~C7), 2nd peak (E3~F15), which were diluted to 1: 5 and 1:10 for assay.

4.2.8. Modified FVIII purification procedure

Although we have established the FVIII expressing stable cell lines, it is difficult to purify the pure FVIII proteins in the medium due to the inherent instability of FVIII, and the use of serum-free conditions (without any additional supplements) which lead to cell death, which prevents multiple harvests of the medium. Finally, maintaining the activity of FVIII during purification is difficult due to the high salt buffer (1.5M NaCl) used for elution step from the FVIIISelect column during purification. For this reason, we developed the protocol described in Figure 4.12 below.

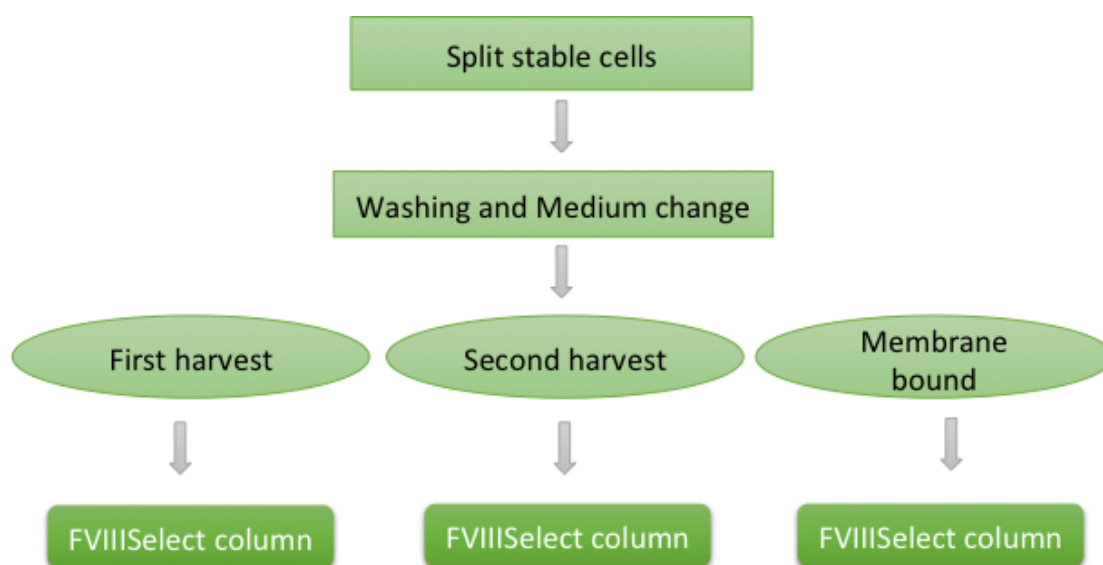


Figure 4.12. Schematic diagram of optimised FVIIISelect Purification

The chart illustrates that the purification procedure for FVIII stable cell lines which will be collected in three different conditions.

4.2.9. FVIII select column purification for remaining variants

The chromatograms showed very similar patterns for each FVIII variant (Fig.4.13). Therefore the same fractions were collected for each variant from the elution trace of the FVIIISelect column. Individual purified fractions were kept at -80°C (Individual peak data not shown).

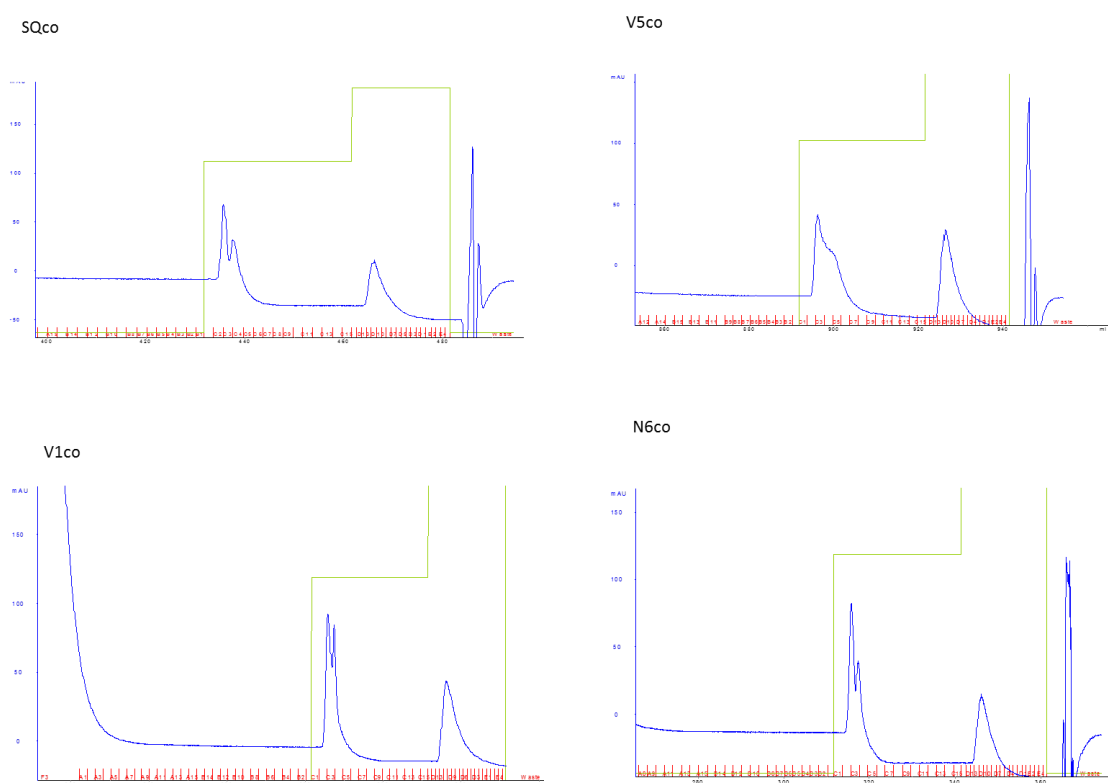


Figure 4.13. FVIIISelect column chromatograms for FVIII variants

Further purification carried out with the same protocol as FVIII-V3 purification. The SQco, V5co, V1co and N6co show similar profiles in FVIIISelect column. The second peak fractions were collected and stored at -80°C freezer for later DEAE column purification.

4.2.10. Optimisation of FVIII concentration using DEAE column

The FVIIISelect chromatography step enriched for FVIII, although there were other proteins eluted alongside as detected in the silver stained protein gel (Fig.4.4). Therefore to increase the purity and concentration, which is essential for further characterisation, an additional chromatography step was included. DEAE is a weak anion-exchange resin and was reported by Tang et al. as part of their FVIII purification process (Tang *et al.*, 2013). The DEAE step will also increase the concentration of FVIII, which is necessary for the further biochemical analysis.

The FVIII proteins (FVIII activity, 20~35 IU/mL) containing fraction (~12mLs) from the FVIIISelect column were diluted to ~800mLs lower the concentration of ethylene glycol and NaCl and then loaded at the speed of 1mL/minute. After washing the column with a mixture of 80% Buffer C (20mM MOPS, 10mM CaCl₂, 100ppm Tween 80, pH7.0) and 20% of Buffer D (20mM MOPS, 10mM CaCl₂, 1M NaCl, 100ppm Tween 80, pH 7.0) the bound FVIII was eluted with a mixture 60% Buffer C (20mM MOPS, 10mM CaCl₂, 100ppm Tween 80, pH7.0) and 40% of Buffer D (20mM MOPS, 10mM CaCl₂, 1M NaCl, 100ppm Tween 80, pH 7.0), which washed off residual unbound protein and cellular debris. Absorbance at A280 showed three peaks (Fig.4.14); the first peak was contained in fractions A14 to B14 in a total of 4mL, the second peak B2 to C3 in 5mL and the third peak was collected in fractions C13 to D13 in total 6mL.

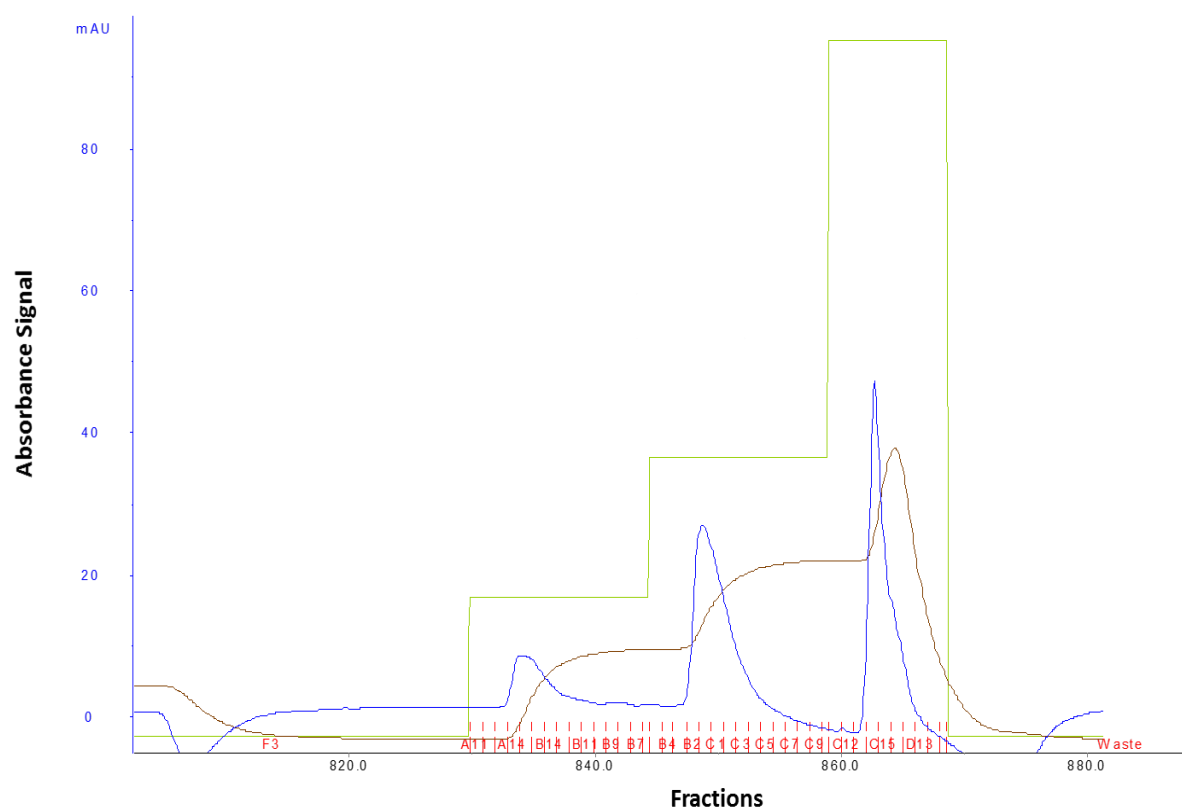


Figure 4.14. Chromatogram of DEAE Sepharose FF, Anion exchange column purification

DEAE anion exchange column used for this purification following manufacturers recommendation. The chromatogram shows three peaks, which relies on three steps gradient elution stage, according to the salt concentration (Green). Absorbance 280 (Blue), Conductivity (Brown), Fraction collect tube number (Red). The elution stage, A280 and Conductivity show similar profiles.

The collected fractions from the peaks were subjected to a FVIII chromogenic assay (Fig.4.15) to identify the peaks containing the active FVIII fractions. The chromogenic assay shows that the 800mL starting material contained 1.69 IU/mL of FVIII (1,352Units in total). The first peak had FVIII activity of 0.07 IU/mL (0.28Unit in total), the second peak 143.4 IU/mL (717Units in totals) and the third peak 3.89 IU/mL (23.34Units in 6mL). These results suggest that the majority of active FVIII is eluted in the second peak of the DEAE step. As a result, the first and third, non-FVIII proteins fractions were discarded and only the second peak that contains the majority of the FVIII was collected in further studies. In addition, the DEAE column increased the concentration by 85-fold, the starting material contained 1.67 IU/mL and the final pool of the second peak was 143.4 IU/mL, the final recovery rate was 52.6% in total.

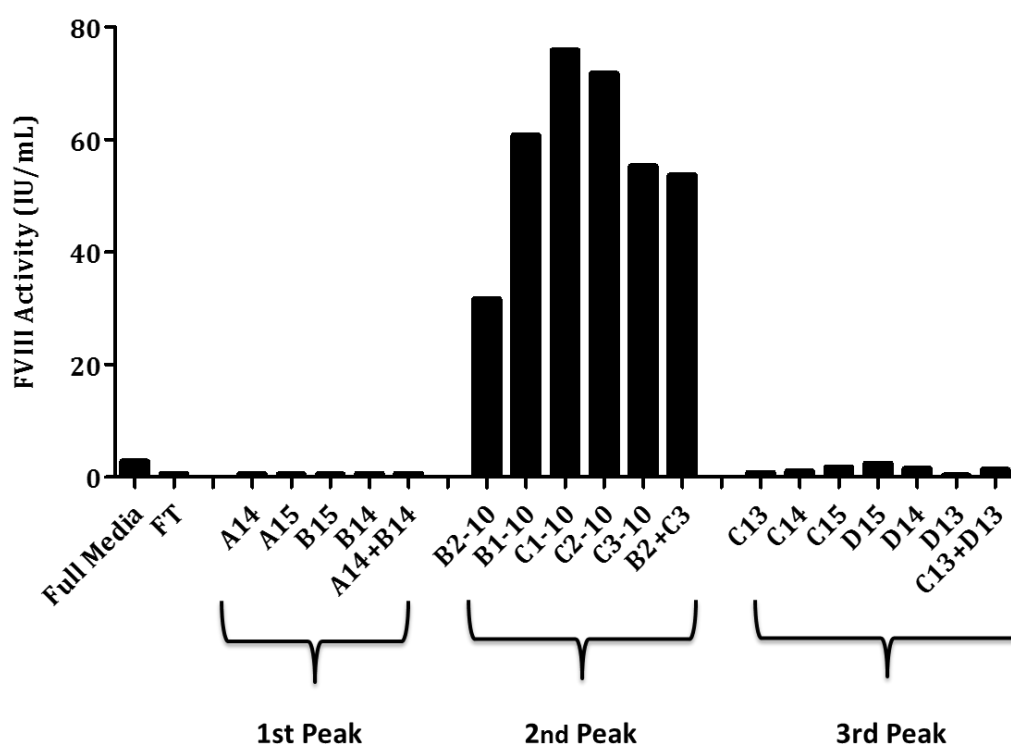


Figure 4.15. Assessment of FVIII activity for fractions corresponding to the DEAE column chromatogram

Three peaks harvested and validated; Full Media-Basic material load on the column, FT-Flow through collect, A14 to B14-1st peak, B2 to C3-2nd peak, C13 to D13- 3rd peak on elution profile following the figure 4.6.1. The second Peak shows dramatically increased FVIII activity, on the other hand, the first and third peaks show very little FVIII activity.

To assess the purity of the purified FVIII in the second peak, 10 μ L of eluents were separated on a SDS-PAGE gel and silver stained. The V3co purified fractions showed 190kDa single chain, 110kDa/90kDa heavy chain bands and 87~73kDa of doublet light chains in all B2 to C3 fractions. We believe that the two light chain bands are the 87kDa a3-A3-C1-C2 domains and the 73kDa A3-C1-C2 domains. The acidic a3 domain in the latter is cleaved at Arg 1689 (Kaufman *et al.*, 1988).

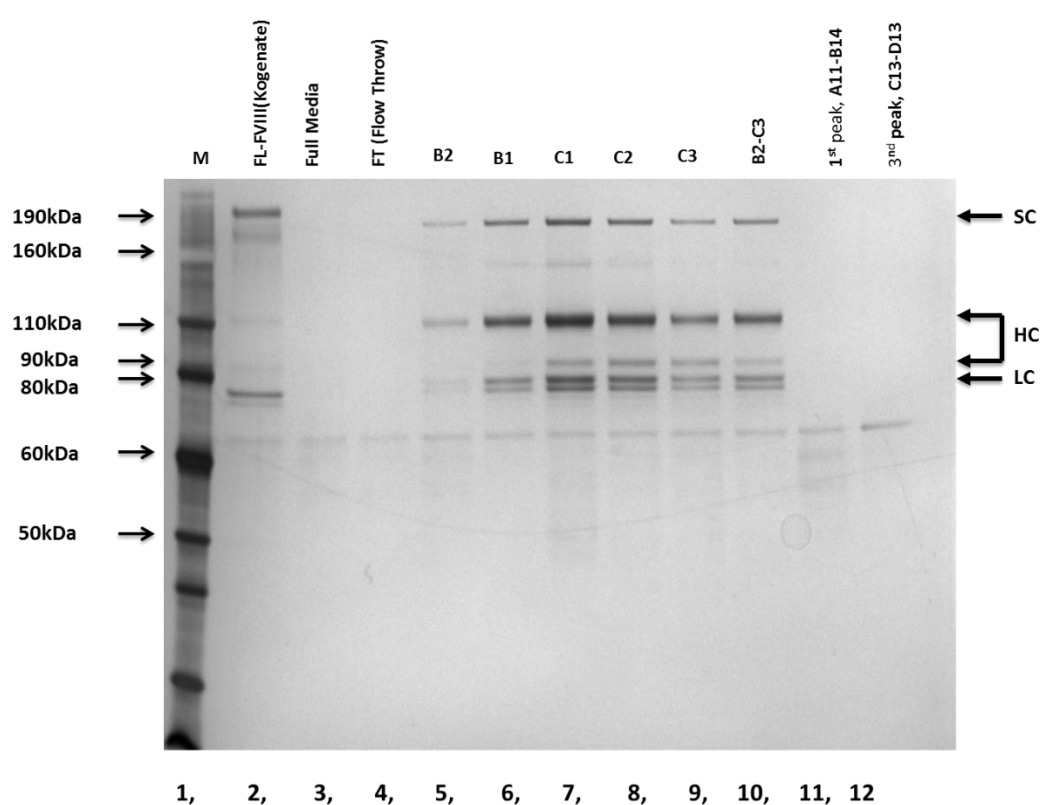


Figure 4.16. Silver staining for fractions corresponding to the DEAE chromatogram

Lane1: Marker, Lane2: Recombinant FL-FVIII (Kogenate, Bayer) Lane3: Full material, Lane4: F3 (Flow through), Lane5: B2, Lane6: B1, Lane7: C1, Lane8: C2, Lane9: C3, Lane10: B2-C3, Lane11: 1st peak A11- B14, Lane12: 3rd peak C13~D13. SC (Single chain, 190kDa), HC (Heavy chains, 110kDa-A1+A2+31aa Linker, 90kDa-A1+A2), LC (A3+C1+C2). The visualised silver stained gel showed that FL-FVIII showed several heterologous bands. Full media and Flow throw exhibit weak protein bands due to FVIII concentration from starting materials were very low in both samples.

To confirm that the protein bands seen on the silver stain were FVIII, a western blot was carried out with a polyclonal antibody that detects both the heavy and light chain of FVIII (Fig.4.17). The result shows typical protein bands (FL-FVIII; 210kDa~90kDa of broad heavy chains, 87~73kDa light chain bands. FVIII V3; 190kDa of a single chain, 110~90kDa heavy chain and ~80kDa light chains (doublet) shows purified fractions in B2 to C3). These results imply that our approach of dual column purification is an efficient method for further FVIII protein structural and biochemical studies.

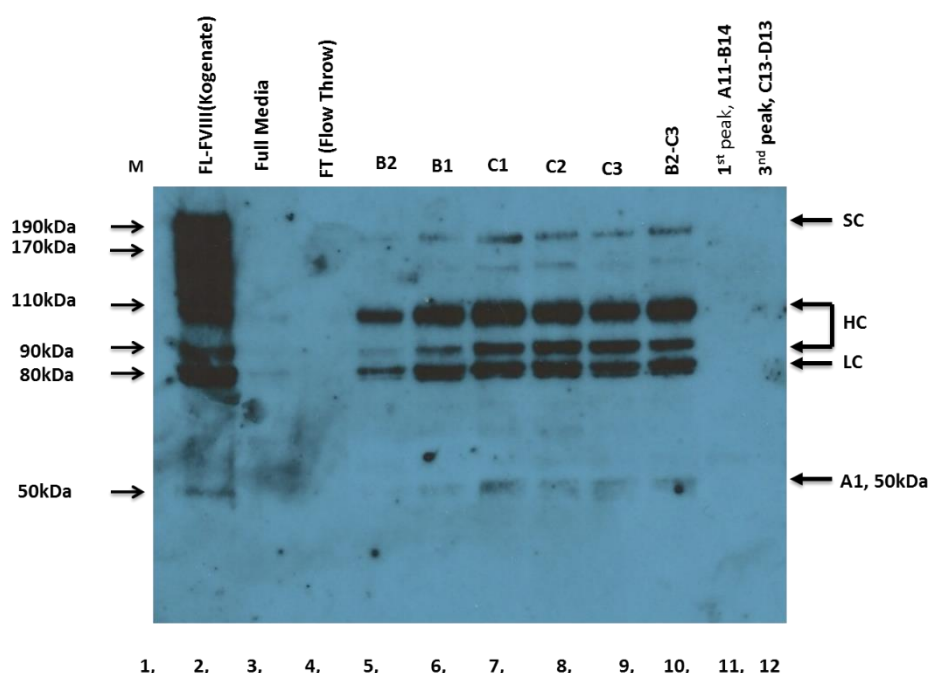


Figure 4.17. Western blot analysis of fractions corresponding to the DEAE chromatogram

Purified proteins show strong FVIII expression, full media and flow through expressions were showed very poor FVIII expression. Lane1: Marker, Lane2: Recombinant FL-FVIII (Kogenate, Bayer) Lane3: Full material, Lane4: FT (Flow through), Lane5: B2, Lane6: B1, Lane7: C1, Lane8: C2, Lane9: C3, Lane10: B2~C3, Lane11: 1st peak A11~B14, Lane12: 3rd peak C13~D13. The lane 2, which is FL-FVIII (kogenate, Bayer) observed as a mixture of heterodimers of a variable-length heavy chain of 210~90kDa, due to fully or partially cleaved B-domain by limited proteolysis. Light chain appeared at a constant length of ~80kDa.

4.2.11. DEAE purification for SQco, V5co, V1co and N6co

FVIII affinity column purified rFVIII was processed by DEAE column purification and elution patterns were similar as V3co (Fig.4.18). The whole process was carried out as previously described for V3co purification. Therefore the same fractions were collected for each variant from the elution trace of the DEAE column (Individual peaks assessment not shown).

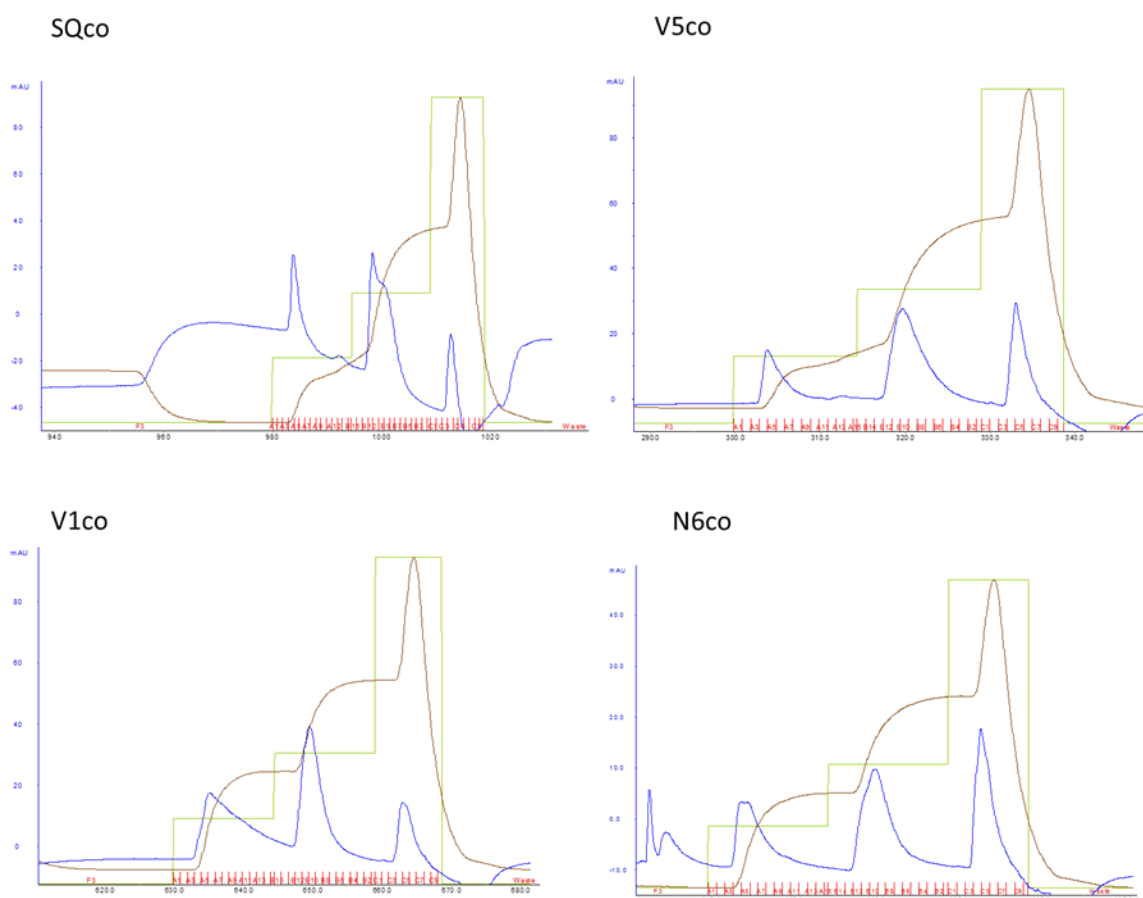


Figure 4.18. DEAE anion exchange column chromatogram for FVIII variants

SQco, V1co, V5co and N6co purified with DEAE anion exchange column, Chromatograms showed each variants were similar profiles.

4.2.12. Dialysis

The next step entailed reformulation of the eluate from the DEAE column, which contained metal ions, and salts, and may disrupt the functional analysis of FVIII. To remove these unwanted components, a dialysis step was included with Ambic Buffer (Ammonium Bicarbonate, pH7.2). A schematic of the final FVIII purification process is shown in Figure 4.19.

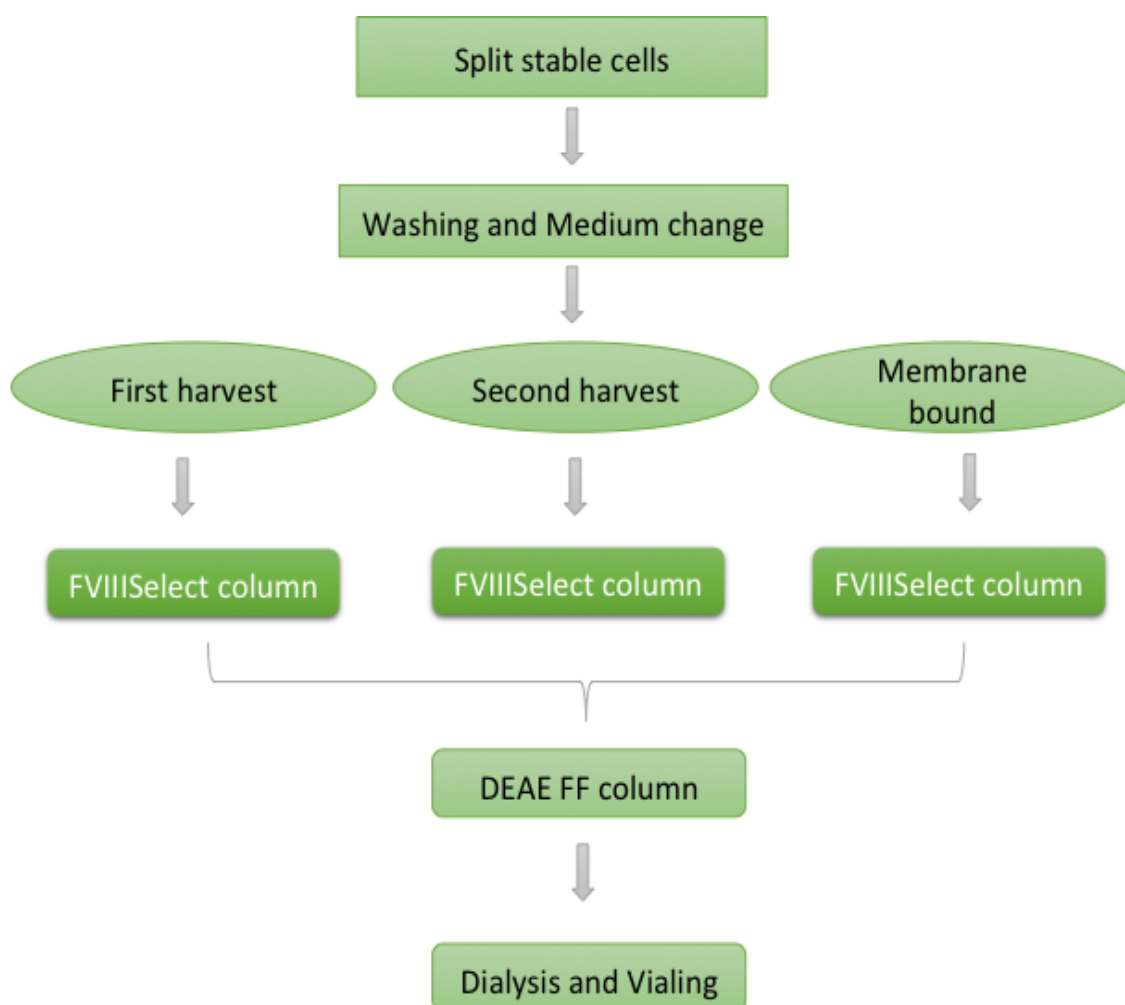


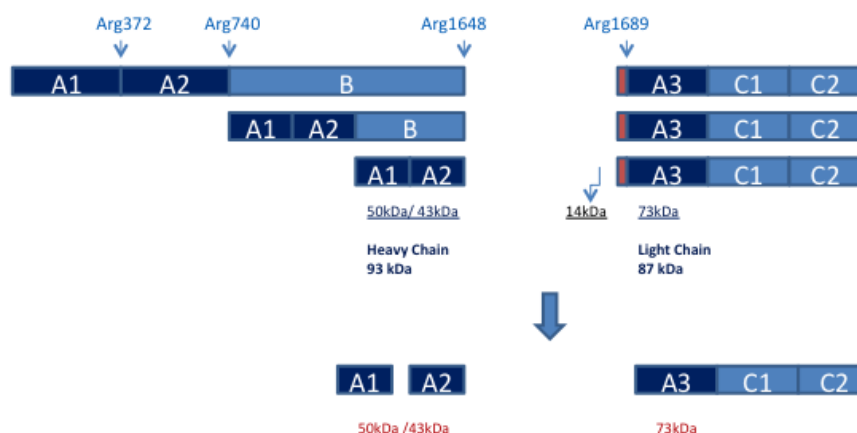
Figure 4. 19. Complete procedure of FVIII purification process

DEAE FF column and Dialysis steps are added following the FVIII select column, which concentrates proteins and removes unnecessary salts and chemicals.

4.2.13. Characterisation of purified variants FVIII materials.

Thrombin is necessary for the activation of FVIII, which cleaves the FVIII molecule after Arg372, Arg740 and Arg1689 (Barrow *et al.*, 1994; Pittman *et al.*, 1994). In the First step Arg1648 is cleaved, so full-length FVIII is initially divided into the A1- A2- B-domain, of 210kDa designated the heavy chain and a3-A3-C1-C2 domain of 87kDa of the light chain. Then cleavage between Arg1689 and Arg740 produces the 93kDa heavy chain (A1 and A2) and the 73kDa light chain (40 amino acid a3 region cleaved from 87kDa). The remnants of the large B-domain are degraded by proteolysis. Finally, Arg372 is cleaved in the middle of A1 and A2, and thus the heavy chain is separated into a 50kDa A1 domain and a 43kDa A2 domain. Finally, thrombin-activated FVIII so produced consists of the 50kDa A1 domain, the 43kDa A2 domain, and the 73kDa light chain (Fig.4.20.A). The thrombin cleavage products of FVIII activation are illustrated schematically in figure 4.20.B.

A



B

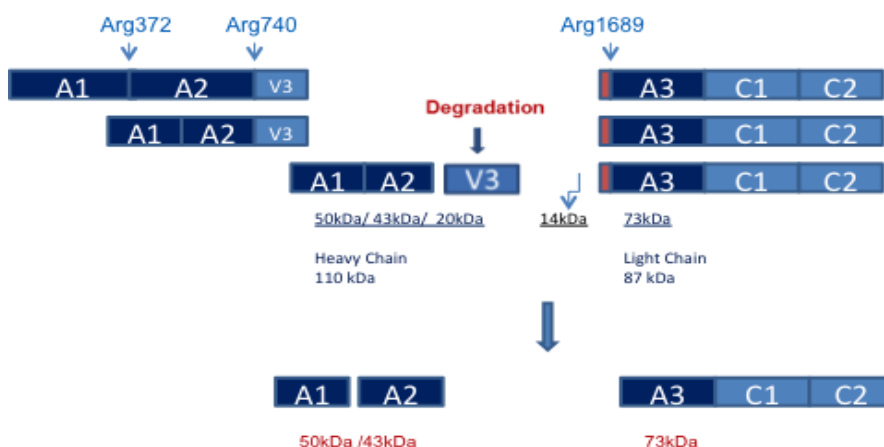


Figure 4.20. Schematic representation of FL-FVIII and FVIII V3 domain cleavage by thrombin activation

A) The diagram shows the FL-FVIII expected size fragments produced by thrombin cleavage at Arg372, Arg740, and Arg1689. The cleavages at Arg740 in the heavy chain (A1-A2-B) to release the B-domain, at Arg372 in the heavy chain to form the A1 and A2 subunits, and at Arg1689 in the light chain to produce the A3-C1-C2 subunit. Cleavage at Arg372 is required for the development of intrinsic FXase cofactor activity. Cleavage at Arg1689 releases an acidic 14kDa fragment that leads to dissociation of vWF allowing the association of FVIIIa to phospholipid membranes such as activated platelets.

B) The diagram shows the 31aa novel linker contained FVIII V3 expected size fragments. The potential sites of thrombin cleavages are located at Arg372, Arg740, and Arg1689 (in front of a3). The final fragments predicted as 50kDa for A1 domain, 43kDa for A2 domain and 73kDa for the light chain.

4.2.14. Thrombin digestion of BDD-FVIII and FVIII-V3

Thrombin proteolysis in FVIII is important because proteolytic activation of FVIII is necessary for the development of the FXa complex (Barrow *et al.*, 1994).

The purified 31 amino acid linker FVIII V3co and commercial B-domain deleted 14 amino acid linker ReFacto® (Pfizer) were activated by thrombin to compare the composition of the thrombin activated products. On a Silver stained gel inactivated BDD-FVIII consisted of a 190kDa single chain, 110kDa heavy chain, and 87kDa light chain. After thrombin activation, the light chain has been cleaved to 73kDa, and heavy chain has been cleaved to the A1 and A2 subunits, 50kDa and 43kDa respectively (Fig.4.21). This was confirmed by western blotting using two antibodies, a polyclonal antibody and a monoclonal antibody to the A2 domain of the heavy chain. The polyclonal antibody western blot showed 73kDa (light chain), 50kDa, and 43kDa (A1 and A2 units of the heavy chain) bands for V3co as well as ReFacto®. When the Western was repeated with a monoclonal antibody which recognises the A2 epitope we were only able to detect 43kDa band for both V3co and ReFacto® (Fig.4.22). Therefore the 31 amino acid linker peptide in FVIII-V3co is fully cleaved on activation by thrombin, and this peptide does not appear to hinder thrombin cleavage at other sites. In the silver stained gel and SDS-PAGE western blot, a 37kDa fragment was seen. We believe that this corresponds, to the human α -thrombin. Hence, once activated FVIII V3co has the same profile as ReFacto®.

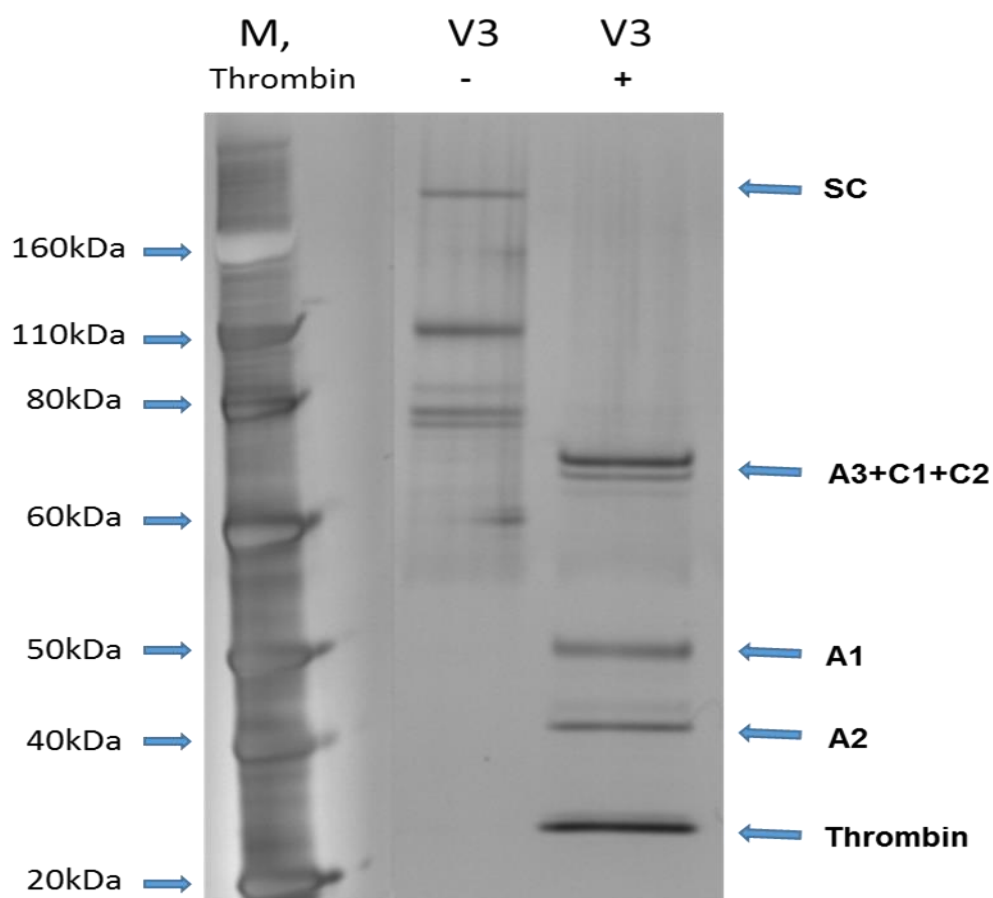


Figure 4.21. Silver staining for thrombin digestion of purified FVIII-V3

Approximately 1unit of FVIII-V3 protein with or without thrombin was separated on a 4-12% Bis-Tris gel in reducing condition. Protein bands were visualised by silver staining. Molecular weights were given in kDa for the standard NuPAGE marker on the left. The naïve rFVIII V3 shows 190kDa single chain (SC), 110kDa/90kDa of heavy chains and doublet 80kDa of light chains. Thrombin digested rFVIII V3 shows 73kDa of A3+C1+C2 light chain, 50kDa of A1 and 43kDa of A2 band visualised in the silver stained gel.

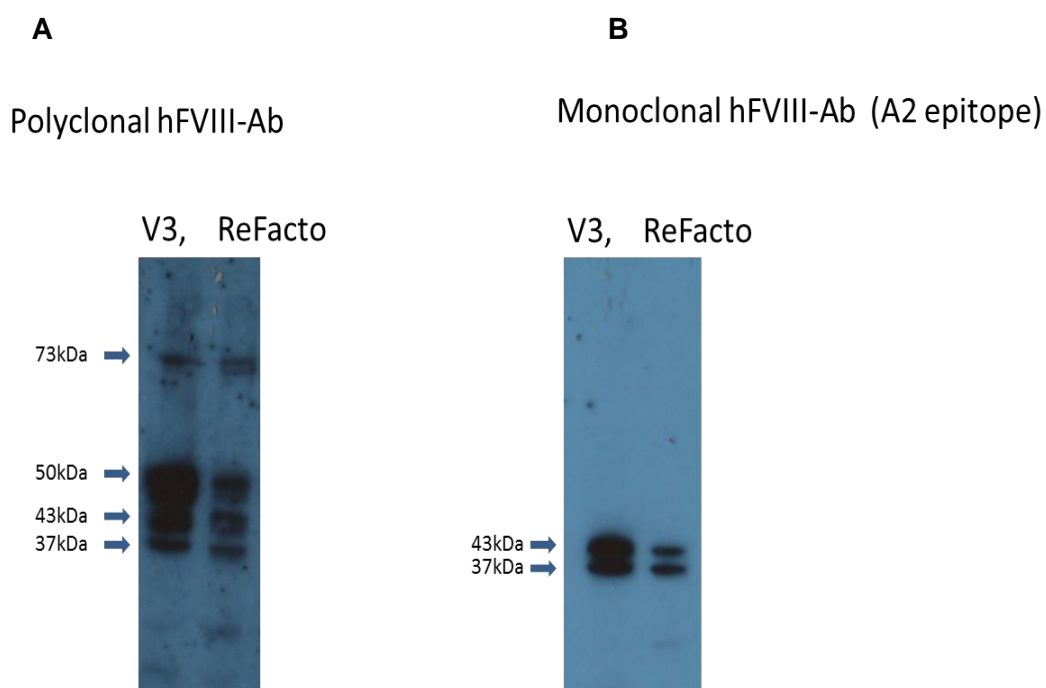


Figure 4.22. Western blotting for thrombin digestion of purified FVIII-V3co

Novel 31 amino acid linker V3 and commercial B-domain deleted recombinant FVIII product (ReFacto®, Pfizer) were activated by thrombin. A) 73kDa, 50kDa and 43kDa polypeptide fragments generated by thrombin digestion, polyclonal hFVIII antibody: 73kDa-A3+C1+C2, 50kDa:A1, 43kDa:A2

B) 43kDa A2 domain detected by the A2 epitope monoclonal antibody, both A and B gels exhibited thrombin band at 37kDa, which nonspecifically binds polyclonal and monoclonal antibody.

4.2.15. FVIII biological activity using the thrombin generation Assay and Thrombogram

Thrombin generation is a key measurement of FVIII function and is a sensitive and reliable method for determining the haemostatic status. Thrombin generation was measured with the Calibrated Automated Thrombogram System (CAT, Stago diagnostic) based on Fluoroskan Ascent Analyser (390nm excitation 460nm emission wavelength: Thrombinoscope, Stago diagnostic). All FVIII variants were measured at a concentration of ~1 unit/mL of a recombinant protein which was determined by the chromogenic assay. FVIII variants were added to FVIII deficient plasma (Hemos/L, Werfen). Thrombin generation was initiated with 1pico mole (pM) of tissue factor (TF) and 4 μ M phospholipid (PPPlow reagent, Thrombinoscope, Stago diagnostic). For the negative control FVIII deficient plasma was used (Hemos/L, Werfen) and Nuwiiq® a recently approved rhFVIII produced in a human cell line (kindly gifted by Octapharma) was used as a positive control to be consistent with the fact that all our FVIII variants were made in HEK-293T cells.

The profiles for all our FVIII variants and Nuwiiq® were similar (Fig.4.23). In addition to the thrombin generation profile four other parameters were measured; lag time, time to peak, peak height and the endogenous thrombin potential (area under the curve).

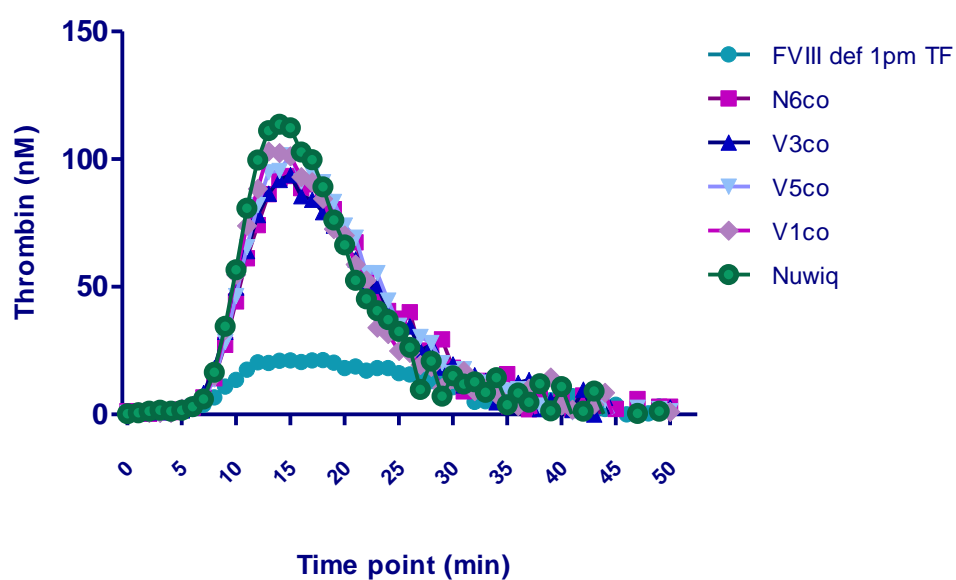


Figure 4.23. Activity of FVIII measured by thrombin generation upon activation of coagulation

FVIII deficient plasma used as a negative control. Purified variants of FVIII did not show any difference compared to each other.

The individual parameters (Fig.4.24) show that the lagtime of all variants and positive control (Nuwig®) ranged in between 7.7 to 8 per minutes and endogenous thrombin potentials (ETP) were in between 1387 to 1463 fluoresce per units (FU). Peaks appeared at 95 to 114 and the time to peak (ttP) started between 14 to 14.67 minutes. The thrombogram indicate that the efficiency of clot formation for all the variants did not show significant differences (Fig. 4.24).

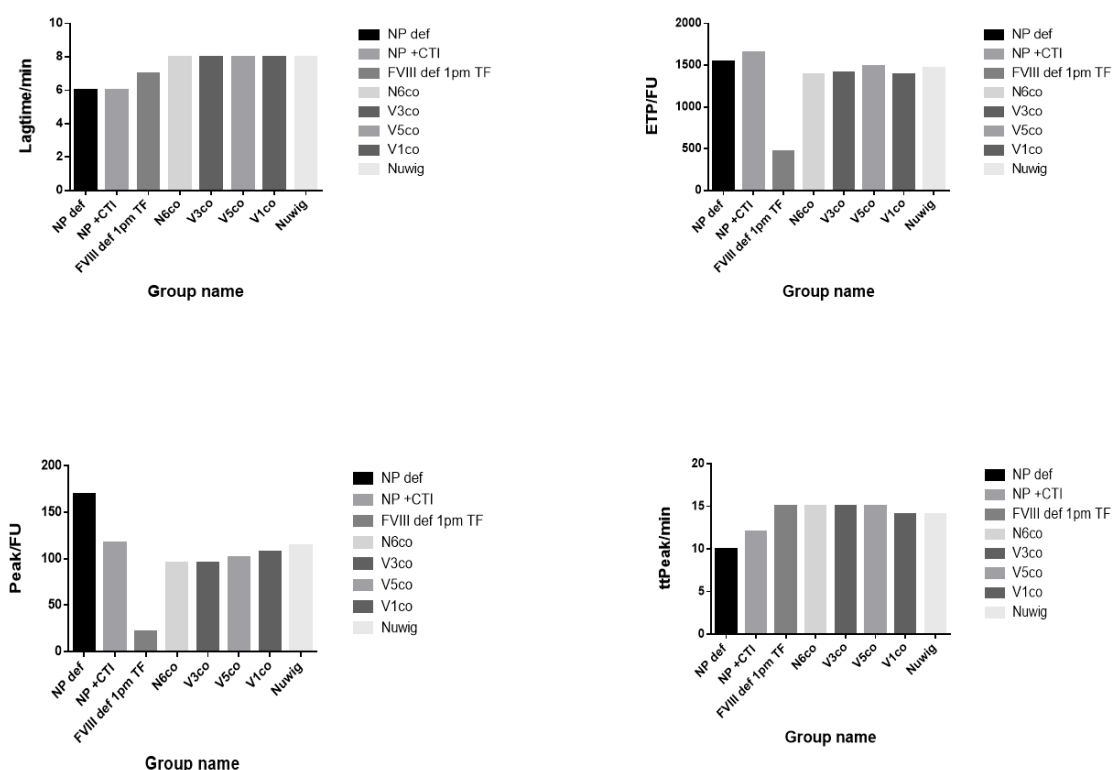


Figure 4.24. Quantitative parameters of the thrombograms for FVIII variants

The lagtime, ETP: endogenous thrombin potential, ttP: Time to peak and Peak height were assessed by CAT machine. Normal plasma deficient (without corn trypsin inhibitor-CTI) and Normal plasma with CTI used as a normal control. Thrombin generation assay was performed at the Royal Free Hospital, London.

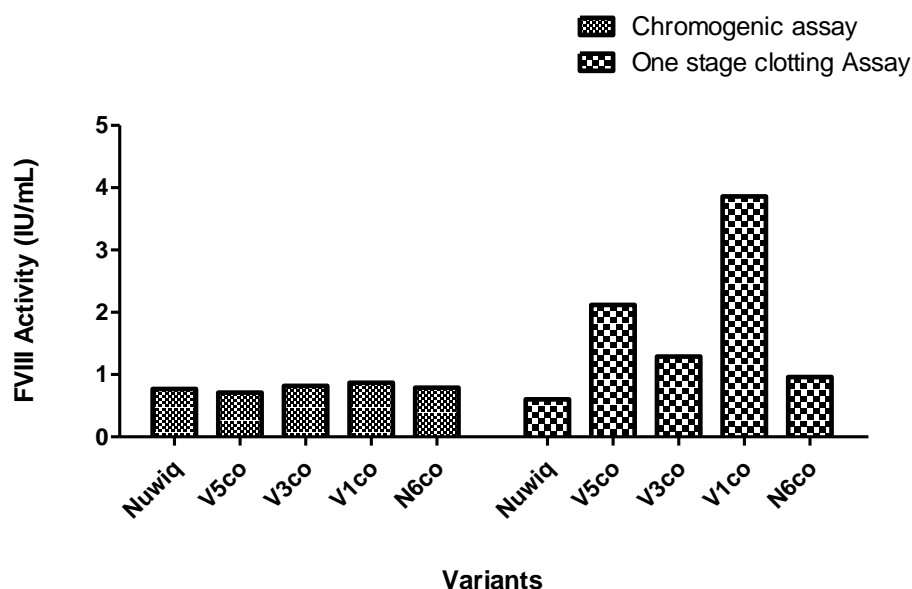
4.2.16. Coagulation assay

The coenzyme FVIII cannot be measured directly. Therefore FVIII activity is measured indirectly through the target enzyme FIX, which converts FX to active FXa (Potgieter *et al.*, 2015). There are three methods for measuring FVIII activity, one stage, two stage and chromogenic assay (which is a development of the two-stage assay). Most diagnostic laboratories use the one-stage and chromogenic assays for measuring FVIII activity. However, discrepancies have been noted between the two assays and were first reported in 1976. It is now known that some mutations (located in the A2 domain) giving rise to mild haemophilia can give a discrepant result between the two methods (Pipe *et al.*, 1999). Since then many cases of different assay results not aligned with patient severity and depending on mutations have been reported, and those assays have discrepancies observed in FVIII proteins (Pipe, 2001; Hakeos *et al.*, 2002). It is advised that haemophilia treatment centre coagulation laboratories should use both one-stage and chromogenic FVIII activity assays, particularly when screening for possible haemophilia A (Potgieter *et al.*, 2015). There are also assay discrepancies when measuring FVIII concentrates, however; improvements in the design of the methods have reduced these discrepancies (Barrowcliffe *et al.*, 1998; Barrowcliffe *et al.*, 2002).

4.2.17. Factor VIII activity measured by Chromogenic Assay and One stage clotting assay

Purified proteins were diluted in the R4 buffer, contained in the chromogenic kit and for the one stage assay FVIII deficient plasma (Biophen, UK). Due to the limited amount of purified FVIII, quantification was carried out on the chromogenic assay with a manual microtiter plate method.

All FVIII variants had a similar level of FVIII activity when measured by the Chromogenic assay. However, when measured by one-stage assay (ReFacto AF as standard) for the same samples N6co, V1co, V3co and V5co had much greater activity values. In particular, V1co and V5co showed 4-fold and 3-fold increased activity with the one-stage assay (Fig. 4.25).



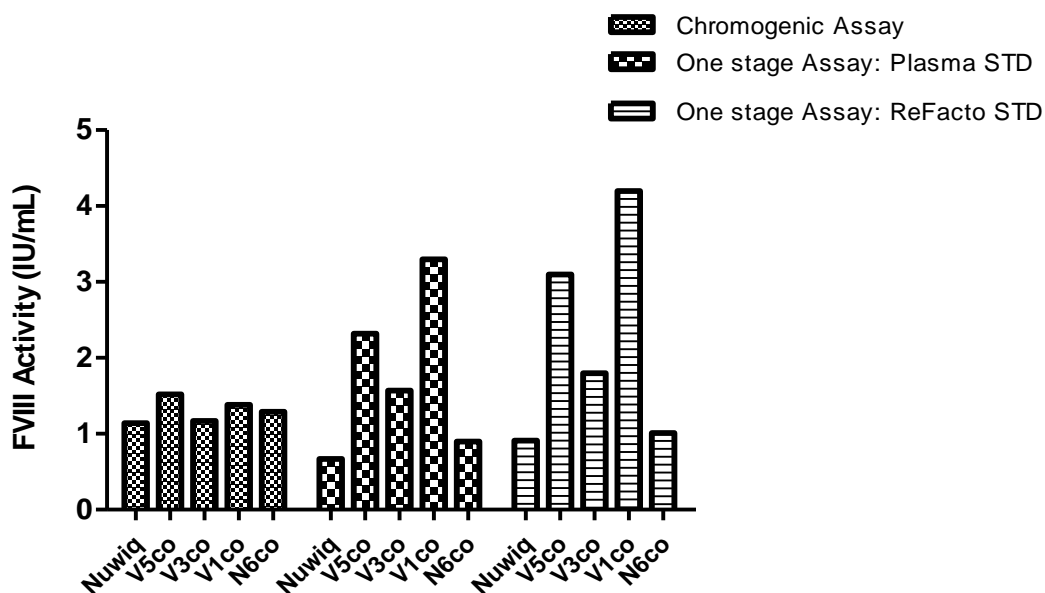
rFVIII	Chromogenic Assay (IU/mL)	One stage Assay: ReFacto STD (IU/mL)
Nuwiq	0.77	0.60
V5co	0.71	2.12
V3co	0.82	1.29
V1co	0.87	3.86
N6co	0.79	0.96

Figure 4.25. Comparison of FVIII activity measured by chromogenic assay and one stage clotting assay

Purified rFVIII variants performed clotting assay. A human cell line derived commercial B-domain engineered FVIII (Nuwiq®, Octapharma) used assay control. Although most of the proteins show some discrepancy, variants V5co and V1co show highly significant difference between the two assays. One stage clotting assay uses ReFacto AF standard, and chromogenic assay used Biophen plasma STD. Statistically not significant between two coagulation assays, column factor ($p=0.16$), row factor ($p=0.467$), (t-test, two tailed). Prism 6.0 (Graph Pad).

To determine if the choice of standard in the one-stage assay had influenced assay discrepancies, activity measurements were repeated with two different FVIII preparations for the one-stage assay, ReFacto® as in the previous experiment and the same plasma calibrator as used in the chromogenic assay (Fig.4.26). However, the previously observed discrepancy between the one-stage and chromogenic assay remained irrespective of the type of FVIII used or the standard (Fig. 4.26).

Assay discrepancies have previously been reported for B-domain deleted FVIII concentrates, where chromogenic assay values were up to 50% higher than the one-stage assay clotting assay (Barrowcliffe *et al.*, 2002; Pahl *et al.*, 2012). In the experiments presented here, ReFacto® shows the same profile as previous reports as does the N6 construct (Fig. 4.26). However, the other FVIII variants have a different profile with increased activity on the one-stage assay when compared to the chromogenic. Therefore, a standardised protocol for the measurement of patient samples and recombinant concentrates is critical.



rFVIII	Chromogenic Assay	One stage Assay: Plasma STD	One stage Assay: ReFacto STD
Nuwiq	1.14	0.67	0.91
V5co	1.52	2.32	3.10
V3co	1.17	1.57	1.80
V1co	1.38	3.30	4.20
N6co	1.29	0.90	1.01

Figure 4.26. Comparison of FVIII activity measured by chromogenic assay and one stage clotting assay using plasma STD and ReFacto AF

Same batch proteins, but the different concentration of proteins (IU/mL) applied to coagulation assay. FVIII activity from one stage clotting assay shows an increment of V5co and V1co as opposed to chromogenic assay. Biophen plasma calibrator was used for chromogenic assay standard. Biophen plasma and ReFacto AF standards were used for one stage clotting assay on an ACL TOP coagulometer (IL, MA, USA).

Statistically significant among the coagulation assays, row factor, $P=0.028$, column factor, $P=0.175$ (Two-way ANOVA). Prism 6.0 (Graph Pad).

4.2.18. FVIII and vWF affinity assay

The half-life and stability of FVIII are an association with the vWF protein, which is the most identified determinant of FVIII survival in blood, as it provides protection from premature clearance or activation of FVIII (Lenting *et al.*, 2007).

My hypothesis was that the B-domain modification of FVIII would not change the vWF binding affinity because vWF binding region on FVIII is not modified.

To test this hypothesis, the purified recombinant FVIII variants proteins (V3co, V5co and V1co) were sent to Dr Mckinnon (Imperial College London) who kindly analysed the binding affinity of vWF to FVIII (rFVIII). ELISA binding assay of vWF-FVIII interaction were undertaken (Fig.4.27). Analysis of binding assays showed that FVIII-Helixate® binds to vWF with a dissociation constant (K_D) of 0.82nM, which is similar to the binding affinity of the B-domain deleted FVIII Nuwiq to vWF (0.63nM). Using the same experimental conditions, we also determined the binding affinity of FVIII variants to vWF which were V1co (0.89nM), V3co (0.65nM) and V5co (0.75nM) respectively; all of which are similar to the wild-type control. This result confirms our hypothesis that the B-domain modification has nothing to do with affinity to vWF.

Overall, the binding assay results suggest that modification of the B-domain region in these variants does not interfere with their biologically important binding function.

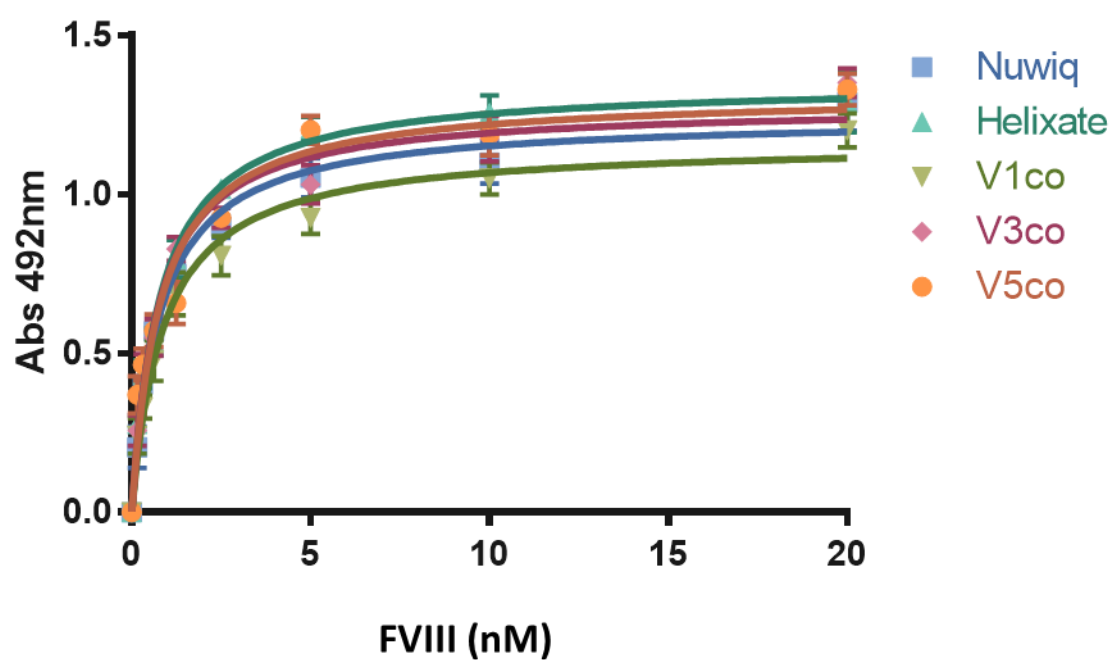


Figure 4.27. Binding analysis of FVIII variants functionality.

Commercial full-length FVIII (Helixate) and Human cell line derived B-domain deleted FVIII (Nuwiq) were assayed as a control. Three purified recombinant FVIII variants were analysed vWF binding affinity by ELISA. Prism 6.0 (Graph Pad).

4.3. Discussion

In this chapter, we have described the expression, purification and characterisation of new recombinant FVIII variants. First of all, we have established a two column chromatographic purification procedure (Fig.4.1). The first step entails the capture of FVIII using FVIIIselect, which is composed of 13kDa recombinant single-domain antibody fragment that is attached to a porous base matrix via a hydrophilic spacer arm (McCue *et al.*, 2009). The total recovery of FVIII from FVIIISelect was 39%, suggesting 61% of the FVIII activity has been lost most probably due to sample degradation during the purification procedure (Fig.4.3).

To increase the overall yield of purified FVIII, we decided to harvest media twice over a 48 hour period. Also, we decided to introduce a 0.5M NaCl wash step to elute FVIII bound to the cell membrane. As a result of these measures, our overall yield of FVIII increased to 1500 Units in 3×10^8 cells (First harvest; 600Unit, Second harvest; 600Unit, and Membrane-bound; 300Units).

A DEAE column step was introduced to enable a ~85-fold concentration of the material isolated from the FVIIISelect column (Fig.4.15). The “concentrated” FVIII showed the expected pattern and bands on a silver staining of SDS-PAGE gel and western blotting, which demonstrate the presence of the single chain FVIII peptides as well as the heavy and light chain FVIII fragments.

The purified and concentrated FVIII was assessed in biological activity/activation assays. A calibrated automated thrombogram system showed (Fig.4.23) that the endogenous thrombin potential was similar and equivalent to commercially available FVIII, implying that the B-domain modification we made (FVIII-V1, FVIII-V3 and FVIII-V5) did not affect thrombin activation.

Discrepancies were seen between the one stage clotting assay and the chromogenic assay as described previously for BDD-FVIII variants (Potgieter *et al.*, 2015). Most of our

B-domain variants showed relatively higher activity as compared to Nuwq® (control, Octapharma) as shown in Figure 4.25 and 4.26. This discrepancy may be procedural with one stage clotting assay requiring relatively longer times for the assay when compared with the chromogenic assay, during which differences in susceptibility to activation of FVIII by contact phase generated proteases can be manifested. The one stage/two stage clotting assay discrepancy between plasma standard compared recombinant protein reference standard has previously been observed and explored (Potgieter *et al.*, 2015). It is also possible that this discrepancy may be because of differences in post-translational modification of the B-domain in the engineered FVIII variants, which is the subject of study in the next chapter. The European Pharmacopoeia and the ISTH (International Society on Thrombosis and Haemostasis) FVIII and FIX Subcommittee recommended the chromogenic assay for reference method. Based on our results we concluded that the chromogenic assay might provide a better indication of FVIII activity after gene transfer than a one stage assay.

Moreover, the vWF and FVIII affinity assay shows a similar affinity for variants with a range in length or sequence of the linker domain substituted for the B-domain, some with and some without *N*-linked glycosylation. Hence affinity to vWF cannot explain the variation in expression of different variants (Fig.4.27).

In summary, we have established a two-step chromatography method for purification of FVIII variants expressed by producer cell line. We showed that the yield of purified FVIII protein was at a level that enabled further biochemical characterisation. Our preliminary studies suggest that FVIII activity and its ability to generate thrombin when added to FVIII deficient plasma was equivalent to that seen with commercial FVIII protein concentrates as was the profile of the FVIII molecule when running in its native form or following thrombin digest when assessed by a silver staining and Western blot analysis. Moreover, the variation in expression cannot relate to vWF binding. This is consistent with the

inference from biochemical studies that the vWF binding domains are in the a3, A3, C1 and C2 regions of FVIII, so do not involve the B-domain.

Chapter 5

Glycomic Profiling of FVIII variants

5.1. Introduction

FVIII is synthesised in the liver, which has been supported by the fact that liver transplantation can cure haemophilia A. Recent data indicates that the liver sinusoidal endothelial cells are responsible for the secretion of FVIII into the circulation (Stel *et al.*, 1983, Nichols and Ginsburg, 1999). However, most of the data on the features of FVIII biosyntheses have been obtained using heterologous expression systems as attempts to immortalise liver sinusoidal endothelial cells have been largely unsuccessful. Before secretion, this single-chain FVIII polypeptide undergoes complex post-translational modification, including significant glycosylation.

The native full-length human FVIII protein has 25 potential *N*-linked glycosylation sites, including 19 sites in the B-domain and three each in heavy (two in A1, one in A2) and light (one in a3, one in A3 and one in C1) chains (Lenting *et al.*, 1998). Of these, 25 sites (19 are located in the B-domain) carry oligosaccharides (Fig.5.1). The B-domain, if human FVIII is therefore extensively glycosylated. Although the amino acid sequence encoding the FVIII B-domain has widely distributed among the human, porcine, and murine genes. The large number of *N*-linked glycosylation sites has remained strikingly conserved between species, suggesting an evolutionary importance (Strasser, 2016).

Within the lumen of the ER, significant folding and modification of newly synthesised FVIII proteins occur. This process is regulated by enzymes and molecular chaperones, including BiP, calnexin and calreticulin (Pipe, 1998). The BiP–FVIII polypeptide complex exhibits ATPase activity; and therefore the isolation of FVIII from BiP and secretion require exceptionally high ATP expenditures, which appears to slow its secretion (Nichols & Ginsburg 1999; Becker *et al.*, 2004). Only correctly folded proteins are allowed to exit the ER. Misfolded protein either is retained within the ER or subject to degradation by the ER-associated protein degradation pathway. These interactions are mediated through *N*-linked glycan structures expressed within the FVIII B-domain.

On successful folding and packaging, newly synthesised FVIII proteins are transported from the ER to the Golgi for additional posttranslational modifications before secretion. This is achieved by formation of COPII vesicles, which bud from the ER lumen and migrate to the Golgi apparatus via the ERGIC. The FV and FVIII have a shared prerequisite for specialised ER-to-Golgi transport machinery. In particular, LMAN1 and MCFD2 are cargo transporters for ER-to-Golgi traffic of FV and FVIII (Nichols *et al.*, 1999; Zhang *et al.*, 2005; Khoriaty *et al.*, 2012). The specific FVIII motif that binds the cargo proteins has not been identified, but *N*-linked oligosaccharides are key to FV/FVIII interactions with the LMAN1/MCFD2 complex. LMAN1 association with FV/FVIII is enhanced by the presence of full glucose trimmed high mannose (9) structures on B-domain located carbohydrates, as demonstrated using a LMAN1 mutant with defective mannose binding ability and, consequently, severely diminished FVIII-LMAN1 interaction. Mutations resulting in the loss of LMAN1 function or disturbing the interaction between LMAN1 and the component of the transport complex MCFD2 cause inherited coagulopathy, a combined deficiency of FV and FVIII (Nichols *et al.*, 1998; Neerman-Arbez *et al.*, 1999, Zhang *et al.*, 2003). Cumulatively, these data serve to emphasise the critical importance of *N*-linked glycan structures in regulating the intracellular trafficking of secretory glycoproteins.

Within the Golgi apparatus, FVIII undergoes further processing, including modification of the *N*-linked oligosaccharides to complex-type structures, *O*-linked glycosylation, and sulphation. Limited proteolysis of the single-chain precursor at residues R1313 and R1648 give rise to a light and a heavy chain, which is occurring in the final stage of FVIII processing in the trans-Golgi prior to secretion. The sites of proteolytic processing correspond to the Arg-X-X-Arg motif can be cleaved by protease furin/PACE (paired basic amino acid cleavage enzyme). However, it remains unclear which signalling protease of the PACE family is responsible for FVIII processing.

In addition to modulating intracellular processing, the glycan can also modulate FVIII susceptibility to proteolysis. The *N*-linked FVIII glycans are commonly capped by terminal negatively charged sialic acid moieties. The removal of capping sialic acid residues leading to exposure of Gal and GalNAc moieties typically results in markedly enhanced glycoprotein clearance mediated primarily via the hepatic lectin asialoglycoprotein receptor (ASGPR). This interaction is mediated through the *N*-linked carbohydrate structures clustered within the B-domain of FVIII. Treatment of ASGPR antagonist significantly inhibited FVIII clearance in mice (Bovenschen *et al.*, 2005a), implying that the ASGPR may contribute to normal physiological clearance of FVIII from plasma.

The natural FVIII circulating in the bloodstream contains multiple forms of the truncated B-domain, which are formed by proteolysis of a full-length two-chain molecule. The procoagulant properties of these FVIII variants shows no differences. Amongst these is the BDD SQ variant (ReFacto®) in which FVIII amino acid residues 746~1639 have been deleted; effectiveness and safety of which has been demonstrated over the past 16 years with its extensive use in patients with severe haemophilia A. Other variants similar to the BDD SQ FVIII e.g. Novo Eight® (deletion of residues 751~1637; NovoNordisk) and Nuwiq® (substitution of the 747~1648 region by the “non-natural” peptide QAYRYRRQ; Octapharma) have been created and tested in humans with good comparable efficacy and safety (Ezban *et al.*, 2014; Sandberg *et al.*, 2012). A FVIII variant carrying the first 226 amino acids of the B-domain and six *N*-linked glycosylation sites (variant 226aa/N6) was found to be secreted 5-fold more efficiently as compared with FVIII with the deletion of the full-length B-domain (Miao *et al.*, 2004). This was thought to be due to the improved transport of the precursor protein from the ER to the Golgi apparatus (as compared with the full-length form) and a decrease in adsorption of the secreted FVIII onto the membrane surface of producer cells (as compared with BDD-FVIII). Additionally, FVIII-N6 has a reduced tendency to give rise an unfolded protein response

when compared to the full length and BDD-hFVIII variant, thus making it a useful variant for further evaluation of gene transfer.

We, therefore, developed a novel FVIII-V3co variant in which the N6/226 amino acids B-domain linker was replaced with a 31 amino acid peptide that contains the six *N*-linked glycosylation signals that were thought to be required for efficient and safe expression of FVIII. FVIII-V1co is identical to FVIII-V3co except that the *N*-linked glycosylation triplets are flanked by additional amino acids that are normally adjacent to these moieties in the native FVIII B-domain, thus extending the size of the B-domain peptide from 31 to 44 amino acids. Finally, FVIII-V5co is identical to FVIII-V3co except that the asparagine in the six *N*-linked glycosylation triplets with the V3co peptide was replaced with alanine (Fig.3.1 & Fig.5.1).

In the studies, we determined the *N*-glycan structures of these different forms of recombinant human FVIII as carbohydrate structures on human FVIII plays important roles in determining stability, circulatory half-life, and biological activity. It is accepted that recombinant FVIII protein will likely have different *N*-glycan structures compared to the endogenously synthesised FVIII protein. Moreover, glycosylation variation has also been described between different commercial recombinant FVIII products that have been synthesised in different mammalian cell lines (including CHO and BHK). For example, rFVIII from Chinese hamster ovary cells express the NeuGc epitope, which accounts for 0.5% of total sialic acid. In contrast, Gal- α (1,3)Gal structures have been detected approximately 3% of BHK expressed rFVIII. Moreover, high levels of antibodies against NeuGc and Gal- α (1,3)Gal naturally generated in the most humans, and specific glycan chains on FVIII could influence dendritic cell uptake mediated by the macrophage mannose receptor (CD206) (Preston *et al.*, 2013; Dasgupta *et al.*, 2007).

In this chapter, we, therefore, attempted to determine how *N*-glycan structures of the FVIII variants using a combination of high performance liquid chromatography (HPLC),

and mass spectrometry, to further develop an understanding of the difference in the glycosylation pattern and how this may influence biological activity.

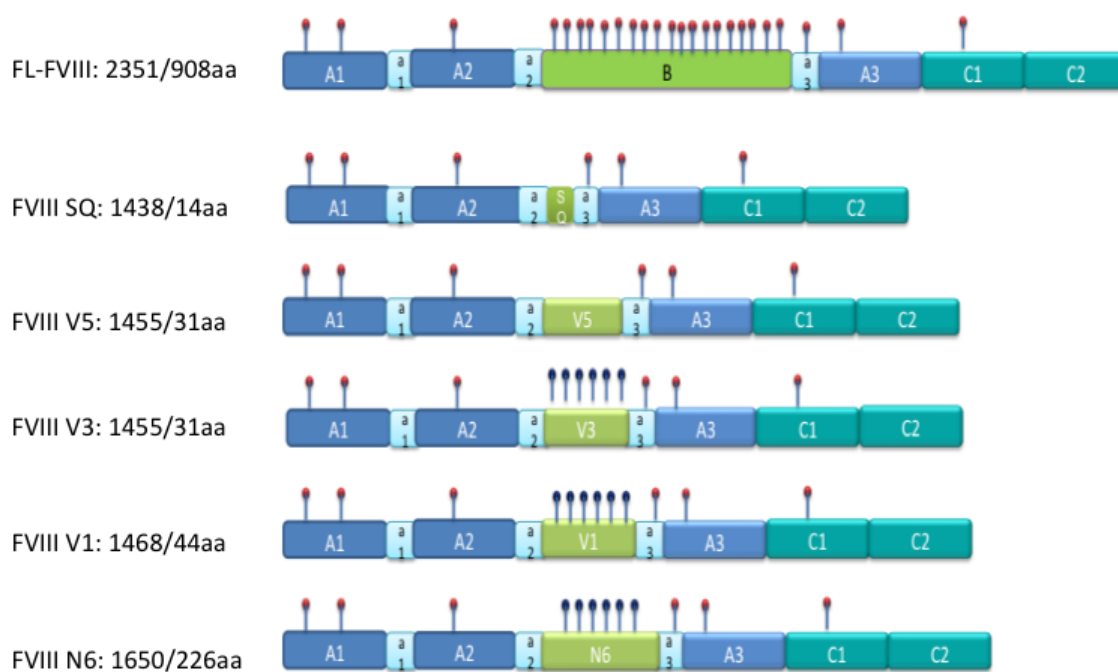


Figure 5.1. Schematic representations of *N*-linked glycosylation sites on FVIII variant domains

Numbers on the left indicate the peptide sequence length of each variant. Total peptide length number/number of linker sequence length. The annotated and potential *N*-linked glycosylation sites of each protein are also displayed on the domain. The red lollipops represent annotated *N*-linked glycosylation sites, and blue lollipops represent non-natural *N*-linked glycosylation sites.

5.2. RESULTS

5.2.1. PNGase F digestion

We compared the *N*-linked glycosylation in our FVIII variants with commercial BDD FVIII SQ (ReFacto®; Pfizer). As an initial evaluation purified, FVIII variants were treated with PNGase F, which cleaves between the innermost GlcNAc and complex oligosaccharides from *N*-linked glycoproteins. Subsequently, unglycosylated protein migrates faster than glycosylated protein in SDS-polyacrylamide gel. PNGase F catalyses the cleavage of an internal glycoside bond in an oligosaccharide. It cleaves all asparagine-linked complex, hybrid, or high mannose oligosaccharides unless the core GlcNAc contains an alpha 1,3-fucose. The asparagine residue, from which the glycan is removed, is deaminated to aspartic acid. PNGase F requires a minimum of two GlcNAc oligosaccharide residues attached to the asparagine in order for catalysis to occur. This enzyme utilises a catalytic triad of cysteine-histidine-aspartate in its active site, which is a common motif for amidases. It is used extensively for characterising *N*-linked glycan structures and for identifying *N*-linked glycosylation sites in proteomic studies.

As the actual status of the potential *N*-linked glycosylation sites in the V3 linker peptides in FVIII-V3co is unknown. We compared PNGase F digest of this molecule with ReFacto® which is produced in CHO cell and our BDD-FVIII SQ made in the same HEK-293T cells as FVIII-V3co (Fig.5.2). The FVIII variant preparations used for this study were purified by double column method described in the previous chapter. We did not observe differences in the de-glycosylated products derived from PNGase F treatment of ReFacto® and BDD-FVIII-SQ. This suggests that that for BDD-FVIII manufacture in different cells lines does not significantly influence glycosylation. A marked shift in 110kDa heavy chain of FVIII-V3co occurred with PNGase F digest compared to undigest cognate suggesting that the linker peptides being heavily glycosylated.

A modest shift in the de-glycosylated products of N6 was observed which has six potential *N*-linked glycosylation sites contained within the 226 amino acid partial B-domain.

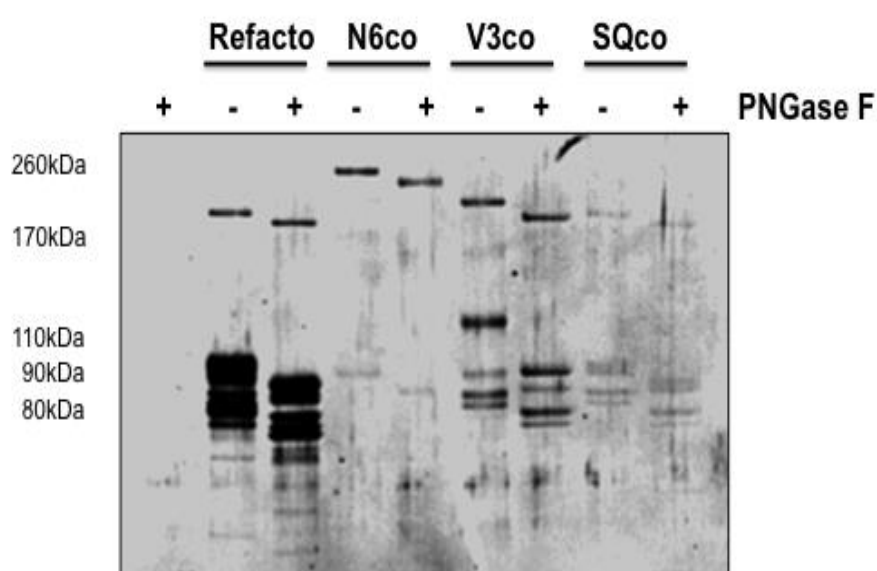


Figure 5.2. PNGase F Digestion of FVIII variants

The purified FVIII variants were subjected to 4~12% Bis-Tris gradient gel electrophoresis under reducing conditions and visualised by SYPro Ruby staining. The samples were treated with PNGase F endoglycosidase for 60 minutes before analysis to demonstrate the presence of *N*-linked glycan modifications. Recombinant human FVIII purified, N6co, V3co, SQco: Digestion with PNGase F. Commercial B-domain deleted ReFacto® was included for comparison. N6co variant gave dominant high molecular weight single chain because of the absence of the furin cleavage sequence in its linker peptide.

5.2.2. Mass spectrometry

The recombinant FVIII proteins (V3co, N6co, V5co, SQco, and V1co) purified by the new protocols were concentrated and up to 100ug was sent to Dr Haslam (Imperial College London) who kindly analysed the glycome profile using MALDI-TOF/TOF MS/MS technology (Appendix 2. 3). Mass spectrometry (MS) has gained widespread use in protein glycosylation analysis and has become an indispensable, powerful analytical technique in this research area. A great advantage of MALDI-TOF MS is that the process of soft ionisation give rise little or no fragmentation of analytes, allowing the molecular ions of analytes to be identified. Moreover, mass mapping of a protein can be achieved by breaking it into specific peptide fragments using amino acid specific proteolytic enzymes. Mass spectrometric analysis of the enzymatic digest generates a profile, which is unique to the analysed protein allowing unambiguous identification by the matching with the database searches.

Hence, glycosylation profiling of our FVIII variants was based on the combination of two basic analyses, which are monosaccharide composition and fragmentation analysis of over 15 glycans per sample. Monosaccharide composition analysis helps to confirm the glycan composition of monosaccharide content as an orthogonal technique. In terms of profiling changes in total glycan composition, monosaccharide analysis can also be used as a technique for identifying various monosaccharide modifications, phosphorylation and sulphation. A refractive index detector is used for monosaccharide composition analysis. In contrast, fluorescence detection is used for saccharide composition analysis of antibody drugs as it provides higher sensitivity. The sugars are not fluorescent; they undergo derivatisation by an appropriate method to make them fluorescent before analysis by high-performance liquid chromatograph with a fluorescence detector.

In contrast, fragmentation analysis is based on mass spectrometry (MALDI) MS. The key aspect of MALDI-MS is to isolate macromolecules in a suitable matrix of highly laser light

absorbing small organic molecules, such as an α -cyano-4-hydroxycinnamic acid (CHCA), sinapinic acid (SA) and 2,5-dihydroxybenzoic acid (DHB). Then it to dry on a MALDI-target into a crystalline deposit throughout which the molecules of the analytes are dispersed. Following excitation of the matrix by a high-intensity laser pulse of short duration, the absorbed energy causes vaporisation and ionisation of the analytes in a very dense MALDI crest. The ions are generated by a point source in space and time then enter a vacuum where they are accelerated by a strong electric field in a tube. They are then separated in time and finally reach to the detector. The time-of-flight (TOF) taken for particular ions. The flight time of an ion relates to its mass-to-charge ratio (m/z). Thus, mass spectra can be generated from simple time measurements.

MS spectra of all five variants are illustrated in figure 5.3 with most abundant glycan structures annotated in association with their m/z values (the full *N*-glycome of the five variants is displayed in Appendix 3).

A wide range of *N*-glycan structures was detected in all samples, specifically, a significant proportion in all five spectra involved high-mannose structures (m/z 1579.8, 1783.9, 1987.9, 2192.0, 2396.2 peaks). In contrast, hybrid structures (i.e., m/z 1824.9) were detected in lower abundance. Prominent bi-antennary (i.e., m/z 2040.0), tri-antennary (i.e., m/z 3415.6) and tetra-antennary (i.e., m/z 4110.1) glycans were also present in the spectra. Their antennae structures consisted primarily of HexNAc-Hex moieties (i.e., m/z 2489.3), with a significant proportion containing *N*-acetylneuraminic acid (sialic acid) (i.e., m/z 3602.7, 3748.8 and 3241.6). Finally, tandem MS analysis confirmed an abundance of core-fucosylated moieties (i.e., m/z 2850.4, 2966.5) in the variant FVIII molecules. In general, the *N*-glycomes were more frequently found in FVIII-N6co, V1co and V3co spectra when compared to V5co and SQco glycomes, in which mainly the intermediate saccharides were found.

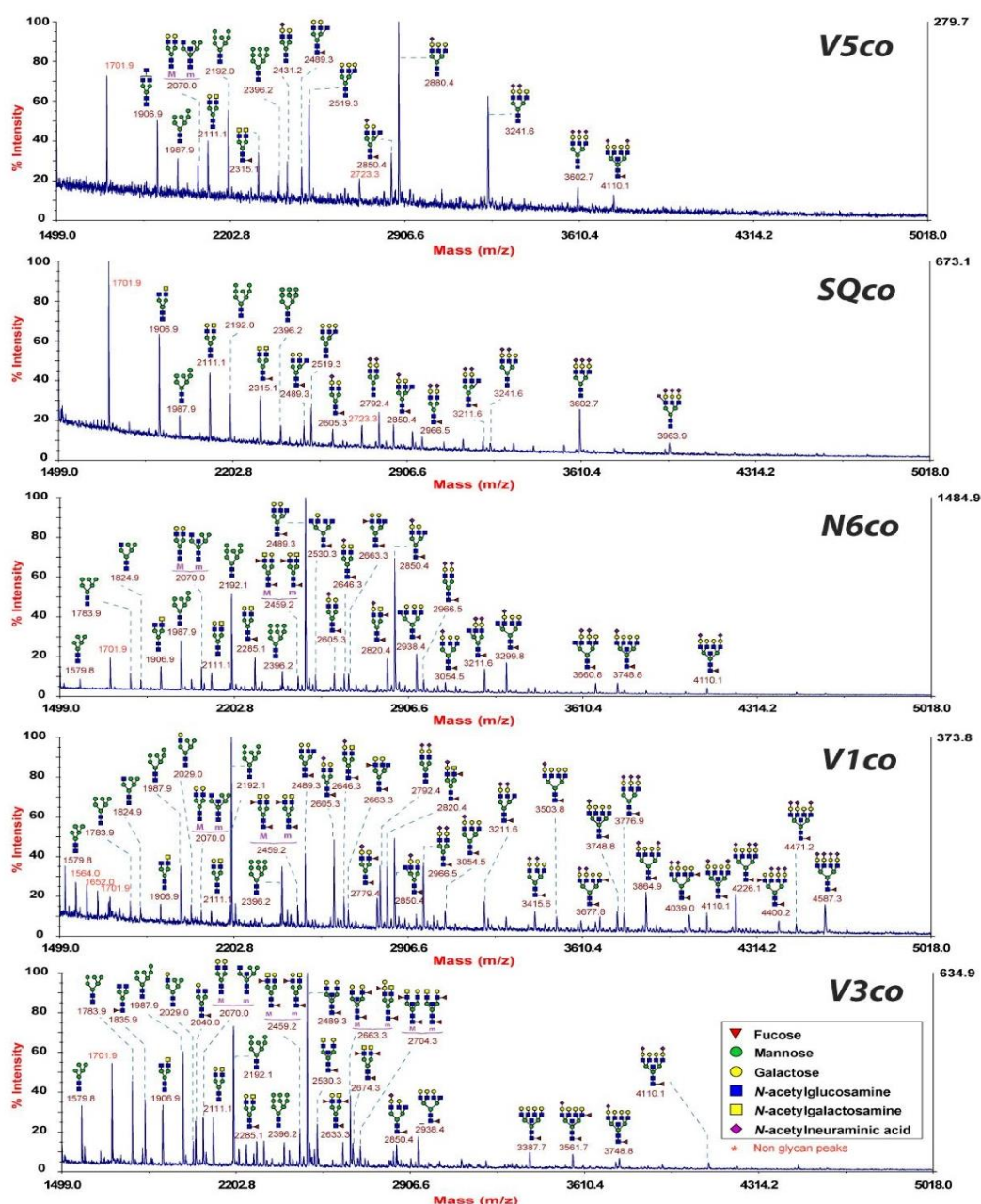


Figure 5.3. MALDI-TOF mass spectra of permethylated *N*-glycans in five FVIII variants

Glycoprotein variants of all spectra display $[M + Na]^+$ molecular ions. Panel intensities were normalised to 100% unless otherwise stated. Only ions with the highest relative abundance are presented here. Structural assignments are based on monosaccharide compositions, knowledge of glycan biosynthesis and fragmentation analyses. In m/z values with more than one structure: M: Major (more abundant) structure; m: minor (less abundant) structure. Data provided by Dr Haslam, imperial college, London.

5.2.3 *N*-glycome analysis separates FVIII variants to two groups

To identify the differences of glycosylation profile of five FVIII protein variants, *N*-glycans were counted, including the difference in the types of structures. The result shows that the total range of *N*-glycan compositions was 37 to 66 in all five variants. Interestingly, 20~30 more glycan structures were found in FVIII-V3co, V1co and N6co as opposed to SQco and V5co (Fig.5.4.A). We speculate that this is likely a reflection of the different constitution of the B-domain peptide in the individual molecules. FVIII- V3co, V1co and N6co, which have six *N*-linked glycosylation sites in the B-domain linker peptides. In contrast in FVIII-V5co substitution of Asparagine with Alanine reduced overall glycosylation of FVIII.

Sialic acid residues protect *N*-glycan moieties from interaction with ASGPR and increase the circulation half-life of FVIII. The sialylation representing approximately one-third of the FVIII glycome levels and differed modestly between the FVIII variants with FVIII-SQco and V1co were showing a slight increase in the number of sialylated glycans (Fig. 5.4.B).

We observed core-fucosylated glycan levels in FVIII-V3co, V1co and N6co when compared to FVIII-V5co and SQco (Fig.5.4.C). Several studies have reported an increase in fucosylated *N*-glycans in recombinant proteins derived from human cell lines (Diaz *et al.*, 2009; Zhang *et al.*, 2010; Böhm *et al.*, 2015). A fucose residue is attached to the first *N*-acetylglucosamine of these complex-type *N*-glycans. The unusual *m/z* 3963.9 ion in FVIII-SQco profile suggests possible contamination derived from FBS (Foetal Bovine Serum), subsequently affecting the ability for further interpreting of this preparation (Appendix 3, SQco) (Monk *et al.*, 2006).

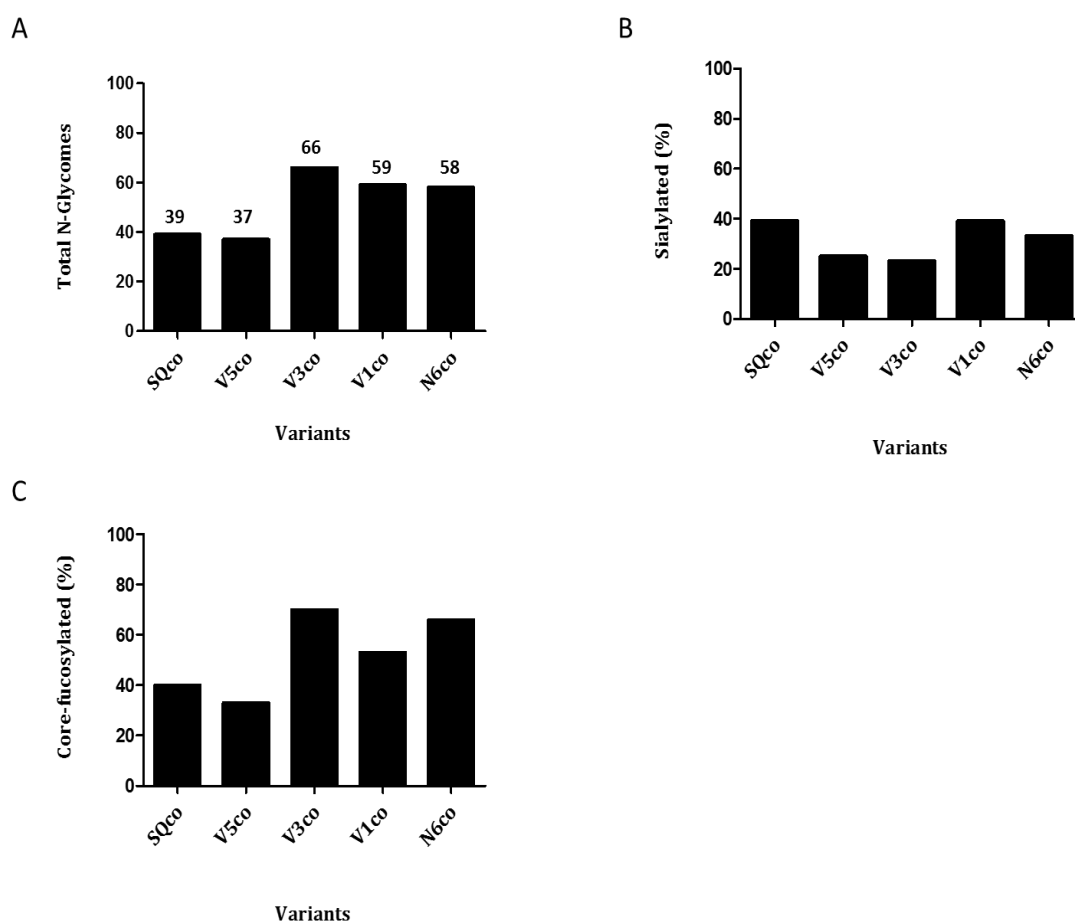


Figure 5.4. Overview of FVIII variants *N*-linked glycosylation

A) Bar chart depicts total number of *N*-glycomes. The quantity of view separate in two groups, SQco, V5co and V3co, V1co, N6co. B) Bar chart illustration of % sialylated observed in *N*-glycomes. C) Bar chart illustration of % core-fucosylated observed in *N*-glycomes.

5.2.4. Distribution of sugar chain and antennary structure profiles of FVIII variants

A similar quantity of high mannose structures in all variants, which corresponds with Kaufman's finding that high mannose structures are common in the light chains of FVIII. Moreover, the hybrid and complex types are more common in the heavy chain, which is more easily degraded than the light chain in serum-free condition (Kaufman *et al.*, 1988). In addition to the qualitative analysis of the glycan structures, detected m/z ion peaks were relatively quantified in each spectrum. Their semi-quantitative distribution shows that more than 80% of *N*-glycans are complex types in each of the five variants (Fig. 5.5.B). The quantity of high mannose-type structure was similar in FVIII- SQco and V5co, which have no Asn-X-Thr/Ser peptides sequences in their B-domain linkers. In contrast, FVIII-V3co, V1co and N6co variants, which contain six potential *N*-linked glycosylation sites in their linker peptides, displayed a prominent enrichment in high-mannose type (Man5 to Man8), hybrid, bi-antennary, tri-antennary and tetra-antennary structures in a quantitative manner (Fig. 5.5.A).

These molecules had a dominance of tetra-antennary antennae structures while FVIII- SQco and V5co displayed tri-antennary structures. This may reflect the difference in the Asn-X-Thr/Ser sites in the B-domain peptide in these variants when compared to FVIII- SQco and V5co. However, further glycoproteomic mapping of the *N*-glycan repertoire of each Asn (*N*) site is necessary to prove this unequivocally.

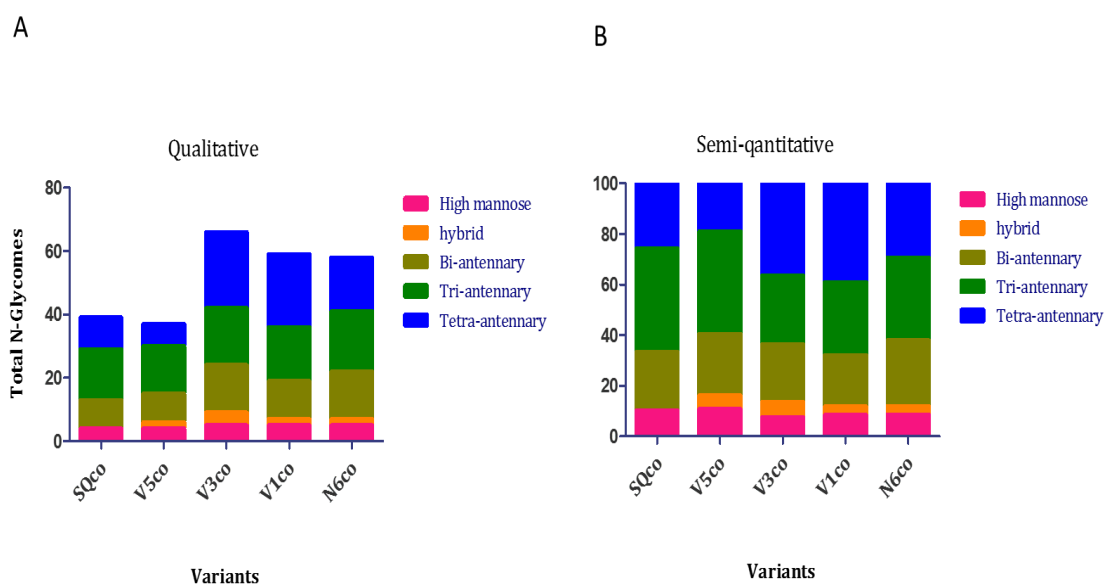


Figure 5.5. Qualitative and semi-quantitative analysis of *N*-glycan structures

A) Condensed bar depicts the qualitative distribution of five *N*-glycan structure groups in variants. B) Semi-Quantitative distribution of five *N*-glycan structure groups in variants. Complex type bi-tri-tetra-antennary structures were shown to constitute approximately 90% of the glycans identified, accompanied by a minority of high mannose type and hybrid. The majority of *N*-glycan structures were of complex-type in all five variants.

5.2.5. Biologically significant common epitopes

Figure 5.6 shows the commonly detected epitopes and glycan features in each FVIII variant. Specifically, the presence of blood group antigen Lewis^{x/a} (Hex1Fuc1HexNAc1) and LacdiNAc with fucosylated LacdiNAc (Fuc1GalNAc1 GlcNAc1) epitopes were observed all variants. The Lewis ^{x/a} epitope is present all five FVIII variants including commercial recombinant Nuwiq® (Octapharma), which may be due to the products being produced in cell lines of embryonic origin (HEK-293 cells). However, the Lewis ^{y/b} (Fuc2Hex1HexNAc1) antigens were detected only in FVIII-V3co and N6co. The fucosylated LacdiNAc (Fuc-LacdiNAc) epitope reported from human HEK293F produced recombinant Nuwiq® (Octapharma), in which the epitope is not present in plasma-derived FVIII but kidney cell line produced Nuwiq® and five variants appeared (Kannicht *et al.*, 2013).

Most importantly, the antigenic Gal- α 1,3-Gal and *N*-glycolylneuraminic acid (Neu5Gc) glycoforms detected in recombinant human FVIII variants expressed in BHK and CHO cells, respectively (Valentino *et al.*, 2014), however, human cell line produced Nuwiq and any of the five variants *N*-glycans were not present. The human anti- α -Gal is one of the most abundant natural antibodies, representing approximately the 1% of the human circulating immunoglobulin. It has also been shown that anti- α Gal prevents porcine xenograft organs transplantation in humans, as it binds to α -Gal epitopes expressed in porcine cells, mediating rejection (Galili, 2005). Similar studies revealed that the majority of the remaining anti- α -Gal antibodies in healthy human serum are specific against the Neu5Gc epitope. The so-called Hanganutziu-Deicher (HD) antigen, Neu5Gc, exists in almost all other animals except humans and has been associated with hyperacute rejection during xenotransplantations (Zhu and Hurst, 2002). As was previously described, expression of FVIII in human cell lines for pharmaceutical purposes avoids

the potential for incorporation of such non-human epitopes, leading to a higher safety level.

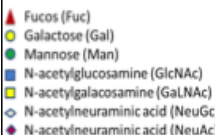
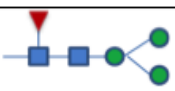



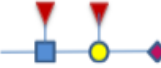




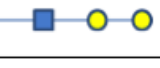
Core structure	Terminal structure		pdFVIII	V3	V1	N6	SQ	V5
		High Mannose N1->6	+	+	+	+	+	+
		LacNac	+	+	+	+	+	+
		Sialyl-LacNac	+	+	+	+	+	+
		Sialyl-Lewis x/a	+	+	+	+	+	+
		Sialyl-Lewis y/b	-	+	-	+	-	-
		Fuc-LacdiNac	-	+	+	+	+	+
		Blood Group A,B,O	+	-	-	-	-	-
			-	-	-	-	-	-
		Neu5GC	-	-	-	-	-	-
		Gal-α 1,3 -Gal	-	-	-	-	-	-

Figure 5.6. Common epitopes of *N*-glycans on FVIII variant glycoproteins

A Synoptic view of epitopes with biological significance, presented in samples *N*-glycomes. Structures of the present (+) or absent (-) glycan features in each profile are indicated next to their respective names. pdFVIII: plasma-derived FVIII, Table adopted from Kannicht *et al.*, 2013 (Kannicht *et al.*, 2013).

5.3. Discussion

Glycosylation is one of the most common posttranslational modifications of proteins. It has important roles in protein structure, stability and function. Differences in protein glycosylation occur in recombinant proteins expressed in mammalian, yeast and insect cells as well as between different mammalian cell lines (Diaz *et al.*, 2009; Croset *et al.*, 2012). Recombinant proteins derived from HEK-293 cells are found to have lower degrees of terminal sialic acids on the *N*-glycans and higher levels of fucosylation compared with other cell lines and naturally occurring forms of glycans (Böhm *et al.*, 2015).

PNGase assay performed on the FVIII proteins (N6co, V3co, and SQco) demonstrated a shift banding pattern as shown in figure 5.2 suggesting that FVIII is heavily glycosylated.

The glycan repertoire of five FVIII variants was identified based on the compositional analysis (MALDI-TOF), fragmentation analyses (MALDI-TOF/TOF) and knowledge of glycan biosynthesis. All FVIII variants displayed a complex profile, comprising of different oligosaccharide structures: high mannose, hybrid and complex (bi-, tri- and tetra-antennary) structures. Sialylated glycan levels were relatively similar among the FVIII variants, representing approximately one-third of their profiles (Fig.5.4). Prominent epitopes Lewis ^{x/a}, LacdiNAc, and Fuc-LacdiNAc antigen were detected in various *N*-glycans in all five variants, including commercially approved recombinant human FVIII (Nuwiq®, Octapharma). We believe that this is possibly attributable to the fact that these proteins were expressed HEK-293T cells, which is derived from embryonic tissues. Most importantly, the antigenic Gal- α 1,3-Gal and Neu5Gc glycan structures, which have been demonstrated to trigger immune responses in humans, were absent from all profiles. In addition, all FVIII variants exhibited an increased population of *N*-glycan structures

including enrichment of high-mannose structures when compared to a recent report of the glycan pattern in the B-domain deleted recombinant human FVIII protein (Kannicht *et al.*, 2013). This could reflect differences in the method for generating the FVIII variants, the sensitivity of the method of analysis and possibly by differences in the B-domain linker sequence and cell culture conditions.

Differences were however noted between FVIII- SQco and -V5co and FVIII- V3co, -V1co and -N6co (Fig.5.3) as summarised below:

- Higher average number of glycan moieties in FVIII- V3co, -V1co and -N6co.
- Relatively higher levels of core-fucosylated glycans in FVIII- V3co, -V1co and -N6co
- Lewis ^{y/b} epitope present exclusively in the in FVIII- V3co and -N6co (Fig. 5.6)

These difference could be explained by the presence of six potential *N*-linked glycosylation sites in the FVIII-V3co, -V1co and -N6co B-domain linker regions. However, further glycoproteomic studies are required to prove this hypothesis.

Our knowledge of the biological significance of these complete glycans on FVIII function is still not clear. Additional studies (i.e. B-domain peptide analysis) could be performed to identify the exact type of the epitopes. Substitutions of Asn residues from the *N*-linked consensus sequences Asn-X-Ser/Thr in the FVIII-V3co with alanine resulted in a substantial change in the glycosylation pattern. However, the activity of FVIII-V5co appeared to be higher in *in-vitro* studies (previous chapter) than FVIII-SQco even though their glycosylation pattern was similar. In ReFacto® (BDD-FVIII) ~80% of the *N*-linked glycosylation sites were deleted when compared to full-length wild-type FVIII but without loss of specific activity and stability. These data suggest that the glycans present in B-domain may not be critical for the clotting activity and possibly stability of the protein. However, the B-domain has been shown to be important for intracellular trafficking and binding to asialoglycoprotein receptor. Therefore, glycans in the heavy

chain (A1 and A2 domains) and the light chain (A3 and C1 domains) may be responsible for the activity. This is contrary to study by Kosloski et al, where they showed that deglycosylation of the full-length protein led to ~32% loss of protein activity (Kosloski *et al.*, 2009).

In this chapter, I have explored the difference in the glycosylation of FVIII variants containing different B-domain linkers using deglycosylation enzymes and MALDI-TOF/TOF tandem mass spectrometry methods. While FVIII is heavily glycosylated we observed the distinct difference in the glycosylation pattern observed with FVIII variants V1co, V3co and N6co compared with FVIII-V5co and SQco suggesting that the configuration of the B-domain peptide configuration influences the overall glycosylation pattern.

Chapter 6

***In-vivo* Analysis of B-domain Engineered Human Factor VIII Expression from Adeno associated viral vectors**

6.1. Introduction

Haemophilia A caused by a deficiency of FVIII is well suited for a gene replacement approach because a modest increase in the level of FVIII (>1% of normal) could be able to improve the severe bleeding phenotype (Ljung, 1999). Among the gene transfer approaches for haemophilia, AAV vectors are showing exceptional promise due to an excellent safety profile and ability to direct long-term transgene expression from post-mitotic cells, making them useful for genetic modification and analysis of wide range of tissues (Nathwani *et al.*, 2007). Indeed, a single vein administration of a FIX AAV vector to haemophilia B patients increased FIX expression from <1% to 1~6% of normal levels, this enabled four of the seven patients to stop their prophylactic infusions, and the other three patients were able to extend the interval between infusion (Nathwani *et al.*, 2014).

However, the use of AAV vectors for haemophilia A gene therapy is challenging, due to the large size of the *F8* gene and a low level of FVIII expression. FVIII is highly inefficient compared to other coagulation factors such as FV (Kaufman *et al.*, 1989; Nichols and Ginsburg, 1999). AAV packaging capacity is limited to 4.7 kb, although it has been demonstrated that large transgenes can be packaged with sufficient expression levels (Allocca *et al.*, 2008). However, this finding has not been recapitulated by others (Lu *et al.*, 2008; Wu *et al.*, 2010). Therefore, the ~7.0 kb size of the *F8* gene is not suitable for AAV. However, the deletion of FVIII B-domain, which is not required for haemostatic function resolves the size constraint problem, reducing the total size of the *F8* gene and increasing secretion of FVIII by the 30% (Pittman *et al.*, 1993; Kaufman *et al.*, 1997; Miao *et al.*, 2004). Moreover, it has been demonstrated that improved secretion of FVIII is mediated through *N*-linked glycosylation with the

mechanism facilitated by binding with LMAN1 and MCFD2 (Kaufman *et al.*, 1988; Zhang *et al.*, 2003; Graw *et al.*, 2005).

Our innovative approaches in Chapter 3 demonstrated that the six *N*-linked glycosylation triplets, juxtaposed in the V3 linker peptide sequences, promote the best expression of FVIII among the variants studied. Therefore, FVIII-V3, composed of a short B-domain linker sequence, allows the use of the AAV gene transfer system, as the total cassette size is 5.13 kb, only marginally over AAV's packaging capacity. Secondly, we showed with the mutant V5, where *N*-linked glycosylation sites are removed expression was not altered compared to V3 (Fig.3.14), suggesting the configuration or confirmation of linker amino acids may have a role in FVIII expression other than *N*-linked glycosylation.

In this chapter, we tested whether we can recapitulate the FVIII expression of the V5, V2 and V1 variants *in-vivo*, by single peripheral vein administration of AAV vector to C57BL/6 mice. We demonstrate with the V5 construct the *N*-linked glycosylation is not required for efficient expression of FVIII. We further characterise alternative deletions around the V3 linker.

6.2. Results

6.2.1 Construction of FVIII variant expressing AAV

We demonstrated in chapter five that the purified FVIII V3 variants were heavily glycosylated. We showed modified linker V5, where putative *N*-linked glycosylation sites were removed, and overall *N*-linked glycosylation decreased, did not exhibit lower FVIII activity. This suggested that perhaps linker configuration or conformation may have more influence on FVIII expression than the number of *N*-linked glycosylation sites. To this end, we showed with variant V1 adding amino acids between the glycosylation triplets (N-X-T/X), does not influence the level of glycosylation yet a decrease in FVIII activity compared to V3 was observed (Fig.3.15 and Fig.5.4). This result further supports the concept that conformation of the linker sequences is more important than the number of *N*-linked glycosylations in the linker. Therefore, we set out to test whether the *in-vitro* findings are recapitulated *in- vivo*.

For *in-vivo* testing, the FVIII variants were incorporated into AAV vectors. Details of AAV expressing the FVIII variants is illustrated in a schematic diagram (Fig.6.1.A). The AAV expression cassettes were designed to compare the effect of linker V5, V2 and V1 with V3 in liver cells for FVIII production, the liver-specific capsid serotype eight (AAV8) was used for packaging (Sands, 2014). In addition, a hybrid liver specific promoter (HLP) was used to drive tissue-specific transgene expression.

Coomassie blue staining was used to assess virion assembly and detection of capsid proteins. All variants show clear separation of the capsid protein VP1, VP2 and VP3 corresponding to upper middle and lower band, respectively (Fig.6.1.B). The alkaline gel showed full packaging and fragmented or partial packaging viral DNAs (Fig.6.1.C).

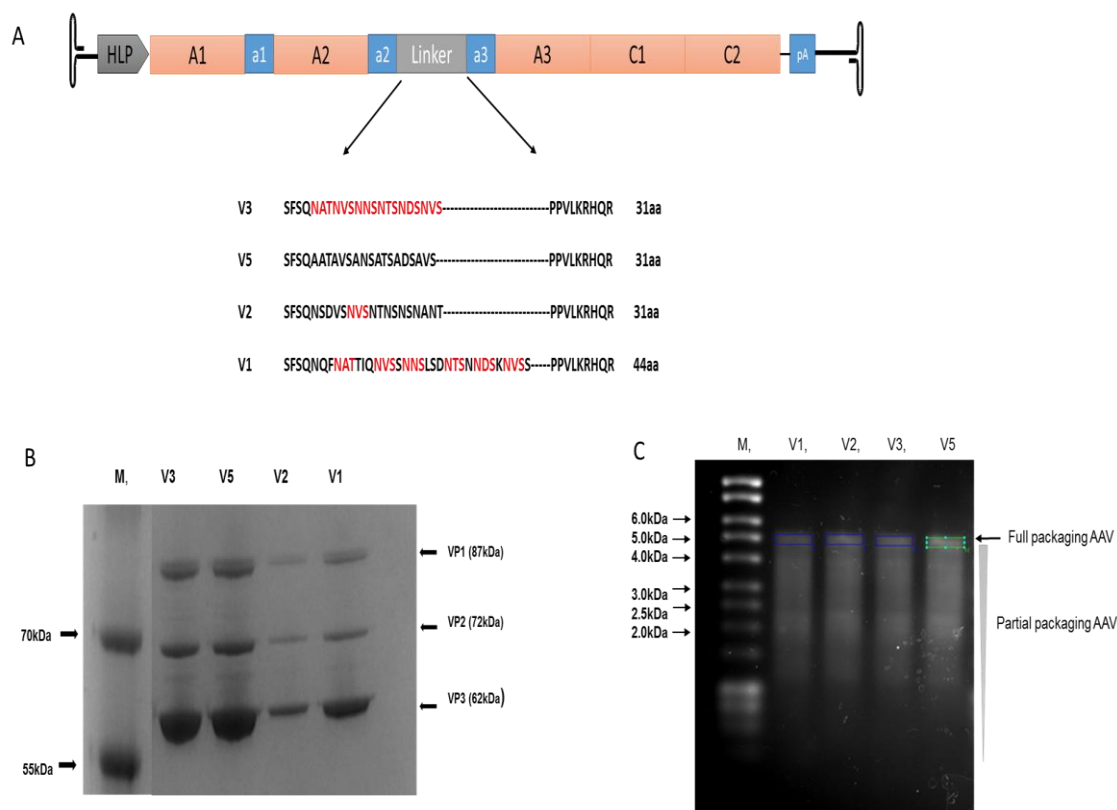


Figure 6.1. Characterization of AAV particles harbouring FVIII variants (V1, V2, V3, and V5)

A) Schematic diagram of four AAV vector genomes encoding FVIII variants under the control of HLP promoter and synthetic polyadenylation sites. The V3 linker (31aa) composed of six *N*-linked glycosylation triplets (17aa) juxtaposed between the remainder sequence of original part of B-domain (14aa). The V5 linker (31aa) of 17aa substitute Asn(M) to Ala(A) to destroy glycosylation triplets sequences. The V2 linker (31aa) is a scrambled sequence of V3. The V1 linker (44aa) has six *N*-linked glycosylation motifs each separated by additional amino acids.

B) Coomassie staining of purified AAV particles (V3: 1×10^{13} vg/mL, V5: 1.5×10^{13} vg/mL, V2: 2×10^{12} vg/mL, and V1: 8×10^{12} vg/mL). Three capsid viral proteins (VP)s were separated on 10% SDS-PAGE gel. VP1; 87kDa, VP2; 72kDa; VP3; 62kDa respectively and molecular weight marker representing 70kDa and 55kDa.

C) Alkaline gel analysis shows full packaging approximately between 5.3kb to 5.1kb top band (square box), which was followed by partial or fragmented DNAs band,

6.2.2. Comparison of AAV FVIII variants *in-vivo*

Intravenous injections of FVIII expressing AAV into C57BL/6 mice were performed to test the efficacy of newly designed FVIII variants, according to the procedure approved by the UK Home Office and institutional guidelines at University College London.

Maximum of 200µL of viral vectors were administered into each animal, containing approximately 2.5×10^{11} viral genome copies per body weight (vg/kg).

Mice were sacrificed four weeks after the injection, liver tissues and blood samples were collected.

Human FVIII expression was determined by FVIII: Antigen assay in murine plasma at 4 weeks using human FVIII monoclonal antibodies based ELISA (Stago). Results showed that the percentage expression of FVIII: Antigen (%) in mouse plasma samples, were V3 (237±27), V5 (123±54), V2 (60±18) and V1 (48±19) respectively (Fig. 6.2.A).

The rAAV-hFVIII gene transfer efficiency was assessed based on viral copy number in the liver determined at four weeks after administration of AAV.

Genomic DNA was isolated from liver tissue, and quantitative PCR (Q-PCR) was performed to determine the copy number of the viral genome in transduced liver tissues. Primers, which were designed to amplify the FVIII A2 domain (Heavy chain), were used for all rAAV-HLP FVIII variants injected mice. The proviral copies per cell of all variants showed relatively similar copy number from V3 (1.86±0.69), V5 (0.98±0.4), V2 (2.51±0.26) and V1 (1.63±0.6) respectively, suggesting equivalent dosing of vectors (Fig.6.2.B).

Due to the logical inference that transgene expression varies depending on proviral copy number, i normalised FVIII expression between vectors according to proviral copy numbers. After normalisation, FVIII antigen(%) expression/transgene copy was V3 (140±52), V5 (121±23), V2 (24±9) and V1 (30±13), respectively (Fig. 6.2.C).

The correction for proviral copy number shows that the expression of V3 was similar to V5 (ns). These results are in agreement with the *in-vitro* study, which implies that the *N*-linked glycosylation modification on the linker sequence is not responsible for the enhanced FVIII expression. Importantly, extending the size of the B-domain peptide from V3 (31aa) to 44 amino acids V1 decreased the FVIII expression *in-vivo* (** $p < 0.005$), further supporting our hypothesis that the number of *N*-linked glycosylation is not a major factor for improving FVIII expression.

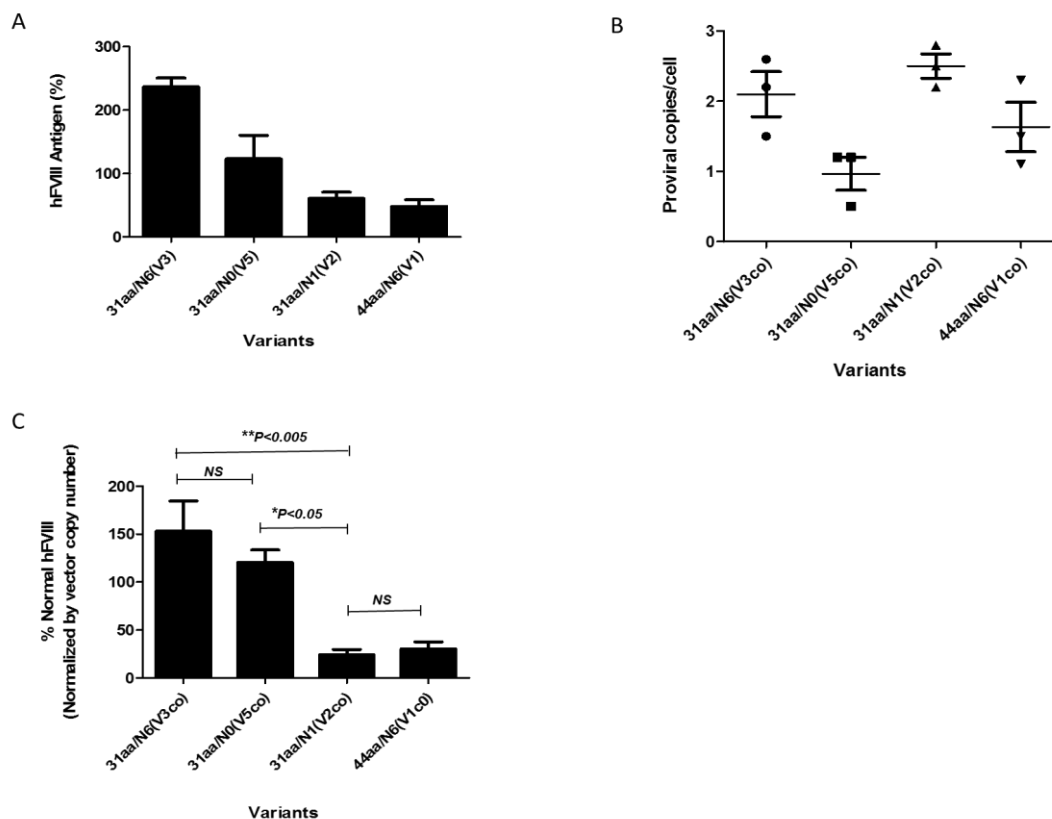


Figure 6.2. Evaluation of AAV FVIII variants *in-vivo*

A) Analysis of FVIII antigen expressions at four weeks after gene transfer, hFVIII expression determined by ELISA specific for hFVIII:Ag. B) Quantitative PCR was used to determine the number of viral genomes in transduced livers. A standard was prepared to consist of pAV2 HLP FVIII V3 plasmid linearized with single cutter restriction enzyme digestion and serial dilutions made between 1×10^8 to 1×10^3 for FVIII DNA standard curve. Mouse liver tissues genomic DNA was extracted and serial dilutions made from 500ng to 3.9ng for the standard curve for GAPDH housekeeping gene. Primers directed against the FVIII A2 domain were used to determine the number of viral genome copies of this domain per cell for all mice receiving rAAV-HLP FVIII variants. Mouse GAPDH primer designed and used to determine mouse liver GAPDH expression. C) Proviral copy number correction normalised antigen levels. Data presented as mean \pm SEM, $n \geq 3$. One-way ANOVA (Bonferroni simultaneous test), Prism 6.0 (Graph Pad).

6.2.3 Modification of V3 linker sequences according to size

Having demonstrated that either interruption (V1) or complete rearrangement (V2) of the linker sequence decreases FVIII levels in the mouse plasma, it may be inferred that the configuration of the amino acid sequence in the linker influences FVIII expression. To further understand how configuration of linker influences FVIII expression, we constructed additional variants, N0-N5. We took the original variant the V3 linker sequence which was built by adjoining six N-X-T/S sites and then juxtaposed to the remainder of the B-domain deleted amino acid sequences (SFSQ-PPVLKRHR). Systematic deletion according to the number of *N*-linked glycosylation motif was used to evaluate the influence of linker length and composition. These new linkers are shown in figure 6.3.A.

These new variants were packaged into AAV, pseudotyped with AAV8 capsid, purified and characterised (Fig.6.3.B.C). To determine the efficacy of these new variants, we injected a dose of 2.5×10^{11} vg/kg into the tail vein of male C57BL/6 mice with V3 linker deleted version of FVIII variants.

The human FVIII expression was determined by FVIII: Antigen assay, using human FVIII specific monoclonal antibodies was used for ELISA (Stago, UK). The level of FVIII expression from each of the variants was determined by ELISA and compared to V3. The assay results showed that the highest levels of FVIII:Ag (%) among the new variants were with construct N2 (174 ± 68) followed by N1 (126 ± 66), N3 (101 ± 47), N0 (82 ± 36), N4 (67 ± 61) and N5 (42 ± 22) respectively (Fig. 6.4.A).

The results demonstrate that the serial deletion of linker sequence (N series) showed relatively lower FVIII antigen (%) expression compared to V3co (237 ± 27). Interestingly, N5, in which NVS amino acid in the V3 linker sequence is deleted, showed the lowest FVIII expression (42 ± 22) suggesting the NVS motif has an important role for FVIII

expression. In contrast, further deletion between N4 to N2 showed recovery of FVIII expression. The result of N2 suggests that linker sequence conformation change between N2~N4 alters the FVIII expressions. Furthermore, N1 and N0 showed that the further deletion of amino acids from N2 decrease FVIII expression.

The proviral copies per liver cell of all variants showed relatively similar copy number from N0 (1.91 ± 0.3), N1 (1.86 ± 1.29), N2 (1.19 ± 0.22), and N5 (1.65 ± 1.48) respectively (Fig.6.3.B). In contrast, N3 (3.35 ± 2.74) and N4 (5.82 ± 5.6) showed relatively high copy number due to the one or two mice with high copy number of viral genomes transduced in the liver (Fig. 6.4.B).

We normalised FVIII expression between vectors according to proviral copy numbers. The normalised FVIII antigen(%) expression /transgene copy was N0 (43 ± 20), N1 (90 ± 65), N2 (142 ± 38), N3 (49 ± 37), N4 (14 ± 9), N5 (47 ± 35), V3 (140 ± 52) respectively (Fig. 6.4.C). The result showed that N4 is the lowest expressing construct after copy correction due to high proviral copies for this insert (** $P < 0.005$, significant compared to V3 and N2) (Fig.6.4.C). However, the trend of FVIII expression was not changed between N4~N2. Importantly, the FVIII expression level of N2 is similar with V3 suggesting that a shorter linker sequence derived from V3 can be achieved without comprising FVIII expression.

While this study is only preliminary, we show that the triplet deletion exhibited unique FVIII expression patterns. It is important to note that the natural c-terminal end of B-domain peptide “PPVLKRHQR” is preceded by a glycosylation triplet (NXT/S) motif. Here, we found that FVIII expression was dramatically altered when amino acid valine-serine (VS) motif is deleted from in front of PPVLKRHQR, as in variants N0, N1, N4 and N5. Therefore, we can propose that N2 shows similar activity with V3, despite four more deletions of glycosylation motifs, due to a structural conformation between VS (Valine-Serine) and PPVLKRHQR. This result may support the hypothesis that V5

exhibits similar activity with V3 through PPVLKRHQR although its *N*-linked glycosylation motifs are all disabled.

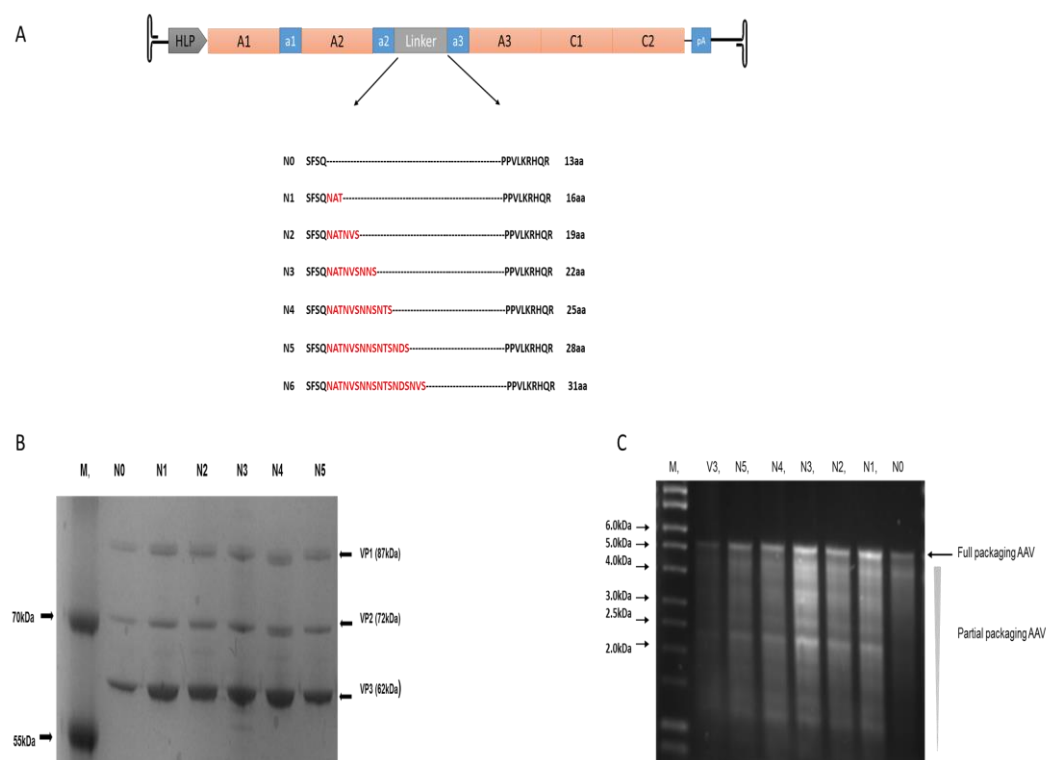


Figure 6.3. Characterisation of AAV particles harbouring FVIII V3 linker deletion variants

A) Schematic diagram of six AAV vector genomes encoding FVIII variants under the control of HLP promoter and synthetic polyadenylation sites. FVIII-N0; B-domain deleted 13aa linker, Gln744 fused Pro1641, None for *N*-linked glycosylation, FVIII-N1; 16aa linker but 3aa substitute, one *N*-linked glycosylation, FVIII-N2; 19aa linker 6aa substitute, two *N*-linked glycosylation, FVIII-N3: 21aa linker, 9aa substitute, potential three *N*-linked glycosylation, FVIII-N4: 24aa linker, 12aa substitute, potential four *N*-linked glycosylation, FVIII-N5: 27aa linker and original 31aa FVIII-V3.

B) Coomassie staining of purified AAV particles (N0:1x10¹² vg/mL, N1:5x10¹²vg/mL, N2: 4x10¹² vg/mL, N3:5x10¹²vg/mL, N4:5x10¹²vg/mL and N5:4x10¹² vg/mL) of three capsid viral proteins (VP)s were separated on 10% SDS-PAGE gel.

C) Alkaline gel analysis shows heavily fragmented or partial packaing AAV.

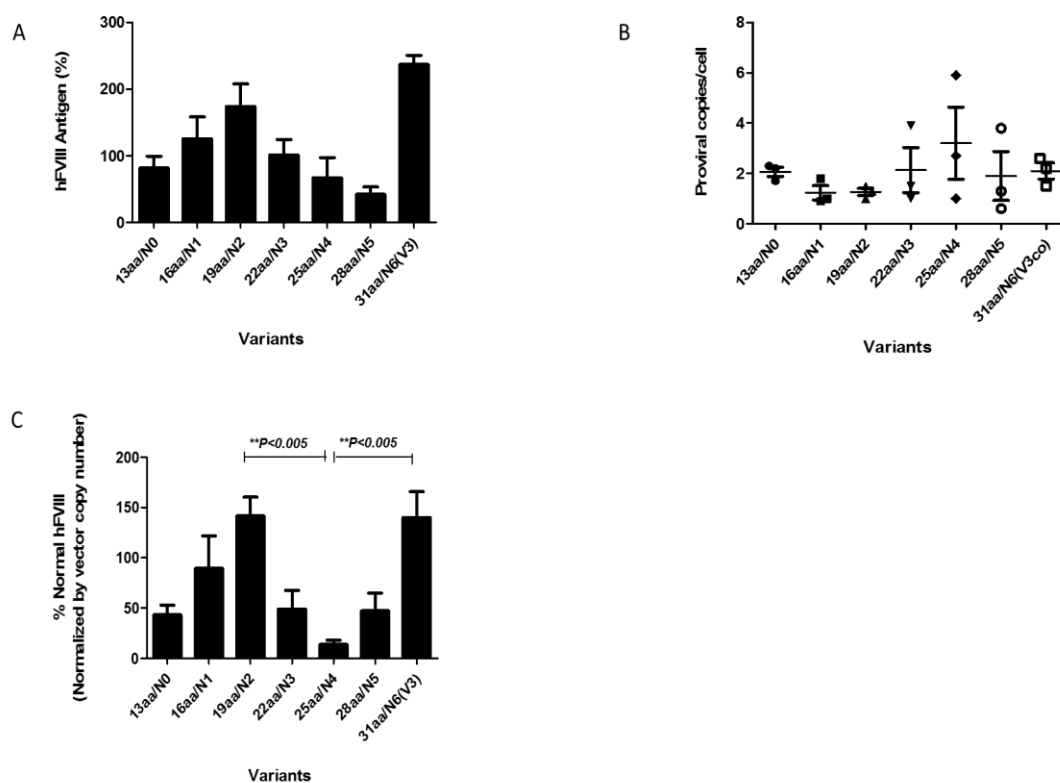


Figure 6.4. Evaluation of AAV hFVIII V3 linker deletion variants *in-vivo*

A) Analysis of FVIII antigen expressions from rAAV vectors produced from FVIII variants *in-vivo*. The FVIII antigen expression illustrated as mean of %FVIII levels \pm SEM.

B) Proviral copies/cell in the liver. A Q-PCR assay determined proviral copy number on murine liver samples collected four weeks after transduction with 2.5×10^{11} vg/kg of each vector depicted. Results are presented as mean proviral copies/cell \pm SEM.

C) Proviral copy number correction normalised antigen. Data presented as mean \pm SEM, (n \geq 3).

One-way ANOVA (Bonferroni simultaneous test), Prism 6.0 (Graph Pad).

6.2.4. Other modified FVIII constructs

To test the hypothesis that the NVS motif is key to the high level of FVIII expression, four additional modified linkers were generated by amino acid substitution.

The first variant N1 (SFSQNATPPVLKRHQR) of NAT substituted to NVS, which we named N1.5 (SFSQNVSPPVLKRHQR), while N2 (SFSQNATNVSPPVLKRHQR) changed NVS to NDS and is named N2.5 (SFSQNATNDSPPVLKRHQR).

As we demonstrated that the V1 expression was poor, although it has the same number of *N*-linked glycosylation motifs as V3. Moreover, the V2, which has scrambled linker sequence of V3, showed significantly low expression of FVIII, implying the constitution of linker sequence may alter the FVIII expression. Therefore, we replaced c-terminal linker VSS (V1) to VVS (V1.5) and ANT (V2) to AVS (V2.5) (Table 6.1).

Name	Linker peptides/ N-linked glycosylation	Peptide sequences	Design and description
V3	31aa/N6	SFSQ NAT VSNNSTNSDS NVS ----- PPVLKRHQR	Gln744 and Non-natural 3aa peptides NAT substitution in front of Pro1641., NAT is the first N-glycosylation peptide sequences in B-domain
N1	16aa/N1	SFSQ NAT ----- PPVLKRHQR	Gln744 and Non-natural 3aa peptides NAT substitution in front of Pro1641., NAT is the first N-glycosylation peptide sequences in B-domain
N1.5	16aa/N1	SFSQ NVS ----- PPVLKRHQR	N1: NAT-> NVS
N2	19aa/N2	SFSQ NATNVS ----- PPVLKRHQR	Gln744 and Non-natural 6aa peptides NATNVS substitution in front of Pro1641., NATNVS is the first and second N-glycosylation peptide sequences in B-domain
N2.5	19aa/N2	SFSQ NATNDS ----- PPVLKRHQR	N2: NATNVS->NAT NDS : N2 expression was higher than other substituted constructors, VS -> DS change amino acid makes any difference?
V2	31aa/N1	SFSQ NSDVS NVSNSTNSNS NANT ----- PPVLKRHQR	Gln744 and Non-natural 18aa peptide substitution in front of Pro1641., one of the V3 scrambled peptide sequences
V2.5	31aa/N1	SFSQ NSDVS NVSNSTNSNS NAVS ----- PPVLKRHQR	V2: ANT-> AVS : V3 and V5 variants both VS sequences in front of proline.
V1	44aa/N6	SFSQ NQFNATTIQNVSSNNSLSDNTSNNDSKNVSS PPVLKRHQR	Gln744 and Non-natural 31aa peptides substitution in front of Pro1641, the 31 amino acid was 226amino acid B-domain's rearranged due to the reduced transgene size
V1.5	44aa/N6	SFSQ NQFNATTIQNVSSNNSLSDNTSNNDSKNVVS PPVLKRHQR	V1: VSS-> VVS :V1 expression levels were poor both in vitro and in-vivo

Table 6.1. Additional modified FVIII constructs cloned into single stranded AAV backbone

Variants of V3 linker sequences, N1.5, N2.5, V2.5 and V1.5 were designed and cloned into AAV vectors using Q5 site direct mutagenesis kit.

The table describes their designated names and a description of the structure of each gene. To test the efficacy of newly designed FVIII variants *in-vivo*, AAV vectors were prepared and injected into C57BL/6 mice as previously described.

The *in-vivo* plasma FVIII:Ag (%) expressions were N1 (125±65), N1.5 (185±95), N2 (173±68), N2.5 (448±336), V2 (60±18), V2.5 (24±1.1), V1 (48±18), and V2.5 (25±3) respectively. N2.5 dramatically increased FVIII:Ag expression compared with other versions (Fig. 6.5.A). These results may suggest that the substitution on N2.5 may enhance FVIII expression.

The proviral copies were determined by quantitative-PCR, which demonstrated that similar copy numbers were delivered to treated cohorts; N1 (1.86±1.29), N1.5 (1.58±0.41), N2 (1.19±0.22), N2.5 (1.45±0.94), V2 (2.5±0.26), V2.5 (0.89±0.38), V1 (1.63±0.60), and V2.5 (0.56±0.05) respectively (Fig. 6.5. B).

The normalised FVIII antigen(%) expression, which shows that N1 (89±64), N1.5 (109±34), N2 (141±37), N2.5 (297±115), V2 (24±9.5), V2.5 (32±14), V1 (30±12.8), and V2.5 (43±4) respectively (Fig.6.5.C). Statistical analysis performed by using Mann Whitney showed that N2.5 (a 2.5-fold increase of FVIII expression), as opposed to N2, was not significant (ns). The data from this study does not suggest that VS (Valine-Serine) peptide sequences in front of PPVLKRHQR are important in the enhanced expression with the FVIII constructor. The exact mechanism behind the linker improvements remains unclear, and further analysis is required.

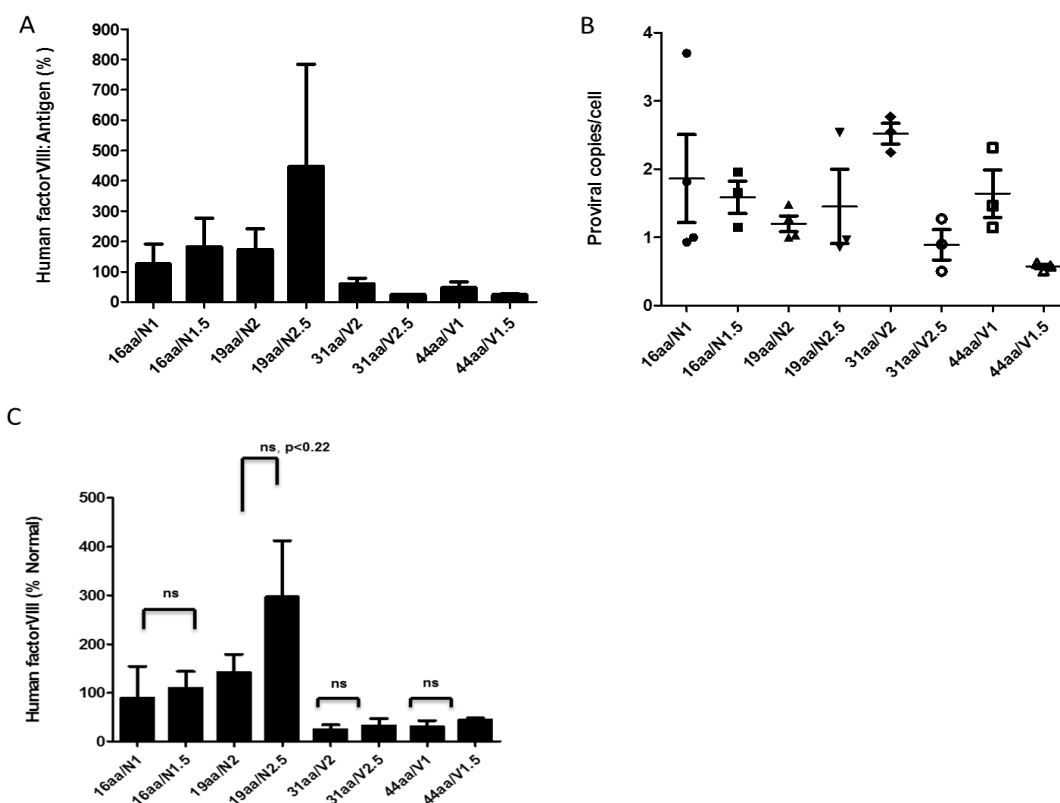


Figure 6.5. V-S to D-S modification of N2 (N2.5) increased FVIII expression

A) FVIII:Ag expression in mouse plasma. B) Proviral copy number in mouse liver cell.

C) Normalised FVIII:Ag with proviral copies. Data presented as mean \pm SEM, ($n \geq 3$), Mann Whitney test, ns: not significant. Prism 6.0 (Graph Pad).

6.3. Discussion

FVIII consists of a large portion of B-domain which has no functional role in the coagulation process. Currently, the well established B-domain modified version of FVIII is SQ, containing a 14 amino acid linker between the a2 and a3 domains are commercially available as ReFacto® (Pfizer). The B-domain deleted version of “SQ” has been tested *in-vivo* using lentiviral vectors (Ward *et al.*, 2011; Spencer *et al.*, 2015). This construct has been also utilised in AAV vectors where capability was tested for a long-term therapeutic effect in haemophilia A (McIntosh *et al.*, 2013). The *in-vitro* expression of B-domain modified versions of FVIII SQ, V1, V3 and V5 have been investigated.

In this chapter, we investigated the expression of V1, V2, V3 and V5 constructs *in-vivo* using AAV gene transfer. Based on FVIII expression in plasma, we did not observe a significant difference in potency between constructs containing linker V3 and V5 (ns). However scrambled V3 sequence in the V2 variant, decreased FVIII expression approximate 7-fold (**p<0.005).

To further understand and optimise the linker sequence, we developed ten other variants with various deletions and substitutions. The best performers were N2 and N2.5. These results are in line with previous report Srour *et al.* (Srour *et al.*, 2008).

In this report, three additional consensus *N*-linked glycosylation sites in the FVIII-BDD were created by inserting the 14 amino acid sequence (ADNSSTMLSLSNGS), resulting in FVIII-BDD-G3. The Asn(N) mutated to Gln(Q) of FVIII-BDD-G3, leading to FVIII-BDD-G0. The FVIII expression levels showed no significant difference between the expression of G3 and G0 constructs (Srour *et al.*, 2008). This result supports our findings that the glycosylation deleted version V5 was not significantly different compared with V3 regarding FVIII expression.

In contrast, Miao et al., performed a similar study where the FVIII linker sequence version FVIII-N6 (266aa/N6) had Asn(N) mutated to Gln(Q) at the consensus site for *N*-linked glycosylation. This constructs fully devoid of *N*-linked oligosaccharides within the partial B-domain fragments and was named as FVIII-266aa/N1. The FVIII-266aa/N1 construct showed significantly lower FVIII expression than 266/N6 in COS-1 cells (Miao et al., 2004). Additional studies have shown the deglycosylation of wild-type FVIII by endoglycosidases resulted in substantial loss of activity (by about 32%) compared to glycosylated FVIII (Kosloski et al., 2009). These result may suggest that the glycosylation of total protein may change the total FVIII expression, but partially modified glycosylation on the B-domain or a linker is not influential.

Here we confirm that glycosylation of the linker sequence in our original FVIII variant, V3 is not a key factor in it's improved expresssion profile.

To further understand the linker modifications that affect expression we studied a series of linker variants. Our next question for a modifier of the FVIII-V3 is confirmation change by deletion of the linker sequence. The deletion of V3 linker study shows glycosylation of the linker sequence is not an important factor, but conformation change may be the key for the Improved expresssion profie.

We showed lowest FVIII expressions from N4 suggesting structural confirmation influences efficiency of FVIII expression (Fig. 6.4). Furthermore, the FVIII expression from N2 was similar to V3 implying that V3 linker sequence can be shortened without affecting FVIII protein expression. Our data is similar to Kolind et al., where vectors containing a serial deletion of wild-type B-domain of FVIII demonstrated the shortest B-domain of 21aa, without *N*-linked glycosylation motif was the most efficiently expressed FVIII (Kolind et al., 2010). Our preliminary data with 19aa linker variant N2 and N2.5 suggest smaller linkers can be used without sacrificing expression level.

Overall, I conclude that *N*-linked glycosylation of V3 linker is not the main determinant of FVIII expression, but the conformation change of the linker imposes the key for the cryptic effect of B-domain linker sequences of V3 on expression efficiency of FVIII.

Chapter 7

General Discussion and Future Directions

Discussion and Future Directions

Haemophilia A therapy has been reliant on plasma derived or recombinant protein products, which are widely used for prophylaxis and treatment in clinical practice. One of the major complications seen in the past was the transmission of blood born viruses. Another serious complication of replacement therapy is inhibitor development. Also, the lack of stability of the FVIII protein in the circulation means that frequent infusions must be given to prevent or treat bleeding. Since recombinant FVIII replacement therapy has been applied to patients, the first of those problems was eliminated from the management of haemophilia (Boedeker, 1992). However, the potential immunogenicity of recombinant FVIII proteins, which generate inhibitor antibodies against FVIII in blood appears to be increased over the plasma-derived products while the stability of recombinant proteins *in-vivo* is similar to that of plasma-derived concentrates (Schwartz *et al.*, 1990; Bray *et al.*, 1994). Therefore, the further biological characterisation and understanding of FVIII products are required.

The main focus of this thesis was the development of stable cell lines for the production, purification and biological characterisation of novel FVIII variants. In addition, preliminary studies incorporating these variants in an AAV gene therapy vector was undertaken.

Previous work within our group developed novel FVIII proteins, in which the B-domain is substituted with potential *N*-linked glycosylation motifs in linker sequences (McIntosh *et al.*, 2013). McIntosh *et al.* demonstrated that codon optimisation of FVIII containing a 266 amino acid B-domain linker under the hybrid liver-specific promoter (HLP) exhibited 10-fold higher FVIII expression levels in mice compared with non-codon optimised variants (McIntosh *et al.*, 2013). Further improvement was achieved by replacing the 266 amino acid N6 spacer with the 31 amino acid peptide (V3co), in which the six-*N*-linked glycosylation motifs from N6 were re-arranged in immediate

proximity to make the shortest possible linker still containing the motifs. As a result, V3co shows not only increased potency up to 2-fold but also achieved more efficiently packaged AAV virions. Importantly, FVIII levels were continuously expressed from *F8* knockout mice following administration of V3co vector. This thesis set out to perform an in-depth exploration to dissect the improved expression of V3co, using various gene delivery or engineering methods.

To study novel FVIII variants, the generation of FVIII stable cell lines was required. Utilising a lentiviral gene transfer system we established stable integration of the FVIII variants in HEK-293T cells, initially as polyclonal populations before refinement to the generation of single clone homogenous stable cell lines. Our results are in agreement with Oberbek et al., who reported the use of lentivirus for the generation of stable cell lines in CHO cells. They reported the stable expression of transgene over three months in serum-free conditions (Oberbek *et al.*, 2011). In the current study, we performed a preliminary test for FVIII variants expressing lentivirus with different MOIs. As a result, we found that an MOI of 10 exhibited the best concentrations for transduction into HEK-293T cell lines.

The initial cell lines were a mixed population of clones, due to the random lentiviral integration of FVIII, which resulted in variation in FVIII expression levels. Subsequently, using a selection process of serial dilutions in 96-well plates, we achieved single clonal cell cultures, which showed uniform growth conditions and protein expression. A benefit of having established single clone is the possibility of tighter quality control. Unlike Oberbek's methods, FACS cannot be applied to our approach because our FVIII does not contain green fluorescent protein (GFP) therefore the selection process had to be performed by serial dilution on 96-well plates, which was time-consuming.

The McIntosh report found that the codon optimised V3 exhibited greater expression among the B-domain modified variants. This suggested that the six *N*-linked

glycosylation motifs may have a critical role for the expression. This conclusion was further supported by our finding that elimination of *N*-linked glycosylation motif by mutating amino acid Asparagine (*N*) to Alanine (*A*) in the modified version variant V5co decreased by approximately 40% FVIII antigen expression as compared to V3co *in-vitro* (Fig.3.15). This result corresponds to a 2-fold change of mRNA expression level between V3co and V5co (Fig.3.13). Although the mechanism for this increased transcription or different secretion levels was not further investigated, it is possible that BiP interaction with the B-domain may be involved (Pittman *et al.*, 1994). Furthermore, Kaufman *et al.* showed by immuno-precipitation that most FVIII is bound with 78kDa BiP and 80% of FVIII in the rough ER is associated with BiP, which prevents FVIII secretions (Kaufman *et al.*, 1988). The glycosylation state and association with BiP could be correlated with secretion efficiency, unglycosylated protein and BiP association increased stability and retention in the ER, thus blocking efficient secretion (Dorner *et al.*, 1987). However, we can argue that the FVIII activity (Fig.3.14) was not significantly changed between V3co and V5co, suggesting potential *N*-linked glycosylation does not influence biological activity on the B-domain linker.

In relation to the *N*-linked glycosylation of the B-domain, the biology of FVIII secretion from the cell system is a core mechanism for FVIII production. *N*-linked glycosylation of V3co may have improved ER to Golgi trafficking through the high mannose oligosaccharides which bind within the ER to a cargo protein-LMAN1 (Moussalli *et al.*, 1999; Cunningham *et al.*, 2003; Miao *et al.*, 2004). Our study in Figure 3.16 demonstrates that the codon optimised V3 co-localised with ER/Golgi and the ER-Golgi trafficking inhibitor BFA lead to accumulation of FVIII in the Golgi compartment. However, the pattern of accumulation in the ER/Golgi was similar between variants, which prevents us from ruling this out as a cause of the discrepancy in expression.

Therefore, further experiments are required to understand the exact mechanisms for the differences in FVIII expression.

Since FVIII is a secreted protein, it is a requirement that FVIII containing vesicles are fused to the plasma membrane in the course of release from cells (Fig.1.5). Kolind et al., reported that 90% of recombinant FVIII is bound to cell membrane when the FVIII contained a short B-domain (21 amino acid), suggesting the size of B-domain is inversely correlated with FVIII attachment to the membrane (Kolind et al., 2010). They also showed that *N*-linked glycosylation within the B-domain has no influence on either total expression level or membrane attached FVIII. In contrast, we showed that the FVIII-V5co (31 amino acid) exhibited 2.4-fold increased membrane bound FVIII under the serum-free condition as opposed to V3co (31 amino acid), suggesting that lack of *N*-linked glycosylation on the V5co B-domain linker leads to accumulation of FVIII on the membrane surface of the HEK-293T cells (Fig.3.16). Although we demonstrate contradictory result to Kolind et al., *N*-linked glycosylation of amino acids juxtaposed in V3co may be structurally different from Kolind's short 21 amino acid B-domain linker. Therefore, we conclude that *N*-linked glycosylation difference between V3co and V5co has an effect on membrane binding, at least in our FVIII-V3co system.

Taken together, B-domain modified short linker version of FVIII, V3co has been confirmed as the best expressing FVIII protein among the variants. FVIII V3co was expressed at approximately 2.5-fold greater levels in HEK-293T cells compared with FVIII SQco, 30% more antigen detected than for FVIII V5co and these observations were made using both cell lines and gene transfer methodologies. The increased expression resulted from increased levels of FVIII V3co mRNA and increased secretion efficiency.

To purify a large amount of recombinant FVIII, I have developed an optimised purification procedure, which allowed me to concentrate FVIII up to 100ug in total for further PTM characterisation.

Thrombin activation of the protein by proteolytic cleavage was characterised. We showed that the thrombin cleavage pattern of FVIII-V3co corresponds exactly with wild-type FVIII (Fig.4.21 and Fig. 4.22), implying FVIII-V3co is biologically active.

Regarding the stability of FVIII, vWF protein is the most identified determinant of FVIII survival in blood, as it provides protection from premature clearance or activation of FVIII and vWF deficiency leads to a secondary deficiency of FVIII (Bendetowicz *et al.*, 1998; Lenting *et al.*, 2007). Our vWF and FVIII binding affinity assay demonstrated that the marked difference in expression between FVIII variant constructs has nothing to do with affinity to vWF (Fig.4.27) suggesting the B-domain region modified FVIII variants are not interfering with vWF and their biological function.

In this study, the biochemical properties of FVIII were characterised by using MS (MALDI-TOF) and MS/MS (MALDI-TOF/TOF) technology. For the production of FVIII, cell culture and purification conditions were optimised for all variant cell lines to test the differences between the five variants (SQco, V5co, V3co, V1co and N6co). Then, all five variants were analysed for *N*-glycans, and the results exhibit unique patterns that can separate into two groups depending on *N*-linked glycosylation motifs in their respective linkers. The result from SQco and V5co variants showed a relatively low glycosylation rate as opposed to the V1co, V3co and N6co, where a high number of glycan structures were observed. Importantly, the most highly glycosylated FVIII variant was V3co, which is in agreement with our initial hypothesis that V3co harbours potential *N*-linked glycosylation sites. In terms of PTM, the enrichment of high-mannose structures was similarly exhibited in all five variants. V3co, V1co and N6co also demonstrated higher levels of core-fucosylated glycans than the SQco and V5co

group. In contrast, sialylated glycan levels were observed in one-third of their total glycan profiles and were relatively similar among variants.

In this respect, the sialic acid residues on the *N*-glycans are important because of protection from being recognised by the asialoglycoprotein receptor in the liver, which affects the circulation half-life of glycoproteins in the blood (Zhang *et al.*, 2010). In this study all FVIII variants exhibit similar levels of sialylated glycan, implying that slight difference between the variants may not influence FVIII half-life significantly.

The mass spectrometry data showed the terminal structure of recombinant FVIII, including complex-, hybrid- and high mannose-type glycosylation, are present at the same sites as in native human plasma-derived FVIII (Kannicht *et al.*, 2013). Our data show the prominent epitopes Lewis x/a, LacdiNAc, and Fuc-LacdiNAc antigen were detected in various *N*-glycans in the FVIII variants (Fig.5.6). The presence of Fuc-LacdiNAc in all five variants, including recombinant human FVIII (Nuwiq®, Octapharma), is possibly attributable to the expression cell line HEK-293T cells which are derived from a kidney cell line and might affect the biological properties of the protein, as this epitope was not found in the native plasma-derived FVIII protein. Regarding immunogenicity, antigenic carbohydrate epitopes Neu5Gc and α -Gal are detected in FVIII that is produced in non-human cell lines. For example, the Gal α -1.3 Gal epitopes were detected in FVIII produced in BHK (Kogenate®, Baxter). However, Nuwiq® (Octapharma) derived from human cell line HEK-293T does not contain either antigenic carbohydrate epitope (Kannicht *et al.*, 2013). This is consistent with our FVIII variant results in fig. 5.6. Overall we discovered that the *N*-linked glycosylation profile of FVIII-V3 is almost identical to the human cell line derived commercial rFVIII (Nuwiq®) and plasma-derived FVIII. As mentioned above, glycan structures were identified based on the compositional analysis (MALDI-TOF), fragmentation analyses

(MALDI-TOF/TOF) and knowledge upon glycan biosynthesis. Additional assays, such as linkage analysis and galactosyl-transferase assay could be performed to increase the depth of the current structural analysis. Moreover, targeted glycoproteomic techniques could be used to further explore the distribution of the identified *N*-glycan in each of the *N*-linked glycosylation sites, possibly elucidating their biological significance upon FVIII function.

X-ray crystal structure analysis of FVIII is necessary to obtain high-resolution structural information, which triangulates the linker structure and *N*-glycosylation pattern of B-domain. For example, the tertiary structure of B-domain deleted FVIII permits unambiguous modelling of the relative orientations of the five domains of rFVIII (Ngo *et al.*, 2008; Shen *et al.*, 2008). Overall crystal structures give much information to better understand the FVIII tertiary structure and domain organisation. However, due to the time required for producing a large amount of recombinant protein and subsequent crystallography methods, this approach was not feasible in the current study.

The final section of this thesis focused on AAV gene transfer of the novel FVIII variants *in-vivo*. While AAV gene therapy is showing exceptional promise for a range of genetic disease a major obstacle for its use in haemophilia A is the limited packaging capacity of this vector. The packaging limit of rAAV is about 4.7kb, whereas FVIII cDNA has a size of 7kb. To overcome this, several novel AAV vector technologies have been developed to increase the genome capacity for AAV or enhance gene expression using trans-splicing or hybrid vectors (Yan *et al.*, 2000; Trapani *et al.*, 2014). Although this system allows for the incorporation of transgenes, which exceed the packaging limitation of AAV, the gene transfer efficiency was lower than conventional AAV vector system (Daya and Berns, 2008). The ability to achieve functional gene transfer with

large genomes in AAV has been shown, with the mechanism of expression being partially packaged sequences complementary to each other to restore a full expression cassette (Hirsch *et al.*, 2010). The two potential pathways of large gene reconstruction from the partially packaged AAV vectors is recombination at overlapping homologous genome sequences and direct annealing of opposite polarity partial large-transgene fragments because the ITRs are thought to stimulate intermolecular recombination and non-homologous end joining (Wu *et al.*, 2010). However, neither relying on transgene recombination or trans-splicing is ideal. Therefore ways to reduce genome size is required. Previously, we have demonstrated the reconstitution of partially packaged AAV-FVIII-V3co by using southern blot which clearly exhibited the fully assembled 5.2kb bands (McIntosh *et al.*, 2013), suggesting more efficient large gene delivery is available with an AAV system. McIntosh *et al.*, exhibit significant enhancement of FVIII gene transfer through successful downsized FVIII V3co, which allows AAV delivery *in-vivo* to target liver and administration of AAV-FVIII V3co to *F8* knockout mice and non-human primates, demonstrating constant production of FVIII (McIntosh *et al.*, 2013). However, the role of V3 B-domain linker sequence for enhancement of FVIII expression was not investigated.

In this study, we further explored the mechanism by which modification of length or conformation change of V3 B-domain linker influences expression *in-vivo* using AAV gene transfer. According to *in-vitro* FVIII variants study, disabling *N*-linked glycosylation sites (V5) does not inhibit FVIII production suggesting the linker amino acids themselves have an effect on FVIII production other than glycosylation. AAV administration of V5 to mouse tail vein also showed that the *N*-linked glycosylation profile did not affect FVIII expression. Therefore, the high FVIII expression from AAV-FVIII-V3 may due to the conformational change of B-domain of FVIII. We showed here that this hypothesis is supported by developing a variety of linker deletion mutants.

The deletion of the V3 linker in the N0-N5 series showed that the number of deletions fluctuates the FVIII expression levels. Indeed, AAV-FVIII-N2 (19 amino acids), has a shorter linker than AAV-FVIII-V3co (31 amino acid), but their FVIII expression is similar. We conclude that it is a conformation change of B-domain linker polypeptide influenced by linker length and composition that dramatically affects the FVIII expressions.

While AAV mediated gene therapy has shown promise for the treatment of haemophilia B, clinical trials targeting FVIII deficiency are limited. However, BioMarin Pharmaceutical (BMN 270), who licenced the UCL technology described by McIntosh et al (McIntosh *et al.*, 2013) announced preliminary data that no serious adverse events were observed when an AAV vector encoding the UCL codon optimised BDD FVIII pseudotyped with AAV5 capsid was administered into patients with severe haemophilia A. Steady state FVIII expressions at therapeutic levels (range 12-150%) was observed in the 7 patients recruited to the high dose level (6×10^{13} vg/kg) over a period of 34 to 50 weeks (<https://www.hemophilia.org/Newsroom/Industry-News/BioMarin-s-Hemophilia-A-Gene-Therapy-Trial-Demonstrates-Increased-FVIII-Levels>). BDD-FVIII-SQ version was used for this trial although FVIII-V3 expression is at least 2-fold higher because of the established safety profile of BDD-FVIII protein concentrates in the clinic over the past 16 years. In terms of establishing AAV gene therapy as a routine treatment option for haemophilia A, there are many hurdles to overcome. However, our studies contribute to providing fundamental data for the safety of future gene therapy for newly engineered FVIII variants.

To conclude, I have critically evaluated the role of V3 B-domain linker in the context of human FVIII expression in cellular models and AAV gene transfer *in-vivo*. In all cases, the FVIII-V3 variant performed better than the B-domain deleted FVIII (SQ).

The basic mechanism behind V3 B-domain linker was evaluated by analysing hFVIII mRNA levels following gene transfer. Our results are indicative of improved transduction of liver cells and enhanced transcription levels and/or improved mRNA stability. The expression of FVIII-V3 was improved compared to other variants both *in-vitro* and *in-vivo*. The biological activity of the purified recombinant FVIII V3 variant was the same as control (full-length FVIII and commercial BDD FVIII), assessed by thrombin generation, and vWF/FVIII binding affinity assay. Although mutations within the *N*-linked glycosylation sites in V5 decrease the number of *N*-glycans, V5 did not significantly change the FVIII expression. These results suggest the enhanced FVIII expression by the V3 linker is not due to the *N*-linked glycosylation motifs. In addition, deletion series of the V3 linker showed that a shorter form FVIII-N2 exhibited similar FVIII expression as FVIII-V3. Thus, B-domain linkers enable higher levels of expression possibly through a conformational change, but this requires further studies. Whilst the precise mechanism remains unclear, future therapy for haemophilia A will utilise a variety of new methods to improve efficacy and safety. The mechanistic insights into the role of V3 described in this thesis will help advance the field in this regard. In particular, our observation that smaller peptides in FVIII-N2 and -N2.5 may also be suitable for effective AAV-mediated gene transfer for haemophilia A. Therefore, the results presented here suggest that FVIII V3co and variants may be efficacious for replacement therapy and/or gene therapy for haemophilia A. This thesis has utilised many of different approaches to understanding the role of FVIII B-domain and how this could be used for future bioengineering of FVIII.

References:

- Abdalla, S.E., and Adam, H.T. (2013). Coagulation Profile (PT, APTT, fibrinogen level and platelets count) in Sudanese patients with acute pancreatitis. *Merit Res J Microbiology* 2(1), 1-4.
- Ahmadian, H., Hansen, E.B., Faber, J.H., Sejergaard, L., Karlsson, J., Bolt, G., Hansen, J.J., and Thim, L. (2016). Molecular design and downstream processing of turoctocog alfa (NovoEight), a B-domain truncated factor VIII molecule. *Blood Coagul. Fibrinolysis* 27(5), 568-575.
- Allocca, M., Doria, M., Petrillo, M., Colella, P., Garcia-Hoyos, M., Gibbs, D., Kim, S.R., Maguire, A., Rex, T.S., Di Vicino, U., et al. (2008). Serotype-dependent packaging of large genes in adeno-associated viral vectors results in effective gene delivery in mice. *The Journal of Clinical Investigation* 118, 1955–1964.
- Ashkenas, J., and Byers, P.H. (1997). The final stage of gene expression: chaperones and the regulation of protein fate. *American Journal of Human Genetics* 61, 267–272.
- Ayuso, E., Mingozzi, F., Montane, J., Leon, X., Anguela, X.M., Haurigot, V., Edmonson, S.A., Africa, L., Zhou, S., High, K.A., et al. (2009). High AAV vector purity results in serotype- and tissue-independent enhancement of transduction efficiency. *Gene Therapy* 17, 503–510.
- Baines, A.C., and Zhang, B. (2007). Receptor-mediated protein transport in the early secretory pathway. *Trends in Biochemical Sciences* 32, 381–388.
- Barr, P.J. (1991). Mammalian subtilisins: the long-sought dibasic processing endoproteases. *Cell* 66, 1–3.
- Barrow, R.T., Healey, J.F., and Lollar, P. (1994). Inhibition by heparin of thrombin-catalyzed activation of the factor VIII-von Willebrand factor complex. *J. Biol. Chem.* 269, 593–598.
- Barrowcliffe, T.W., Raut, S., and Hubbard, A.R. (1998). Discrepancies in potency assessment of recombinant FVIII concentrates. *Haemophilia* 4, 634–640.
- Barrowcliffe, T.W., Raut, S., Sands, D., and Hubbard, A.R. (2002). Coagulation and chromogenic assays of factor VIII activity: general aspects, standardization, and recommendations. *Semin. Thromb. Hemostasis* 28, 247–256.
- Bendetowicz, A.V., Morris, J.A., Wise, R.J., Gilbert, G.E., and Kaufman, R.J. (1998). Binding of Factor VIII to von Willebrand Factor Is Enabled by Cleavage of the von Willebrand

Factor Propeptide and Enhanced by Formation of Disulfide-Linked Multimers. *Blood* 92, 529–538.

Becker, S., Simpson, J.C., Pepperkok, R., Heinz, S., Herder, C., Grez, M., Seifried, E., and Tonn, T. (2004). Confocal microscopy analysis of native, full length and B-domain deleted coagulation factor VIII trafficking in mammalian cells. *Thromb. Haemostasis* 92, 23–35.

Berns, K.I. (1990). Parvovirus replication. *Microbiological Reviews* 54(3), 316–329.

Bihoreau, N., Pin, S., Kersabiec, A.M., Vidot, F., and Fontaine Aupart, M.P. (1994). Copper-atom identification in the active and inactive forms of plasma-derived FVIII and recombinant FVIII-ΔII. *The FEBS Journal* 222, 41–48.

Blesch, A. (2004). Lentiviral and MLV based retroviral vectors for ex vivo and in vivo gene transfer. *Methods* 33, 164–172.

Boedeker, B.G. (1992). The manufacturing of the recombinant factor VIII, Kogenate. *Transfus Med Review* 6, 256–260.

Bolton-Maggs, P., and Pasi, K.J. (2003). Haemophilias a and b. *The Lancet* 361 (9371), 1801–1809.

Bovenschen, N., Rijken, D.C., Havekes, L.M., Vlijmen, B.J.M., and Mertens, K. (2005a). The B domain of coagulation factor VIII interacts with the asialoglycoprotein receptor. *Journal of Thrombosis and Haemostasis* 3, 1257–1265.

Bovenschen, N., Mertens, K., Hu, L., Havekes, L.M., and van Vlijmen, B.J.M. (2005b). LDL receptor cooperates with LDL receptor-related protein in regulating plasma levels of coagulation factor VIII in vivo. *Blood* 106, 906–912.

Böhm, E., Seyfried, B.K., Dockal, M., Graninger, M., Hasslacher, M., Neurath, M., Konetschny, C., Matthiessen, P., Mitterer, A., and Scheiflinger, F. (2015). Differences in N-glycosylation of recombinant human coagulation factor VII derived from BHK, CHO, and HEK293 cells. *BMC Biotechnology* 15, 87.

Boël, G., Letso, R., Neely, H., Price, W.N., Wong, K.-H., Su, M., Luff, J.D., Valecha, M., Everett, J.K., Acton, T.B., et al. (2016). Codon influence on protein expression in *E. coli* correlates with mRNA levels. *Nature* 529, 358–363.

Bray, G.L., Gomperts, E.D., Courter, S., Gruppo, R., Gordon, E.M., Manco-Johnson, M., Shapiro, A., Scheibel, E., White, G.3., and Lee, M. (1994). A multicenter study of

recombinant factor VIII (recombinate): safety, efficacy, and inhibitor risk in previously untreated patients with hemophilia A. The Recombinate Study Group. *Blood* 83, 2428–2435.

Brooks, S.A. (2004). Appropriate Glycosylation of Recombinant Proteins for Human Use: Implications of Choice of Expression System. *Mb* 28, 241–256.

Brown, H.C., Gangadharan, B., and Doering, C.B. (2011). Enhanced biosynthesis of coagulation factor VIII through diminished engagement of the unfolded protein response. *Journal of Biological Chemistry* 286, 24451–24457.

Brown, H.C., Wright, J.F., Zhou, S., Lytle, A.M., Shields, J.E., Spencer, H.T., and Doering, C.B. (2014). Bioengineered coagulation factor VIII enables long-term correction of murine hemophilia A following liver-directed adeno-associated viral vector delivery. *Mol Ther Methods Clin Dev* 1, 14036.

Buller, R.M.L., Janik, J.E., Sebring, E.D., and Rose, J.A. (1981). Herpes Simplex Virus Types 1 and 2 Completely Help Adenovirus-Associated Virus Replication. *Journal of Virology* 40, 241–247

Bushman, F., Lewinski, M., Ciuffi, A., Barr, S., Leipzig, J., Hannenhalli, S., and Hoffmann, C. (2005). Genome-wide analysis of retroviral DNA integration. *Nat. Rev. Microbiology* 3, 848–858.

Butler, M. (2005). Animal cell cultures: recent achievements and perspectives in the production of biopharmaceuticals. *Appl. Microbiol. Biotechnology* 68, 283–291.

Calcedo, R., Morizono, H., Wang, L., McCarter, R., He, J., Jones, D., Batshaw, M.L., and Wilson, J.M. (2011). Adeno-Associated Virus Antibody Profiles in Newborns, Children, and Adolescents. *Clinical and Vaccine Immunology* 18, 1586–1588.

Cannarozzi, G., Cannarozzi, G., Schraudolph, N.N., Faty, M., Rohr, von, P., Friberg, M.T., Roth, A.C., Gonnet, P., Gonnet, G., and Barral, Y. (2010). A role for codon order in translation dynamics. *Cell* 141, 355–367.

Casademunt, E., Martinelle, K., Jernberg, M., Winge, S., Tiemeyer, M., Biesert, L., Knaub, S., Walter, O., and Schröder, C. (2012). The first recombinant human coagulation factor VIII of human origin: human cell line and manufacturing characteristics. *Eur J Haematology* 89, 165–176.

Casonato, A., Pontara, E., Zerbinati, P., Zucchetto, A., and Girolami, A. (1998). The evaluation of factor VIII binding activity of von Willebrand factor by means of an ELISA

method: significance and practical implications. *Am. J. Clin. Pathology* 109, 347–352.

Chao, H., and Walsh, C.E. (2001). Induction of tolerance to human factor VIII in mice. *Blood* 97, 3311–3312.

Chao, H., Mao, L., Bruce, A.T., and Walsh, C.E. (2000). Sustained expression of human factor VIII in mice using a parvovirus-based vector. *Blood* 95, 1594–1599.

Coster, H.G.L., and Chilcott, T.C. (2002). Electric field effects in proteins in membranes. *Bioelectrochemistry* 56, 141–146.

Croset, A., Delafosse, L., Gaudry, J.-P., Arod, C., Glez, L., Losberger, C., Begue, D., Krstanovic, A., Robert, F., Vilbois, F., et al. (2012). Differences in the glycosylation of recombinant proteins expressed in HEK and CHO cells. *J. Biotechnology* 161, 336–348.

Cunningham, M.A., Pipe, S.W., Zhang, B., Hauri, H.-P., Ginsburg, D., and Kaufman, R.J. (2003). LMAN1 is a molecular chaperone for the secretion of coagulation factor VIII. *J. Thromb. Haemostasis* 1, 2360–2367.

Dasgupta, S., Navarrete, AM., Bayry, J., Delignat, S., Wootla, B., André, S., Christophe, O., Nascimbeni, M., Jacquemin, M., Martinez-Pomares, L., Teunis B. Geijtenbeek, H., Moris, A., Saint-Remy, JM., Kazatchkine, MD., Kaveri, SV., and Lacroix-Desmazes, S. (2007). A role for exposed mannose in presentation of human therapeutic self-proteins to CD4+ T lymphocytes. *Proceedings of the National Academy of Sciences* 104(21), 8965–8970.

Davie, E.W., and Ratnoff, O.D. (1964). Waterfall Sequence for Intrinsic Blood Clotting. *Science* 145, 1310–1312.

Daya, S., and Berns, K.I. (2008). Gene Therapy Using Adeno-Associated Virus Vectors. *Clinical Microbiology Reviews* 21, 583–593.

Deribe, Y.L., Pawson, T., and Dikic, I. (2010). Post-translational modifications in signal integration. *Nature Structural & Molecular Biology* 17, 666–672.

Diaz, S.L., Padler-Karavani, V., and Ghaderi, D. (2009). Sensitive and Specific Detection of the Non-Human Sialic Acid N-Glycolylneuraminic Acid in Human Tissues and Biotherapeutic Products. *PLoS One* 4(1), e4241

Dorner, A.J., Bole, D.G., and Kaufman, R.J. (1987). The relationship of N-linked glycosylation and heavy chain-binding protein association with the secretion of

glycoproteins. *The Journal of Cell Biology* 105, 2665–2674.

Drickamer, K. (1996). Selective Sugar Binding to the Carbohydrate Recognition Domains of the Rat Hepatic and Macrophage Asialoglycoprotein Receptors. *Journal of Biological Chemistry* 271, 6686–6693.

Dull, T., Zufferey, R., Kelly, M., Mandel, R.J., Nguyen, M., Trono, D., and Naldini, L. (1998). A third-generation lentivirus vector with a conditional packaging system. *Journal of Virology* 72, 8463–8471.

Dumont, J.A., Liu, T., Low, S.C., Zhang, X., Kamphaus, G., Sakorafas, P., Fraley, C., Drager, D., Reidy, T., McCue, J., et al. (2012). Prolonged activity of a recombinant factor VIII-Fc fusion protein in hemophilia A mice and dogs. *Blood* 119, 3024–3030.

Duncan N, Roberson C, Lail A, Donfield S, Shapiro A. (2014). A haemophilia disease management programme targeting cost and utilization of specialty pharmaceuticals. *Haemophilia* 20, 519-26

Earnshaw, S.R., Graham, C.N., McDade, C.L., Spears, J.B., and Kessler, C.M. (2015). Factor VIII alloantibody inhibitors: cost analysis of immune tolerance induction vs. prophylaxis and on-demand with bypass treatment. *Haemophilia* 21, 310–319.

Eaton, D.L., Wood, W.I., Eaton, D., Hass, P.E., Hollingshead, P., Wion, K., Mather, J., Lawn, R.M., Vehar, G.A., and Gorman, C. (1986a). Construction and characterization of an active factor VIII variant lacking the central one-third of the molecule. *Biochemistry* 25, 8343–8347.

Eaton, D.L., Wood, W.I., Eaton, D., Hass, P.E., Hollingshead, P., Wion, K., Mather, J., Lawn, R.M., Vehar, G.A., and Gorman, C. (1986b). Construction and characterization of an active factor VIII variant lacking the central one-third of the molecule. *Biochemistry* 25, 8343–8347.

Eckhardt, C.L., van Velzen, A.S., Peters, M., Astermark, J., Brons, P.P., Castaman, G., Cnossen, M.H., Dors, N., Escuriola-Ettingshausen, C., Hamulyak, K., et al. (2013). Factor VIII gene (F8) mutation and risk of inhibitor development in nonsevere hemophilia A. *Blood* 122, 1954–1962.

Eggens, I., Fenderson, B., Toyokuni, T., Dean, B., Stroud, M., and Hakomori, S. (1989). Specific interaction between Lex and Lex determinants. A possible basis for cell recognition in preimplantation embryos and in embryonal carcinoma cells. *Journal of Biological Chemistry* 264, 9476–9484.

- Ellies, L.G., Ditto, D., Levy, G.G., Wahrenbrock, M., Ginsburg, D., Varki, A., Le, D.T., and Marth, J.D. (2002). Sialyltransferase ST3Gal-IV operates as a dominant modifier of hemostasis by concealing asialoglycoprotein receptor ligands. *Proceedings of the National Academy of Sciences* 99, 10042–10047.
- Ezban, M., Vad, K., and Kjalke, M. (2014). Turoctocog alfa (NovoEight®)--from design to clinical proof of concept. *Eur J Haematology* 93, 369–376.
- Fahs, S.A., Hille, M.T., Shi, Q., Weiler, H., and Montgomery, R.R. (2014). A conditional knockout mouse model reveals endothelial cells as the principal and possibly exclusive source of plasma factor VIII. *Blood* 123, 3706–3713.
- Fallaux, F.J., Hoebe, R.C., Cramer, S.J., van den Wollenberg, D.J., Briët, E., van Ormondt, H., and van der Eb, A.J. (1996). The human clotting factor VIII cDNA contains an autonomously replicating sequence consensus- and matrix attachment region-like sequence that binds a nuclear factor, represses heterologous gene expression, and mediates the transcriptional effects of sodium butyrate. *Molecular and Cellular Biology* 16, 4264–4272.
- Fang, H., Wang, L., and Wang, H. (2007). The protein structure and effect of factor VIII. *Thromb. Reseach* 119(1), 1-13.
- Fay, J., Kelehan, P., Lambkin, H., and Schwartz, S. (2009). Increased expression of cellular RNA-binding proteins in HPV-induced neoplasia and cervical cancer. *Journal of Medical Virology* 81, 897–907.
- Fay, P.J., Haidaris, P.J., and Smudzin, T.M. (1991). Human factor VIIIa subunit structure. Reconstruction of factor VIIIa from the isolated A1/A3-C1-C2 dimer and A2 subunit. *Journal of Biological Chemistry* 266(14), 957-962
- Fay, P.J. (2004). Activation of factor VIII and mechanisms of cofactor action. *Blood Review* 18, 1–15.
- Ferreira, J.A., Magalhães, A., Gomes, J., Peixoto, A., Gaiteiro, C., Fernandes, E., Santos, L.L., and Reis, C.A. (2016). Protein glycosylation in gastric and colorectal cancers: Toward cancer detection and targeted therapeutics. *Cancer Letter* (16), 30016-30017.
- Foster, P.A., and Zimmerman, T.S. (1989). Factor VIII structure and function. *Blood Review* 3, 180–191.

- Foster H., Sharp P.S., Athanasopoulos T., Trollet C., Graham I.R., Foster K., Wells D.J., and Dickson G. (2008). Codon and mRNA sequence optimization of microdystrophin transgenes improves expression and physiological outcome in dystrophic mdx mice following AAV2/8 gene transfer. *Mol Therapy* 16(11), 1825-1832.
- Fowler, W.E., Fay, P.J., Arvan, D.S., and Marder, V.J. (1990). Electron microscopy of human factor V and factor VIII: correlation of morphology with domain structure and localization of factor V activation fragments. *Proceedings of the National Academy of Sciences of the United States of America* 87, 7648–7652.
- Galili, U. (2005). The alpha-gal epitope and the anti-Gal antibody in xenotransplantation and in cancer immunotherapy. *Immunology and Cell Biology* 83, 674–686.
- Garrick, D., Fiering, S., David I.K., Martin and Whitela, E (1998). Repeat-induced gene silencing in mammals. *Nature Genetics* 18, 56 – 59.
- Ghosh, A., Yue, Y., Lai, Y., and Duan, D. (2008). A hybrid vector system expands adeno-associated viral vector packaging capacity in a transgene-independent manner. *Mol. Therapy* 16, 124–130.
- G.A., Capon, D.J., and Lawn, R.M. (1984). Characterization of the human factor VIII gene. *Nature* 312, 326–330.
- Goudemand, J., Rothschild, C., Demiguel, V., Vinciguerrat, C., Lambert, T., Chambost, H., Borel-Derlon, A., Claeysens, S., Laurian, Y., Calvez, T., et al. (2006). Influence of the type of factor VIII concentrate on the incidence of factor VIII inhibitors in previously untreated patients with severe hemophilia A. *Blood* 107, 46–51.
- Graw, J., Brackmann, H.-H., Oldenburg, J., Schneppenheim, R., Spannagl, M., and Schwaab, R. (2005). Haemophilia A: from mutation analysis to new therapies. *Nature Reviews. Genetics* 6, 488–501.
- Grillberger, L., Kreil, T.R., Nasr, S., and Reiter, M. (2009). Emerging trends in plasma-free manufacturing of recombinant protein therapeutics expressed in mammalian cells. *Biotechnol J* 4, 186–201.
- Gringeri, A. (2003). Cost of care and quality of life for patients with hemophilia complicated by inhibitors: the COCIS Study Group. *Blood* 102, 2358–2363.

- Gringeri, A., Tagliaferri, A., Tagariello, G., Morfini, M., Santagostino, E., Mannucci, P., ReFacto-AICE Study Group (2004). Efficacy and inhibitor development in previously treated patients with haemophilia A switched to a B domain-deleted recombinant factor VIII. *British Journal of Haematology* 126, 398–404.
- Halbert, C.L., Allen, J.M., and Miller, A.D. (2002). Efficient mouse airway transduction following recombination between AAV vectors carrying parts of a larger gene. *Nat Biotechnology* 20, 697–701.
- Hammond, C., Braakman, I., and Helenius, A. (1994). Role of *N*-linked oligosaccharide recognition, glucose trimming, and calnexin in glycoprotein folding and quality control. *Proceedings of the National Academy of Sciences of the United States of America* 91, 913–917.
- Hakeos, W. H., Miao, H. M., Sirachainan, N., Kemball-Cook, G., Pipe, S. (2002). Haemophilia A Mutations within the FVIII A2-A3 subunit interface Destabilize FVIIIa and Cause One-stage/Two- stage Activity Discrepancy. *Thromb Haemostasis* 88, 781-787.
- Hastie, E., and Samulski, R.J. (2015). Adeno-associated virus at 50: a golden anniversary of discovery, research, and gene therapy success-a personal perspective. *Hum. Gene Therapy* 26, 257–265.
- Hebert, D.N., Foellmer, B., and Helenius, A. (1995). Glucose trimming and reglucosylation determine glycoprotein association with calnexin in the endoplasmic reticulum. *Cell* 81, 425–433.
- High, K.H., Nathwani, A., Spencer, T., and Lillicrap, D. (2014). Current status of haemophilia gene therapy. *Haemophilia* 20 Suppl 4, 43–49.
- High, K.A., and Anguela, X.M. (2015). Adeno-associated viral vectors for the treatment of hemophilia. *Human Molecular Genetics* 25(1), 36-41
- Hirsch, M.L., Agbandje-McKenna, M., and Samulski, R.J. (2010). Little vector, big gene transduction: fragmented genome reassembly of adeno-associated virus. *Mol. Therapy* 18, 6–8.
- Hoeben, R.C., Fallaux, F.J., Cramer, S.J., van den Wollenberg, D.J., van Ormondt, H., Briët, E., and van der Eb, A.J. (1995). Expression of the blood-clotting factor-VIII cDNA is repressed by a transcriptional silencer located in its coding region. *Blood* 85, 2447–2454.

- Hoffman, M., and Monroe, D.M. (2001). A cell-based model of hemostasis. *Thromb. Haemost* 85, 958–965.
- Hoffman, M. (2003). A cell-based model of coagulation and the role of factor VIIa. *Blood Review* 17 Suppl 1, S1–S5.
- Holst, S., Deuss, A.J.M., van Pelt, G.W., van Vliet, S.J., Garcia-Vallejo, J.J., Koeleman, C.A.M., Deelder, A.M., Mesker, W.E., Tollenaar, R.A., Rombouts, Y., et al. (2016). N-glycosylation Profiling of Colorectal Cancer Cell Lines Reveals Association of Fucosylation with Differentiation and Caudal Type Homebox 1 (CDX1)/Villin mRNA Expression. *Molecular & Cellular Proteomics: MCP* 15, 124–140.
- Hossler, P., Mulukutla, B.C., and Hu, W.-S. (2007). Systems analysis of N-glycan processing in mammalian cells. *PloS One* 2, e713.
- Hubbard, A.R., Dodt, J., Lee, T., Mertens, K., Seitz, R., Srivastava, A., Weinstein, M., Factor VIII and Factor IX Subcommittee of the Scientific and Standardisation Committee of the International Society on Thrombosis and Haemostasis (2013). Recommendations on the potency labelling of factor VIII and factor IX concentrates. *J. Thromb. Haemostasis* 11, 988–989.
- Inagaki, K., Ma, C., Storm, T.A., Kay, M.A., and Nakai, H. (2007). The Role of DNA-PKcs and Artemis in Opening Viral DNA Hairpin Termini in Various Tissues in Mice. *Journal of Virology* 81, 11304–11321.
- Ing, M., Gupta, N., Teyssandier, M., Maillère, B., Pallardy, M., Delignat, S., Lacroix-Desmazes, S., ABIRISK consortium (2016). Immunogenicity of long-lasting recombinant factor VIII products. *Cell. Immunology* 301, 40–48.
- Itin, C., Roche, A.C., Monsigny, M., and Hauri, H.-P. (1996). ERGIC-53 is a functional mannose-selective and calcium-dependent human homologue of leguminous lectins. *Molecular Biology of the Cell* 7, 483–493.
- Johnston, J.M., Denning, G., Doering, C.B., and Spencer, H.T. (2012). Generation of an optimized lentiviral vector encoding a high-expression factor VIII transgene for gene therapy of hemophilia A. *Gene Therapy* 20, 607–615.
- Kalkhoran, F., Behzadian, F., Sabahi, F., Karimi, M., Mirshahabi, H. (2013). Construction and eukaryotic expression of recombinant large hepatitis delta antigen. *Reports of Biochemistry & Molecular Biology* 2(1), 28–34.

- Kannicht, C., Ramström, M., Kohla, G., Tiemeyer, M., Casademunt, E., Walter, O., and Sandberg, H. (2013). Characterisation of the post-translational modifications of a novel, human cell line-derived recombinant human factor VIII. *Thromb. Research* 131, 78–88.
- Kasper, C.K., Aledort, L., Aronson, D., Counts, R., Edson, J.R., van Eys, J., Fratantoni, J., Green, D., Hampton, J., Hilgartner, M., et al. (1975). Proceedings: A more uniform measurement of factor VIII inhibitors. *Thromb Diath Haemorrh* 34, 612.
- Kaufman, R.J. (1999). Advances toward Gene Therapy for Hemophilia at the Millennium. *Human Gene Therapy* 10(13), 2091-2107
- Kaufman, R.J., Wasley, L.C., and Dorner, A.J. (1988). Synthesis, processing, and secretion of recombinant human factor VIII expressed in mammalian cells. *Journal of Biological Chemistry* 263, 6352–6362.
- Kaufman, R.J., Wasley, L.C., Davies, M.V., Wise, R.J., Israel, D.I., and Dorner, A.J. (1989). Effect of von Willebrand factor coexpression on the synthesis and secretion of factor VIII in Chinese hamster ovary cells. *Molecular and Cellular Biology* 9, 1233–1242.
- Kauffman, R. J., Pipe, S.W., L, T., M, S., and M, M. (1997). Biosynthesis, assembly and secretion of coagulation factor VIII. *Blood Coagulation & Fibrinolysis* 8 Suppl 2, S3–S14.
- Kay, M.A., Glorioso, J.C., and Naldini, L. (2001). Viral vectors for gene therapy: the art of turning infectious agents into vehicles of therapeutics. *Nature Medicine* 7, 33–40.
- Keeling, D.M., Sukhu, K., and Cook, G.K. (1999). Diagnostic importance of the two-stage factor VIII:C assay demonstrated by a case of mild haemophilia associated with His1954 → Leu substitution in the factor VIII A3 domain. *British Journal of Haematology* 113, 603-615
- Kempton, C.L., and White, G.C. (2009). How we treat a hemophilia A patient with a factor VIII inhibitor. *Blood* 113, 11-17
- Khoriaty, R., Vasievich, M.P., and Ginsburg, D. (2012). The COPII pathway and hematologic disease. *Blood* 120(1), 31-38.
- Kim, V.N., Mitrophanous, K., Kingsman, S.M., and Kingsman, A.J. (1998). Minimal requirement for a lentivirus vector based on human immunodeficiency virus type 1. *Journal of Virology* 72, 811–816.

- Koeberl, D.D., Halbert, C.L., Krumm, A., and Miller, A.D. (1995). Sequences within the coding regions of clotting factor VIII and CFTR block transcriptional elongation. *Hum. Gene Therapy* 6, 469–479.
- Kofler, P. (1998). Liposome-Mediated Gene Transfer into Established CNS Cell Lines, Primary Glial Cells, and In Vivo. *Cell Transplant* 7, 175–185.
- Kolind, M.P., Nørby, P.L., Berchtold, M.W., and Johnsen, L.B. (2011). Optimisation of the Factor VIII yield in mammalian cell cultures by reducing the membrane bound fraction. *J. Biotechnology* 151, 357–362.
- Kolind, M.P., Nørby, P.L., Flintegaard, T.V., Berchtold, M.W., and Johnsen, L.B. (2010). The B-domain of Factor VIII reduces cell membrane attachment to host cells under serum free conditions. *J. Biotechnology* 147, 198–204.
- Kosloski, M.P., Miclea, R.D., and Balu-Iyer, S.V. (2009). Role of glycosylation in conformational stability, activity, macromolecular interaction and immunogenicity of recombinant human factor VIII. *Aaps J* 11, 424–431.
- Kotin, R.M., R.Michael Linden and Kenneth I.Berns. (1992) Characterization of a preferred site on human chromosome 19q for integration of adeno-associated virus DNA by non-homologous recombination. *EMBO* 11 (13), 5071 – 5078.
- Kyöstiö, S.R., Kotin, R.M., and Owens, R.A. (1994). Adeno-associated virus (AAV) Rep proteins mediate complex formation between AAV DNA and its integration site in human DNA. *Proceedings of the National Academy of Sciences of the United States of America* 91(13), 5808-5812.
- Laffan, M.A., Lester, W., O'Donnell, J.S., Will, A., Tait, R.C., Goodeve, A., Millar, C.M., and Keeling, D.M. (2014). The diagnosis and management of von Willebrand disease: a United Kingdom Haemophilia Centre Doctors Organization guideline approved by the British Committee for Standards in Haematology. *British Journal of Haematology* 167, 453–465.
- Lai, Y., Yue, Y., and Duan, D. (2010). Evidence for the failure of adeno-associated virus serotype 5 to package a viral genome ≥ 8.2 kb. *Mol. Therapy* 18, 75–79.
- Lakich, D., Kazazian, H.H., Antonarakis, S.E., and Gitschier, J. (1993). Inversions disrupting the factor VIII gene are a common cause of severe haemophilia A. *Nature Genetics* 5, 236–241.

- Lavoie, C., Paiement, J., Dominguez, M., Roy, L., Dahan, S., Gushue, J.N., and Bergeron, J.J.M. (1999). Roles for α 2p24 and COPI in Endoplasmic Reticulum Cargo Exit Site Formation. *The Journal of Cell Biology* 146, 285–299.
- Lee, C.A., Kessler, C.M., Varon, D., Martinowitz, U., Heim, M., JACQUEMIN, M.G., and Saint REMY, J.M.R. (1998). Factor VIII immunogenicity. *Haemophilia* 4, 552–557.
- Lenting, P.J., Neels, J.G., van den Berg, B.M.M., Clijsters, P.P.F.M., Meijerman, D.W.E., Pannekoek, H., Van Mourik, J.A., Mertens, K., and van Zonneveld, A.J. (1999). The Light Chain of Factor VIII Comprises a Binding Site for Low Density Lipoprotein Receptor-related Protein. *Journal of Biological Chemistry* 274, 23734–23739.
- Lenting, P.J., Van Mourik, J.A., and Mertens, K. (1998). The life cycle of coagulation factor VIII in view of its structure and function. *Blood* 92, 3983–3996.
- Lenting, P.J., van Schooten, C.J.M., and Denis, C.V. (2007). Clearance mechanisms of von Willebrand factor and factor VIII. *J. Thromb. Haemostasis* 5, 1353–1360.
- Levinson, B., Bermingham, J.R., Metzenberg, A., Kenwrick, S., Chapman, V., and Gitschier, J. (1992a). Sequence of the human factor VIII-associated gene is conserved in mouse. *Genomics* 13, 862–865.
- Levinson, B., Kenwrick, S., Gamel, P., Fisher, K., and Gitschier, J. (1992b). Evidence for a third transcript from the human factor VIII gene. *Genomics* 14, 585–589.
- Leyte, A., Verbeet, MP., Brodniewicz-Proba, T., Van Mourik, JA., Mertens, K. (1989). The interaction between human blood-coagulation factor VIII and von Willebrand factor. Characterization of a high-affinity binding site on factor VIII. *Biochem Journal* 257(3), 679-683.
- Leyte, A., van Schijndel, HB, Niehrs C., Huttner, WB, Verbeet, MP., Mertens, K., van Mourik, JA. (1991). Sulfation of Tyr1680 of human blood coagulation factor VIII is essential for the interaction of factor VIII with von Willebrand factor. *Journal of Biological Chemistry* 266(2), 740-746.
- Li, H., Chan, S., and Tang, F. (1997a). Transfection of rat brain cells by electroporation. *J. Neurosci Methods* 75(1), 29-32.
- Li, J., Samulski, R.J., and Xiao, X. (1997b). Role for highly regulated rep gene

expression in adeno-associated virus vector production. *Journal of Virology* 71, 5236–5243.

Lind, P., Larsson, K., Spira, J., Sydow-Bäckman, M., Almstedt, A., Gray, E., and Sandberg, H. (1995). Novel forms of B-domain-deleted recombinant factor VIII molecules. Construction and biochemical characterization. *European Journal of Biochemistry* 232, 19–27.

Linden, R.M., and Winocour, E. (1996). The recombination signals for adeno-associated virus site-specific integration. *Proceedings of the National Academy of Sciences of the United States of America* 93(15), 7966-7972.

Lis, H., and Sharon, N. (1993). Protein glycosylation. Structural and functional aspects. *European Journal of Biochemistry* 218, 1–27.

Liu, F., and Huang, L. (2002). Electric gene transfer to the liver following systemic administration of plasmid DNA. *Gene Therapy* 9, 1116–1119.

Liu, J., Qian, C., and Cao, X. (2016). Post-Translational Modification Control of Innate Immunity. *Immunity* 45, 15–30.

Ljung, R. C. (1999). Prophylactic infusion regimens in the management of hemophilia. *Thromb Haemostasis* 82(2), 525-530.

Lodish, H.F., Kong, N., Snider, M., and Strous, G.J. (1983). Hepatoma secretory proteins migrate from rough endoplasmic reticulum to Golgi at characteristic rates. *Nature* 304, 80–83.

Lollar, P., Hill-Eubanks, D.C., and Parker, C.G. (1988). Association of the factor VIII light chain with von Willebrand factor. *Journal of Biological Chemistry* 263, 10451-10455

Lu, H., Chen, L., Wang, J., Huack, B., Sarkar, R., Zhou, S., Xu, R., Ding, Q., Wang, X., Wang, H., et al. (2008). Complete Correction of Hemophilia A with Adeno-Associated Viral Vectors Containing a Full-Size Expression Cassette. *Human Gene Therapy* 19, 648–654.

Lucas, M.L., Heller, L., Coppola, D., and Heller, R. (2002). IL-12 plasmid delivery by in vivo electroporation for the successful treatment of established subcutaneous B16.F10 melanoma. *Molecular Therapy* 5, 668–675.

Lusher, J.M., Lee, C.A., Kessler, C.M., Bedrosian, C.L., and Grp, R.P.3.S. (2003). The

safety and efficacy of B-domain deleted recombinant factor VIII concentrate in patients with severe haemophilia A. *Haemophilia* 9, 38–49.

Lynch, C.M., Israel, D.I., Kaufman, R.J., and Miller, A.D. (1993). Sequences in the Coding Region of Clotting Factor VIII Act as Dominant Inhibitors of RNA Accumulation and Protein Production. *Human Gene Therapy* 4, 259–272.

Macfarlane, R.G. (1964). An enzyme cascade in the blood clotting mechanism, and its function as biochemical amplifier. *Nature* 202, 498–499.

Mackman, N. (2009). The Role of Tissue Factor and Factor VIIa in Hemostasis. *Anesthesia & Analgesia* 108, 1447–1452.

Manno, C.S., Chew, A.J., Hutchison, S., Larson, P.J., Herzog, R.W., Arruda, V.R., Tai, S.J., Ragni, M.V., Thompson, A., Ozelo, M., et al. (2003). AAV-mediated factor IX gene transfer to skeletal muscle in patients with severe hemophilia B. *Blood* 101, 2963–2972.

Manno, C.S., Pierce, G.F., Arruda, V.R., Glader, B., Ragni, M., Rasko, J.J., Ozelo, M.C., Hoots, K., Blatt, P., Konkle, B., et al. (2006). Successful transduction of liver in hemophilia by AAV-Factor IX and limitations imposed by the host immune response. *Nature Medicine* 12, 342–347.

Mannucci, P.M., and Tuddenham, E.G. (2001). The hemophilias--from royal genes to gene therapy. *N. Engl. J. Medicine* 344, 1773–1779.

McCue, J.T., Selvitelli, K., and Walker, J. (2009). Application of a novel affinity adsorbent for the capture and purification of recombinant factor VIII compounds. *J Chromatography A* 1216, 7824–7830.

McCue, J., Kshirsagar, R., Selvitelli, K., Lu, Q., Zhang, M., Mei, B., Peters, R., Pierce, G.F., Dumont, J., Raso, S., et al. (2015). Manufacturing process used to produce long-acting recombinant factor VIII Fc fusion protein. *Biologicals* 43, 213–219.

McIntosh, J., Lenting, P.J., Rosales, C., Lee, D., Rabbani, S., Raj, D., Patel, N., Tuddenham, E.G.D., Christophe, O.D., McVey, J.H., et al. (2013). Therapeutic levels of FVIII following a single peripheral vein administration of rAAV vector encoding a novel human factor VIII variant. *Blood* 121, 3335–3344.

Meex, S. J., Andreo, U., Sparks, J. D., and Fisher, E. A. (2011). Huh-7 or HepG2 cells: which is the better model for studying human apolipoprotein-B100 assembly and secretion. *J Lipid Reseach* 52(1), 152–158.

- Mei, B., Pan, C., Jiang, H., Tjandra, H., Strauss, J., and Chen, Y. (2010). Rational design of a fully active, long-acting PEGylated factor VIII for hemophilia A treatment | Blood Journal. *Blood* 116(2), 270-279
- Messerschmidt, A., and Huber, R. (1990). The blue oxidases, ascorbate oxidase, laccase and ceruloplasmin Modelling and structural relationships. *The FEBS Journal* 187, 341–352.
- Messner, P. (2004). Prokaryotic glycoproteins: unexplored but important. *J. Bacteriology* 186, 2517–2519.
- Miao HZ, Sirachainan N, Palmer L, Kucab P, Cunningham MA, Kaufman RJ, Pipe SW. (2004). Bioengineering of coagulation factor VIII for improved secretion. *Blood* 103(9), 3412-3419.
- Mingozzi, F., and High, K.A. (2013). Immune responses to AAV vectors: overcoming barriers to successful gene therapy. *Blood* 122, 23–36.
- Moestrup, S.K., Gliemann, J., and Pallesen, G. (1992). Distribution of the alpha 2-macroglobulin receptor/low density lipoprotein receptor-related protein in human tissues. *Cell Tissue Research* 269, 375–382.
- Monahan, P.E., Lothrop, C.D., Sun, J., Hirsch, M.L., Kafri, T., Kantor, B., Sarkar, R., Tillson, D.M., Elia, J.R., and Samulski, R.J. (2010). Proteasome inhibitors enhance gene delivery by AAV virus vectors expressing large genomes in hemophilia mouse and dog models: a strategy for broad clinical application. *Molecular Therapy* 18, 1907–1916.
- Monk, C.R., Sutton-Smith, M., Dell, A., and Garden, O.A. (2006). Preparation of CD25(+) and CD25(-) CD4(+) T cells for glycomic analysis--a cautionary tale of serum glycoprotein sequestration. *Glycobiology* 16, 11G–13G.
- Mononen, I., and Karjalainen, E. (1984). Structural comparison of protein sequences around potential N-glycosylation sites. *Biochimica Biophysica Acta - Protein Structure and Molecular Enzymology* 788, 364–367.
- Moussalli, M., Pipe, S.W., Hauri, H.-P., Nichols, W.C., Ginsburg, D., and Kaufman, R.J. (1999). Mannose-dependent Endoplasmic Reticulum (ER)-Golgi Intermediate Compartment-53-mediated ER to Golgi Trafficking of Coagulation Factors V and VIII. *Journal of Biological Chemistry* 274, 32539–32542.

- Nakabayashi, H., Taketa, K., Miyano, K., Yamane, T., and Sato, T. (1982). Growth of Human Hepatoma Cell Lines with Differentiated Functions in Chemically Defined Medium. *Cancer Research* 42, 3858-3863.
- Naldini, L., Blömer, U., Gage, F.H., Trono, D., and Verma, I.M. (1996). Efficient transfer, integration, and sustained long-term expression of the transgene in adult rat brains injected with a lentiviral vector. *Proceedings of the National Academy of Sciences of the United States of America* 93(21), 11382-11388.
- Nathwani, A.C., Davidoff, A.M., and Linch, D.C. (2005). A review of gene therapy for haematological disorders. *British Journal of Haematology* 128, 3–17.
- Nathwani, A.C., Gray, J.T., McIntosh, J.M., Ng, C.Y., Zhou, J., Spence, Y., Cochrane, M., Gray, E., Tuddenham, E.G.D., Davidoff, A.M. (2007). Safe and efficient transduction of the liver after peripheral vein infusion of self-complementary AAV vector results in stable therapeutic expression of human FIX in nonhuman primates. *Blood* 109, 1414-1421.
- Nathwani, A.C., Tuddenham, E.G., Rangarajan, S., Rosales, C., McIntosh, J., Linch, D.C., Chowdary, P., Riddell, A., Pie, A.J., Harrington, C., et al. (2011). Adenovirus-associated virus vector-mediated gene transfer in hemophilia B. *N. Engl. J. Medicine* 365, 2357–2365.
- Nathwani, A.C., Reiss, U.M., Tuddenham, E.G.D., Rosales, C., Chowdary, P., McIntosh, J., Peruta, Della, M., Lheriteau, E., Patel, N., Raj, D., et al. (2014). Long-Term Safety and Efficacy of Factor IX Gene Therapy in Hemophilia B. *N. Engl. J. Medicine* 371, 1994–2004.
- Neerman-Arbez, M., Johnson, K.M., Morris, M.A., McVey, J.H., Peyvandi, F., Nichols, W.C., Ginsburg, D., Rossier, C., Antonarakis, S.E., and Tuddenham, E.G. (1999). Molecular analysis of the ERGIC-53 gene in 35 families with combined factor V-factor VIII deficiency. *Blood* 93, 2253–2260.
- Newell, J.L., and Fay, P.J. (2007). Proteolysis at Arg740 facilitates subsequent bond cleavages during thrombin-catalyzed activation of factor VIII. *Journal of Biological Chemistry* 282, 25367–25375.
- Ngo, J.C.K., Huang, M., Roth, D.A., Furie, B.C., Furie, B. (2008). Crystal Structure of Human Factor VIII: Implications for the Formation of the Factor IXa-Factor VIIIa Complex. *Structure* 16(4), 597–606.
- Nichols, W.C., and Ginsburg, D. (1999). From the ER to the Golgi: insights from the

study of combined factors V and VIII deficiency. *American Journal of Human Genetics* 64, 1493–1498.

Nichols, W.C., Seligsohn, U., Zivelin, A., Terry, V.H., Hertel, C.E., Wheatley, M.A., Moussalli, M.J., Hauri, H.-P., Ciavarella, N., Kaufman, R.J., et al. (1998). Mutations in the ER–Golgi Intermediate Compartment Protein ERGIC-53 Cause Combined Deficiency of Coagulation Factors V and VIII. *Cell* 93, 61–70.

Nicolau, C., Legrand, A., and Grosse, E. (1987). Liposomes as carriers for in vivo gene transfer and expression. *Meth. Enzymology* 149, 157–176.

Nordfang, O., and Ezban, M. (1988). Generation of active coagulation factor VIII from isolated subunits. *Journal of Biological Chemistry* 263, 1115–1118.

Nufer, O., Kappeler, F., Guldbrandsen, S., and Hauri, H.-P. (2003). ER export of ERGIC-53 is controlled by cooperation of targeting determinants in all three of its domains. *Journal of Cell Science* 116, 4429–4440.

Nyfeler, B., Zhang, B., Ginsburg, D., Kaufman, R.J., and Hauri, H.-P. (2006). Cargo selectivity of the ERGIC-53/MCFD2 transport receptor complex. *Traffic* 7, 1473–1481.

Oberbek, A., Matasci, M., Hacker, D.L., and Wurm, F.M. (2011). Generation of stable, high-producing CHO cell lines by lentiviral vector-mediated gene transfer in serum-free suspension culture. *Biotechnol. Bioengineering* 108, 600–610.

Oldenburg, J., and Albert, T. (2014). Novel products for haemostasis - current status. *Haemophilia* 20 Suppl 4, 23–28.

Oldenburg, J., and Pavlova, A. (2006). Genetic risk factors for inhibitors to factors VIII and IX. *Haemophilia* 12 Suppl 6, 15–22.

Olsen, J.V., and Mann, M. (2013). Status of large-scale analysis of post-translational modifications by mass spectrometry. *Molecular & Cellular Proteomics* 12, 3444–3452.

Ostedgaard, L.S., Rokhlina, T., Karp, P.H., Lashmit, P., Afione, S., Schmidt, M., Zabner, J., Stinski, M.F., Chiorini, J.A., and Welsh, M.J. (2005). A shortened adeno-associated virus expression cassette for CFTR gene transfer to cystic fibrosis airway epithelia. *Proceedings of the National Academy of Sciences of the United States of America* 102, 2952–2957.

Pagel, O., Loroch, S., Sickmann, A., and Zahedi, R.P. (2015). Current strategies and findings in clinically relevant post-translational modification-specific proteomics. *Expert*

Review of Proteomics 12, 235–253.

Palmberger, D., Ashjaei, K., Strell, S., Hoffmann-Sommergruber, K., and Grabherr, R. (2014). Minimizing fucosylation in insect cell-derived glycoproteins reduces binding to IgE antibodies from the sera of patients with allergy. *Biotechnol Journal* 9, 1206–1214.

Pan, J., Liu, T., Kim, J.Y., Zhu, D., Patel, C., Cui, Z.H., Zhang, X., Newgren, J.O., Reames, A., Canivel, D., et al. (2009). Enhanced efficacy of recombinant FVIII in noncovalent complex with PEGylated liposome in hemophilia A mice. *Blood* 114, 2802–2811.

Park, E.I., Manzella, S.M., and Baenziger, J.U. (2003). Rapid Clearance of Sialylated Glycoproteins by the Asialoglycoprotein Receptor. *Journal of Biological Chemistry* 278, 4597–4602.

Pedroso de Lima MC., Simões S., Pires P., Faneca H and Düzgüneş N. (2001). Cationic lipid-DNA complexes in gene delivery: from biophysics to biological applications. *Adv Drug Deliv Review* 47(2-3), 277-94.

Peel, A.L., and Klein, R.L. (2000). Adeno-associated virus vectors: activity and applications in the CNS. *J. Neurosci. Methods* 98, 95–104.

Pemberton, S., Lindley, P., Zaitsev, V., Card, G., Tuddenham, E.G., and Kemball-Cook, G. (1997). A molecular model for the triplicated A domains of human factor VIII based on the crystal structure of human ceruloplasmin. *Blood* 89, 2413–2421.

Peyvandi, F., Garagiola, I., and Seregini, S. (2013). Future of coagulation factor replacement therapy. *J. Thromb. Haemost* 11 Suppl 1, 84–98.

Pipe, S.W. (1998). Differential Interaction of Coagulation Factor VIII and Factor V with Protein Chaperones Calnexin and Calreticulin. *Journal of Biological Chemistry* 273, 8537–8544.

Pipe, S.W. (2001). Hemophilia A mutations associated with 1-stage/2-stage activity discrepancy disrupt protein-protein interactions within the triplicated A domains of thrombin-activated factor VIIIa. *Blood* 97, 685–691.

Pipe, S.W. (2009). Functional roles of the factor VIII B domain. *Haemophilia* 15, 1187–1196.

Pipe, S.W., Eickhorst, A.N., McKinley, S.H., Saenko, E.L., and Kaufman, R.J. (1999). Mild hemophilia A caused by increased rate of factor VIII A2 subunit dissociation:

evidence for nonproteolytic inactivation of factor VIIIa in vivo. *Blood* 93, 176–183.

Pipe, S.W. (2008). Recombinant clotting factors. *Thromb. Haemostasis* 99, 840–850.

Pittman, D.D., Alderman, E.M., Tomkinson, K.N., Wang, J.H., Giles, A.R., and Kaufman, R.J. (1993). Biochemical, immunological, and in vivo functional characterization of B-domain-deleted factor VIII. *Blood* 81, 2925–2935.

Pittman, D.D., Marquette, K.A., and Kaufman, R.J. (1994). Role of the B domain for factor VIII and factor V expression and function. *Blood* 84, 4214–4225.

Pollmann, H., Externest, D., Ganser, A., Eifrig, B., Kreuz, W., Lenk, H., Pabinger, I., Schramm, W., Schwarz, T.F., Zimmermann, R. (2007). Efficacy, safety and tolerability of recombinant factor VIII (REFACTO) in patients with haemophilia A: interim data from a postmarketing surveillance study in Germany and Austria. *Haemophilia* 13, 131–143.

Potgieter, J.J., Damgaard, M., and Hillarp, A. (2015). One-stage vs. chromogenic assays in haemophilia A. *Eur J Haematology* 94, 38–44.

Powell, J.S., Josephson, N.C., Quon, D., Ragni, M.V., Cheng, G., Li, E., Jiang, H., Li, L., Dumont, J.A., Goyal, J. (2012). Safety and prolonged activity of recombinant factor VIII Fc fusion protein in hemophilia A patients. *Blood* 119, 3031–3037.

Powell, J.S., Ragni, M.V., White, G.C., Lusher, J.M., Hillman-Wiseman, C., Moon, T.E., Cole, V., Ramanathan-Girish, S., Roehl, H., Sajjadi, N. (2003). Phase 1 trial of FVIII gene transfer for severe hemophilia A using a retroviral construct administered by peripheral intravenous infusion. *Blood* 102, 2038–2045.

Poznansky, M., Lever, A., Bergeron, L., Haseltine, W., and Sodroski, J. (1991). Gene transfer into human lymphocytes by a defective human immunodeficiency virus type 1 vector. *Journal of Virology* 65(1), 532–536.

Presnyak, V., Alhusaini, N., Chen, Y., Martin, S., Morris, N., Kline, N., Olson, S., Weinberg, D., Baker, A, E., Graveley, B.R and Collier, J. (2015). Codon Optimality Is a Major Determinant of mRNA Stability. *Cell* 160, 1111–1124.

Preston, R.J.S., Rawley, O., Gleeson, E.M., and O'Donnell, J.S. (2013). Elucidating the role of carbohydrate determinants in regulating hemostasis: insights and opportunities. *Blood* 121, 3801–3810.

Radcliffe, P.A., Sion, C.J.M., Wilkes, F.J., Custard, E.J., Beard, G.L., Kingsman, S.M., and Mitrophanous, K.A. (2007). Analysis of factor VIII mediated suppression of

lentiviral vector titres. *Gene Therapy* 15, 289–297.

Reiser, J., Harmison, G., Kluepfel-Stahl, S., Brady, R.O., Karlsson, S., and Schubert, M. (1996). Transduction of nondividing cells using pseudotyped defective high-titer HIV type 1 particles. *Proceedings of the National Academy of Sciences of the United States of America* 93, 15266–15271.

Rodgers, S.E., Duncan, E.M., Barbulescu, D.M., Quinn, D.M., and Lloyd, J.V. (2007). In vitro kinetics of factor VIII activity in patients with mild haemophilia A and a discrepancy between one-stage and two-stage factor VIII assay results. *British Journal of Haematology* 136, 138–145.

Roth, D.A., Tawa, N.E., O'Brien, J.M., Treco, D.A., Selden, R.F., Factor VIII Transkaryotic Therapy Study Group (2001). Nonviral transfer of the gene encoding coagulation factor VIII in patients with severe hemophilia A. *N. Engl. J. Medicine* 344, 1735–1742.

Rudolph, K.L.M., Schmitt, B.M., Villar, D., White, R.J., Marioni, J.C., Kutter, C., and Odom, D.T. (2016). Codon-Driven Translational Efficiency Is Stable across Diverse Mammalian Cell States. *PLoS Genetics* 12, e1006024.

Sadler J, E. (1998). Biochemistry and genetics of von Willebrand factor. *Annu Rev Biochemistry* 67, 395-424.

Saenko, E.L., Shima, M., Rajalakshmi, K.J., and Scandella, D. (1994). A role for the C2 domain of factor VIII in binding to von Willebrand factor. *Journal of Biological Chemistry* 269, 11601–11605.

Saenko, E.L., Scandella, D. (1997). The acidic region of the factorVIII light chain and the C2 domain together form the high affinity binding site for von Willebrand factor. *Journal of Biological Chemistry* 272(29), 18007-18014

Saenko, E.L., Yakhyaev, A.V., Mikhailenko, I., Strickland, D.K., and Sarafanov, A.G. (1999). Role of the low density lipoprotein-related protein receptor in mediation of factor VIII catabolism. *Journal of Biological Chemistry* 274, 37685–37692.

Samulski, R.J., Srivastava, A., Berns, K.I., and Muzyczka, N. (1983). Rescue of adeno-associated virus from recombinant plasmids: Gene correction within the terminal repeats of AAV. *Cell* 33, 135–143.

Sandberg, H., Almstedt, A., Brandt, J., Gray, E., Holmquist, L., Oswaldsson, U.,

- Sebring, S., and Mikaelsson, M. (2001). Structural and functional characteristics of the B-domain-deleted recombinant factor VIII protein, r-VIII SQ. *Thromb. Haemostasis* 85, 93–100.
- Sandberg, H., Kannicht, C., Stenlund, P., Dadaian, M., Oswaldsson, U., Cordula, C., and Walter, O. (2012). Functional characteristics of the novel, human-derived recombinant FVIII protein product, human-cl rhFVIII. *Thromb. Reseach* 130, 808–817.
- Sands, M, S. AAV-Mediated Liver-Directed Gene Therapy. (2014). *Methods Mol Biology* 807, 141–157.
- Santagostino, E. (2014). A new recombinant factor VIII: from genetics to clinical use. *Drug Des Devel Therapy* 8, 2507–2515.
- Sarafanov, A.G., Ananyeva, N.M., Shima, M., and Saenko, E.L. (2001). Cell Surface Heparan Sulfate Proteoglycans Participate in Factor VIII Catabolism Mediated by Low Density Lipoprotein Receptor-related Protein. *Journal of Biological Chemistry* 276, 11970–11979.
- Schmidbauer, S., Witzel, R., Robbel, L., Sebastian, P., Grammel, N., Metzner, H.J., and Schulte, S. (2015). Physicochemical characterisation of rVIII-SingleChain, a novel recombinant single-chain factor VIII. *Thromb. Reseach* 136, 388–395.
- Schnepp, B C., Ryan L. Jensen, Chun-Liang Chen, Philip R. Johnson, K. Reed Clark. (2005). Characterization of Adeno-Associated Virus Genomes Isolated from Human Tissues. *J. Virology* 79 (23), 14793-14803.
- Schulte, S. (2013). Innovative coagulation factors: albumin fusion technology and recombinant single-chain factor VIII. *Thromb. Reseach* 131, S2–S6.
- Schwaab, R., Brackmann, H.H., Meyer, C., Seehafer, J., Kirchgesser, M., Haack, A., Olek, K., Tuddenham, E.G., and Oldenburg, J. (1995). Haemophilia A: mutation type determines risk of inhibitor formation. *Thromb. Haemostasis* 74, 1402–1406.
- Schwartz, R.S., Abildgaard, C.F., and Aledort, L.M. (1990). Human recombinant DNA-derived antihemophilic factor (factor VIII) in the treatment of hemophilia A. *England Journal of Medicine* 323(26), 1800-1805.
- Shen BW, Spiegel PC, Chang CH, Huh JW, Lee JS, Kim J, Kim YH, Stoddard BL. (2008). The tertiary structure and domain organization of coagulation factor VIII. *Blood* 111(3), 1240-1247.

- Shestopal, S.A., Hao, J.J., Karnaukhova, E., Liang,Y., Ovanesov, M,V ., Lin M., Kurasawa ,J,H., Lee, T,K., McVey, J,H., Sarafanov, A,G. (2017). Expression and characterization of a codon-optimized blood coagulation factor VIII. *J Thromb. Haemostasis* 15(4), 709-720.
- Shevtsova, Z., Malik, J.M.I., Michel, U., Bähr, M., and Kügler, S. (2005). Promoters and serotypes: targeting of adeno-associated virus vectors for gene transfer in the rat central nervous system in vitro and in vivo. *Exp. Physiology* 90, 53–59.
- Skinner, M.W. (2012). WFH: Closing the global gap-achieving optimal care. *Haemophilia* 18, 1–12.
- Solá, R.J., and Griebenow, K. (2010). Glycosylation of therapeutic proteins: an effective strategy to optimize efficacy. *BioDrugs* 24, 9–21.
- Spencer,H,T., Denning, G., Gautney,R,E., Dropulic,B., Roy,A,J., Baranyi,L., Gangadharan,B., Parker,E,T., Lollar,P., and Doering,C,E. (2011). Lentiviral Vector Platform for Production of Bioengineered Recombinant Coagulation Factor VIII. *Molecular Therapy* 19(2), 302–309.
- Srivastava, C.H., Samulski, R.J., Lu, L., Larsen, S.H., and Srivastava, A. (1989). Construction of a recombinant human parvovirus B19: adeno-associated virus 2 (AAV) DNA inverted terminal repeats are functional in an AAV-B19 hybrid virus. *Proceedings of the National Academy of Sciences of the United States of America* 86, 8078–8082.
- Srour,M,A., Grupp,J., Aburubaiha,Z., Albert, T., Brondke, H., Oldenburg, J., Schwaab, R. (2008). Modified expression of coagulation factor VIII by addition of a glycosylation site at the N terminus of the protein. *Ann Hematology* 87(2), 107-112.
- Stel, H.V., van der Kwast, T.H., and Veerman, E.C.I. (1983). Detection of factor VIII/coagulant antigen in human liver tissue. *Nature* 303, 530–532.
- Stennicke, H.R., Kjalke, M., Karpf, D.M., Balling, K.W., Johansen, P.B., Elm, T., Øvlisen, K., Möller, F., Holmberg, H.L., Gudme, C.N., et al. (2013). A novel B-domain O-glycoPEGylated FVIII (N8-GP) demonstrates full efficacy and prolonged effect in hemophilic mice models. *Blood* 121, 2108–2116.
- Stephanie A. Smith, Dvm, MS Dacvim. (2009). The cell-based model of coagulation. *Journal of Veterinary Emergency and Critical Care* 19(1), 3–10
- Stockert, R.J. (1995). The asialoglycoprotein receptor: relationships between

structure, function, and expression. *Physiological Reviews* 75, 591–609.

Stoylova, S.S., Lenting, P.J., Kemball-Cook, G., and Holzenburg, A. (1999). Electron Crystallography of Human Blood Coagulation Factor VIII Bound to Phospholipid Monolayers. *Journal of Biological Chemistry* 274, 36573–36578.

Strasser, R. Plant protein glycosylation. (2016). *Glycobiology* 26(9), 926–939.

Swiech, K., Kamen, A., Ansorge, S., Durocher, Y., Picanço-Castro, V., Russo-Carbolante, E.M.S., Neto, M.S.A., and Covas, D.T. (2011). Transient transfection of serum-free suspension HEK 293 cell culture for efficient production of human rFVIII. *BMC Biotechnology* 11, 114.

Swiech, K., Picanço-Castro, V., and Covas, D.T. (2012). Human cells: new platform for recombinant therapeutic protein production. *Protein Expr. Purification* 84, 147–153.

Swystun, L.L., and Lillicrap, D. (2016). Gene Therapy for Coagulation Disorders. *Circ. Research* 118, 1443–1452.

Tang, L., Leong, L., Sim, D., Ho, E., Gu, J.M., Schneider, D., Feldman, R.I., Monteclaro, F., Jiang, H., and Murphy, J.E. (2013). von Willebrand factor contributes to longer half-life of PEGylated factor VIII in vivo. *Haemophilia* 19, 539–545.

Taranejoo, S., Liu, J., Verma, P., and Hourigan, K. (2015). A review of the developments of characteristics of PEI derivatives for gene delivery applications. *Journal of Applied Polymer Science* 132.

Toole, J.J., Knopf, J.L., Wozney, J.M., Sultzman, L.A., Buecker, J.L., Pittman, D.D., Kaufman, R.J., Brown, E., Shoemaker, C., and Orr, E.C. (1984). Molecular cloning of a cDNA encoding human antihemophilic factor. *Nature* 312, 342–347.

Toole, J.J., Pittman, D.D., Orr, E.C., Murtha, P., Wasley, L.C., and Kaufman, R.J. (1986). A large region (approximately equal to 95 kDa) of human factor VIII is dispensable for in vitro procoagulant activity. *Proceedings of the National Academy of Sciences of the United States of America* 83, 5939–5942.

Trapani, I., Colella, P., Sommella, A., Iodice, C., Cesi, G., de Simone, S., Marrocco, E., Rossi, S., Giunti, M., Palfi, A., et al. (2014). Effective delivery of large genes to the retina by dual AAV vectors. *EMBO Mol Medicine* 6, 194–211.

Triplett, D.A. (2000). Coagulation and bleeding disorders: review and update. *Clinical*

Chemistry 46, 1260–1269.

Trono, D. (2000). Lentiviral vectors: turning a deadly foe into a therapeutic agent. *Gene Therapy* 7, 20–23.

Tuller, T., Carmi, A., Vestsigian, K., Navon, S., Dorfan, Y., Zaborske, J., Pan, T., Dahan, O., Furman, I., and Pilpel, Y. (2010). An evolutionarily conserved mechanism for controlling the efficiency of protein translation. *Cell* 141, 344–354.

Turecek PL, Bossard MJ, Graninger M, Gritsch H, Höllriegl W, Kaliwoda M, Matthiessen P, Mitterer A, Muchitsch EM, Purtscher M, Rottensteiner H, Schiviz A, Schrenk G, Siekmann J, Varadi K, Riley T, Ehrlich HJ, Schwarz HP, Scheiflinger F. (2012). BAX 855, a PEGylated rFVIII product with prolonged half-life. Development, functional and structural characterisation. *Hamostaseologie* 32 Suppl 1, S29-38.

Turner, N.A., and Moake, J.L. (2015). Factor VIII Is Synthesized in Human Endothelial Cells, Packaged in Weibel-Palade Bodies and Secreted Bound to ULVWF Strings. *PloS One* 10, e0140740.

Valentino, L.A., Negrier, C., Kohla, G., Tiede, A., Liesner, R., Hart, D., and Knaub, S. (2014). The first recombinant FVIII produced in human cells--an update on its clinical development programme. *Haemophilia* 20 Suppl 1, 1–9.

Varki, A. (1993). Biological roles of oligosaccharides: all of the theories are correct. *Glycobiology* 3, 97–130.

Varki, A., and Gagneux, P. (2012). Multifarious roles of sialic acids in immunity. *Annals of the New York Academy of Sciences* 1253, 16–36.

Veeraraghavan, S., Baleja, J.D., and Gilbert, G.E. (1998). Structure and topography of the membrane-binding C2 domain of factor VIII in the presence of dodecylphosphocholine micelles. *Biochem. Journal* 332(2), 549–555.

Vehar, G.A., Keyt, B., Eaton, D., Rodriguez, H., O'Brien, D.P., Rotblat, F., Oppermann, H., Keck, R., Wood, W.I., Harkins, R.N., et al. (1984). Structure of human factor VIII. *Nature* 312, 337–342.

Velloso, L.M. (2002). Crystal Structure of the Carbohydrate Recognition Domain of p58/ERGIC-53, a Protein Involved in Glycoprotein Export from the Endoplasmic Reticulum. *Journal of Biological Chemistry* 277, 15979–15984.

Versteeg, H.H., Heemskerk, J.W.M., Levi, M., and Reitsma, P.H. (2013). New

Fundamentals in Hemostasis. *Physiological Reviews* 93, 327–358.

Wakabayashi, H., Koszelak, M.E., Mastro, M., and Fay, P.J. (2001). Metal ion-independent association of factor VIII subunits and the roles of calcium and copper ions for cofactor activity and inter-subunit affinity. *Biochemistry* 40, 10293–10300.

Walsh, G., and Jefferis, R. (2006). Post-translational modifications in the context of therapeutic proteins. *Nat. Biotechnology* 24, 1241–1252.

Ward, N.J., Buckley, S.M.K., Waddington, S.N., VandenDriessche, T., Chuah, M.K.L., Nathwani, A.C., McIntosh, J., Tuddenham, E.G.D., Kinnon, C., Thrasher, A.J., et al. (2011). Codon optimization of human factor VIII cDNAs leads to high-level expression. *Blood* 117, 798–807.

Washbourne, P., and McAllister, A.K. (2002). Techniques for gene transfer into neurons. *Current Opinion in Neurobiology* 12(5), 566-573.

Weerapana, E., and Imperiali, B. (2006). Asparagine-linked protein glycosylation: from eukaryotic to prokaryotic systems. *Glycobiology* 16(6), 91R-101R.

Weiss, H.J., Sussman, I.I., and Hoyer, L.W. (1977). Stabilization of factor VIII in plasma by the von Willebrand factor. Studies on posttransfusion and dissociated factor VIII and in patients with von Willebrand's disease. *The Journal of Clinical Investigation* 60, 390–404.

White, G.C., Rosendaal, F., and Aledort, L.M. (2001). Definitions in hemophilia. *Thrombosis and Haemostasis* 85(3), 560.

Wiethoff, C.M., and Middaugh, C.R. (2003). Barriers to nonviral gene delivery. *Journal of Pharmaceutical Sciences* 92, 203–217.

Winge, S., Yderland, L., Kannicht, C., Hermans, P., Adema, S., Schmidt, T., Gilljam, G., Linhult, M., Tiemeyer, M., Belyanskaya, L., et al. (2015). Development, upscaling and validation of the purification process for human-cl rhFVIII (Nuwiq®), a new generation recombinant factor VIII produced in a human cell-line. *Protein Expr. Purification* 115, 165–175.

Wion, K.L., Kelly, D., Summerfield, J.A., Tuddenham, E.G., and Lawn, R.M. (1985). Distribution of factor VIII mRNA and antigen in human liver and other tissues. *Nature* 317, 726–729.

- Wise, R.J., Dorner, A.J., Krane, M., Pittman, D.D., Kaufman, R.J. (1991). The role of von Willebrand factor multimers and propeptide cleavage in binding and stabilization of factor VIII. *Journal of Biological Chemistry* 266(32), 21948-21955.
- Wood, W.I., Capon, D.J., Simonsen, C.C., Eaton, D.L., Gitschier, J., Keyt, B., Seeburg, P.H., Smith, D.H., Hollingshead, P., Wion, K.L., et al. (1984). Expression of active human factor VIII from recombinant DNA clones. *Nature* 312, 330–337.
- Wu, Z., Yang, H., and Colosi, P. (2010). Effect of genome size on AAV vector packaging. *Mol. Therapy* 18, 80–86.
- Wurm, F.M. (2004). Production of recombinant protein therapeutics in cultivated mammalian cells. *Nat. Biotechnology* 22, 1393–1398.
- Xiao, X., Li, J., and Samulski, R.J. (1998). Production of high-titer recombinant adeno-associated virus vectors in the absence of helper adenovirus. *Journal of Virology* 72, 2224–2232.
- Yamane-Ohnuki, N., and Satoh, M. (2009). Production of therapeutic antibodies with controlled fucosylation. *MAbs* 1, 230–236.
- Yan, Z., Zhang, Y., Duan, D., and Engelhardt, J.F. (2000). Trans-splicing vectors expand the utility of adeno-associated virus for gene therapy. *Proceedings of the National Academy of Sciences of the United States of America* 97, 6716–6721.
- Yan, Z., Zak, R., Zhang, Y., and Engelhardt, J.F. (2005). Inverted terminal repeat sequences are important for intermolecular recombination and circularization of adeno-associated virus genomes. *Journal of Virology* 79, 364–379.
- Zanolini, D., Merlin, S., Feola, M., Ranaldo, G., Amoroso, A., Gaidano, G., Zaffaroni, M., Ferrero, A., Brunelleschi, S., Valente, G., Gupta, S., Prat, M., Follenzi, A. (2015). Extrahepatic sources of factor VIII potentially contribute to the coagulation cascade correcting the bleeding phenotype of mice with hemophilia A. *Haematologica* 100, 881-892.
- Zhang, B., Cunningham, M.A., Nichols, W.C., and Bernat, J.A. (2003). Bleeding due to disruption of a cargo-specific ER-to-Golgi transport complex. *Nature Genetics* 34, 220-225.
- Zhang, B., Kaufman, R.J., and Ginsburg, D. (2005). LMAN1 and MCFD2 form a cargo receptor complex and interact with coagulation factor VIII in the early secretory

pathway. *Journal of Biological Chemistry* 280, 25881–25886.

Zhang, L., Nolan, E., Kreitschitz, S., and Rabussay, D.P. (2002). Enhanced delivery of naked DNA to the skin by non-invasive in vivo electroporation. *Biochimica Biophysica Acta* 1572, 1–9.

Zhang, P., Tan, D.L., Heng, D., Wang, T., Mariati, Yang, Y., and Song, Z. (2010). A functional analysis of *N*-glycosylation-related genes on sialylation of recombinant erythropoietin in six commonly used mammalian cell lines. *Metab. Eng* 12, 526–536.

Zheng, C., and Baum, B.J. (2008). Evaluation of promoters for use in tissue-specific gene delivery. *Methods Mol. Biology* 434, 205–219.

Zheng, C., Page, R.C., Das, V., Nix, J.C., Wigren, E., Misra, S., and Zhang, B. (2013). Structural characterization of carbohydrate binding by LMAN1 protein provides new insight into the endoplasmic reticulum export of factors V (FV) and VIII (FVIII). *Journal of Biological Chemistry* 288, 20499–20509.

Zhu, A., and Hurst, R. (2002). Anti-N-glycolylneuraminic acid antibodies identified in healthy human serum. *Xenotransplantation* 9, 376–381.

Zhu, J. (2012). Mammalian cell protein expression for biopharmaceutical production. *Biotechnology Advances* 30, 1158–1170.

Zufferey, R., Dull, T., Mandel, R.J., Bukovsky, A., Quiroz, D., Naldini, L., and Trono, D. (1998). Self-inactivating lentivirus vector for safe and efficient in vivo gene delivery. *Journal of Virology* 72, 9873–9880.

Appendix

.

Appendix. 1, FVIIISelect column Äkta explore profile

ÄKTAdesign

UNICORN 5.20 (Build 500)

Result file: C:\...\default\FVIII V3co 300ml 6e82t1000 20140219 FVIII SELECT 001

```
0.00 Base SameAsMain
0.00 Block System_Volume_Compensation
      (System_Volume_Compensation)
0.00 Base Volume
      (8.00)#Compensation_Volume End_Block
(5.00)#Reequilibrate_with End_Block
```

Documentation

Variables

Column	VIIISelect
Flow_Rate	1.00 {ml/min}
Column_PressureLimit	0.50 {MPa}
Wavelength_1	280 {nm}
Wavelength_2	OFF {nm}
Wavelength_3	OFF {nm}
Averaging_Time_UV	0.01 {sec}
BufferValve_A1_Inlet	A11
Pump_A_Inlet	A1
Pump_B_Inlet	B1
Wash_Inlet_A1	OFF
Wash_Inlet_A2	OFF
Wash_Inlet_B1	OFF
Wash_Inlet_B2	OFF
Column_Position	Position3
Compensation_Volume	8.00 {ml}
Equilibrate_with	5 {CV}
OutletValve_Position	F3
SampleInlet	A11
Injection_Flow_rate	1.00 {ml/min}
Sample_Volume	300.00 {ml}
Wash_column_with	2 {CV}
1_PumpAInlet	A1
1_PumpBINlet	B1
1_Buffer_Inlet_A	A11
1_Wash_Inlet_A1	OFF
1_Wash_Inlet_A2	OFF
1_Wash_Inlet_B1	OFF
1_Wash_Inlet_B2	OFF
1_ConcB_Step	0 {%B}
1_Tube_Type	12mm
1_Fraction_Size	2 {ml}
1_Start_at	FirstTube
1_Length_of_Step	60 {CV}
2_PumpAInlet	A2
2_PumpBINlet	B1
2_Buffer_Inlet_A	A11
2_Wash_Inlet_A1	OFF
2_Wash_Inlet_A2	OFF
2_Wash_Inlet_B1	OFF
2_Wash_Inlet_B2	OFF
2_ConcB_Step	70 {%B}
2_Tube_Type	12mm
2_Fraction_Size	2 {ml}
2_Start_at	NextTube
2_Length_of_Step	60 {CV}

ÄKTAdesign

UNICORN 5.20 (Build 500)

Result file: C:\...\default\rFVIII V3co 300ml 6e82t1000 20140219 FVIII SELECT 001

3_PumpAInlet	A2
3_PumpBInlet	B1
3_Buffer_Inlet_A	A11
3_Wash_Inlet_A1	OFF
3_Wash_Inlet_A2	OFF
3_Wash_Inlet_B1	OFF
3_Wash_Inlet_B2	OFF
3_ConcB_Step	100 { %B }
3_Tube_Type	12mm
3_Fraction_Size	1 { ml }
3_Start_at	NextTube
3_Length_of_Step	20 { CV }
Reequilibrate_with	5.00 { CV }

Scouting

No information to print.

Questions

No 1: Sample Volume and Type
rFVIII V3co, 300ml, 6e8/2-t1000. 2014-02-19 FVIII SELECT

No 2: Column

No 3: Eluent A

No 4: Eluent B

No 5: Remarks

Column(s) :

VIIISelect

Height	3.5 cm
Diameter	0.6 cm
Column volume	0.99 ml
Technique	Affinity
Vt	0.0 ml
Vo	0.0 ml
Max pressure	0.5 MPa
Default flowrate	1.0 ml/min
Max flowrate	
Typ. peak width at base	
pH High value, longterm	
pH Low value, longterm	
pH High value, shortterm	
pH Low value, shortterm	
Average particle diam.	
Code no	
Typical loading range	
Mol. weight range	

ÄKTAdesign

UNICORN 5.20 (Build 500)

Result file: C:\...\default\rFVIII V3co 300ml 6e82t1000 20140219 FVIII SELECT 001

Scan rate

Start Notes

No information to print.

Run Notes

No information to print.

Evaluation Notes

No information to print.

Calibration

P900Press Calibrated 18/12/2013 10:20:24 by default

P950Press Calibrated 08/06/2010 17:54:20 by default

pH Calibrated 18/12/2013 11:04:39 by default

Reference Value 1 : 9.000000 pH

Reference Value 2 : 2.700000 pH

P950Flow Calibrated 23/01/2013 12:03:56 by default

Reference Value 1 : 5.000000 ml

Reference Value 2 : 5.000000 ml

Logbook

0.00 min Method Run 19/02/2014, 08:31:22 GMT Standard Time, Method : FVIII
 direct load imadiazole, Result : C:\...\default\rFVIII V3co 300ml 6e82t1000
 20140219 FVIII SELECT 001.res

0.00 min User default in control of the run
 0.00 min Batch ID: 39C7A226-282C-48D7-B3AF-2B7F7DBC03B8
 0.00 min Base CV, 0.99 {ml}, VIIISelect
 0.05 min Block Flow_Rate
 0.05 min Base SameAsMain
 0.05 min Flow 1.00 ml/min
 0.05 min End Block
 0.05 min Block Column_Pressure_Limit
 0.05 min Base SameAsMain
 0.05 min Alarm Pressure Enabled , 0.50 MPa, 0.00 MPa
 0.05 min End Block
 0.05 min Block Start_Instructions
 0.05 min Base SameAsMain
 0.05 min Wavelength 280 nm, OFF , OFF
 0.05 min AveragingTimeUV 0.01 sec
 0.05 min End Block
 0.05 min Block BufferValve_A1_Inlet
 0.05 min Base SameAsMain
 0.05 min BufferValveA1 A11
 0.05 min End Block
 0.05 min Block Eluent_A_Inlet
 0.05 min Base SameAsMain
 0.05 min PumpAInlet A1

UNICORN 5.20 (Build 500)

Result file: C:\...\default\rFVIII V3co 300ml 6e82t1000 20140219 FVIII SELECT 001

```

0.05 min End Block
0.05 min Block Eluent_B_Inlet
0.05 min Base SameAsMain
0.05 min PumpBINlet B1
0.05 min End Block
0.05 min Block Start_with_PumpWash_Explorer
0.05 min Base SameAsMain
0.05 min PumpWashExplorer OFF , OFF, OFF, OFF
0.12 min End Block
0.12 min Block Start_Conc_B_0_pc_B
0.12 min Base SameAsMain
0.12 min Gradient      0.00 %B,      0.000 CV
0.12 min End Block
0.12 min Block Column_Valve
0.12 min Base SameAsMain
0.12 min ColumnPosition Position3
0.12 min End Block
0.12 min Block System_Volume_Compensation
0.12 min Base Volume {ml}
8.19 min End Block
8.19 min Block Column_Equilibration
8.19 min Base SameAsMain
13.14 min End Block
13.14 min Block AutoZero_UV
13.14 min Base SameAsMain
13.14 min AutoZeroUV
13.14 min End Block
13.14 min Block Flowthrough_Collection
13.14 min Base SameAsMain
13.18 min Pause 19/02/2014, 08:44:30 (Manual)
13.18 min OutletValve F3
13.18 min Continue 19/02/2014, 08:45:03 (Manual)
13.18 min End Block
13.18 min Block Sample_Inlet_BufferValve
13.18 min Base SameAsMain
13.18 min PumpAInlet A1
13.18 min BufferValveA1 A11
13.18 min End Block
13.18 min Block Load_Sample_with_SystemPump
13.18 min Base Volume {ml}
13.18 min InjectionMark
13.18 min Flow      1.00 ml/min
310.94 min Pause 19/02/2014, 13:42:49 (Manual)
310.94 min Next Breakpoint (Manual)
310.94 min Continue 19/02/2014, 13:43:48 (Manual)
310.94 min End Block
310.94 min Block BufferValve_A1_Inlet
310.94 min Base SameAsMain
310.94 min BufferValveA1 A11
310.94 min End Block
310.94 min Block Eluent_A_Inlet
310.94 min Base SameAsMain
310.94 min PumpAInlet A1
310.94 min End Block
310.94 min Block Flow_Rate
310.94 min Base SameAsMain
310.94 min Flow      1.00 ml/min
310.94 min End Block
310.94 min Block Complete_Sample_Loading

```



amersham pharmacia biotech

ÄKTAdesign

UNICORN 5.20 (Build 500)

Result file: C:\...\default\rFVIII V3co 300ml 6e82t1000 20140219 FVIII SELECT 001

```

310.94 min Base Volume {ml}
330.98 min End Block
330.98 min Block Wash_Out_Unbound_Sample
330.98 min Base SameAsMain
332.96 min End Block
332.96 min Block Pump_Inlet_A_Segment_1
332.96 min Base SameAsMain
332.96 min PumpAInlet A1
332.96 min End Block
332.96 min Block Pump_Inlet_B_Segment_1
332.96 min Base SameAsMain
332.96 min PumpBInlet B1
332.96 min End Block
332.96 min Block Buffer_Inlet_A_Segment_1
332.96 min Base SameAsMain
332.96 min BufferValveA1 A11
332.96 min End Block
332.96 min Block Wash_Explorer_1
332.96 min Base SameAsMain
332.96 min PumpWashExplorer OFF , OFF, OFF, OFF
333.03 min Block Delay0p05min
333.03 min Base Time {min}
333.08 min End Block
333.08 min End Block
333.08 min Block ConcB_Step_1
333.08 min Base SameAsMain
333.08 min Gradient 0.00 %B, 0.000 CV
333.08 min End Block
333.08 min Block Fractionation_Segment_1
333.08 min Base SameAsMain
333.08 min Fractionation 12mm , 2.000 ml , FirstTube , Volume
333.10 min End Block
333.10 min Block Step_Segment_1
333.10 min Base SameAsMain
333.10 min Block Step_1
333.10 min Base SameAsMain
392.50 min End Block
392.50 min Block Delay0p02min
392.50 min Base Time {min}
392.52 min End Block
392.52 min End Block
392.52 min Block Pump_Inlet_A_Segment_2
392.52 min Base SameAsMain
392.52 min PumpAInlet A2
392.52 min End Block
392.52 min Block Pump_Inlet_B_Segment_2
392.52 min Base SameAsMain
392.52 min PumpBInlet B1
392.52 min End Block
392.52 min Block Buffer_Inlet_A_Segment_2
392.52 min Base SameAsMain
392.52 min BufferValveA1 A11
392.52 min End Block
392.52 min Block Wash_Explorer_2
392.52 min Base SameAsMain
392.52 min PumpWashExplorer OFF , OFF, OFF, OFF
392.59 min Block Delay0p05min
392.59 min Base Time {min}
392.64 min End Block

```

ÄKTAdesign

UNICORN 5.20 (Build 500)

Result file: C:\...\default\rFVIII V3co 300ml 6e82t1000 20140219 FVIII SELECT 001

```
392.64 min End Block
392.64 min Block ConcB_Step_2
392.64 min Base SameAsMain
392.64 min Gradient 70.00 %B, 0.000 CV
392.64 min End Block
392.64 min Block Fractionation_Segment_2
392.64 min Base SameAsMain
392.64 min Fractionation 12mm , 2.000 ml , NextTube , Volume
392.66 min End Block
392.66 min Block Step_Segment_2
392.66 min Base SameAsMain
392.66 min Block Step_2
392.66 min Base SameAsMain
452.06 min End Block
452.06 min Block Delay0p02min
452.06 min Base Time {min}
452.08 min End Block
452.08 min End Block
452.08 min Block Pump_Inlet_A_Segment_3
452.08 min Base SameAsMain
452.08 min PumpAInlet A2
452.08 min End Block
452.08 min Block Pump_Inlet_B_Segment_3
452.08 min Base SameAsMain
452.08 min PumpBInlet B1
452.08 min End Block
452.08 min Block Buffer_Inlet_A_Segment_3
452.08 min Base SameAsMain
452.08 min BufferValveA1 A11
452.08 min End Block
452.08 min Block Wash_Explorer_3
452.08 min Base SameAsMain
452.08 min PumpWashExplorer OFF , OFF, OFF, OFF
452.15 min Block Delay0p05min
452.15 min Base Time {min}
452.20 min End Block
452.20 min End Block
452.20 min Block ConcB_Step_3
452.20 min Base SameAsMain
452.20 min Gradient 100.00 %B, 0.000 CV
452.20 min End Block
452.20 min Block Fractionation_Segment_3
452.20 min Base SameAsMain
452.20 min Fractionation 12mm , 1.000 ml , NextTube , Volume
452.22 min End Block
452.22 min Block Step_Segment_3
452.22 min Base SameAsMain
452.22 min Block Step_3
452.22 min Base SameAsMain
472.02 min End Block
472.02 min Block Delay0p02min
472.02 min Base Time {min}
472.04 min End Block
472.04 min End Block
472.04 min Block Fractionation_Stop
472.04 min Base SameAsMain
472.04 min FractionationStop
472.06 min Peak_FracStop
472.08 min End Block
```

Appendix 2

Mass Spectrometry Materials and Methods.

2.1 Samples Description

Samples containing five FVIII variants were kindly provided by Dr. Nathwani's group (University College London) in collaboration with the Royal Free Hospital, London, UK. Glycoproteins were expressed in HEK-293T cell lines purified and dispatched to Imperial College London for glycomic analysis. The experimental approach followed in the current study is extensively described in Canis et al., 2012. Unless otherwise stated, all chemical reagents were obtained from Sigma-Aldrich.

2.2 Dialysis

Samples were inserted into dialysis cassettes (MWCO3500, Pierce) and incubated in 50mM ammonium hydrogen carbonate (AMBIC) buffer (pH 8.5) for 48 hours at 4°C with regular buffer replacements. Next, samples were efficiently frozen at -80°C and subsequently freeze-dried.

2.3 Reduction and carboxymethylation

Samples were reduced with dithiothreitol (DTT) and carboxylated using iodoacetic acid (IAA). An initial solution of 0.6M Tris, 4M GuHCl was prepared, its pH was adjusted to 8.5 using HCl and it subjected to de-gas under nitrogen for 20 minutes, in order to make 2mg/mL DTT solution. Then, DTT solution was inserted to sample and incubated at 50°C for 2 hours. A second solution of 0.6M Tris adjusted to pH 8.5 and de-gassed under nitrogen for 20 minutes, in order to make 12mg/mL IAA solution. Next, this solution was added to the sample and incubated at room temperature for 2 hours in the dark. A subsequent dialysis was performed as described above.

2.4 Trypsin digestion

Trypsin digestion of reduced and carboxymethylated samples was performed in 50mM AMBIC buffer, adjusted with diluted ammonia in pH 8.4. For every 100µg of sample, 0.2µg of trypsin (Bovine pancreas, T-1426, Sigma) were used. Samples were incubated for 14 hours at 37°C. The reaction quenched by adding a few drops of Acetic acid. Digested glycopeptides were purified using C18 reversed-phase chromatography column (Oasis HLB Plus) with the PrOH/ 5% Acetic acid method. Then, propanol fractions were combined, their volume was reduced using SpeedVac (Savant), they were frozen at -80°C and lyophilised.

2.5 PNGase F digestion

N-Glycosidase F (PNGase F, Roche) was used to release *N*-glycans from glycopeptides. Lyophilised samples were dissolved in 50mM AMBIC buffer of pH 8.4, adding 3~5 units of PNGase F and incubating for 24 hours at 37°C. The second aliquot of PNGase F was added at an interim interval during incubation. Samples were frozen at -80°C and lyophilised. Samples were re-dissolved in 5% Acetic acid and subjected reversed-phase chromatography with PrOH/ 5% Acetic acid method. *N*-glycans were isolated at the 5% Acetic acid fraction, and along with the other fractions were reduced in volume with SpeedVac, frozen at -80°C and lyophilised. Peptide fragments was collected from the 20% and 40% propanol fractions.

2.6 Reductive elimination

Reductive elimination was performed to release *O*-glycans from glycopeptides. 1 M KBH₄/ 0.1 M KOH solution was used to dissolve lyophilised samples, and the solutions were incubated for 14-16 hours at 45°C. A few drops of Acetic acid were added to terminate the reaction. Then, a column made with Dowex beads (VWR) was constructed to desalt the samples by ion-exchange. The column conditioning was made with 15 mL of 5% Acetic acid; the sample was loaded and eluted (4mL) with 5% Acetic acid in a tube. The eluent was frozen at -80°C and lyophilized. Excess borates were removed by co-evapulating with 10% Methanolic Acetic acid with nitrogen at room temperature.

2.7 Derivatisation of O- and N-glycans

O- and N-glycans were permethylated with DMSO (3mL), and NaOH (5 pellets) slurry with 0.5mL methyl iodide under constant shaking for 15 minutes at room temperature. Reaction terminated by adding 1mL of ultra-pure water. Chloroform (1~2mL) was added to the solutions, and permethylated glycans were extracted with chloroform layer after several washings with water. The samples were dried under nitrogen and purified by reversed-phase chromatography with MeCN/H₂O method (see description below). All fractions collected, reduced in volume with SpeedVac, frozen at -80°C and lyophilised.

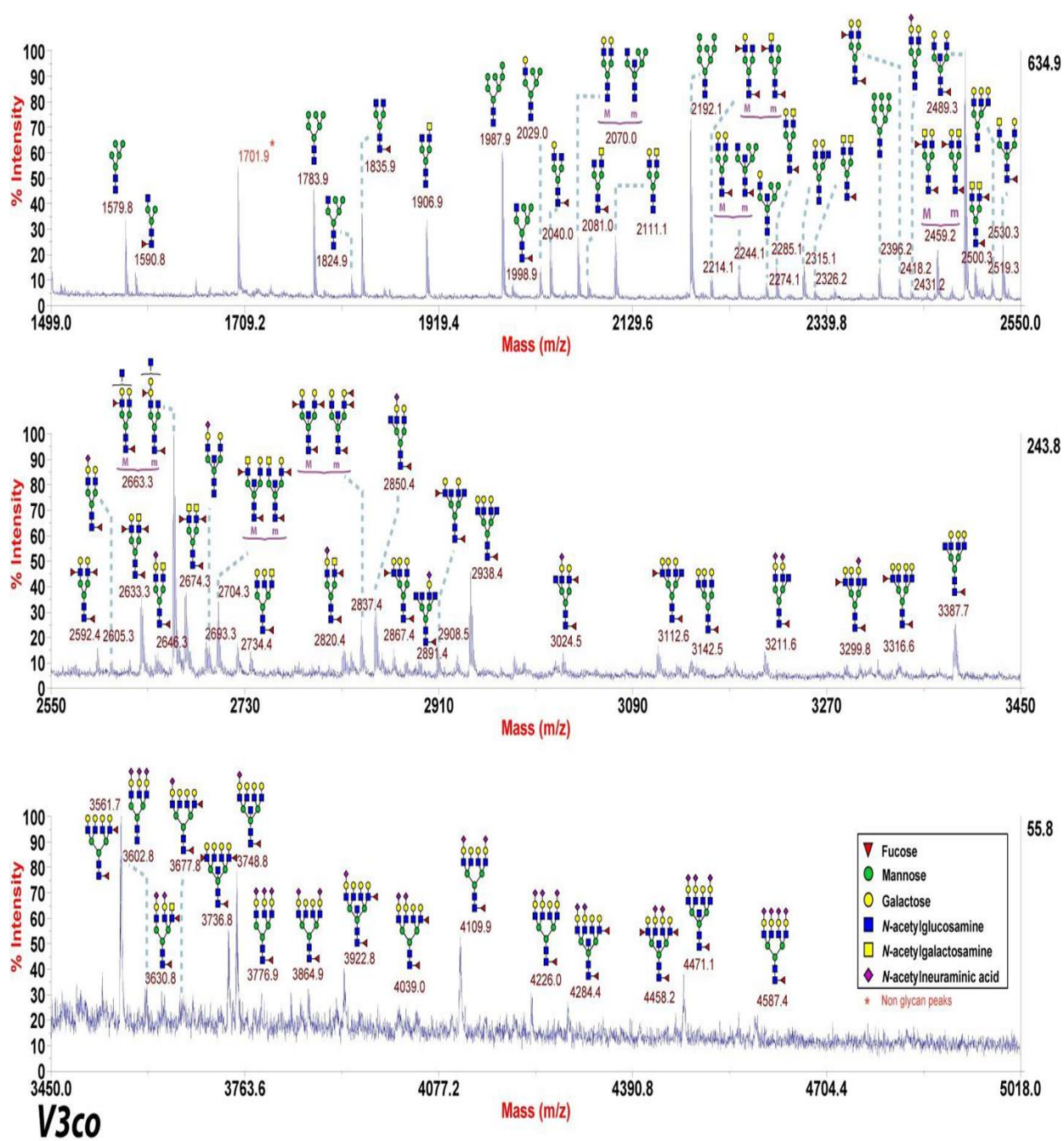
2.8 MALDI-TOF and MALDI-TOF/TOF analysis

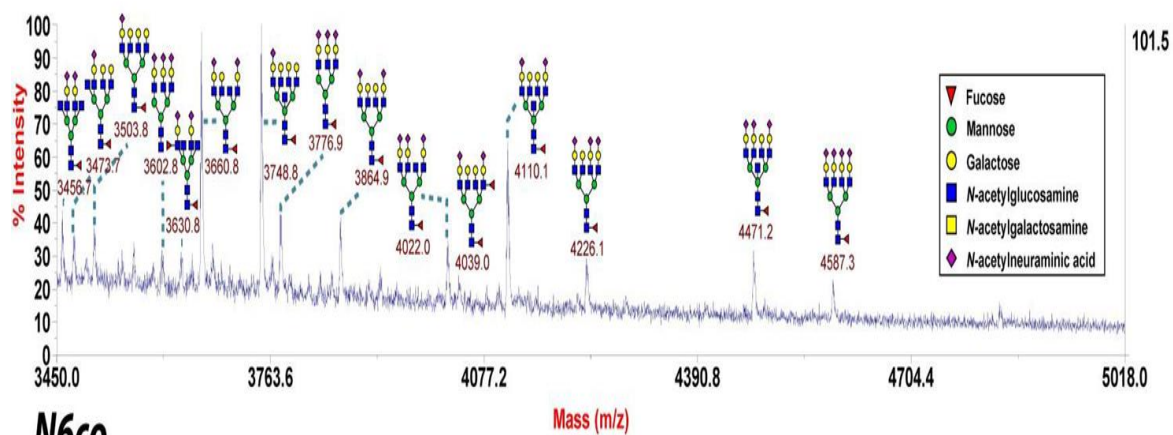
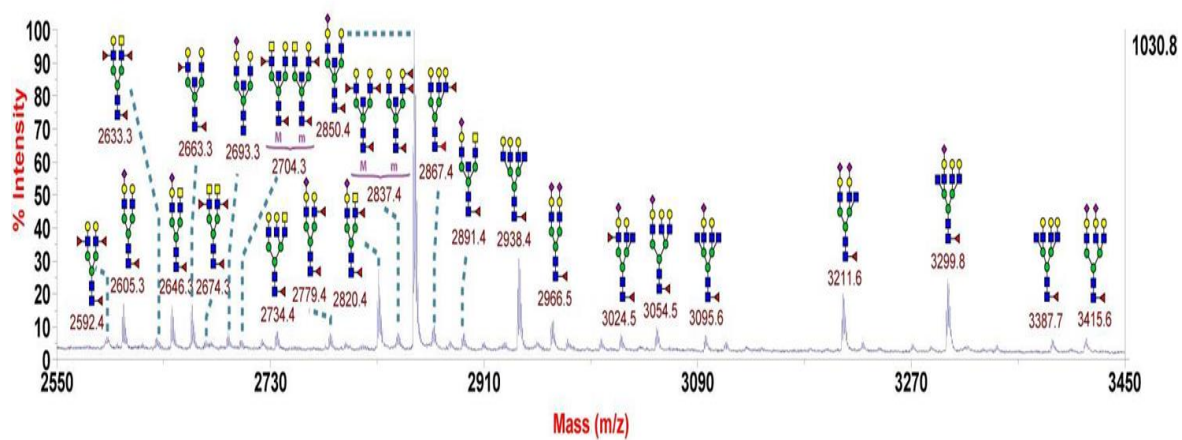
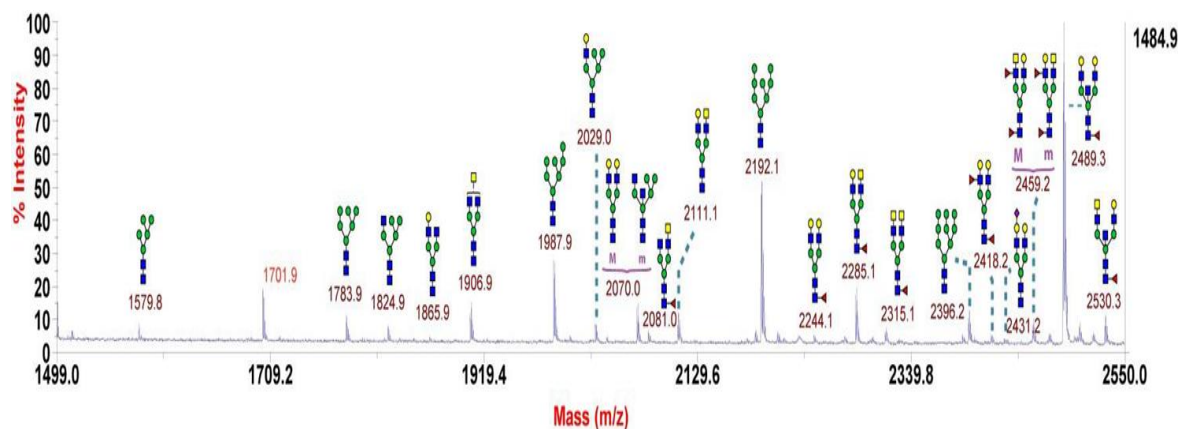
Samples dissolved in 10µL MeOH, and 1µL was mixed 1:1 with matrix (3,4-diaminobenzophenone 20mg/mL in 75% acetonitrile and 25% water), spotted onto MS plate and dried under vacuum. Both MALDI-TOF MS (matrix-assisted laser desorption/ionization time-of-flight Mass spectrometry) and MALDI-TOF/TOF MS/MS analyses were performed on 4700 Proteomics Analyzer (Applied Biosystems). Reversed-phase column chromatography, unless stated otherwise, purifications were carried out with Sep-Pak C18 cartridge (Waters).

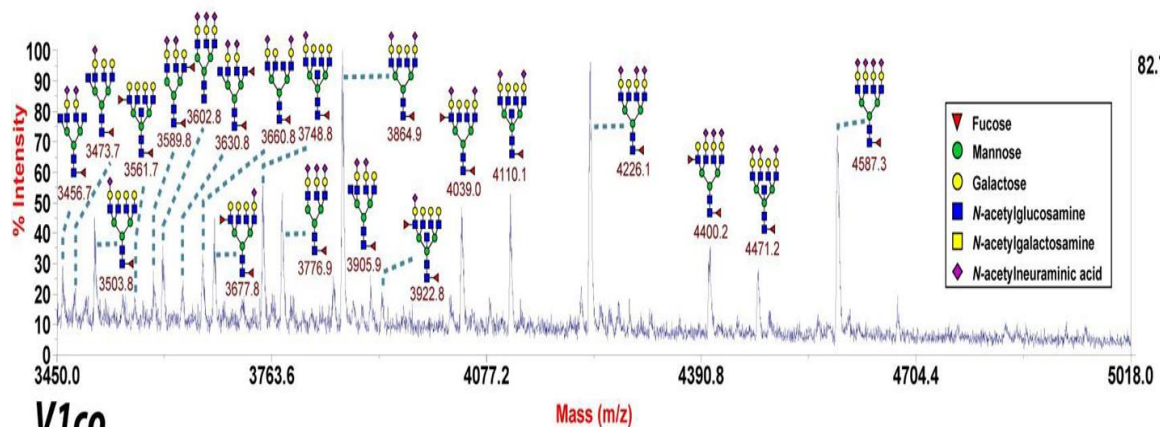
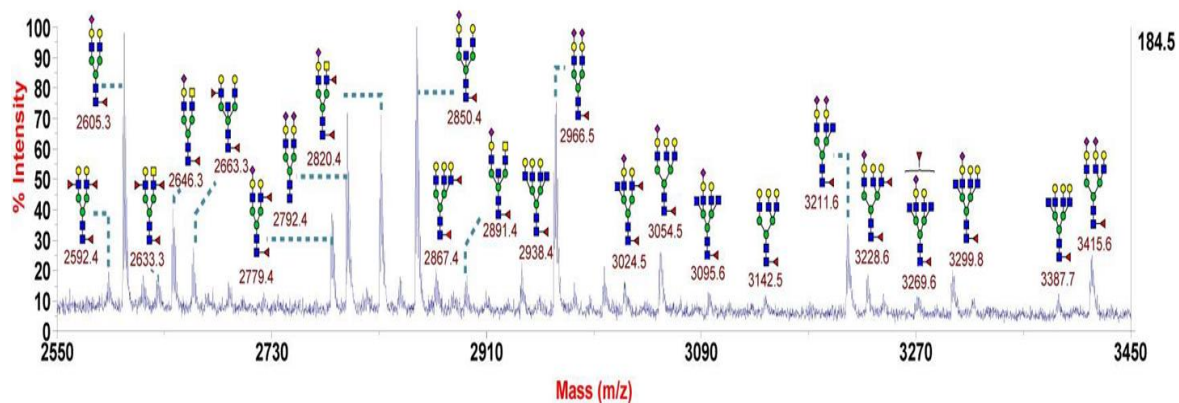
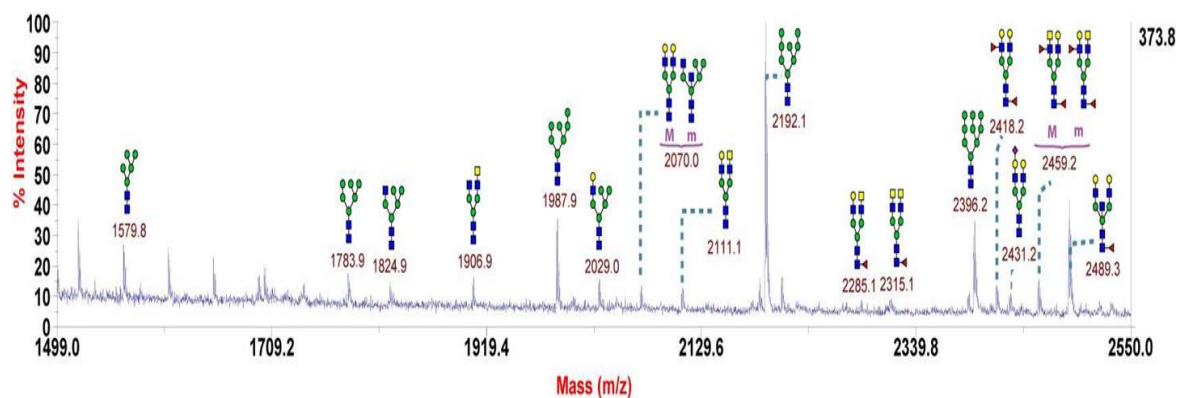
2.9 PrOH/5% Acetic acid system

C18 cartridge conditioning was performed by sequentially adding MeOH (5 mL), 5% Acetic acid (5mL), propanol (4mL), and 5% Acetic acid (15mL). After loading the sample, cartridge washed with 5% acetic acid (3 x 5mL) and samples eluted with 5% Acetic acid (15mL), 20% PrOH (4mL), 40% PrOH (4mL) and 100% PrOH (4mL). MeCN/H₂O system C18 cartridge conditioning was performed by sequentially adding MeOH (5mL), ultra-pure water (5mL), MeCN (5mL), and ultra-pure water (3 x 5mL). After loading the sample, cartridge washed with ultra-pure water (5mL) and the fractions 15%, 35%, 50%, and 75% MeCN (3mL each) were collected.

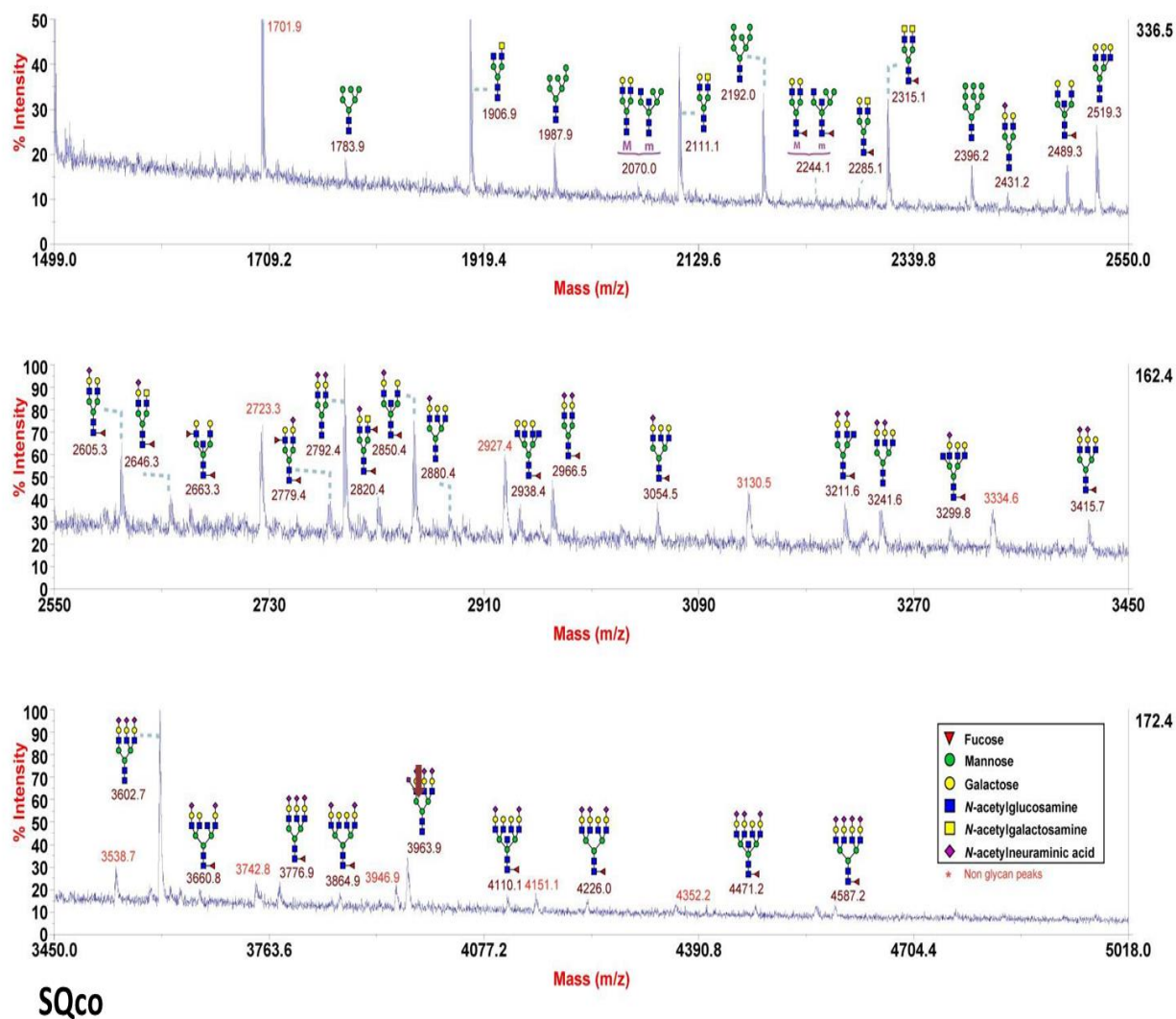
Appendix 3. Mass spectrometry

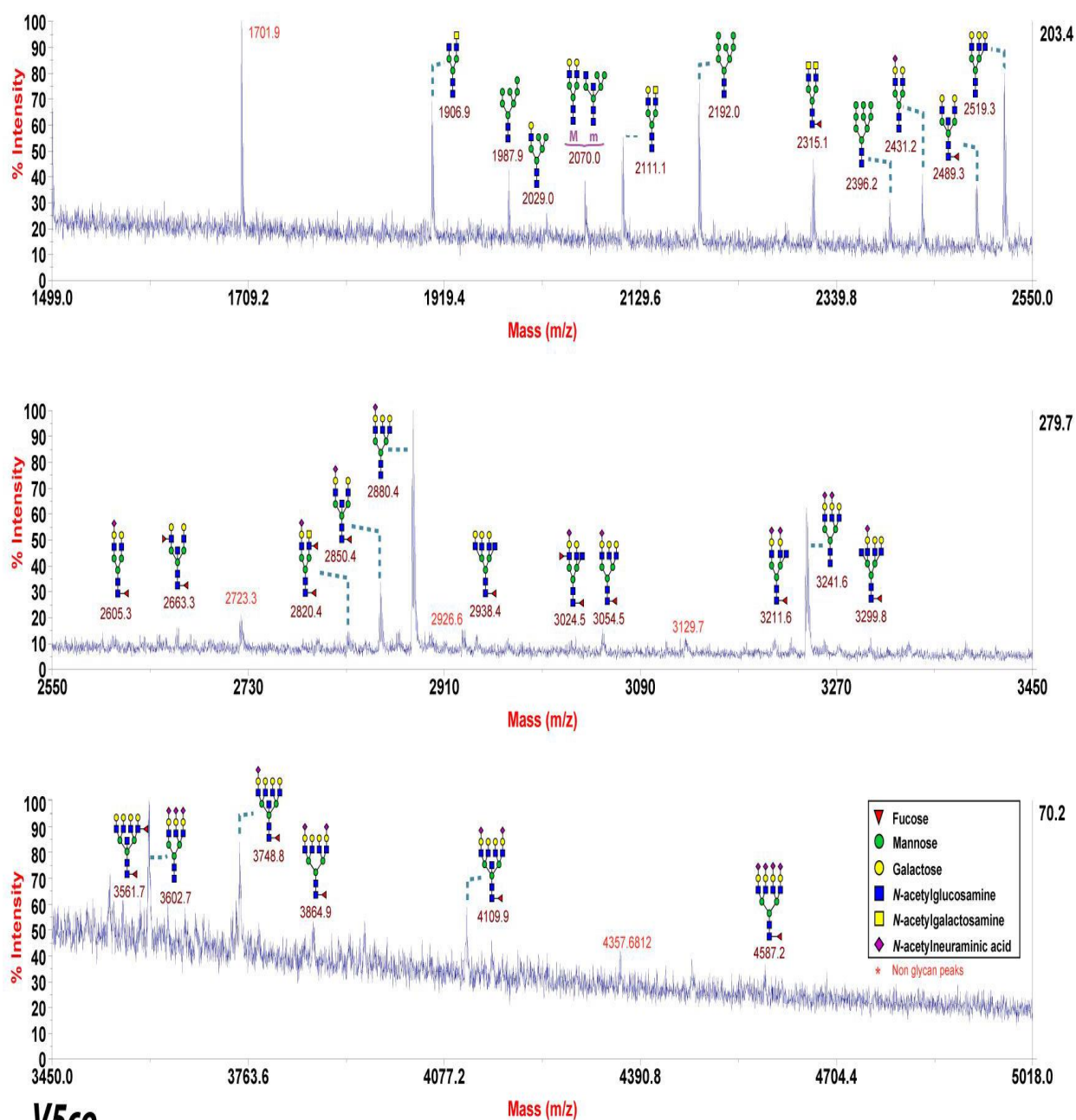


**N6co**



V1co





Full MALDI-TOF mass spectra of samples presenting the total identified *N*-glycomes. Structural assignments are based on monosaccharide compositions, knowledge upon glycan biosynthesis and fragmentation analyses. All spectra display $[M + Na]^+$ molecular ions. Panel intensities were normalized to 100% unless otherwise stated. In m/z values with more than one structures: M: Major (more abundant) structure; m: minor (less abundant) structure, Data provide from Dr Stuart Haslam (Imperial college).